Trade-offs between growth, storage and defense in plants under carbon limitation

Dissertation

To Fulfill the
Requirements for the Degree of
„doctor rerum naturalium“ (Dr. rer. nat.)

Submitted to the Council of the Faculty
of Biology and Pharmacy
of the Friedrich Schiller University Jena

by Jianbei Huang

born on 01.04.1989 in China

Reviewers:

1. Prof. Nicole M. van Dam

   German Centre for Integrative Biodiversity Research, Leipzig, Germany

2. Prof. Anna Sala

   Division of Biological Sciences, The University of Montana, Missoula, USA

3. Dr. Henrik Hartmann

   Max Planck Institute for Biogeochemistry, Jena, Germany

Date of defense: 24 September 2018

Dissertation, Friedrich Schiller University Jena, 2018

Table of Contents

ACKOWLEDGEMENTS

First and foremost, I would like to thank my supervisors, Dr. Henrik Hartman and Prof. Susan Trumbore at Max Planck Institute for Biogeochemistry (MPI-BGC), for giving me this opportunity to join this prestigious institute and this nice group, for their encouragement, guidance and support throughout my Ph.D study. My “eyes” are opened to science because of you.

I am also grateful to Prof. Nicole van Dam and Prof. Anna Sala for supervising my Ph.D study and giving constructive feedback. I would like to thank Dr. Almuth Hammerbacher and Prof. Dr. Jonathan Gershenzon at Max Planck Institute for Chemical Ecology (MPI-CE), for giving me an opportunity to work in your lab and for your guidance on secondary metabolites. Special thanks go to Dr. Michael Reichelt for his great expertise and support in GC-MS and HPLC-MS.

I would also like to thank Dr. Thomas Behrendt for his supervision and great support in the BVOC study. I would like to thank Dr. Alexander Weinhold, Dr. Heidi Hellén, Prof. Armin Wisthaler for their support in BVOC measurements.

I appreciate the technical assistance during my Ph.D experiment. I would like to thank Savoyane Lambert for her continuous and dedicated support from greenhouse preparation and sampling to lab work, Waldemar Ziegler for his enormous assistance in greenhouse and teaching in experimental manipulations, and Martin Göbel for his assistance in phytochamber and chamber constructions. I thank Iris Kuhlmann for her teaching and assistance in the lab, Anett Enke and Jessica Heublein for NSC measurements. I acknowledge the support from the service groups at MPI-BGC including Field Experiments group, Workshop, IsoLab, GasLab, Speclab, RoMA and Building Services, especially Olaf Kolle and René Schwalbe for their assistance in CO_2 manipulation, Heike Geilmann and Michael Rothe for isotopic measurements, Johannes Schwarz for gas preparation. My PhD study would have been impossible without all of their support.

I would like thank all my colleagues and friends at MPI-BGC. In particular, I would like to thank my fellow office mates, Somak Chowdhury, Carsten Simon, Simon Benk. It was really a pleasure working and relaxing in the office with such nice people. I also thank my group members, Haiyang Zhang, Gabriela Pereyra, Lenka Forkelova, David Herrera, Juliane Helm and Sarah Fischer for providing constructive discussions and support. I thank my Chinese friends in Munich for their company and encouragements. Special thanks to Yunpeng Luo, Su Ding, Jinhong Guan, Yan Li, Chuanfang Jin, and my friends at MPI-CE, Zhiling Yang, Dechang Cao, Chenyong Lang and Jingyuan Chen. You guys provided me a home feeling. Our lunch group members, Ingo Schöning, Jenia Singh, Hueiying Gan and Kasun Gayantha, thanks for your company. I will also remember our summer barbecue parties together with John Kim and Stefan Karlowsky and other colleagues. I am grateful to Dr. Steffi Rothhardt for organizing the training and courses, and John Kula for applying residence permit. Many thanks to Kerstin Lohse for her support in organizing business trips and administrative stuff. I also want to thank the Chinese basketball team in Winzerla sports gym, and particularly, my friends at MPI-BGC for your friendship in my life.

I acknowledge Chinese Scholarship Council (CSC) and Max Plank society (MBG) for funding my position and research, and support from International Max-Planck research school for global biogeochemical cycles (IMPRS).

For those who have helped me in any way since I started in Germany, I am grateful for your help.

Last but not the least, I would like to thank my family for their endless and unconditionally love.

ABOUT MYSELF

I was born and raised in China. Ever since I was a child, I have been motivated and told by my parents, who have been working as tailors for 30 years, that knowledge is very important for future.

As expected I went to the university and studied in the Faculty of Geography. After completing a bachelor degree, I joined the Faculty of Forest for my master in Sichuan Agricultural University and completed my master with a project on allelopathic effects of walnut leaf litter on winter wheat photosynthesis, growth and antioxidant systems. While the main focus of the study was to see the consequences, I was fascinated by the underlying mechanisms. So I decided to write a proposal on plant responses to changing environmental conditions and submitted it to Chinese Scholarship Council (CSC) in order to pursue Ph.D study abroad. Luckily I was funded for a four-year PhD study in Germany, and then started in Munich in OCT 2013 with full of hope, but left with full of disappointment after six month.

I moved from Munich to Jena where my research was reborn with a new Ph.D project under the supervision of Dr. Henrik Hartmann and Prof. Susan Trumbore. At the beginning of my PhD, an international workshop aiming to improve our understanding of tree mortality was initiated by Dr. Henrik, and this made me realize that understanding how plants allocate carbon is of critical importance for understanding how plants may respond to environmental changes. Ever since, I have been interested in exploring plant carbon allocation, with particular focus on the trade-offs between growth, storage and defense.

CHAPTER 1 General introduction

1.1 Carbon allocation across functional sinks

Carbon is the central element of life because it can bind with other elements such as hydrogen and oxygen, as well as many other elements and carbon atoms, to form complex molecules important for life. Thus, 'the fate of carbon', i.e. carbon allocation, plays a fundamental role in growth, survival and reproduction of organisms, particularly sessile organisms like plants that cannot escape harsh environmental conditions thus have to deal with stress with locally limited resources. Hence, for more than 40 years, carbon allocation has been of interest to plant scientists (Mooney, 1972). Rapidly changing climate in recent years, for example drought and heat-enhanced insect outbreaks (Allen *et al.*, 2010), and elevated atmospheric CO_2 concentrations (Becklin *et al.*, 2017) as well as rising air temperature (Way & Oren, 2010), have sparked our interest in understanding, among others, how plants allocate carbon into growth, storage (Hartmann & Trumbore, 2016) and defense (Anderegg *et al.*, 2015b). Despite extensive research efforts on plant carbon allocation (Atkin, 2015), our understanding of carbon allocation patterns and their changes during organ ontogeny (young vs. old) and across organ types (leaf vs. stem vs. root) or plant species with different life-history strategies (herbaceous vs. woody plants), is still very limited (Dietze *et al.*, 2014).

Where does the carbon go (Fig. 1)? Carbon enters the plant via photosynthetic uptake of atmospheric CO_2 (source activity) and is then partitioned among several sinks, including respiration, structural growth, non-structural carbohydrates (NSC) and secondary metabolites (SM), as well as carbon export such as biogenic volatile organic compounds (BVOC) and root exudates. Hence, plant carbon allocation patterns are generally explained by the balance between source activity and sinks strength. Such a balance, however, can be altered by changes in resource availability, such as water, nutrients, temperature, light and CO_2 (Fatichi *et al.*, 2014). In general, the former three resources influence both source activity and sink strength, while the latter two resources only influence source activity thereby allowing investigations on the roles of source activity in carbon allocation. In particular, plants can be forced via reductions of CO_2 availability into trade-off situations in carbon allocation, i.e. preferential

allocation to one sink must come at the expense of others (Hartmann & Trumbore, 2016). Such information is of critical importance for understanding how plants allocate carbon in general and in particular in the context of environmental change.

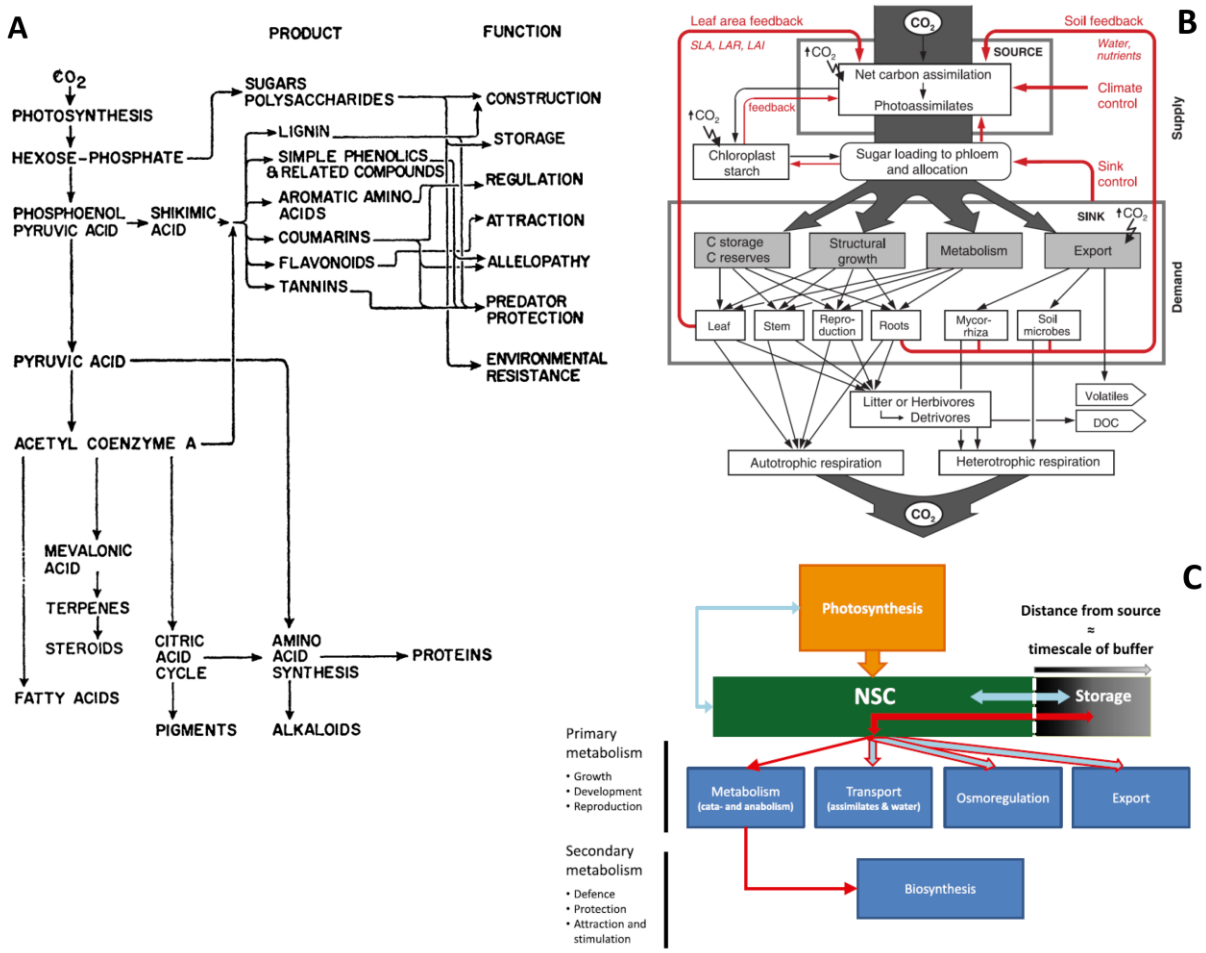

Figure 1.1 Schematic representation of carbon allocation. A): Main carbon products and their metabolic pathways (taken from Mooney (1972)). B): Functional (e.g., storage, growth and metabolism) and spatial (e.g., leaf, stem and roots) carbon pools and their feedback responses to environmental changes (taken from Körner (2006)). C): The central role of nonstructural carbohydrates (NSC) in plant carbon allocation (taken from Hartmann and Trumbore (2016)).

In the following sections, I will briefly discuss the role of different carbon sinks in plants and how carbon allocation to these sinks may be influenced by changes in availability of resources in particular carbon.

1.1.1 Regulation of respiration

Respiration is an essential metabolic process providing carbon intermediates for photosynthesis and energy for metabolic processes such as sucrose synthesis and phloem loading as well as protein turnover. At the whole-plant level, respiration may represent up to 30–50% of the gross photosynthetic CO_2 uptake, and due to the interdependency between respiration and photosynthesis, this percentage was relatively constant in herbaceous plants across a large range of atmospheric CO_2 (Gifford, 1995), temperature (Atkin *et al.*, 2007) and irradiance (Pons & Poorter, 2014). Not only energy demand but also substrate availability may influence respiration rates. Studies have shown that under extremely low CO_2 (40 ppm, Hartmann *et al.*, 2013a) or complete shading (Sevanto *et al.*, 2014; Fischer *et al.*, 2015), respiration rates decreased over time as NSC storage declined, suggesting dependence of respiration rate on substrate availability.

1.1.2 Regulation of growth

Whether and to what extent growth can be limited by carbon availability has been recently debated (Wiley & Helliker, 2012; Palacio *et al.*, 2014). It has been shown that abiotic stresses such as drought, cold and nutrient limitation decrease growth (C demand) earlier and to a greater degree than photosynthesis (C supply). This suggests that growth is limited by environmental physical factors rather than C supply. However, recent evidence showed that tree growth can also be limited by carbon availability under defoliation (Wiley *et al.*, 2013; Wiley *et al.*, 2017a), drought (Galiano Pérez *et al.*, 2017) and low CO_2 (Hartmann *et al.*, 2015).

Phytohormones play an important role in growth regulation in response to changing resource availability. Auxin (indole-3-acetic acid, IAA) was recognized as an essential plant growth promoter more than 70 years ago (Enders & Strader, 2015). While studies have shown that elevated CO_2 increases IAA concentrations and promotes growth in *Arabidopsis thaliana* (Teng *et al.,* 2006; Niu *et al.,* 2011; Hachiya *et al.,* 2014) and tomato seedlings *(Lycopersicon esculentum,* Wang *et al.*, 2009*)*, much less is known about its role in modulating plant growth under reduced carbon availability (Kazan, 2013). During drought, rice (Oryza sativa, Zhang *et al.*, 2009) and *Arabidopsis (*Skirycz *et al.*, 2010*)* may down-regulate growth via a reduction in auxin concentrations, possibly to divert carbon away from growth to promote survival. Similarly,

gibberellin (GA)– dependent down-regulation of growth has been observed under salt (Achard *et al.*, 2006), cold (Achard *et al.*, 2008) and osmotic stress (Skirycz *et al.*, 2010). In contrast to IAA and GA, Abscisic acid (ABA) has been known as a growth inhibitor, and activation of the ABA signalling pathway was involved in inhibition of root growth under osmotic stress (Achard *et al.*, 2006; Rowe *et al.*, 2016), suggesting that plants may actively regulate growth in response to abiotic stresses via modulation of phytohormones.

1.1.3 Regulation of storage

Nonstructural carbohydrates, NSC, including mostly sugars and starches but also lipid and proteins, are building blocks for plant growth and substrates for metabolism (Hartmann & Trumbore, 2016). In many studies, NSC are viewed as the major component of carbon storage that buffers the asynchrony of carbon supply and demand (Dietze *et al.*, 2014), but there is also evidence that lipids and proteins are substrates for supporting metabolism under shading (Fischer *et al.*, 2015). During drought and cold, rates of growth (C demand) decrease faster than rates of photosynthesis (C supply), thereby causing plants to accumulate NSC (Figure 1.2). This has led to the view that NSC pools simply build up when carbon supply exceeds demand (accumulation, Palacio *et al.*, 2014), rather than storage being a sink for C that might compete with other demands such as growth or defense. However, recent studies demonstrated that allocation to storage may be prioritized over growth under defoliation (Wiley *et al.*, 2017a), drought (Galiano Pérez *et al.*, 2017) and low CO_2 (Hartmann *et al.*, 2015) thereby suggesting a trade-off between growth and NSC storage (reserve formation).

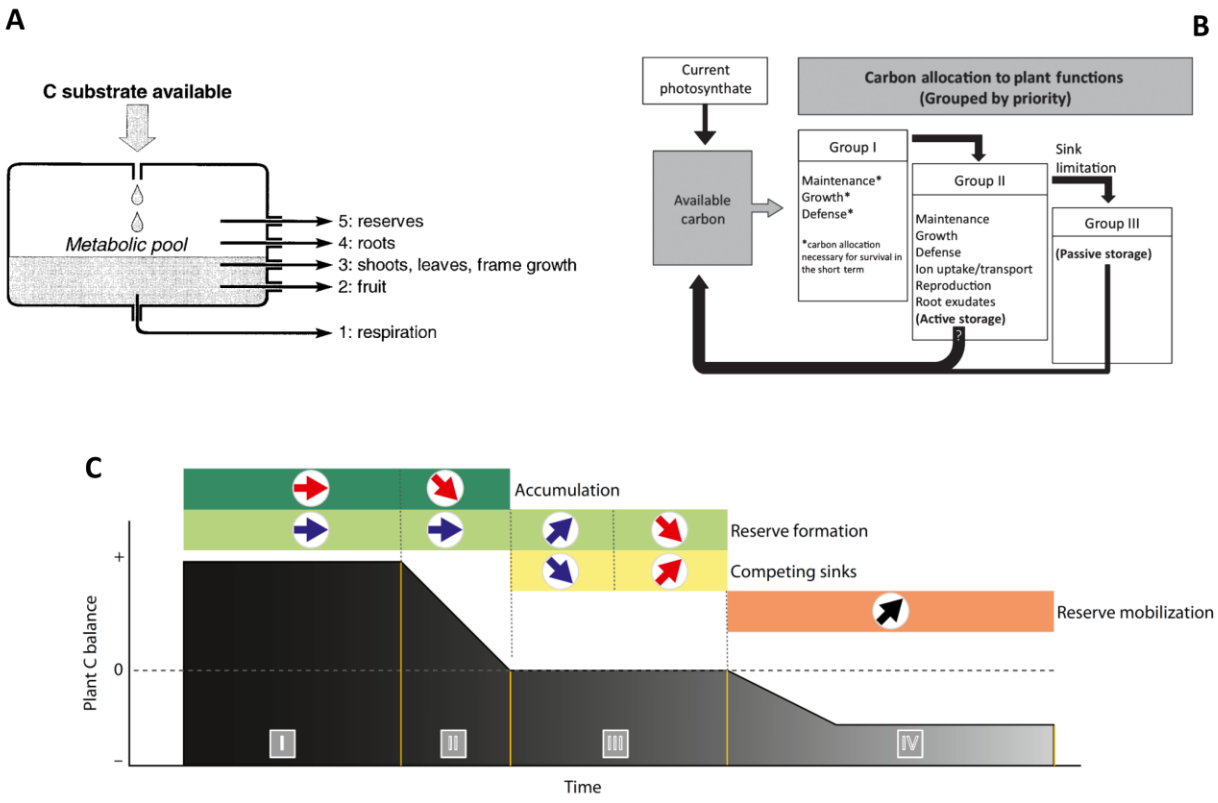

Figure 1.2 Schematic representations of NSC dynamics. A): Allocation to NSC is considered as a purely overflow process, i.e. NSC only accumulate when carbon supply exceeds carbon demand for respiration, growth and reproduction (taken from Lacointe (2000)). B): Build-up of NSC storage may result from two phases: under source limitation, allocation to NSC can compete with other sinks (e.g. growth) in order to enhance future survival (reserve formation), and accumulation occurs when sinks (e.g. growth) are directly limited by environmental factors other than carbon (taken from Wiley and Helliker (2012)). C): Hypothetical NSC dynamics along a gradient of carbon balance. Red arrows indicate allocation to storage is an overflow process while blue arrows indicate active regulation. Dark green boxes indicate accumulation, light green boxes indicate reserve formation. When C supply exceeds C demand (positive C balance, phase I), storage pools are composed of accumulation through overflow process and reserve formation through active regulation. As C availability decreases (phase II), accumulation declines while reserve formation remains constant via active regulation. When plants reach a C compensation point where net C assimilation equals net C losses (phase III), reserve formation may compete with other sinks (yellow boxes). Under negative C balance (phase IV), storage must be mobilized (black arrows) to support metabolisms necessary for sustaining life. Changes in storage pools (orange boxes) are independent of storage regulation (taken from Hartmann & Trumbore, 2016).

1.1.4 Regulation of secondary metabolite production

Secondary metabolites, SM, which are compounds not directly involved in primary metabolic activities (e.g. growth, development and reproduction), but are constructed for the purposes of detoxification and defense. Construction of these compounds represent a large carbon cost, for example, total phenolic compounds can account for up to 10%–20% of foliar dry weight in *Populus* (Donaldson *et al.*, 2006; Harding *et al.*, 2009; Boeckler *et al.*, 2013; Holeski *et al.*, 2013), willow (Salix myrsinifolia, Paajanen *et al.*, 2011) and spruce (Virjamo *et al.*, 2013; Virjamo *et al.*, 2014). However, allocation to SM may ultimately enhance overall plant C balance through their roles in protection against damage from periods of stresses (drought, cold, herbivory) (Vickers *et al.*, 2009).

How plants balance the costs and benefits of SM in a changing environment? The carbon-nutrient balance hypothesis, developed more than 30 years ago (Bryant *et al.*, 1983), provides a framework based on the carbon balance between C supply via photosynthesis and C demand for growth. It suggests that shading decreases C availability thereby resulting in lower concentrations of SM, whereas moderate nutrient limitation decreases growth more than photosynthesis, thereby increasing the availability of C for SM production. This hypothesis has been more recently expanded by the growth-differentiation balance hypothesis (Herms & Mattson, 1992), which suggests that any environment factor that limits growth more than photosynthesis may result in accumulation of NSC thereby increasing the C pool available for SM production. Hence, both hypotheses assume that limited carbon is preferentially allocated to growth rather than to SM (Figure 1.3).

Analogous to NSC, one could question whether there is a threshold below which allocation to SM can occur at the cost of growth, i.e. SM receive allocation priority over growth because the plant's ability to survive under stress relies more on SM (Figure 1.3). While some studies have shown the negative relationships between growth and SM among different genotypes (Donaldson *et al.*, 2006; Osier & Lindroth, 2006; Donaldson & Lindroth, 2007; Paul-Victor *et al.*, 2010), the increase in SM observed in these studies could simply result from a decrease in growth due to limited environmental resources (e.g. water and nutrients), rather that

prioritizing allocation to SM to achieve a trade-off. In addition, carbon-based SM generally increase under elevated CO_2 (Robinson *et al.*, 2012) and decrease under shading (Roberts & Paul, 2006), i.e. they are related to the rate of C supply. As growth also increases under elevated CO_2 and declines with shading, there is no direct evidence that supports a trade-off between use of limited C to construct plant structural tissues versus SM. Hence, experiments that manipulate carbon availability to varying degrees including low availability are needed to determine whether there is a trade-off between growth and SM.

Jasmonic acid (JA) and salicylic acid (SA) (Khan *et al.*, 2015) are the main phytohormones controlling SM biosynthesis. For example, JA has been shown to induce production of phenolic acids (Kim *et al.*, 2007), flavonoids (Gundlach *et al.*, 1992), putrescine (Horbowicz *et al.*, 2011), benzoxazinoid derivatives (Oikawa *et al.*, 2002) and monoterpenes (Martin *et al.*, 2002). Exogenous application of SA can also enhance concentrations of glucosinolates (Kiddle *et al.*, 1994) and anthocyanins (Godoy-Hernández & Loyola-Vargas, 1997). In addition, changes in JA and SA have been associated with SM regulation in response to drought and salinity (Herrera-Vásquez *et al.*, 2015; Riemann *et al.*, 2015). Recent studies also showed that elevated CO_2 can enhance SA-dependent defense but repress JA-dependent defense (Zavala *et al.*, 2013; Sun *et al.*, 2016). How JA and SA may regulate SM production at low carbon availability remains unknown.

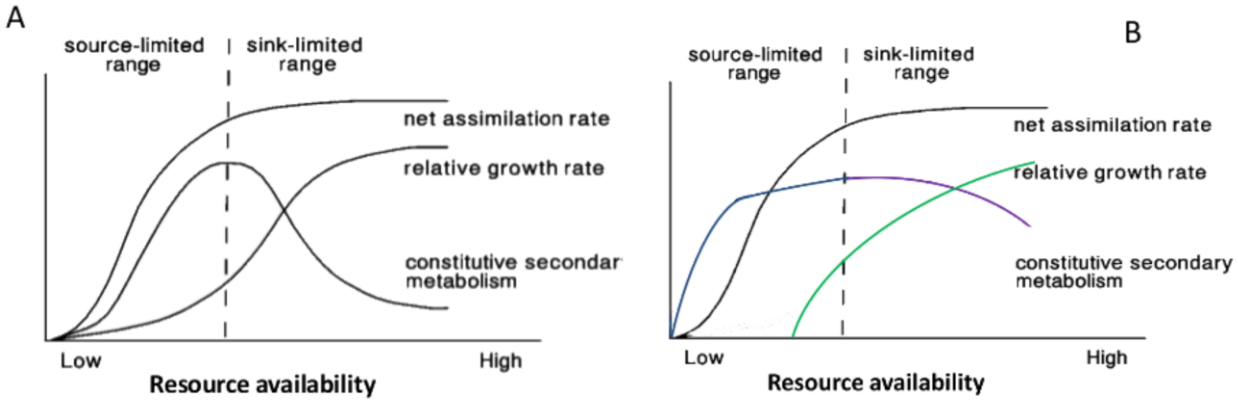

Figure 1.3 Schematic representations of secondary metabolites (SM) dynamics along a gradient of resource availability. A): patterns of SM predicted by the growth-differentiation balance hypothesis. Reducing resource availability from high to moderate levels decreases growth

more than net assimilation, thereby increasing the availability of carbon for SM production (taken from Herms and Mattson (1992)); reducing resource availability from moderate to low levels decreases SM faster than growth as growth receives a higher allocation priority of limited carbon. B): In source-limited plants, allocation to SM (blue line) maybe prioritized over growth (green line) in order to enhance future survival.

1.1.5 Regulation of BVOC

Biologically produced volatile organic compounds, BVOC, are one subset of secondary metabolites that have been specifically studied because their volatility means they are emitted from plants to the atmosphere. These compounds play a variety of roles for the plant, though they are not fully understood – e.g. scavenging harmful reactive oxygen species, communicating with symbiotic organisms and attracting pollinators. Once in the atmosphere, BVOC play important roles in atmospheric chemistry and climate by altering the oxidative capacity of the atmosphere (Di Carlo *et al.*, 2004; Lelieveld *et al.*, 2008; Nölscher *et al.*, 2013), ozone production in the presence of NO and NO_2 (Monks *et al.*, 2015), and the formation of secondary organic aerosols (Hallquist *et al.*, 2009). Globally, plants are the largest source of BVOC to the atmosphere, representing up to ~90% of total global emissions (Guenther *et al.*, 1995), with isoprenoids (isoprene, mono- and sesquiterpenes) and oxygenated VOC (i.e. methanol and acetone) being the most abundant BVOC emitted into the atmosphere (Sindelarova *et al.*, 2014; Messina *et al.*, 2016).

It is well known that BVOC emissions are largely dependent on temperature and light, and isoprene emission rates decrease with increasing atmospheric CO_2 (Sharkey & Monson, 2014). However, we know little about how changes in carbon availability may influence emissions of other important BVOC including mono- and sesquiterpenes as well as oxygenated BVOC. Under elevated CO_2 monoterpene emissions remain constant or may even increase (reviewed in Penuelas & Staudt, 2010), and the response of methanol and acetone emissions vary with seasons, organ types and species (Kreuzwieser *et al.*, 2002; Velikova *et al.*, 2009). It remains unknown that how emissions of these BVOC may be influenced by low CO_2 and resulting low carbon availability.

1.1.6 Other compounds involved in plant C balance

Plants export large amounts of carbon to symbiotic partners (i.e. mycorrhizae and Rhizobia) in exchange for nutrients, and directly exude carbon into the rhizosphere. Although the quantification of exudation usually is limited to short-term observations, 5–20% of gross production may be allocated to arbuscular mycorrhizal fungal (Johnson *et al.*, 2002; Grimoldi *et al.*, 2006) while the magnitude of root exudation was highly variable, ranging from 0.27 to 10 % (Farrar *et al.*, 2003; Johansson *et al.*, 2009; Phillips *et al.*, 2009). Because of the technical limitations in measuring exudation fluxes I could not address these in my study.

Plants export large amounts of carbon compounds to symbiotic partners (i.e. microbial partners such as mycorrhizae and rhizobia) in exchange for nutrients, and directly exude carbon into the rhizosphere. Although the quantification of exudation usually is limited to short-term observations, 5–20% of gross production may be allocated to arbuscular mycorrhizal fungi (Johnson *et al.*, 2002; Grimoldi *et al.*, 2006). The magnitude of root exudation can also be highly variable, ranging from 0.27 to 10 % of gross production (Farrar *et al.*, 2003; Johansson *et al.*, 2009; Phillips *et al.*, 2009). Plants also directly or indirectly provide sugars to insect symbionts in exchange for defense. Because of the technical limitations in measuring exudation fluxes I could not address these functions in my study, though they can clearly be important sinks for plant C.

1.2 Allocation to different organs and during development

1.2.1 Organ types

Different plant organs play distinct roles in carbon allocation. For example, leaves assimilate carbon from the atmosphere which is then exported to roots in exchange for nutrients and water. To optimize resource acquisition, plants are assumed to invest carbon preferentially into organs that are responsible for acquiring the most limiting resource, as suggested by functional equilibrium hypothesis (Poorter *et al.*, 2012). Accordingly a meta-analyses showed that plants growing under carbon limitation induced by low light and/or low CO_2, generally increase allocation of biomass to leaves but decrease allocation to roots (Poorter *et al.*, 2012). In addition to biomass, responses of NSC and SM pools to changing resource availability may also

vary among organ types, given that organs that are of greater value to plants may be well supplied with resources while being better protected from stresses. Recent studies showed that drought increased NSC concentrations in roots but not in aboveground organs in *Pinus radiata* (Mitchell *et al.*, 2013), *Quercus alba* and *Liriodendron tulipifera* (Kannenberg *et al.*, 2017) likely to maintain osmotic potential in roots. The opposite pattern, i.e. decreases in NSC pools in roots during drought, were observed in *Picea abies* (Hartmann *et al.*, 2013b) and two *Eucalyptus* species (Mitchell *et al.*, 2013) likely due to impeded phloem transport. These observations highlight the need to investigate organ-specific allocation patterns in response to changing resource availability.

1.2.2 Organ ontogeny

Organ ontogeny may also influence carbon allocation patterns by altering source-sink relationships. During advanced leaf ontogeny, when carbon supply via photosynthesis increases (Miyazawa & Terashima, 2001; Pantin *et al.*, 2012), carbon from external sources required for growth (Pantin *et al.*, 2012), respiration (Armstrong *et al.*, 2006), NSC storage (Hoch *et al.*, 2003) and SM production (Barton & Koricheva, 2010) decrease. As a result, allocation trade-offs may be less constrained as organs develops. Studies have shown that leaves of dicots may experience sink-to-source transitions when leaves reach 30−60% of their final size (Pantin *et al.*, 2012). Carbon allocation trade-offs therefore mainly occur in young leaves and largely depend on carbon transported from mature source leaves. Hence, organ ontogeny needs to be taken into consideration when studying carbon allocation patterns in response to changing carbon availability.

1.2.3 Plant species

Plants with contrasting life-history strategies may also differ in carbon allocation strategies. Trees experience the asynchrony of carbon supply and demand not only on diurnal and seasonal scales which are also experienced by annual herbaceous plants, but also on interannual scales with asynchronies that can span years to decades (Dietze *et al.*, 2014). Annual herbaceous plants die at the end of the growing or fruiting season; hence allocation to NSC storage and SM in the absence of stress would reduce both growth and final reproductive

success in these plants. By contrast, the long lifespan of trees increases the risk to encounter periods of abiotic (i.e. drought, heat waves and cold) or biotic stresses (i.e. insect attack and pathogen infestation) and a conservative allocation strategy that prioritize NSC and SM at the expense of growth and respiration may therefore ensure long-term survival (Sala *et al.*, 2012; Becklin *et al.*, 2014), particularly in those evergreen tree species that organs have long lifespan. In this thesis, we explored two different plant types: wheat (an annual) and spruce trees.

1.3 Carbon dioxide

Atmospheric CO_2 concentrations have risen from about 170–200 ppm during glacial periods to the current 400 ppm, and are predicted to reach between 430 and 1000 ppm by 2100 (Cubasch *et al.*, 2013). Understanding the mechanisms by which increasing CO_2 have influenced plant carbon allocation in the past will help to unravel mechanisms regulating plant carbon allocation to future elevated CO_2 but also to changing carbon availability as may occur during shading, cold or drought. For example, at high CO_2, i.e. when carbon availability is not limiting for growth, other factors like nutrients (Lewis *et al.*, 2010; Reich *et al.*, 2014) or water availability may reduce growth sink strength for carbon (Reich *et al.*, 2014; Faralli *et al.*, 2017); by contrast, at low CO_2, photosynthesis and growth can both be strongly carbon-limited (Lewis *et al.*, 2010; Schmid *et al.*, 2017) as during glacial periods (Gerhart *et al.*, 2012). However, the influence of changing CO_2 on the trade-off between allocation to growth, storage and defence is uncertain.

To do so, we manipulated the whole-plant carbon balance under a gradient of CO_2 concentrations using a previously built greenhouse facility in Max-Planck Institute for Biogeochemistry (Hartmann *et al.*, 2013a). Ambient air from a compressor was passed through a molecular sieve to remove all CO_2 and most VOC. Pure CO_2 was then added to the CO_2-free air to achieve target concentrations. Wheat plants were grown at CO_2 concentrations of 170, 400 and 700 ppm to study effects of C supply on allocation in an annual plant. In a second study with spruce trees, we progressively induced C limitation by decreasing CO_2 from 400 ppm to 280 ppm (preindustrial) or 170 ppm (glacial) conditions (depending on the experiment) and then to 120 ppm or 50 ppm CO_2 (to induce negative plant C balance). In the spruce treatments,

CO_2 re-added to the CO_2-free air had a $\delta^{13}C$ of -38‰ and thus introduced continuously labeled C to be traced through plant metabolism. To achieve a thorough understanding of plant carbon allocation, we assessed all aspects of carbon cycle, including fluxes (net C assimilation and net C lost through respiration and as BVOC), biomass growth and partitioning (total biomass, NSC and SM) as well as the phytohormones (IAA, ABA, JA and SA) at the whole-plant level (leaves, stems and roots).

Twelve aquarium-style glass chambers (80 cm high × 75 cm long × 45 cm wide) were attached to the CO_2 manipulation system to isolate the atmosphere around the plants. To avoid BVOC adsorption to chamber walls, we built four cylindrical chambers (height=70 cm, diameter=70 cm, volume=270 L) covered with Teflon foil. BVOC emissions were continuously monitored using proton transfer reaction mass spectrometry (PTR-MS).

1.4 Objectives

My overall objective was to improve our understanding of allocation trade-offs and the underlying control mechanisms, in both herbaceous plants (winter wheat, *Triticum aestivum*) and trees (Norway spruce, *Picea abies* L.).

More specifically, I aim to (1) uncover the carbon allocation tradeoffs between functional carbon sinks in wheat plants, and (2) explore whether and to what extent changes in phytohormones are associated with these allocation patterns; (3) assess allocation tradeoffs in spruce trees using continuous isotope labelling to trace the fate of newly-assimilated C in small spruce trees and (4) report in detail how changes in CO_2 may influence BVOC emissions in spruce trees (Fig 1.4).

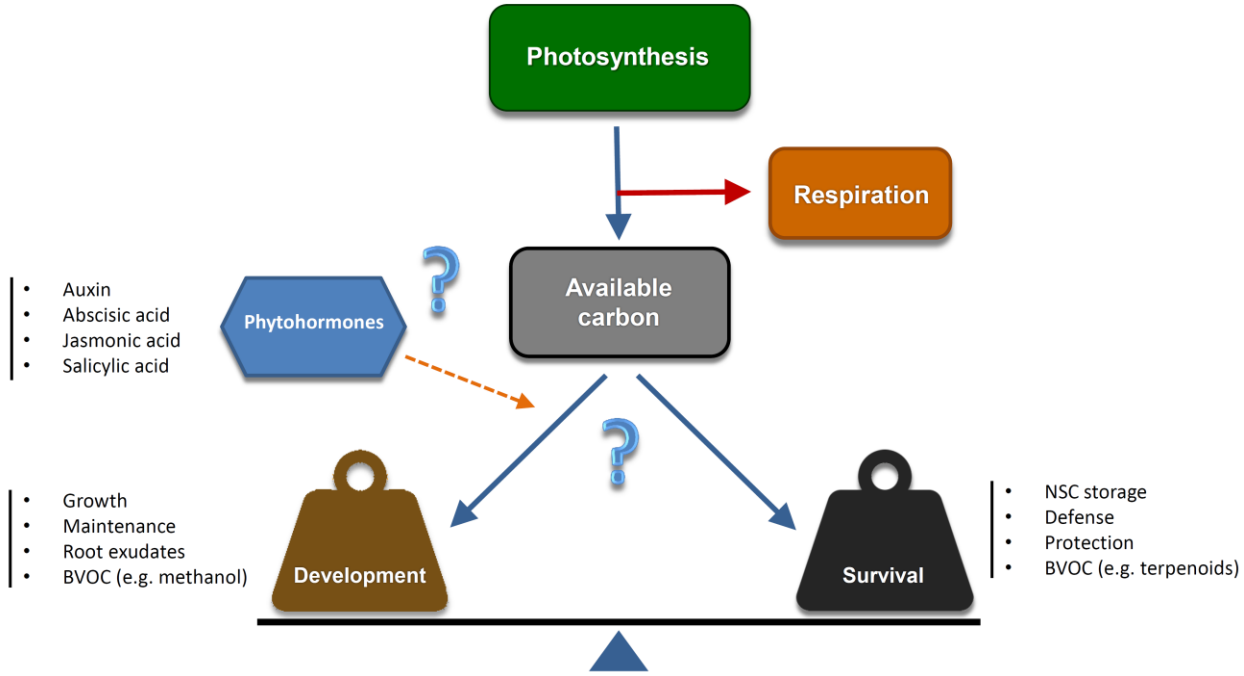

Figure 1.4 Schematic representation of allocation trade-offs between development (e.g. growth) and survival (NSC and defense) and the underlying phytohormonal regulation.

1.5 Thesis structure

The thesis comprises in total six chapters. Chapter 1 (this chapter) briefly introduces the background of carbon allocation, and indicates the main research frontiers involved in each functional carbon sink. In chapter 2 and 3, I quantify the percentage of net carbon assimilation allocated to respiration, growth, NSC and SM along a gradient of CO_2 (170, 400 and 700 ppm) in wheat plants and assess the relationship between phytohormones and allocation patterns. Chapter 4 further investigates allocation patterns in spruce trees exposed to a gradient of CO_2 (400, 280, 170, 120 and 50 ppm) and traces the fate of newly-assimilated carbon using continuous isotope labelling. In chapter 5, we report on-line measurements of BVOC emissions from whole-aboveground of Norway spruce exposed to a gradient of CO_2 (400, 180 and 50 ppm) over three weeks, followed by reverting the lower CO_2 treatments back up to 400 ppm. In chapter 6, we summarize the results and discussed the main findings, remaining open questions and future directions.

CHAPTER 2

Plant, Cell & Environment

Plant, Cell and Environment (2017) **40**, 672–685 doi: 10.1111/pce.12885

Original Article

Release of resource constraints allows greater carbon allocation to secondary metabolites and storage in winter wheat

Jianbei Huang[1], Almuth Hammerbacher[2,3], Lenka Forkelová[1] & Henrik Hartmann[1]

[1]*Max Planck Institute for Biogeochemistry, Hans-Knöll-Str. 10, 07745 Jena, Germany,* [2]*Max Planck Institute for Chemical Ecology, Hans-Knöll-Str. 8, 07745 Jena, Germany and* [3]*Department of Microbiology and Plant Pathology, Forestry and Agricultural Biotechnology Institute, University of Pretoria, Private Bag X20, Pretoria 0028, South Africa*

ABSTRACT

The atmospheric CO_2 concentration ($[CO_2]$) is rapidly increasing, and this may have substantial impact on how plants allocate metabolic resources. A thorough understanding of allocation priorities can be achieved by modifying $[CO_2]$ over a large gradient, including low $[CO_2]$, thereby altering plant carbon (C) availability. Such information is of critical importance for understanding plant responses to global environmental change. We quantified the percentage of daytime whole-plant net assimilation (A) allocated to night-time respiration (R), structural growth (SG), nonstructural carbohydrates (NSC) and secondary metabolites (SMs) during 8 weeks of vegetative growth in winter wheat (*Triticum aestivum*) growing at low, ambient and elevated $[CO_2]$ (170, 390 and 680 ppm). R/A remained relatively constant over a large gradient of $[CO_2]$. However, with increasing C availability, the fraction of assimilation allocated to biomass (SG + NSC + SMs), in particular NSC and SMs, increased. At low $[CO_2]$, biomass and NSC increased in leaves but decreased in stems and roots, which may help plants achieve a functional equilibrium, that is, overcome the most severe resource limitation. These results reveal that increasing C availability from rising $[CO_2]$ releases allocation constraints, thereby allowing greater investment into long-term survival in the form of NSC and SMs.

Key-words: carbon allocation; CO_2; growth; respiration; storage carbohydrates.

INTRODUCTION

For more than 40 years, the control mechanisms of whole-plant carbon (C) allocation have been of central interest to plant scientists (Mooney, 1972). Plants fix CO_2 from the atmosphere and partition the resulting photosynthetic products (carbohydrates) among several uses, including growth of structural biomass, synthesis of secondary metabolites and metabolic processes like respiration and osmoregulation. The atmospheric CO_2 concentration ($[CO_2]$) has increased from 170 ppm during glacial periods of the past million years to the current ~400 ppm and is expected to increase up to 430 ppm to 1000 ppm by the year 2100 (Cubasch *et al.*, 2013). However, little is known about how increased $[CO_2]$ alters partitioning of fixed C among different sinks or about the processes regulating allocation (Dietze *et al.*, 2014).

Historically, the regulation of plant C partitioning was thought to be driven by C supply (i.e. source activity), but recent evidence suggests that sink activity may be the main determinant (Fatichi *et al.*, 2014; Korner, 2015). Experiments manipulating source activity via $[CO_2]$ availability can elucidate the contributions of sources and sinks for whole-plant C allocation (Fatichi *et al.*, 2014). However, such studies are still sparse, not only because of the expense of manipulating $[CO_2]$ (Gerhart & Ward, 2010), but also because of challenges in assessing both whole-plant C balance (assimilation minus respiration; A – R) and how non-respired C is distributed among sink components, that is, structural growth (SG), nonstructural carbohydrates (NSC), secondary metabolites (SMs) and export (e.g. to rhizosphere symbionts or as volatile organic compounds (VOCs)) (Fig. 1).

In many plant species, short-term stimulation of leaf-level photosynthesis by elevated $[CO_2]$ (Franks *et al.*, 2013; Gerhart & Ward, 2010) is often associated with down-regulation of photosynthesis in the long term (Lee *et al.*, 2011; Long *et al.*, 2004). However, leaf-level net photosynthetic rates cannot be directly scaled up to whole-plant assimilation for a number of reasons. For example, leaf-level assimilation measurements are usually done under ideal light and temperature conditions (Kirschbaum, 2011) and therefore may overestimate actual assimilation rates. Scaling up from leaf to whole-plant gas exchange also requires parameterization of leaf phenology and light distribution. In addition, photosynthesis in non-leaf tissues (bark, stems) may not scale in the same way as in leaves. Therefore, direct whole-plant assessment of gas exchange is a more suitable method for determining whole-plant responses to different $[CO_2]$ (Atkin *et al.*, 2007; Boote *et al.*, 2013).

Respiration (R) is an essential plant functional process providing energy and metabolic intermediates needed for photosynthesis, which in turn provides substrates for R. Some studies have reported that whole-plant R may account for up to 30–50% of the gross photosynthetic CO_2 uptake in herbaceous plants, and due to the interdependency of these processes this proportion remains relatively constant under a gradient of

Correspondence: J. Huang. E-mail: hjianbei@bgc-jena.mpg.de

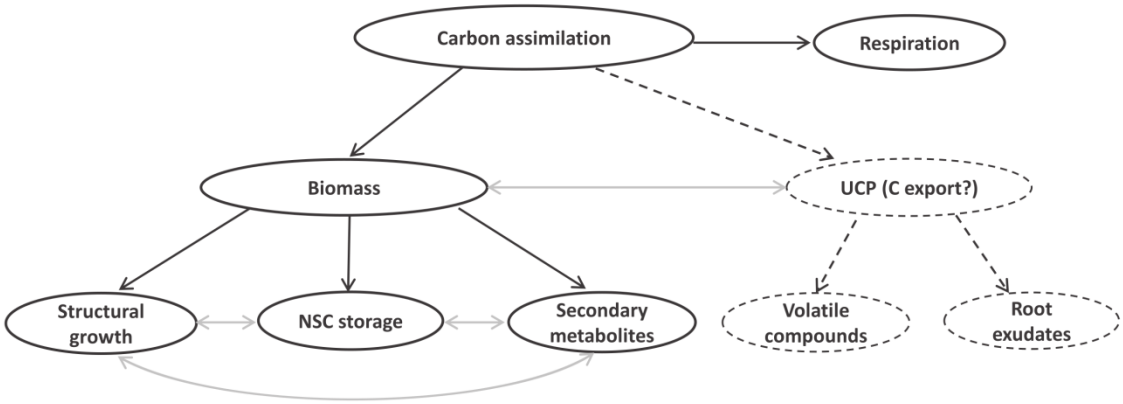

Figure 1. Conceptual model for trade-offs in carbon allocation to functional pools respiration, biomass (structural growth + non-structural carbohydrates (NSC) + secondary metabolites) and an – operationally defined – unaccounted carbon pool (UCP, potentially export to volatile compounds and root exudates). Black solid arrows indicate established (based on literature) carbon flow between pools, while black dashed arrows indicate flows that remain uncertain mainly due to technical difficulties in measuring them. Such flows require further investigation (see Discussion and Outlook sections). Grey solid arrows indicate trade-off situation between different carbon pools, as suggested by growth-defence hypotheses and different carbon storage paradigms.

environmental conditions (Atkin *et al.*, 2007; Gifford, 1995; Pons & Poorter, 2014). In our study, we measured net C assimilation; during the day-time, this is the difference between A and R; at night, as there is no assimilation it represents only R.

Species adapted to low resource availability have intrinsically lower growth rates than species adapted to high resource availability (Endara & Coley, 2011). Therefore, modern plants adapted to current [CO_2] may not be able to utilize higher [CO_2] assimilation for growth (Tissue & Lewis, 2012). Under elevated [CO_2], growth may also be constrained by environment factors such as water and nutrients (Kirschbaum, 2011; Palacio *et al.*, 2014). A 30–40% increase in leaf-level photosynthesis leads only to a 10% increase in relative growth rate (reviewed in Kirschbaum, 2011). By contrast, plants grown at low [CO_2] may fully utilize all assimilated C for growth while concurrently reduce C loss to exports, particularly in the form of VOCs and rhizodeposits, at least when nutrients are provided and freely accessible (Fig. 1).

Plants maintain large pools of NSC compounds that can enhance plant survival during stresses (Dietze *et al.*, 2014; Hartmann & Trumbore, 2016), and strategies of C allocation to NSC pools have been discussed for more than 25 years (Chapin *et al.*, 1990). NSC pools have often been considered as reservoirs filled with C that is available in excess of demand (accumulation of NSC) (Palacio *et al.*, 2014). However, an alternate model suggests that plants allocate C to NSC to ensure future C availability even at the expense of other C sinks such as SG (reviewed in Dietze *et al.*, 2014; Wiley & Helliker, 2012). Recent studies provide evidence of C allocation to NSC storage even in half defoliated *Quercus velutina* saplings (Wiley *et al.*, 2013) and in *Picea abies* saplings grown under low [CO_2] (Hartmann *et al.*, 2015).

Plants may allocate a substantial proportion of available C to SMs that play important roles in biotic and abiotic interactions (Neilson *et al.*, 2013). For example, glucosinolates are one of the major classes of defensive SMs (Halkier & Gershenzon, 2006), and up to 15% of total photosynthetic energy may be required for glucosinolate production in *Arabidopsis thaliana* (Bekaert *et al.*, 2012). This large C investment, however, may divert resources away from other metabolic processes. The growth-differentiation balance hypothesis (GDBH) (Herms & Mattson, 1992) suggests that allocation to SMs is driven by C availability in excess of growth demand. Under ideal conditions, this trade-off may be less constrained, and plants can grow larger leaf canopies with higher SM production than under resource limitation. In support of this hypothesis, C-based SMs increased under elevated [CO_2] (Robinson *et al.*, 2012), while O'Neill *et al.* (2010) found that only quercetin triglycoside increased but genistein decreased in soybean (*Glycine max*) foliage.

Trade-off situations in allocation occur not only across functional sinks but also across plant tissues and organs. Plants are thought to invest C preferentially into tissues that are responsible for acquiring the most limiting resource; this is termed 'functional equilibrium'. Such an optimal allocation strategy has been observed in biomass partitioning under low [CO_2] where plants allocated proportionally more C to above-ground than to belowground tissues (Poorter *et al.*, 2012; Temme *et al.*, 2013; Zhang *et al.*, 2015), but data on the partitioning to different functional sinks, like NSC (Hartmann *et al.*, 2015) and SMs, and across different plant tissues and organs are still very sparse.

The objective of this study was to investigate C allocation tradeoffs in winter wheat (*Triticum aestivum* L.) during the vegetative growth phase. Previous studies have shown that elevated [CO_2] will cause photosynthetic acclimation of wheat plants (Aranjuelo *et al.*, 2011; Aranjuelo *et al.*, 2015), but much less is known about allocation priorities across functional sinks under these conditions. Such priorities can be deduced from assessments of allocation patterns along a plant C availability gradient, including low [CO_2] (Hartmann *et al.*, 2015). Although shading may be a much simpler

approach for reducing plant C availability, it may also trigger phytochrome-induced growth stimulation (Casal, 2013) and defence suppression (Ballare, 2014), independent of C availability. Direct manipulations of atmospheric [CO_2] suffer less from such side effects and allow plants to adjust to C (rather than light) availability.

Because allocation is a continuous process, the whole-plant fluxes (A – R derived from gas exchange) and pools were monitored over the vegetative growth phase using a unique chamber design implemented in a greenhouse. Supplemental nutrients were applied to the substrate in order to minimize nutrient limitations on plants. Allocation to reproduction (seed production) was purposely excluded in this study because pollination has been shown to be problematic and incomplete in these growth chambers, likely due to light limitation. Changes in primary (NSC, including soluble sugars, starch and fructans) and SMs (including flavonoid glycosides and benzoxazinoids) of plant tissues (leaves, stems and roots) were used to partition biomass into SG (SG = Biomass – NSC – SMs) and nonstructural components (NSC and SMs). Specifically, we hypothesized that, with increasing [CO_2] (170, 390 and 680 ppm): (1) the proportion of C allocated to R remains constant but decreases in biomass (SG + NSC + SMs) (relative to A); (2) NSC and SMs increase while SG decreases; and (3) biomass (SG + NSC + SMs) increases in stems and roots but decreases in leaves, in accordance with the functional equilibrium hypothesis.

MATERIALS AND METHODS

Plant material

A cultivar of winter wheat from a local seed plantation (Bioland Hof Jeebel Biogartenversand, Salzwedel, Germany) adapted to Central Europe was used in our study. On 7 January 2015, seeds were germinated in plates filled with sand and were watered every day. On 13 and 14 January 2015, seedlings of similar height were transplanted into pots (diameter 11 cm, height 24 cm) filled with C-free quartz sand. Four pots (12 seedlings per pot) and two pots (10 seedlings per pot) were randomly placed in each plant chamber immediately after transplanting (Fig. 2). We provided the plants with supplemental nutrients by watering pots with a continuous through-flow of a modified Hoagland nutrient solution (Hoagland & Arnon, 1950) to avoid nutrient limitation (other than C).

Growth chambers

Twelve aquarium-style glass chambers (80 cm high × 75 cm long × 45 cm wide) were used to isolate the atmosphere around the plants and allowed controlling [CO_2] (Fig. 2). Chambers were placed on a greenhouse table covered with closed-cell rubber foam mats made of ethylene propylene diene monomer for airtight sealing (as in Hartmann *et al.* (2013)). Air in the chambers was flushed continuously at a flow rate of 14 l min^{-1} through inlet tubing located at the bottom and outlet tubing at the top of the chamber. The [CO_2] of incoming air was controlled by first scrubbing all CO_2 from atmospheric air using a molecular sieve and then adding pure CO_2 from a gas tank (Schnyder, 1992). The CO_2-free air was separated into three air circuits (four chambers per circuit); in each circuit, [CO_2] was measured sequentially with a Vaisala® (*GMP 343*) at intervals of 10 min, using a custom-built switching valve controlled by a micro-logger (Campbell® CR1000). Measured [CO_2] were compared against pre-set values (170, 390 and 680 ppm, respectively), and, if required, CO_2 supply to the airstream was adjusted via mass flow controllers to maintain target [CO_2] levels. To minimize differences in light levels, treatments were randomly assigned on the table, and three of four chambers per treatment were used to grow plants while the other one was used to monitor [CO_2] directly in the chamber.

In each chamber, air temperature and photosynthetic photon flux density were monitored continuously (see Hartmann *et al.*, 2013). During the day, average temperatures increased

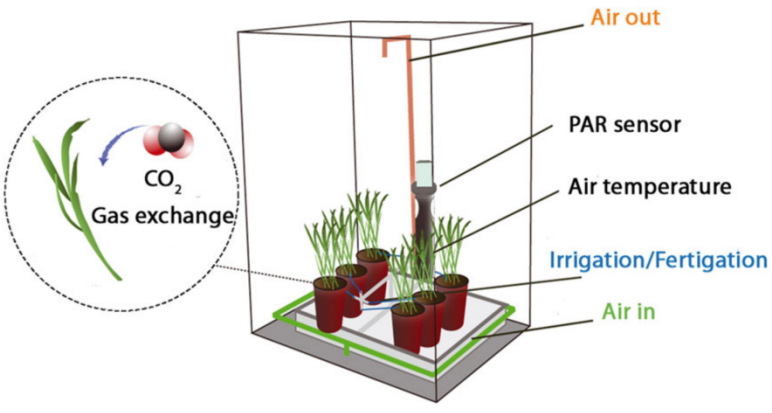

Figure 2. Schematic view of one of the 12 chambers showing the ventilation system and the photosynthetically active radiation (PAR) sensor. Air was flushed continuously through inlet tubing located at the bottom and outlet tubing at the top of the chamber. Four pots (12 seedlings per pot) and two pots (10 seedlings per pot) were randomly placed in each plant chamber. Note that only pots containing 12 seedlings were harvested. Supplemental nutrients were provided by watering the pots with a continuous through-flow of a modified Hoagland nutrient solution.

from ca. 12 °C at 6:30 (local time) to ca. 20–24 °C in the afternoon, and then decreased to ca. 16.5 °C at 22:00. During the night, air temperature declined from ca. 16 to 11 °C. All plants were grown in a 16/8 h light/dark regime using supplemental greenhouse lamps (Son-T Agro® 430 W HPS bulbs, primary light range = 520–610 nm, Philips® Lighting Co., Somerset, NJ, USA). The average daily total photosynthetic photon flux density inside the chambers from 23 January to 20 March was 7.79 ± 0.92 mol m^{-2} d^{-1}.

Destructive harvesting and biomass processing

Allocation priorities likely differ between growth stages of winter wheat (seedling, tillering, stem elongation, flowering and grain filling), and we concentrated on the vegetative growth period (seedling and tillering stage) to rule out the potential confounding effects of developmental stage on plant allocation. According to the growth scale of Zadoks *et al.* (1974), seedling growth of winter wheat is achieved before the occurrence of nine unfolded leaves on the main shoot. Plants were therefore harvested when three, six and eight leaf sheaths were completely developed, denoted as 3 L, 6 L and 8 L periods, respectively. For 390 and 680 ppm treatments, this occurred 3, 7 and 9 weeks after transplanting, respectively, while development in the low [CO_2] treatment was slower, and plants were sampled 3.5, 8 and 10.5 weeks after transplanting. Sampling was always conducted between 16:00 and 21:00. At each sampling, three pots (12 seedlings per pot) from three chambers of each [CO_2] treatment were destructively harvested. Fresh biomass of whole-plant leaves, stems and roots of each pot were determined, and then all tissues were shock-frozen in liquid nitrogen and stored at −80 °C, freeze-dried and weighted for dry biomass. Dry tissues were homogenized and ground to fine powder using a ball mill (Retsch® MM400, Haan, Germany) and stored at −20 °C until analysis.

Whole-plant gas exchange

Gas exchange data were measured with a Picarro® 2101-i (precision 0.01–0.4%, Picarro Inc. Santa Clara, CA, USA) for the first 7 weeks (extending beyond the 6 L period) under 680, 390 and 170 ppm [CO_2]. However, because the Picarro failed after week 7, gas exchange for week 8, 9, 10 and 11 were measured with a Spectronus® FTIR (Fourier transform infrared spectroscopy, Ecotech Pty Ltd., Knoxfield, VIC, Australia) using otherwise the same hardware and the same sequence protocol as mentioned above. Reference gases were used to verify and ensure comparability across devices.

Within 2 h, the [CO_2] of air leaving the 12 chambers and 6 reference air samples (taken from the air circuit) were measured sequentially at intervals of 6 min 40 s, and the sequence was controlled by a micro-logger (Campbell® CR1000) and a custom-built switching valve unit. Transition periods after valve switching were excluded from analysis, and a core period of 3 min 20 s was used to estimate instantaneous whole-plant gas exchange, defined as:

$$\Delta[CO_2] = \frac{[CO_2]_{\text{non-plant}} - [CO_2]_{\text{plant}}}{M} \quad (1)$$

where $[CO_2]_{\text{non-plant}}$ is the [CO_2] of outgoing air from the chamber without plants, and $[CO_2]_{\text{plant}}$ is the [CO_2] of outgoing air from chambers with plants. M is the number of plants grown in the chamber.

The whole-plant gas exchange rate was assumed to be constant within the 2 h cycle and whole-plant C flux at hour j was calculated as:

$$C_j\ (\text{g h}^{-1}) = \frac{\Delta[CO_2](\ \mu\text{mol mol}^{-1}) * \text{VFR}\ (\text{l min}^{-1}) * 60\ \text{min} * 12\ (\text{g mol}^{-1})}{22.4\ (\text{l mol}^{-1}) * 1000000} \quad (2)$$

where VFR is the volumetric flow rates of air going through the chambers, that is, 14 l min^{-1}, and 22.4 l mol^{-1} is the molar volume of gas at normal conditions. The cumulative daily whole-plant net C assimilation (A_{cum_n}) and night-time respiration (R_{cum_n}) over the duration of the experiment (n = number of days d, j = hour of day) were then computed using the following equation:

$$A_{cum\_n} = \sum_{i=1}^{n} \sum_{j=7}^{22} C_j \quad (3)$$

$$R_{cum\_n} = \sum_{i=1}^{n} \sum_{j=23}^{24} C_j + \sum_{i=1}^{n} \sum_{j=1}^{06} C_j. \quad (4)$$

A_{cum_n} and R_{cum_n} between 3 L and 6 L were used to calculate the fraction of C allocated to R. Whole-plant A and R collected over the last two or three days prior to biomass sampling were averaged for calculations of mass-based (i.e. specific) rates of daily net assimilation and respiration.

While C-free quartz sand was used to avoid any C input into the system other than from plant photosynthesis, it was technically impossible to sterilize the all components of such a greenhouse facility (air, water, plant material) to a degree that would completely avoid microbial infestation. Hence, microbial respiration of root exudates or litter may be included in the gas exchange measurements. However, given that root exudation (Grayston *et al.*, 1997; Phillips *et al.*, 2009) represents a much smaller C flux than respiration (<10% versus 30–50%) (Atkin *et al.*, 2007; Gifford, 1995; Pons & Poorter, 2014), gas exchange data represent mainly plant assimilation and respiration (Hartmann *et al.*, 2015; Hartmann *et al.*, 2013).

NSC analysis

Concentrations of soluble sugars and starch in plant tissues were determined using methods described in Raessler *et al.* (2010). For soluble sugars, usually 1 ml (or 0.5 ml for small samples) of sterilized water was added to 50 mg (or 10 mg for small samples) dry biomass. The mixture was vortexed, incubated at 65 °C for 10 min and then centrifuged at 12 000 *g* for 10 min. The supernatant was collected and stored on ice, and the remaining pellet was re-extracted twice using the same procedure. The supernatants were pooled and then diluted at a ratio of 1:20 (or 1:8 for small samples) and stored at −20 °C. For starch, 50 mg (or 10 mg for small samples) dry biomass

were extracted with 0.35 ml (or 0.175 ml for small samples) of water and 0.5 ml (or 0.25 ml for small samples) of perchloric acid (52%). The mixture was vortexed, incubated at 65 °C for 10 min and then centrifuged at 12 000 *g* for 10 min. The supernatant was collected, and the remaining pellet was re-extracted. The supernatants were pooled and then diluted at a ratio of 1:55, stored at −20 °C.

Sucrose, glucose and fructose of both soluble sugars and starch extractions were determined by High-Performance Liquid Chromatography coupled with Pulsed Amperometric Detection (HPLC-PAD), using a Dionex® ICS 3000 ion chromatography system equipped with an autosampler (Thermo Fisher GmbH, Idstein, Germany). Starch concentrations were calculated by subtracting glucose and half of the sucrose concentrations in water-soluble extract from glucose concentrations in the hydrolyzed extract then multiplying a conversion factor of 0.9 (Sullivan, 1935). Fructan concentrations were calculated using the same method but with fructose instead of glucose concentrations, given that fructan is one of the most important C storage compounds in wheat (Pollock & Cairns, 1991). Total NSC concentrations reported are the sum of soluble sugars, starch and fructans.

SM analysis

Samples from 680 ppm at 8 L were used for the identification of major SMs in leaf, stem and root tissues; 800 μl methanol and two glass beads were added to 30 mg of dry biomass. The mixture was bead-beaten for 40 s at 6.0 m s^{-1} with a FastPrep Instrument (MP Biomedicals, Santa Ana, USA), then vortexed and centrifuged at 13 000 *g* for 5 min. The supernatant was collected and then analysed by HPLC coupled to a mass spectrometer. Compounds were separated on a Nucleodur Sphinx RP18ec column with dimensions of 250 × 4.6 mm and a particle size of 5 μm (Macherey Nagel, Dueren, Germany) using an Agilent 1100 series HPLC with a flow rate of 1.0 ml min^{-1}. The column temperature was maintained at 20 °C. Phenolic compounds were separated using 0.2% (v/v) formic acid and acetonitrile as mobile phases A and B, respectively, with the following elution profile: 0–28 min, 5–61% B in A; 28–30 min 100% B; and 30–35 min 5% B.

Compound detection and quantification were accomplished with an Esquire 6000 ESI ion-trap mass spectrometer (Bruker Daltronics, Bremen, Germany). Flow coming from the column was diverted in a ratio of 4:1 before entering the mass spectrometer electrospray chamber. ESI-MS was operated in negative mode scanning $m\ z^{-1}$ between 50 and 1600 with an optimal target mass of 400 $m\ z^{-1}$. The mass spectrometer was operated using the following specifications: skimmer voltage, 60 V; capillary voltage, 4200 V; nebulizer pressure, 35 psi; drying gas, 11 l min^{-1}; gas temperature, 330 °C. Capillary exit potential was kept at −121 V. Compounds of leaves and stems were identified by comparing the fragmentation patterns with previously reported wheat phenolic profiles (Moheb *et al.*, 2011; Wojakowska *et al.*, 2013). Root compounds were identified based on profiles of benzoxazinoids in grasses (Wouters *et al.*, 2014).

For quantification, 500 (300) μl 95% methanol and two glass beads were added into 50 (30) mg samples, the mixture extracted using the same procedure described above but the remaining pellet was re-extracted again. Supernatants were pooled and then analysed by HPLC-UV using the same chromatographic conditions as above. The UV wavelengths 240, 260, 280 and 330 nm were monitored. All compounds were quantified using external standard curves. Feruoylputrescine (HPC Standards GmbH, Cunnersdorf, Germany) was used to quantify ferulic acid-based compounds in leaves and stems, and also putrescine-containing compounds in roots. Luteolin 6-C-glucoside and apigenin 6-C-glucoside (Sigma-Aldrich) were used to quantify luteolin-based and apigenin-based compounds in leaves, respectively. Chrysoeriol (LGC standards, Middlesex, UK) was used to quantify chrysoeriol-based and tricin-based compounds in leaves. DIMBOA-Glc and HDMBOA-Glc in roots were quantified by standards DIMBOA-Glc and HDMBOA-Glc purified from maize roots (Wouters et al., 2014). Leaf and stem compounds were quantified at a UV absorption spectrum of 330 nm, and root compounds at 280 nm.

Elemental analysis

C and N concentrations of tissues were determined by an elemental analyser (varioEL II). To do so, 15 mg dry samples were weighed into tin foil, combusted and separated by specific columns, and then assessed with a thermal conductivity detector.

C balance

Tissue-specific C, NSC and SM content was calculated by multiplying tissue-specific C (Supporting Information Table S1), NSC and SM concentrations by tissue dry mass. C content in tissue-specific NSC and SM was then calculated by multiplying tissue-specific NSC and SM content by their mass proportion of C (0.4 for NSC and specific fraction to each compound for the different SMs (Supporting Information Table S2)). C allocation to biomass, NSC and SMs was defined as the difference in C content of whole-plant biomass, NSC and SMs between 6 L and 3 L divided by the difference in A_{cum_n} between 6 L and 3 L. Note that quantifying allocation to biomass requires relatively large increase in biomass; therefore, C allocation between 8 L and 6 L is not reported, given that average biomass increment of low [CO_2] plants was smaller than its standard deviation within and across chambers.

When net C gain estimated from gas exchange exceeded the C that accumulated in biomass, the difference was attributed to an 'unaccounted carbon pool' (UCP). UCP was calculated by mass balance using the following equation:

$$UCP = A_{cum\_n} - R_{cum\_n} - SG - NSC - SMs. \quad (5)$$

Data analysis

All of the data were analysed using Levene tests and Tukey's HSD tests that treated each growth chamber as a biological

replicate ($n = 3$), to check homogeneity of variances and detect significant differences between treatments, respectively. Data were log-transformed when variance was not homoscedastic. All statistical analysis was conducted in R, version 3.23 (R Development Core Team, 2014).

RESULTS

Whole-plant gas exchange and tissue biomass

Whole-plant daily assimilation, respiration and net carbon gain increased with increasing [CO_2], but the increase was much stronger at 170 ppm (compared to 390 ppm) than at 390 ppm (compared to 680 ppm) (Fig. 3a–c). However, after 9 weeks, plants grown at 390 and 680 ppm exhibited no significant difference in day-time assimilation (A), night-time respiration (R) and net carbon gain (A – R; Fig. 3a–c). Initially, R/A in plants grown at 170 and 390 ppm [CO_2] were higher than that in plants grown at 680 ppm [CO_2], but the difference was not statistically significant and disappeared over time (Fig. 3d). At 3 L, mass-based A increased with increasing [CO_2] (Fig. 4a). Mass-based R was higher at 390 and 680 ppm [CO_2] that at 170 ppm [CO_2], but there was no significant difference between the two higher [CO_2] treatments (Fig. 4b). Both mass-based A and R declined strongly over time at 390 and 680 ppm [CO_2] but much less at 170 ppm [CO_2] (Fig. 4a,b).

Biomass varied with [CO_2] in a way similar to whole-plant assimilation and respiration. At 3 L and 6 L, the dry mass of all tissues increased with increasing [CO_2], and the increase was much greater comparing plants grown between 170 and 390 ppm than between 390 and 680 ppm (Fig. 5a–d). However, at 8 L, there was no significant difference in all tissues between 390 and 680 ppm [CO_2] treatments (Fig. 5a–d).

NSC and SMs

The response of soluble sugars and total NSC (soluble sugars + starch + fructans) to [CO_2] differed between tissues and developmental stages. At 3 L, plant leaves grown at 170 ppm [CO_2] had slightly higher concentrations of soluble sugars and total NSC than plant leaves grown at 390 ppm [CO_2], but the opposite was observed in stems and roots (Fig. 6a–f). However, while the concentrations of soluble sugars and total NSC (soluble sugars + starch + fructans) remained relatively constant at 170 ppm [CO_2] between 3 L and 6 L, they doubled at 390 ppm [CO_2] and increased by more than three times at 680 ppm [CO_2] over the same period (Fig. 6a–f). Whole-plant NSC content increased in proportions that were much higher than increases in total plant biomass (Fig. 7). At 6 L, concentrations of soluble sugars and total NSC (soluble sugars + starch + fructans) were significantly higher at 680 ppm than at 390 ppm [CO_2] while the difference between 390 and 170 ppm [CO_2] was much smaller. Between 6 L and 8 L, the concentrations of soluble sugars and total NSC (soluble sugars+ starch + fructans) increased at 390 ppm [CO_2] but showed a declining trend at 680 ppm [CO_2] (Fig. 6a–f).

SM concentrations were much higher in leaves and roots than that in stems (Fig. 6g–i). Leaf SM concentrations significantly increased with increasing [CO_2] over all developmental stages (Fig. 6g). At 3 L, stem SM concentrations significantly

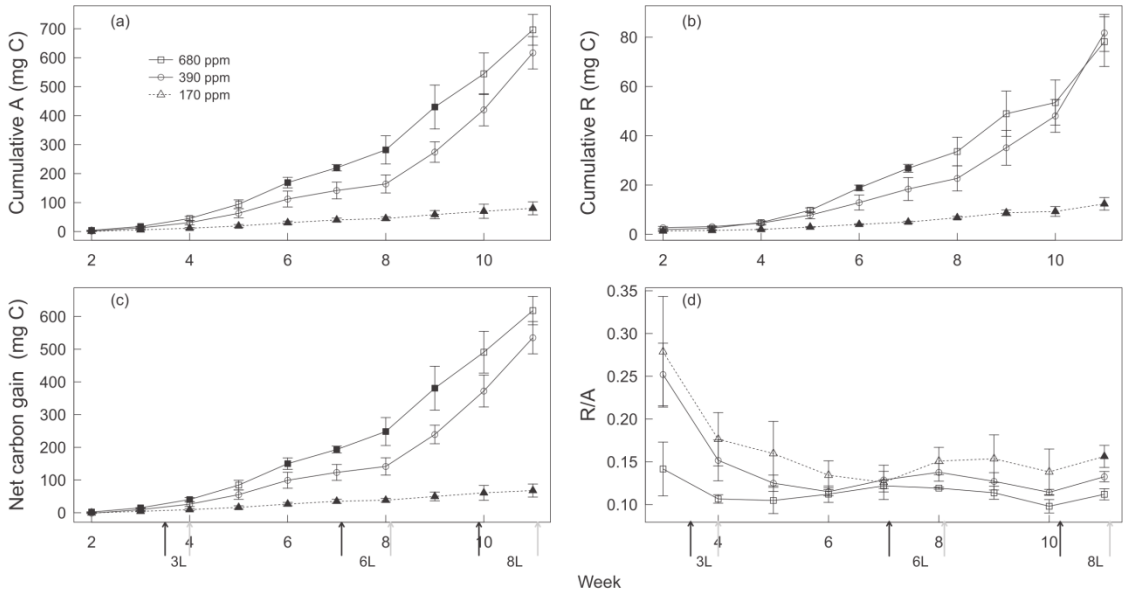

Figure 3. Weekly cumulative whole-plant net carbon assimilation A (a), respiration R (b), net carbon gain (c) and R/A (d) of winter wheat (*Triticum aestivum* cv. Genius) for the three [CO_2] treatments: 680 ppm [CO_2] (squares, black line); 390 ppm [CO_2] (circles, black line); 170 ppm [CO_2] (triangles, dashed line). Values are the means (mg C) of three individual chambers; error bars represent ±1 SD. Black arrows indicate sampling dates for 680 and 390 ppm [CO_2] treatments; grey arrows indicate sampling dates for 170 ppm [CO_2] treatment. Significant differences between 680 and 170 ppm [CO_2] treatments compared to ambient [CO_2] (390 ppm) are indicated by filling of symbols ($P < 0.05$, Tukey's HSD). Harvests were carried out after emergence of three, six and eight leaf sheaths; denoted as 3 L, 6 L and 8 L periods, respectively.

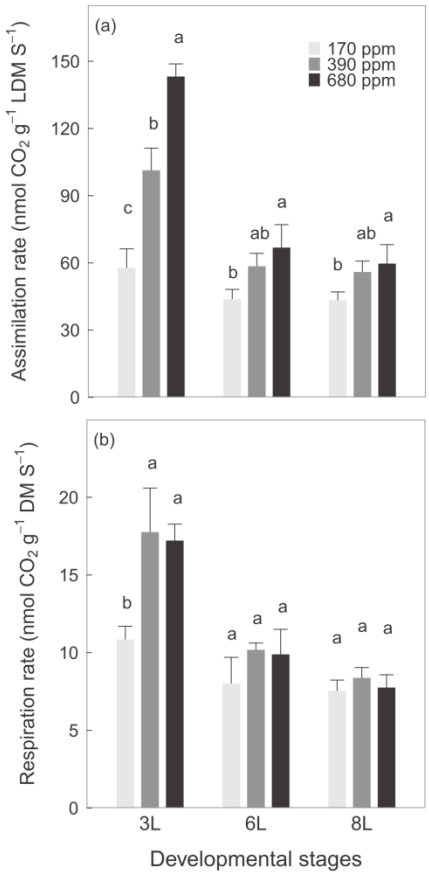

Figure 4. Leaf mass-based net assimilation rate (a) and whole-plant mass-based night-time respiration rate (b) of winter wheat (*Triticum aestivum* cv. Genius) for the three [CO_2] treatments: 680 ppm [CO_2] (black bars); 390 ppm [CO_2] (dark grey bars); 170 ppm [CO_2] (light grey bars). Values are the means (nmol CO_2 g^{-1} s^{-1}) of three individual chambers; error bars represent ±1 SD. Different letters indicate significant differences between [CO_2] treatments ($P < 0.05$, Tukey's HSD). Harvests were carried out after emergence of three, six and eight leaf sheaths; denoted as 3 L, 6 L and 8 L periods, respectively.

increased with increasing [CO_2], but at 6 L and 8 L there was no significant difference across [CO_2] treatments (Fig. 6h). At 6 L and 8 L, root SM concentrations were significantly lower at 170 ppm than at 390 ppm [CO_2]. By contrast, root SM concentrations were slightly higher at 390 ppm than at 680 ppm [CO_2], although this difference was statistically not significant (Fig. 6i). Note that most leaf SMs are C-based compounds whereas most root SMs contain N (Supporting Information Figs S1 & S2). Within leaves, low [CO_2] tended to decrease the concentrations of Luteolin-based, chrysoeriol-based, tricin-based and apigenin-based SMs, rather than ferulic acid-based SMs (Supporting Information Fig. S1). In addition, the concentrations of ferulic acid-based, luteolin-based and chrysoeriol-based SMs decreased from 3 L to 8 L across all [CO_2] treatments, whereas tricin-based and apigenin-based SMs increased at 680 ppm [CO_2] but remained relatively constant at 390 and 170 ppm [CO_2] (Supporting Information Fig. S1). Within roots, low [CO_2] tended to decrease DIMBOA-Glc (38%) more than HDMBOA-Glc (25%) (Supporting Information Fig. S2).

The response of SMs/NSC to [CO_2] differed between tissues and developmental stages (Fig. 6j–l). At 3 L and 6 L, leaf SMs/NSC was lower at 170 ppm [CO_2] than at 390 ppm [CO_2], but at 8 L there was no difference in leaf SMs/NSC across [CO_2] treatments (Fig. 6j). By contrast, stem and root SMs/NSC was higher at 170 ppm than at 390 and 680 ppm [CO_2] (Fig. 6k,l).

Proportional C allocation to respiration, structural growth, NSC and SMs

Proportional C allocation to R (R/A) remained relatively constant across [CO_2] treatments (Fig. 8). The proportion of C allocation to biomass (SG + NSC + SMs) was lower in plants grown at 170 ppm [CO_2] than at 680 ppm [CO_2], although this was not statistically significant (Fig. 8). Proportional C allocation to NSC was significantly higher in plants grown at 680 ppm than at 390 and 170 ppm [CO_2], and proportional C allocation to SMs significantly increased with increasing [CO_2] (Fig. 8). The unaccounted C pool (A – R – SG – NSC – SMs) showed large variations and no discernible trend with [CO_2].

Within-plant partitioning of biomass, NSC and SMs

Allocation of total plant biomass and NSC to leaves, stems and roots differed with [CO_2] (Fig. 9a–f). With increasing [CO_2], allocation of biomass and NSC to leaves decreased but allocation to stems and roots increased (Fig. 9a–f). However, allocation of SMs was not affected by [CO_2]; plants in all treatments showed the highest proportions in leaves and the lowest proportions in stems (Fig. 9g–i).

DISCUSSION

Continuous measurements of gas exchange combined with the recurrent quantification of whole-plant NSC and SMs allowed us to track C fluxes to different plant organs and functional pools. Manipulations of the whole-plant C balance provided insights into the response of plant C allocation to changes in C availability. Our study revealed that C allocation to respiration is maintained as a fixed proportion of net plant C gain, even over a large gradient of [CO_2]. With increasing C availability, the fraction of assimilation allocated to biomass (SG + NSC + SMs), in particular NSC and SMs, increased. Moreover, biomass and NSC increased more in stems and roots than in leaves with increasing C availability. However, under low C availability resource constraints favoured the establishment of a functional equilibrium, that is, biomass and NSC increased in leaves, the tissue responsible for the acquisition of the most limiting resource, CO_2. Increasing C availability released this constraint and allowed plants to invest proportionally more C into NSC and SMs.

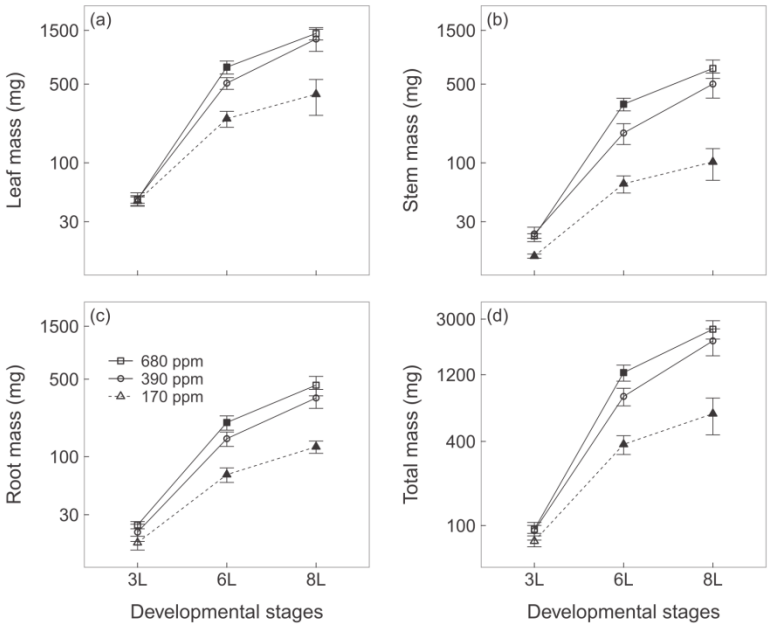

Figure 5. The dry mass of leaf (a), stem (b), root (c) and total mass (d) of winter wheat (*Triticum aestivum* cv. Genius) for the three [CO_2] treatments: 680 ppm [CO_2] (squares, black line); 390 ppm [CO_2] (circles, black line); 170 ppm [CO_2] (triangles, dashed line). Values are the means (mg) of three individual chambers; error bars represent ±1 SD. Significant differences between 680 and 170 ppm [CO_2] treatments compared to ambient [CO_2] (390 ppm) are indicated by filling of symbols ($P < 0.05$, Tukey's HSD). Note the dry mass is plotted on a log scale. Harvests were carried out after emergence of three, six and eight leaf sheaths; denoted as 3 L, 6 L and 8 L periods, respectively.

Minimizing carbon loss – with increasing C availability the proportion of C in biomass (in particular nonstructural components) increases but respiration does not

The higher relative allocation to respiration in the first weeks of the experiment (until 3 L) in the two lower [CO_2] treatments may be due to relatively greater carbon supply from seed storage than from photosynthesis. Because seed storage (~46 mg seed mass on average) was depleted rapidly over time, as indicated by strong increases in plant dry biomass (ca. 230 and 1150 mg at 3 L and 6 L at low [CO_2]), R/A decreased dramatically at low and ambient [CO_2] while it remained quite constant at elevated [CO_2]. Whole-plant R/A remained relatively constant across [CO_2] treatments afterwards, corroborating previously observed homeostasis of leaf-level R/A in response to changing [CO_2] in *Eucalyptus saligna* (Ayub *et al.*, 2011), *G. max* (Ayub *et al.*, 2014) and wheat (Gifford, 1995). The homeostasis of whole-plant R/A was also observed across a range of temperatures in two *Plantago* species (Atkin *et al.*, 2007) and at different irradiance levels in five herbaceous species (Pons & Poorter, 2014). However, all these studies assessed gas exchange during several hours or up to few days only, and hence our study, spanning many weeks, provides further insights into long-term responses of R/A to changes in [CO_2]. Note that our estimates of the R/A ratio (ca. 10–14%) were based on nighttime respiration (R) and daytime net photosynthesis (i.e. A = gross photosynthesis – daytime respiration), not on total respiration and gross photosynthesis as in other studies. Assuming daytime respiration rates equal those measured at night, the ratio of total respiration to gross photosynthesis would be ~30% and within the range of proportions previously reported (ca. 30–50%) (Atkin *et al.*, 2007; Gifford, 1995; Pons & Poorter, 2014).

Whole-plant assimilation and respiration are largely dependent on plant size and, therefore, do not represent photosynthetic or respiratory efficiency. By contrast, mass-based rates can indicate whether other factors than CO_2 availability, like leaf N or sugar concentrations, may constrain assimilation or respiration. Leaf mass-based net day-time assimilation declined over time and correlated negatively with leaf NSC concentrations but positively with leaf N concentrations in all [CO_2] treatments (Supporting Information Figs S3 & S4). Moreover, it decreased to a greater extent at elevated [CO_2] than at low [CO_2] as leaf NSC increased and N concentrations decreased to a greater extent at elevated [CO_2]. These findings support previously reported sugar- (reviewed in Long *et al.*, 2004) and Rubisco-mediated (Aranjuelo *et al.*, 2011; Pinto *et al.*, 2014) photosynthetic regulation under elevated [CO_2] but may also indicate proportionally greater light limitation at elevated than at low [CO_2] in the growth chambers.

The tight coupling between assimilation and respiration across [CO_2] treatments suggests that a large proportion of respiration serves to provide energy required during assimilation, for example, for processes like sucrose synthesis and phloem loading (Crous *et al.*, 2011). However, assimilation was not the only factor influencing respiration. In absence of

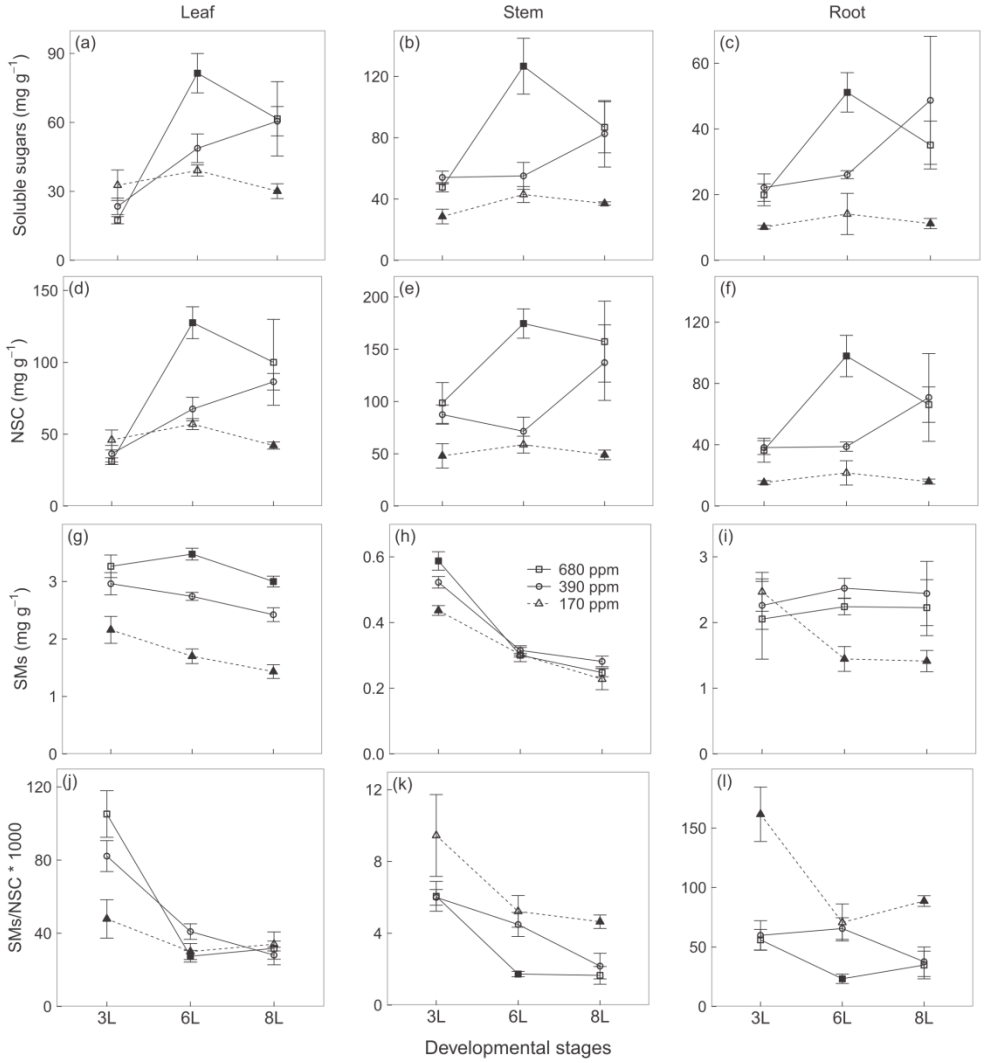

Figure 6. Concentrations of soluble sugars (mg g^{-1} dry weight, a–c), total non-structural carbohydrates (NSC, mg g^{-1} dry weight, d–e), secondary metabolites (SMs, mg g^{-1} dry weight, g–i) and ratios of SMs to NSC (j–l) in leaves, stems and roots of winter wheat (*Triticum aestivum* cv. Genius) for the three [CO_2] treatments: 680 ppm [CO_2] (squares, black line); 390 ppm [CO_2] (circles, black line); 170 ppm [CO_2] (triangles, dashed line). Total NSC concentrations were calculated as the sum of concentrations of soluble sugars, starch and fructans. Values are the means of three individual chambers; error bars represent ±1 SD. Significant differences between 680 and 170 ppm [CO_2] treatments compared to ambient [CO_2] (390 ppm) are indicated by filling of symbols ($P < 0.05$, Tukey's HSD). Note the different scales on *y*-axes. Harvests were carried out after emergence of three, six and eight leaf sheaths; denoted as 3 L, 6 L and 8 L periods, respectively.

assimilation, that is, during nights, respiration rates were quite low, but these may have been the result of low night-time temperatures in the greenhouse. The negative correlation between mass-based night-time respiration and whole-plant NSC concentrations (Supporting Information Fig. S3) indicates that substrate supply, at least at ambient and elevated [CO_2], was not a limiting factor for respiration.

Interestingly and contrary to our expectations, plants grown at high [CO_2] invested relatively more C in biomass (in particular in NSC and SMs) than plants grown at low [CO_2]. In these plants, a down-regulation of growth via modulation of phytohormones under stress (Achard *et al.*, 2006; Park *et al.*, 2007; Zhang *et al.*, 2009) could provide an explanation for the different allocation patterns. By contrast, at elevated [CO_2], photosynthesis was apparently light-, not C-limited, and plants tended to utilize more C for biomass. This is consistent with the growth rate hypothesis (Coley *et al.*, 1985; Endara & Coley, 2011) stating that plants in resource-rich environments generally grow faster in order to be able to compete for other resources such as water, nutrients or, as in our study, for light. Greenhouse light intensities were much lower than those occurring in the field. While this may put an upper limit on absolute resource fluxes, the general agreement of allocation patterns in our study with those observed in field-grown plants downplays the impact of greenhouse light limitation on allocation patterns.

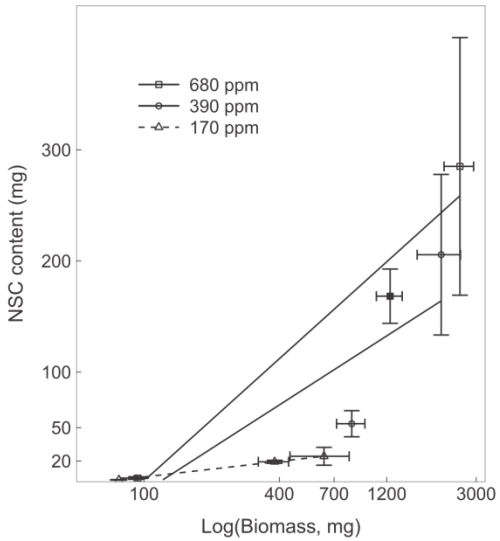

Figure 7. Correlations between whole-plant nonstructural carbohydrates (NSC) content and biomass in winter wheat (*Triticum aestivum* cv. Genius) for the three [CO_2] treatments: 680 ppm [CO_2] (squares, black line); 390 ppm [CO_2] (circles, black line); 170 ppm [CO_2] (triangles, dashed line). Values are the means (mg) of three individual chambers; error bars represent ±1 SD. Note the dry mass is plotted on a log scale. Significant differences in NSC content and biomass between 680 and 170 ppm [CO_2] treatments compared to ambient [CO_2] (390 ppm) are indicated by filling of symbols ($P < 0.05$, Tukey's HSD).

The unaccounted C pool showed relatively large variations across treatments, which may be attributed, at least partially, to changes in C export, like root exudation or the emission of VOCs. Plants release root exudates as a means to facilitate organic matter decomposition presumably for nutrient acquisition, and several studies found that root exudation was much lower in plants grown at ambient than at elevated [CO_2] (Johansson *et al.*, 2009; Phillips *et al.*, 2009). In our experiment, nutrients were provided and freely accessible (sand and nutrient solution) thus making nutrient uptake facilitation unnecessary. However, other studies showed that plants subjected to low [CO_2] always exhibited higher emissions of VOCs (Possell & Hewitt, 2011; Wilkinson *et al.*, 2009), likely for quenching reactive oxygen species (Harrison *et al.*, 2013; Loreto & Schnitzler, 2010) that are increasingly produced during inhibition of the photosynthetic electron transfer chain under limited CO_2 availability to the Calvin cycle (Brosché *et al.*, 2010).

Ensuring long-term survival – larger increases in NSC and SMs than structural growth with increasing C availability

How plants build up NSC remains a conceptual paradigm with potentially far-reaching implications for both understanding and predicting plant responses to environmental changes (Dietze *et al.*, 2014; Hartmann & Trumbore, 2016). There is substantial evidence suggesting that environmental stress limits growth faster than photosynthesis thus leading to an initial excess C accumulating as NSC (Palacio *et al.*, 2014). By contrast, trade-off allocation to NSC, that is, allocation of C to storage at the cost of growth, was directly assessed only in few recent studies (Gibon *et al.*, 2009; Hartmann *et al.*, 2015; Wiley *et al.*, 2013) but may represent an important insurance strategy against potential future threats like herbivory and thus promote long-term survival (Wiley & Helliker, 2012).

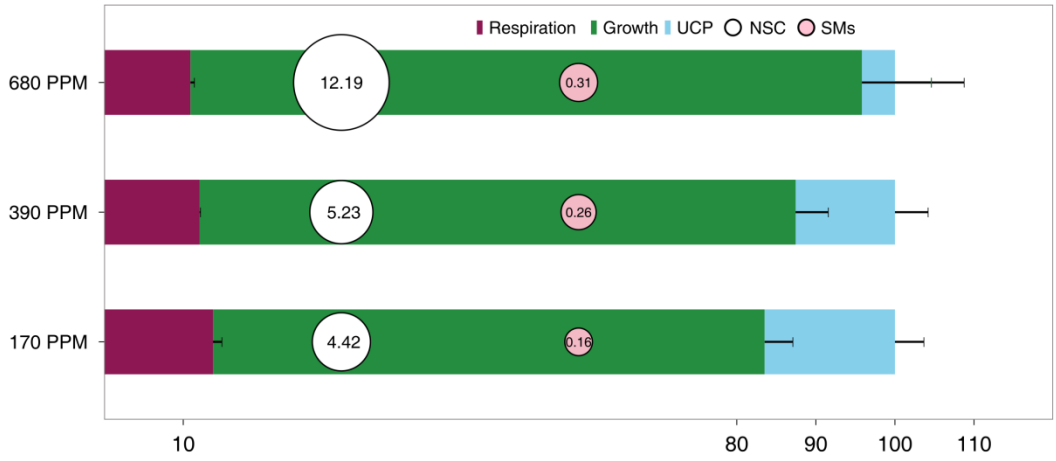

Figure 8. Percentage proportions of cumulative net carbon assimilation between 3 L and 6 L allocated to respiration (violet bars), growth (green bars), unaccounted carbon pool (UCP, blue bars), total nonstructural carbohydrates (NSC, white bubbles) and secondary metabolites (SMs, pink bubbles) of winter wheat (*Triticum aestivum* cv. Genius) for the three [CO_2] treatments: 680 ppm [CO_2]; 390 ppm [CO_2]; 170 ppm [CO_2]. All concentration data were scaled up to whole-plant content by multiplying them with tissue dry mass, and then converted to carbon content before calculating proportions. The numbers in the white and pink bubbles indicate the percentage of net carbon assimilation allocated to NSC and SMs, respectively. Note, however, that the size of these bubbles has been adjusted to allow numbers to be printed and is not linearly related to the pool sizes. Values are means of three individual chambers; error bars represent ±1 SE.

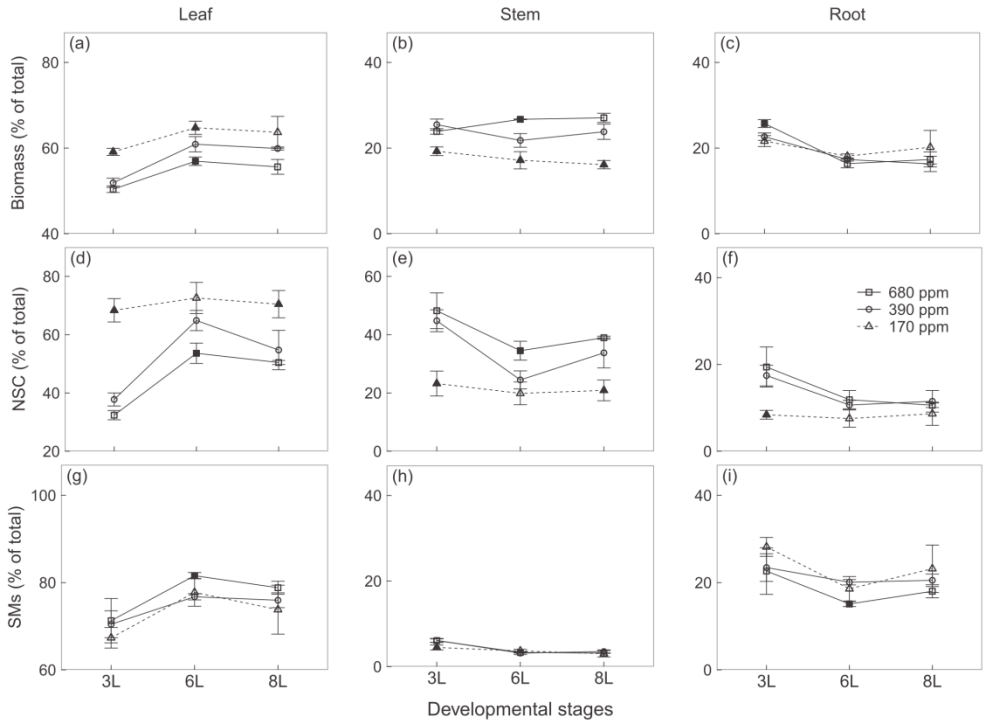

Figure 9. Percentage proportion of biomass (a–c), non-structural carbohydrates (NSC, d–e) and secondary metabolites (SMs, g–i) allocated to leaves, stems and roots of winter wheat (*Triticum aestivum* cv. Genius) for the three [CO_2] treatments: 680 ppm [CO_2] (squares, black line); 390 ppm [CO_2] (circles, black line); 170 ppm [CO_2] (triangles, dashed line). Values are the means of three individual chambers; error bars represent ±1 SD. Significant differences between 680 and 170 ppm [CO_2] treatments compared to ambient [CO_2] (390 ppm) are indicated by filled symbols ($P < 0.05$, Tukey's HSD). Note the different scales on *y*-axes. Harvests were carried out after emergence of three, six and eight leaf sheaths; denoted as 3 L, 6 L and 8 L periods, respectively.

As a result of positive C balance between 3 L and 6 L, total NSC (soluble sugars + starch + fructans) concentrations doubled at 390 ppm [CO_2] and increased by more than three times at 680 ppm [CO_2]. Therefore, greater C availability increased total NSC concentrations and whole-plant NSC content in proportions that were much higher than increases in total plant biomass. At ambient and elevated [CO_2], SG may be limited by environmental factors such as nutrients and water (Kirschbaum, 2011; Palacio *et al.*, 2014). The much higher C/N ratio at elevated than at ambient [CO_2] also suggests that SG was likely N-, rather than C-limited (Supporting Information Table S1). At 8 L, the subsequent decline in NSC concentrations at elevated [CO_2] may be due to photosynthetic acclimation of wheat plants to elevated [CO_2] (Aranjuelo *et al.*, 2011; Aranjuelo *et al.*, 2015). In addition, under elevated [CO_2], the size of the C pool in whole-plant NSC is equivalent to twice the whole-plant daily net assimilation at 6 L (1.5 times at 8 L). Thus, NSC at elevated [CO_2] may represent a multiple-day buffer pool for supporting metabolic activities.

Many manipulative studies have investigated the effects of elevated [CO_2] or of shading (to reduce C availability) on SMs (Lindroth, 2012), but little is known about the responses of whole-plant SMs over a large gradient of C availability. Leaf SM concentrations increased with increasing C availability, which is in accord with the GDBH and suggests that the SM pool is filled with C that is available in excess of growth demand (Herms & Mattson, 1992). Plants grown under low C availability may gain immediate benefits by reducing C investments into SMs. However, SMs can serve multiple functions, such as detoxification, primary metabolism and chemical defence (Neilson *et al.*, 2013). Large costs needed to repair and regrow plant tissues following stress conditions such as herbivory could reduce the long-term fitness of low [CO_2] plants with low SMs, as suggested by the growth rate hypothesis (Coley *et al.*, 1985). In addition, plants at 3 L had relatively more young leaves and higher leaf and stem SMs than plants at 8 L. Greater leaf and stem SMs in young vulnerable leaves that also have greater photosynthetic capacity may represent an investment insurance strategy.

N-rich SMs play important roles in ecological interactions, but very few studies investigated how they may respond to elevated [CO_2] (Lindroth, 2012). As expected, low [CO_2] decreased N-containing SMs (benzoxazinoid derivatives) in roots. This is consistent with the GDBH and suggests that limited C resources are preferentially invested in SG rather than SMs. Furthermore, low [CO_2] tended to decrease DIMBOA-Glc more than HDMBOA-Glc (Supporting Information Fig. S2), possibly because HDMBOA-Glc is more efficient against pathogens and insect herbivory (Glauser *et al.*, 2011) and represents

the better investment under C limitation. By contrast, concentrations of these compounds were slightly lower at elevated [CO_2] than at ambient [CO_2], likely because the production of these N-rich SMs (putrescine-based and benzoxazinoids) may have been limited by N supply rather than C supply (Supporting Information Table S1). This interpretation is in agreement with results from other studies showing that elevated [CO_2] inhibited nitrate assimilation in wheat (Bloom *et al.*, 2010). Given the defensive role of benzoxazinoid derivatives (Ahmad *et al.*, 2011), the responses observed in our study support previously reported increases in egg densities of western corn rootworm (*Diabrotica virgifera virgifera*) in the soil of soybean fields under elevated [CO_2] (Schroeder *et al.*, 2006).

The trade-off between allocation to NSC versus SMs was tissue specific and depended on the developmental stage of the plants. At 3 L, leaf SMs/NSC increased with increasing C availability, indicating that leaves tend to invest more NSC into SM production. By contrast, root SMs/NSC declined with increasing C availability, suggesting that plant roots grown at ambient and elevated [CO_2] increase NSC more than SMs, likely due to a potential N limitation on root SM production, as discussed above.

Achieving a functional equilibrium – with increasing C availability wheat plants prioritize allocation of biomass and NSC to stems and roots over leaves

Allocation patterns of biomass and NSC are consistent with the 'functional equilibrium' hypothesis (Poorter *et al.*, 2012). At low [CO_2], plants were apparently constrained to invest proportionally more biomass and NSC in leaves, while with increasing C availability biomass and NSC increased in stems and roots. Under low [CO_2], this optimization strategy allows plants to counteract C limitation, while a more balanced resource partitioning was required to support taller plants under elevated [CO_2]. Moreover, export of NSC from leaves to stems and roots in plants at elevated [CO_2] may help plants to build storage and avoid high NSC-induced negative feedback on assimilation (Long *et al.*, 2004). By contrast, proportional allocation to SMs across plant organs did not vary between treatments, likely because leaf SMs and root SMs differed in C and N cost.

OUTLOOK

While our experimental design allowed us to quantify several functional sinks of the plant C balance, it did not allow direct assessments of root exudates and VOCs and thereby prevented differentiating among C exports. The high variability in the unaccounted C pool in our experiment is likely due to the accumulation of uncertainties across different measurements and devices (Vaisala, Picarro, FTIR, elemental analyser, HPLC-PAD and HPLC-UV). Thus, future studies would benefit from direct assessment of 'export' C fluxes, including root exudates and VOCs, while keeping in mind that very short-lived or rapidly decomposed export may be detected in experimental set-ups as respiration (i.e. CO_2).

Given that SMs can serve multiple functions, the role of C allocation to SMs as a strategic investment for defence can only be assessed by simultaneously evaluating responses of herbivores and/or pathogens. Such studies have been conducted on soybean under elevated [CO_2] (reviewed in Zavala *et al.*, 2013) and can guide future studies with low C availability ([CO_2]). Because our knowledge about the mechanisms controlling plant allocation is still very limited, future studies should also focus on biochemical and molecular regulation of growth (Claeys *et al.*, 2014) and explore regulatory mechanisms of other allocation sinks like storage and SMs.

ACKNOWLEDGEMENTS

We thank Savoyane Lambert, Iris Kuhlmann and Somak Chowdhury for their help with sample processing, Ines Hilke for elemental analysis, and Michael Rässler and Jessica Heublein for measurements of sugars, starch and fructans. Jonathan Gershenzon and Michael Reichelt supported us for measurements of secondary metabolites. Waldemar Ziegler, Olaf Kolle and René Schwalbe assisted in setting up the [CO_2] manipulation. Daniel Rzesanke helped with the FTIR manipulation. We thank Susan Trumbore for helpful comments and language revision of the manuscript. J.H. was funded by Chinese Scholarship Council and Max Planck Institute.

REFERENCES

Achard P., Cheng H., De Grauwe L., Decat J., Schoutteten H., Moritz T. & Harberd N.P. (2006) Integration of plant responses to environmentally activated phytohormonal signals. *Science* **311**, 91–94.

Ahmad S., Veyrat N., Gordon-Weeks R., Zhang Y.H., Martin J., Smart L. & Ton J. (2011) Benzoxazinoid metabolites regulate innate immunity against aphids and fungi in maize. *Plant Physiology* **157**, 317–327.

Aranjuelo I., Cabrera-Bosquet L., Morcuende R., Avice J.C., Nogués S., Araus J. L. & Pérez P. (2011) Does ear C sink strength contribute to overcoming photosynthetic acclimation of wheat plants exposed to elevated CO_2? *Journal of Experimental Botany* **62**, 3957–3969.

Aranjuelo I., Erice G., Sanz-Sáez A., Abadie C., Gilard F., Gil-Quintana E. & Tcherkez G. (2015) Differential CO_2 effect on primary carbon metabolism of flag leaves in durum wheat (*Triticum durum* Desf.). *Plant, Cell & Environment* **38**, 2780–2794.

Atkin O.K., Scheurwater I. & Pons T.L. (2007) Respiration as a percentage of daily photosynthesis in whole plants is homeostatic at moderate, but not high, growth temperatures. *New Phytologist* **174**, 367–380.

Ayub G., Smith R.A., Tissue D.T. & Atkin O.K. (2011) Impacts of drought on leaf respiration in darkness and light in *Eucalyptus saligna* exposed to industrial-age atmospheric CO_2 and growth temperature. *New Phytologist* **190**, 1003–1018.

Ayub G., Zaragoza-Castells J., Griffin K.L. & Atkin O.K. (2014) Leaf respiration in darkness and in the light under pre-industrial, current and elevated atmospheric CO_2 concentrations. *Plant Science* **226**, 120–130.

Ballare C.L. (2014) Light regulation of plant defense. *Annual Review of Plant Biology* **65**, 335–363.

Bekaert M., Edger P.P., Hudson C.M., Pires J.C. & Conant G.C. (2012) Metabolic and evolutionary costs of herbivory defense: systems biology of glucosinolate synthesis. *New Phytologist* **196**, 596–605.

Bloom A.J., Burger M., Asensio J.S.R. & Cousins A.B. (2010) Carbon dioxide enrichment inhibits nitrate assimilation in wheat and *Arabidopsis*. *Science* **328**, 899–903.

Boote K.J., Jones J.W., White J.W., Asseng S. & Lizaso J.I. (2013) Putting mechanisms into crop production models. *Plant, Cell & Environment* **36**, 1658–1672.

Brosché M., Overmyer K., Wrzaczek M., Kangasjärvi J. & Kangasjärvi S. (2010) Stress signaling III: reactive oxygen species (ROS). In *Abiotic Stress Adaptation in Plants: Physiological, Molecular and Genomic Foundation* (eds Pareek A., Sopory S.K. & Bohnert J.H.), pp. 91–102. Springer Netherlands, Dordrecht.

Casal J.J. (2013) Photoreceptor signaling networks in plant responses to shade. *Annual Review of Plant Biology* **64**, 403–427.

Chapin F.S., Schulze E.-D. & Mooney H.A. (1990) The ecology and economics of storage in plants. *Annual Review of Ecology and Systematics* **21**, 423–447.

Claeys H., De Bodt S. & Inze D. (2014) Gibberellins and DELLAs: central nodes in growth regulatory networks. *Trends in Plant Science* **19**, 231–239.

Coley P.D., Bryant J.P. & Chapin F.S. (1985) Resource availability and plant antiherbivore defense. *Science* **230**, 895–899.

Crous K.Y., Zaragoza-Castells J., Löw M., Ellsworth D.S., Tissue D.T., Tjoelker M.G. & Atkin O.K. (2011) Seasonal acclimation of leaf respiration in *Eucalyptus saligna* trees: impacts of elevated atmospheric CO_2 and summer drought. *Global Change Biology* **17**, 1560–1576.

Cubasch U., Wuebbles D., Chen D., Facchini M.C., Frame D., Mahowald N. & Winther J.-G. (2013) Introduction. In *Climate Change 2013: The Physical Science Basis. Contribution of Working Group I to the Fifth Assessment Report of the Intergovernmental Panel on Climate Change* (eds Stocker T.F., Qin D., Plattner G.-K., Tignor M., Allen S.K., Boschung J. & Midgley P.M.), pp. 119–158. Cambridge University Press, Cambridge, United Kingdom and New York, NY, USA.

Dietze M.C., Sala A., Carbone M.S., Czimczik C.I., Mantooth J.A., Richardson A.D. & Vargas R. (2014) Nonstructural carbon in woody plants. *Annual Review of Plant Biology* **65**, 667–687.

Endara M.J. & Coley P.D. (2011) The resource availability hypothesis revisited: a meta-analysis. *Functional Ecology* **25**, 389–398.

Fatichi S., Leuzinger S. & Korner C. (2014) Moving beyond photosynthesis: from carbon source to sink-driven vegetation modeling. *New Phytologist* **201**, 1086–1095.

Franks P.J., Adams M.A., Amthor J.S., Barbour M.M., Berry J.A., Ellsworth D.S. & von Caemmerer S. (2013) Sensitivity of plants to changing atmospheric CO_2 concentration: from the geological past to the next century. *New Phytologist* **197**, 1077–1094.

Gerhart L.M. & Ward J.K. (2010) Plant responses to low [CO_2] of the past. *New Phytologist* **188**, 674–695.

Gibon Y., Pyl E.-T., Sulpice R., Lunn J.E., Höhne M., Günther M. & Stitt M. (2009) Adjustment of growth, starch turnover, protein content and central metabolism to a decrease of the carbon supply when *Arabidopsis* is grown in very short photoperiods. *Plant, Cell & Environment* **32**, 859–874.

Gifford R.M. (1995) Whole plant respiration and photosynthesis of wheat under increased CO_2 concentration and temperature: long-term vs. short-term distinctions for modelling. *Global Change Biology* **1**, 385–396.

Glauser G., Marti G., Villard N., Doyen G.A., Wolfender J.-L., Turlings T.C.J. & Erb M. (2011) Induction and detoxification of maize 1,4-benzoxazin-3-ones by insect herbivores. *The Plant Journal* **68**, 901–911.

Grayston S.J., Vaughan D. & Jones D. (1997) Rhizosphere carbon flow in trees, in comparison with annual plants: the importance of root exudation and its impact on microbial activity and nutrient availability. *Applied Soil Ecology* **5**, 29–56.

Halkier B.A. & Gershenzon J. (2006) Biology and biochemistry of glucosinolates. *Annual Review of Plant Biology* **57**, 303–333.

Harrison S.P., Morfopoulos C., Dani K.G.S., Prentice I.C., Arneth A., Atwell B.J. & Wright I.J. (2013) Volatile isoprenoid emissions from plastid to planet. *New Phytologist* **197**, 49–57.

Hartmann H., McDowell N.G. & Trumbore S. (2015) Allocation to carbon storage pools in Norway spruce saplings under drought and low CO_2. *Tree Physiology* **35**, 243–252.

Hartmann H. & Trumbore S. (2016) Understanding the roles of nonstructural carbohydrates in forest trees – from what we can measure to what we want to know. *New Phytologist* **211**, 386–403.

Hartmann H., Ziegler W., Kolle O. & Trumbore S. (2013) Thirst beats hunger – declining hydration during drought prevents carbon starvation in Norway spruce saplings. *New Phytologist* **200**, 340–349.

Herms D.A. & Mattson W.J. (1992) The dilemma of plants: to grow or defend. *The Quarterly Review of Biology* **67**, 283–335.

Hoagland D.R. & Arnon D.I. (1950) The water culture method for growing plants without soil. *Calif Agric. Exp. Station Circular* **347**, 1–32.

Johansson E.M., Fransson P.M.A., Finlay R.D. & van Hees P.A.W. (2009) Quantitative analysis of soluble exudates produced by ectomycorrhizal roots as a response to ambient and elevated CO_2. *Soil Biology and Biochemistry* **41**, 1111–1116.

Kirschbaum M.U.F. (2011) Does enhanced photosynthesis enhance growth? Lessons learned from CO_2 enrichment studies. *Plant Physiology* **155**, 117–124.

Korner C. (2015) Paradigm shift in plant growth control. *Current Opinion in Plant Biology* **25**, 107–114.

Lee T.D., Barrott S.H. & Reich P.B. (2011) Photosynthetic responses of 13 grassland species across 11 years of free-air CO_2 enrichment is modest, consistent and independent of N supply. *Global Change Biology* **17**, 2893–2904.

Lindroth R.L. (2012) Atmospheric change, plant secondary metabolites and ecological interactions. In *Ecology of Plant Secondary Metabolites: From Genes to Global Processes* (eds Iason G.R., Dicke M. & Hartley S.E.), pp. 120–153. Cambridge University Press, Cambridge, United Kingdom and New York, NY, USA.

Long S.P., Ainsworth E.A., Rogers A. & Ort D.R. (2004) Rising atmospheric carbon dioxide: plants face the future. *Annual Review of Plant Biology* **55**, 591–628.

Loreto F. & Schnitzler J.-P. (2010) Abiotic stresses and induced BVOCs. *Trends in Plant Science* **15**, 154–166.

Moheb A., Ibrahim R.K., Roy R. & Sarhan F. (2011) Changes in wheat leaf phenolome in response to cold acclimation. *Phytochemistry* **72**, 2294–2307.

Mooney H.A. (1972) The carbon balance of plants. *Annual Review of Ecology and Systematics* **3**, 315–346.

Neilson E.H., Goodger J.Q.D., Woodrow I.E. & Møller B.L. (2013) Plant chemical defense: at what cost? *Trends in Plant Science* **18**, 250–258.

O'Neill B.F., Zangerl A.R., Dermody O., Bilgin D.D., Casteel C.L., Zavala J.A. & Berenbaum M.R. (2010) Impact of elevated levels of atmospheric CO_2 and herbivory on flavonoids of soybean (*Glycine max* Linnaeus). *Journal of Chemical Ecology* **36**, 35–45.

Palacio S., Hoch G., Sala A., Körner C. & Millard P. (2014) Does carbon storage limit tree growth? *New Phytologist* **201**, 1096–1100.

Park J.-E., Park J.-Y., Kim Y.-S., Staswick P.E., Jeon J., Yun J. & Park C.-M. (2007) GH3-mediated auxin homeostasis links growth regulation with stress adaptation response in *Arabidopsis*. *Journal of Biological Chemistry* **282**, 10036–10046.

Phillips R.P., Bernhardt E.S. & Schlesinger W.H. (2009) Elevated CO_2 increases root exudation from loblolly pine (*Pinus taeda*) seedlings as an N-mediated response. *Tree Physiology* **29**, 1513–1523.

Pinto H., Sharwood R.E., Tissue D.T. & Ghannoum O. (2014) Photosynthesis of C-3, C-3-C-4, and C-4 grasses at glacial CO_2. *Journal of Experimental Botany* **65**, 3669–3681.

Pollock A. & Cairns A.J. (1991) Fructan metabolism in grasses and cereals. *Annual Review of Plant Physiology and Plant Molecular Biology* **42**, 77–101.

Pons T.L. & Poorter H. (2014) The effect of irradiance on the carbon balance and tissue characteristics of five herbaceous species differing in shade-tolerance. *Frontiers in Plant Science* **5**, 14.

Poorter H., Niklas K.J., Reich P.B., Oleksyn J., Poot P. & Mommer L. (2012) Biomass allocation to leaves, stems and roots: meta-analyses of interspecific variation and environmental control. *New Phytologist* **193**, 30–50.

Possell M. & Hewitt C.N. (2011) Isoprene emissions from plants are mediated by atmospheric CO_2 concentrations. *Global Change Biology* **17**, 1595–1610.

R Development Core Team (2014) R: a language and environment for statistical computing. R foundation for Statistical computing, URL http://www.r-project.org., Vienna, Austria.

Raessler M., Wissuwa B., Breul A., Unger W. & Grimm T. (2010) Chromatographic analysis of major non-structural carbohydrates in several wood species – an analytical approach for higher accuracy of data. *Analytical Methods* **2**, 532–538.

Robinson E.A., Ryan G.D. & Newman J.A. (2012) A meta-analytical review of the effects of elevated CO_2 on plant–arthropod interactions highlights the importance of interacting environmental and biological variables. *New Phytologist* **194**, 321–336.

Schnyder H. (1992) Long-term steady-state labelling of wheat plants by use of natural $^{13}CO_2/^{12}CO_2$ mixtures in an open, rapidly turned-over system. *Planta* **187**, 128–135.

Schroeder J.B., Gray M.E., Ratcliffe S.T., Estes R.E. & Long S.P. (2006) Effects of elevated CO_2 and O_3 on a variant of the western corn rootworm (Coleoptera: Chrysomelidae). *Environmental Entomology* **35**, 637–644.

Sullivan J.T. (1935) The estimation of starch. *Industrial & Engineering Chemistry Analytical Edition* **7**, 311–314.

Temme A.A., Cornwell W.K., Cornelissen J.H.C. & Aerts R. (2013) Meta-analysis reveals profound responses of plant traits to glacial CO_2 levels. *Ecology and Evolution* **3**, 4525–4535.

Tissue D.T. & Lewis J.D. (2012) Learning from the past: how low [CO_2] studies inform plant and ecosystem response to future climate change. *New Phytologist* **194**, 4–6.

Wiley E. & Helliker B. (2012) A re-evaluation of carbon storage in trees lends greater support for carbon limitation to growth. *New Phytologist* **195**, 285–289.

Wiley E., Huepenbecker S., Casper B.B. & Helliker B.R. (2013) The effects of defoliation on carbon allocation: can carbon limitation reduce growth in favour of storage? *Tree Physiology* **33**, 1216–1228.

Wilkinson M.J., Monson R.K., Trahan N., Lee S., Brown E., Jackson R.B. & Fall R. (2009) Leaf isoprene emission rate as a function of atmospheric CO_2 concentration. *Global Change Biology* **15**, 1189–1200.

Wojakowska A., Perkowski J., Goral T. & Stobiecki M. (2013) Structural characterization of flavonoid glycosides from leaves of wheat (*Triticum aestivum* L.) using LC/MS/MS profiling of the target compounds. *Journal of Mass Spectrometry* **48**, 329–339.

Wouters F.C., Reichelt M., Glauser G., Bauer E., Erb M., Gershenzon J. & Vassão D.G. (2014) Reglucosylation of the benzoxazinoid DIMBOA with inversion of stereochemical configuration is a detoxification strategy in lepidopteran herbivores. *Angewandte Chemie* **126**, 11502–11506.

Zadoks J.C., Chang T.T. & Konzak C.F. (1974) A decimal code for the growth stages of cereals. *Weed Research* **14**, 415–421.

Zavala J.A., Nabity P.D. & DeLucia E.H. (2013) An emerging understanding of mechanisms governing insect herbivory under elevated CO_2. *Annual Review of Entomology* **58**, 79–97.

Zhang H., Ziegler W., Han X., Trumbore S. & Hartmann H. (2015) Plant carbon limitation does not reduce nitrogen transfer from arbuscular mycorrhizal fungi to *Plantago lanceolata*. *Plant and Soil* **396**, 369–380.

Zhang S.W., Li C.H., Cao J., Zhang Y.C., Zhang S.Q., Xia Y.F. & Sun Y. (2009) Altered architecture and enhanced drought tolerance in rice via the down-regulation of indole-3-acetic acid by TLD1/OsGH3.13 activation. *Plant Physiology* **151**, 1889–1901.

Received 22 August 2016; accepted for publication 12 December 2016

SUPPORTING INFORMATION

Additional Supporting Information may be found in the online version of this article at the publisher's web-site:

Table S1. Carbon (C) and nitrogen (N) concentrations and C/N ratios in leaves, stems and roots of winter wheat (*Triticum aestivum* cv. Genius) for the three [CO_2] treatments: 680 ppm [CO_2] 390 ppm [CO_2] and 170 ppm [CO_2]. Values represent the means (±1 SD) of three individual chambers. Different letters indicate significant differences between [CO_2] treatments ($P < 0.05$ Tukey's HSD)

Table S2. Molecular formula, molecular weight and C fraction of standards used for the quantification of secondary metabolites in leaves, stems and roots of winter wheat (*Triticum aestivum* cv. Genius).

Figure S1. Concentrations of ferulic acid-based (a), luteolin-based (b), chrysoeriol-based (c) and tricin-based (d) and apigenin-based (e) secondary metabolites in leaves of winter wheat (*Triticum aestivum* cv. Genius) for the three [CO_2] treatments: 680 ppm [CO_2] (squares, blue line); 390 ppm [CO_2] (circles, black line); 170 ppm [CO_2] (triangles, red line). Values are the means (mg g^{-1}) of three individual chambers; error bars represent ±1 SD. Significant differences between 680 and 170 ppm [CO_2] treatments compared to ambient [CO_2] (390 ppm) are indicated by filled symbols ($P < 0.05$, Tukey's HSD).

Figure S2. Concentrations of Putrescine-based (a), DIMBOA-Glc-based (b) and HDMBOA-Glc-based (c) secondary metabolites in roots of winter wheat (*Triticum aestivum* cv. Genius) for the three [CO_2] treatments: 680 ppm [CO_2] (squares, blue line); 390 ppm [CO_2] (circles, black line); 170 ppm [CO_2] (triangles, red line). Values are the means (mg g^{-1}) of three individual chambers; error bars represent ±1 SD. Significant differences between 680 and 170 ppm [CO_2] treatments compared to ambient [CO_2] (390 ppm) are indicated by filled symbols ($P < 0.05$, Tukey's HSD).

Figure S3. Correlations between leaf nonstructural carbohydrate (NSC) concentrations (mg g^{-1}) and leaf assimilation rate (nmol CO_2 g^{-1} s^{-1}) (a), and correlations between whole-plant NSC concentrations (mg g^{-1}) and respiration rate (nmol CO_2 g^{-1} s^{-1}) (b) in winter wheat (*Triticum aestivum* cv. Genius) for the three [CO_2] treatments: 680 ppm [CO_2] (squares, blue line); 390 ppm [CO_2] (circles, black line); 170 ppm [CO_2] (triangles, red line). Values are the means of three individual chambers; error bars are ±1 SD.

Figure S4. Correlations between leaf nitrogen (N) concentrations (mg g^{-1}) and assimilation rate (nmol CO_2 g^{-1} s^{-1}) in winter wheat (*Triticum aestivum* cv. Genius) for the three [CO_2] treatments: 680 ppm [CO_2] (squares, blue line); 390 ppm [CO_2] (circles, black line); 170 ppm [CO_2] (triangles, red line). Values are the means of three individual chambers; error bars are ±1 SD.

CHAPTER 3

Journal of Experimental Botany, Vol. 68, No. 5 pp. 1251–1263, 2017
doi:10.1093/jxb/erx008 Advance Access publication 17 February 2017
This paper is available online free of all access charges (see http://jxb.oxfordjournals.org/open_access.html for further details)

RESEARCH PAPER

Increasing carbon availability stimulates growth and secondary metabolites via modulation of phytohormones in winter wheat

Jianbei Huang[1,*], Michael Reichelt[2], Somak Chowdhury[1], Almuth Hammerbacher[2,3] and Henrik Hartmann[1]

[1] Max Planck Institute for Biogeochemistry, Hans-Knöll-Str. 10, D-07745, Jena, Germany
[2] Max Planck Institute for Chemical Ecology, Hans-Knöll-Str. 8, D-07745, Jena, Germany
[3] Department of Microbiology and Plant Pathology, Forestry and Agricultural Biotechnology Institute, University of Pretoria, Private Bag X20, Pretoria 0028, South Africa

* Correspondence: hjianbei@bgc-jena.mpg.de

Received 30 September 2016; Editorial decision 9 January 2017; Accepted 10 January 2017

Editor: Tracy Lawson, University of Essex

Abstract

Phytohormones play important roles in plant acclimation to changes in environmental conditions. However, their role in whole-plant regulation of growth and secondary metabolite production under increasing atmospheric CO_2 concentrations ($[CO_2]$) is uncertain but crucially important for understanding plant responses to abiotic stresses. We grew winter wheat (*Triticum aestivum*) under three $[CO_2]$ (170, 390, and 680 ppm) over 10 weeks, and measured gas exchange, relative growth rate (RGR), soluble sugars, secondary metabolites, and phytohormones including abscisic acid (ABA), auxin (IAA), jasmonic acid (JA), and salicylic acid (SA) at the whole-plant level. Our results show that, at the whole-plant level, RGR positively correlated with IAA but not ABA, and secondary metabolites positively correlated with JA and JA-Ile but not SA. Moreover, soluble sugars positively correlated with IAA and JA but not ABA and SA. We conclude that increasing carbon availability stimulates growth and production of secondary metabolites via up-regulation of auxin and jasmonate levels, probably in response to sugar-mediated signalling. Future low $[CO_2]$ studies should address the role of reactive oxygen species (ROS) in leaf ABA and SA biosynthesis, and at the transcriptional level should focus on biosynthetic and, in particular, on responsive genes involved in $[CO_2]$-induced hormonal signalling pathways.

Key words: Abscisic acid, auxin, elevated CO_2, jasmonic acid, low CO_2, salicylic acid, secondary metabolites, soluble sugars.

Introduction

Plants capture CO_2 from the atmosphere and convert it into sugars as essential building blocks for growth and substrates for metabolism (Hartmann and Trumbore, 2016). Atmospheric CO_2 concentrations ($[CO_2]$) has risen from ~170–200 ppm during glacial periods to the current 400 ppm, and are predicted to reach between 430 ppm and 1000 ppm by 2100 (Cubasch *et al.*, 2013). Understanding the mechanisms by which increasing $[CO_2]$ have influenced whole-plant growth and metabolism in the past will help to unravel mechanisms regulating plant responses to future elevated $[CO_2]$ but also to reduced carbon availability as may occur during shading, cold, or drought. Phytohormones play an important

role in plant acclimation to changing environmental conditions (Peleg and Blumwald, 2011), such as drought (Valluru *et al.*, 2016) and salinity (Albacete *et al.*, 2008). However, our understanding of how phytohormones, such as auxin, abscisic acid (ABA), jasmonic acid (JA), or salicylic acid (SA), are involved in the whole-plant regulation of plant gas exchange, growth, and secondary metabolite (SM) production under changing [CO_2] is still limited.

ABA plays a role in multiple physiological processes for stress acclimation. For example, ABA is the main regulator of stomatal responses to drought and salinity (Osakabe *et al.*, 2014). Elevated [CO_2] reduces stomatal conductance and density (Franks *et al.*, 2013), and this is often (Lake and Woodward, 2008; Chater *et al.*, 2015), but not always (Teng *et al.*, 2006; Merilo *et al.*, 2013) associated with increased leaf ABA concentration. Changes in carbohydrate availability have been proposed to be a sensing pathway by which plants may increase ABA biosynthesis at elevated [CO_2] (Chater *et al.*, 2014). Additional application of glucose can increase ABA biosynthesis (reviewed in León and Sheen, 2003), and the ABA-dependent signalling pathway is essential for sucrose-induced stomatal closure (Kelly *et al.*, 2013). Moreover, the activation of the ABA signalling pathway is involved in inhibition of root growth under osmotic stress (Achard *et al.*, 2006; Rowe *et al.*, 2016).

Auxin (indole-3-acetic acid; IAA) was recognized as an essential plant growth promoter >70 years ago (Enders and Strader, 2015), but much less is known about its role in modulating plant response to abiotic stress (Kazan, 2013). Elevated CO_2 increased carbohydrate and IAA concentrations and promoted growth in *Arabidopsis thaliana* (Teng *et al.*, 2006; Hachiya *et al.*, 2014) and tomato seedlings (*Solanum lycopersicum*; Wang *et al.*, 2009) but reduced IAA concentrations in roots of sweet pepper (*Capsicum annuum*; Piñero *et al.*, 2014). Niu *et al.* (2011) showed that the auxin-dependent signalling pathway is required for enhancing root development under elevated CO_2 in Arabidopsis. Moreover, accumulated soluble sugars may be key elicitors for increased IAA production under elevated [CO_2], as both glucose (Sairanen *et al.*, 2012) and sucrose additions (Lilley *et al.*, 2012) have been shown to stimulate IAA biosynthesis and resulted in higher growth rates in the latter study. In contrast, low [CO_2] reduces carbohydrate availability (Hartmann *et al.*, 2013, 2015) and limits plant growth (Gerhart and Ward, 2010), but whether IAA regulation is involved in these processes remains uncertain.

JA (Riemann *et al.*, 2015) and SA (Khan *et al.*, 2015) play key roles in regulating plant defence responses to abiotic and biotic stresses. The JA signalling pathway involves the isoleucine (Ile) conjugate of JA (JA-Ile), a phytohormone that activates the transcription of JA-dependent defence genes (Thines *et al.*, 2007). In contrast to JA-Ile, the hydroxylated derivatives of JA, such as 12-hydroxy-JA (12-OH-JA, tuberonic acid) may deactivate JA-dependent defence genes (Miersch *et al.*, 2008; Koo and Howe, 2012). Elevated [CO_2] has been shown to enhance SA-dependent defence and repress JA-dependent defence (Zavala *et al.*, 2013; Sun *et al.*, 2016), but how plants regulate JA and SA at low [CO_2] remains uncertain. Furthermore, changes in soluble sugars may regulate production of SMs via modulation of JA and SA. Sucrose (Loreti *et al.*, 2008) and glucose (Guo *et al.*, 2013) play a synergistic role with JA in anthocyanin and glucosinolate biosynthesis, respectively.

Shading and defoliation are common approaches for reducing plant sugar availability, but shading can activate IAA biosynthesis (Casal, 2013) and suppress JA biosynthesis via changes in phytochromes (Ballare, 2014), and defoliation itself is a wounding treatment that can trigger JA biosynthesis with cascading effects on other phytohormones (Erb *et al.*, 2012). Directly manipulating [CO_2] suffers less from such side effects and allows plants to regulate phytohormones under contrasting carbon (rather than light) availability.

Here, we present an analysis of whole-plant phytohormone dynamics in winter wheat (*Triticum aestivum*) grown along a gradient of atmospheric CO_2 concentrations (170, 390, and 680 ppm). We investigated correlations between phytohormone concentrations and stomatal conductance, relative growth rate (RGR), and soluble sugar and SM concentrations. In this study, we focused on ABA, IAA, SA, and JA as well as its derivatives JA-Ile and 12-OH-JA, although we are aware that other phytohormones such as cytokinin and ethylene also play important roles in the regulation of growth. Based on knowledge about hormonal regulation of growth and secondary metabolite production at the tissue/organ level, we explore whether the following relationships hold true at the whole-plant level: with increasing [CO_2], plants (i) reduce stomatal conductance via increasing ABA; (ii) promote growth via increasing IAA; (iii) increase biosynthesis of SMs via increasing JA, JA-Ile, and SA; and (iv) show higher carbohydrate concentrations that, in turn, induce the biosynthesis of phytohormones.

Materials and methods

Plant material

We used a cultivar of winter wheat (*Triticum aestivum* cv. Genius) adapted to Central Europe. On 7 January 2015, seeds were germinated on plates filled with sand and watered every day. After 6 d, we transplanted 10–12 seedlings with similar height into each pot (11 cm diameter, 24 cm height) pre-filled with quartz sand. Six pots were randomly placed in each growth chamber. All pots were irrigated with a continuous through-flow of a modified Hoagland solution (Hoagland and Arnon, 1950).

Growth chambers and treatments

Plants were grown in glass chambers (75 cm long×45 cm wide×80 cm high) flushed continuously with air at a flow rate of 14 l min^{-1} (for more details, see Hartmann *et al.*, 2013). Concentrations of the different CO_2 treatments were produced by first scrubbing all CO_2 from incoming air using a molecular sieve, and then injecting pure CO_2 (Schnyder, 1992). The [CO_2] of incoming air for the three [CO_2] treatments was measured with a Vaisala® (GMP 343) at intervals of 10 min. A micro-logger (Campbell® CR1000) compared these concentrations against pre-set values (170, 390, and 680 ppm) and adjusted them accordingly via mass flow controllers. For each [CO_2] treatment, three chambers were used to grow plants and one chamber was used to monitor [CO_2] reference levels.

In each chamber, we monitored air temperature and photosynthetic photon flux density (PPFD) continuously (for more details,

see Hartmann *et al.*, 2013). During the day, average temperature increased from ~12 °C at 06:30 h (local time) to ~20–24 °C and then decreased to ~16.5 °C at 22:00 h. Plants were grown in a light/dark regime of 16/8 h using supplemental greenhouse lamps. The average PPFD from 23 January 2015 to 20 March 2015 was 7.79 ± 0.92 mol m^{-2} d^{-1}.

Destructive harvesting

To rule out potential effects of plant development on hormone levels, we harvested plants in different treatments independently of calendar dates and when three, six, and eight leaf sheaths were completely developed, denoted as 3L, 6L, and 8L periods, respectively. The experiment was only conducted during the vegetative growth period (seedling growth and tillering stage). Plants grown in 390 ppm and 680 ppm [CO_2] chambers were sampled 3, 7, and 9 weeks after transplanting, whereas plants grown in low [CO_2] chambers were sampled 3.5, 8, and 10.5 weeks after transplanting. Harvests were always conducted between 16:00 h and 21:00 h to minimize light and temperature effects on hormones and metabolites. For each harvest, we removed one pot from each chamber. Plants were separated into leaves, stems, and roots. Leaf area was determined with a Li 3100A area meter (Li-Cor, Bad Homburg, Germany). All fresh tissues were weighed and frozen in liquid nitrogen and later transferred to a −80 °C freezer. Around 75% of the biomass was freeze-dried, weighed, and ground to fine powder using a ball mill (Retsch® MM400, Haan, Germany) and finally stored at −20 °C until further analysis. The rest of the samples were ground with liquid nitrogen using a mortar and pestle, and stored at −80 °C until analysis.

Whole-plant gas exchange

A Picarro® 2101-i (precision 0.01–0.4%, Picarro Inc., Santa Clara, CA, USA) was used to measure the [CO_2] and [H_2O] of air entering and leaving the growth chambers. The air coming from the 12 chambers and the reference air were measured sequentially at intervals of 6 min 40 s; the cycle was controlled by a micro-logger (Campbell® CR1000) connected to a custom-built valve switching unit, completing a whole cycle within 2 h. Transition periods after valve switching were excluded from analysis.

We assumed whole-plant gas exchange to be constant within the 2 h cycle. The instantaneous whole-plant assimilation (A) and transpiration (E) at hour j was calculated as:

$$[CO_2 \text{ or } H_2O]_j \left(\mu mol\, s^{-1}\right) = \frac{[CO_2 \text{ or } H_2O]_{non-plant} - [CO_2 \text{ or } H_2O]_{plant}}{M} \left(\mu mol\, mol^{-1}\right) \times \frac{VFR\left(1 min^{-1}\right)}{22.4\left(1 mol^{-1}\right) \times 60 s} \quad (1)$$

where [CO_2 or H_2O]$_{non\text{-}plant}$ and [CO_2 or H_2O]$_{plant}$ is the [CO_2 or H_2O] of outgoing air from the reference chambers without plants and from chambers with plants, respectively. M represented the number of plants in the chamber, and VFR was the volumetric flow rate of air going through the chamber (14 l min^{-1}). The value of 22.4 l mol^{-1} is the molar volume of gas under normal conditions. Canopy conductance was then estimated as previously described in McDowell *et al.* (2008):

$$G_S = \frac{E}{VPD} \quad (2)$$

where VPD (kPa) is vapour pressure deficit. Note that the relative humidity of incoming air was very low (<2%) therefore VPD is close to the saturation vapour pressure at chamber temperature. Leaf area-based (i.e. specific) net assimilation, transpiration, and stomatal conductance (G_s) were then calculated by dividing instantaneous whole-plant exchange by leaf area (m^2). To obtain a robust estimate of current whole-plant gas exchange, we averaged whole-plant gas exchange over the last few days prior to biomass sampling.

Analysis of soluble sugars

Concentrations of glucose, sucrose, and fructose were measured using the method of Raessler *et al.* (2010). Briefly, we added 1 ml (0.5 ml for small samples) of sterilized water to 50 mg (10 mg for small samples) of ground sample. The mixture was vortexed, incubated for 10 min at 65 °C, and then centrifuged for 10 min at 12 000 *g*. The supernatant was carefully collected and stored on ice, and the pellet was re-extracted twice. The supernatants were pooled and diluted at a ratio of 1:20 (1:8 for small samples) and stored at −20 °C before measurements. Sucrose, glucose, and fructose were determined by HPLC coupled with pulsed amperometric detection (HPLC-PAD), on a Dionex® ICS 3000 ion chromatography system equipped with an autosampler (Thermo Fisher GmbH, Idstein, Germany).

Analysis of SMs

A 500 µl aliquot (300 µl for small samples) of 95% methanol was added to 50 mg (30 mg for small samples) of freeze-dried tissues. The mixture was bead-beaten for 40 s at 6.0 m s^{-1} with a FastPrep Instrument (MP Biomedicals, Santa Ana, CA, USA), vortexed for 5 min, and then centrifuged at 13 000 *g* for 5 min. The supernatant was collected and the pellet was re-extracted. The supernatants were pooled and stored at 4 °C. Identification and quantification of SMs were achieved by HPLC coupled with MS and a UV Detector. Phenolic compounds were separated on a Nucleodur Sphinx RP18ec column (250 × 4.6 mm, particle size 5 µm, Macherey Nagel, Dueren, Germany) with two mobile phases 0.2% (v/v) formic acid (A) and acetonitrile (B) using the following elution profile: 0–28 min, 5–61% B in A; 28–30 min 100% B; and 30–35 min 5% B. Flow was diverted in a ratio of 4:1 before entering the mass spectrometer electrospray chamber. For identification, ESI-MS was operated at a negative mode scanning *m/z* between 50 and 1600 with an optimal target mass of 400 *m/z*. The MS conditions were: skimmer voltage, 60 V; capillary voltage, 4200 V; nebulizer pressure, 35 psi; drying gas, 11 l min^{-1}; gas temperature, 330 °C; capillary exit potential, −121 V. For quantification, the UV wavelengths 240, 260, 280, and 330 nm were monitored. Compounds of leaves and stems were identified by comparing the fragmentation patterns with previously reported wheat phenolic profiles (Moheb *et al.*, 2011; Wojakowska *et al.*, 2013). Root compounds were identified based on profiles of benzoxazinoids in grasses (Wouters *et al.*, 2014). All compounds were quantified by external standards (for more details, see Huang *et al.*, 2016).

Quantification of hormones

Concentrations of ABA, IAA, SA, and jasmonates, comprising JA, JA-Ile, and 12-OH-JA, were determined using the method of Vadassery *et al.* (2012) with modifications. Briefly, 250 mg of fresh samples were extracted with 1 ml of methanol containing 40 ng of D_6-ABA (Santa Cruz Biotechnology, Santa Cruz, CA, USA), 40 ng of D_5-IAA (Olchemin, Olomouc, Czech Republic), 40 ng of D_4-SA (Sigma-Aldrich), 40 ng of D_6-JA (HPC Standards GmbH, Cunnersdorf, Germany), and 8 ng of JA-[$^{13}C_6$]Ile conjugate as internal standards. JA-[$^{13}C_6$]Ile was synthesized using [$^{13}C_6$]Ile (Sigma-Aldrich) according to Kramell *et al.* (1988). The mixture was vortexed for 10 min and then centrifuged at 13 000 *g* for 10 min. A 800 µl aliquot of the supernatant was then collected and transferred into a 5 ml 96-well plate. The pellet was re-extracted with 500 µl of methanol using the same procedure, and 500 ml of supernatant was collected, pooled, and stored at −20 °C.

Hormone detection and quantification was accomplished with an Agilent 1260 HPLC system (Agilent Technologies,

Santa Clara, CA, USA) coupled to an API 5000 tandem mass spectrometer (Applied Biosystems, Foster City, CA, USA) equipped with a Turbospray ion source. Hormones were separated on a Zorbax Eclipse XDB-C18 HPLC column (1.8 µm, 50 × 4.6 mm; Agilent) at 25 °C, with two mobile phases consisting of 0.05% formic acid in water (solvent A) and acetonitrile (solvent B), at a flow rate of 1.1 ml min^{-1} using the following elution profile: 0–0.5 min, 10% B; 0.5–4.0 min, linear gradient from 10% to 90% B; 4.0–4.02 min, linear gradient from 90% to 100% B; 4.02-4.50 min, 100% B, 4.50-4.51 min, linear gradient from 100% to 10% B; and 4.51–7.00 min, 10% B. The parent ion and their fragments of jasmonates, SA, and ABA were analysed in negative mode by multiple reaction monitoring (MRM) (for more details, see Vadassery *et al.*, 2012). IAA was analysed in the positive ionization mode in a separate chromatographic analysis (same LC conditions as above for other phytohormones) with the following conditions: analyte parent ion→product ion: *m/z* 176→130 for IAA; *m/z* 181→134+*m/z* 181→133 for D_5-IAA. Collision energy (CE) was 19 V; declustering potential (DP) was 31 V. Q1 and Q3 quadrupoles were both maintained at unit resolution. Mass data were collected and processed using analyst 1.6 software (Applied Biosystems). Linearity in ionization efficiencies was confirmed by analysing serial dilutions of a standard mixture. The concentrations of ABA, IAA, SA, JA, and JA-Ile were determined relative to the corresponding internal standard. The concentration of OH-JA was determined relative to D_6-JA by analysing a mixture of OH-JA and D_6-JA at the same concentration. OH-JA was synthesized as described in Nakamura *et al.* (2011) and was kindly provided by Wilhelm Boland (MPI for Chemical Ecology, Jena, Germany).

Data analysis

Each growth chamber was treated as a biological replicate (n=3). We determined homogeneity of variances with the Levene test and log-transformed data when variance was not homoscedastic. Tukey's HSD (P<0.05) was used to detect significant differences between treatments. Weighted phytohormone concentrations were calculated by multiplying tissue-specific concentrations by tissue biomass and dividing their sum by whole-plant mass, as for weighted soluble sugars and SM concentrations. Phytohormones were reported on a fresh weight basis; therefore, to ensure consistency of units, the concentrations of soluble sugars and SMs were converted to fresh weight. We assessed the Pearson's correlation of phytohormones with gas exchange, RGR, soluble sugars, and SMs. All statistical analysis was conducted in R, version 3.23 (R Development Core Team, 2014).

Results

Gas exchange rate

Plants grown at 170 ppm [CO_2] exhibited lower assimilation rates but higher transpiration rates and higher stomatal conductance compared with plants grown at 390 ppm and 680 ppm [CO_2] (Fig. 1a–c). The difference between the two higher [CO_2] treatments, however, varied with developmental stages. At 3L, assimilation rates increased significantly at 680 ppm [CO_2] compared with 390 ppm [CO_2], while at 6L and 8L the increase disappeared (Fig. 1a). At 3L and 6L, transpiration rates and stomatal conductance remained relatively constant between 390 ppm and 680 ppm [CO_2], while at 8L they were higher at 680 ppm than at 390 ppm [CO_2] (Fig. 1b, c).

RGR, soluble sugars, and secondary metabolites

Similar to assimilation, plants grown at 170 ppm [CO_2] exhibited a lower RGR of all tissues than plants grown at 390 ppm [CO_2], across developmental stages (Fig. 2a–c). At 6L, RGR was higher in plants grown at 680 ppm [CO_2] than at 390 ppm [CO_2], but at 8L, plants grown at 390 ppm and 680 ppm [CO_2] exhibited a similar RGR of all tissues (Fig. 2a–c).

The [CO_2] response of soluble sugars varied with developmental stages and tissues. At 3L, all soluble sugar concentrations slightly increased at 170 ppm [CO_2] in leaves, but glucose and fructose concentrations significantly decreased in stems and roots, compared with 390 ppm [CO_2] (Fig. 3a–i). At 6L, there was no significant difference in soluble sugars across tissues between 170 ppm and 390 ppm [CO_2], but glucose and fructose concentrations significantly increased at 680 ppm [CO_2] in all tissues compared with 390 ppm [CO_2] (Fig. 3a–i). Interestingly, at 6L, we did not observe large differences in leaf sucrose concentration between the two higher [CO_2] treatments. From 6L to 8L, while soluble sugars of all tissues showed a declining trend at 680 ppm [CO_2], they accumulated at 390 ppm [CO_2] but slightly decreased at 170 ppm [CO_2] (Fig. 3a–i). Sucrose concentrations were

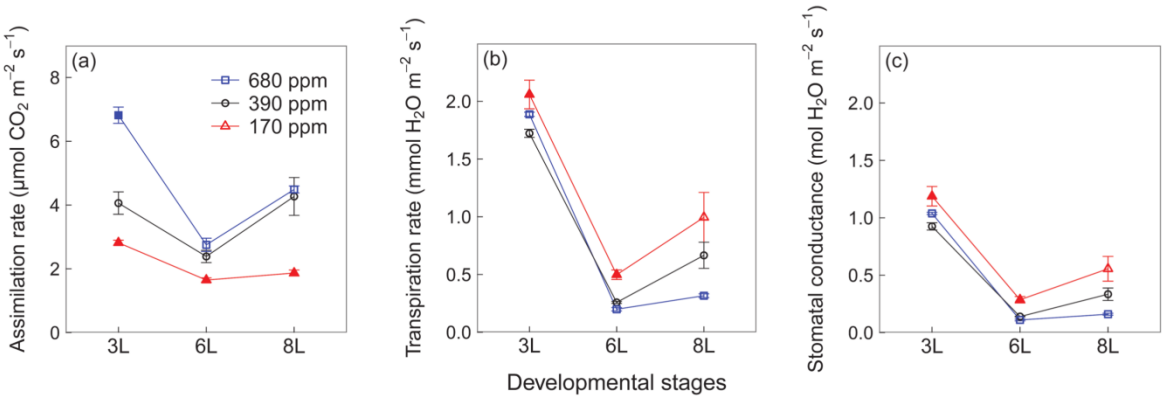

Fig. 1. Leaf area-based net assimilation rate (a), transpiration rate (b), and stomatal conductance of winter wheat (*Triticum aestivum*) for the three [CO_2] treatments (squares, 680 ppm; circles, 390 ppm; triangles, 170 ppm). Values are the mean ±SE of three individual chambers. Filled symbols of 680 ppm and 170 ppm [CO_2] treatments indicate significant differences compared with 390 ppm [CO_2] treatment (P<0.05, Tukey's HSD). We harvested plants after emergence of three, six, and eight leaf sheaths, denoted by 3L, 6L, and 8L, respectively. (This figure is available in colour at *JXB* online.)

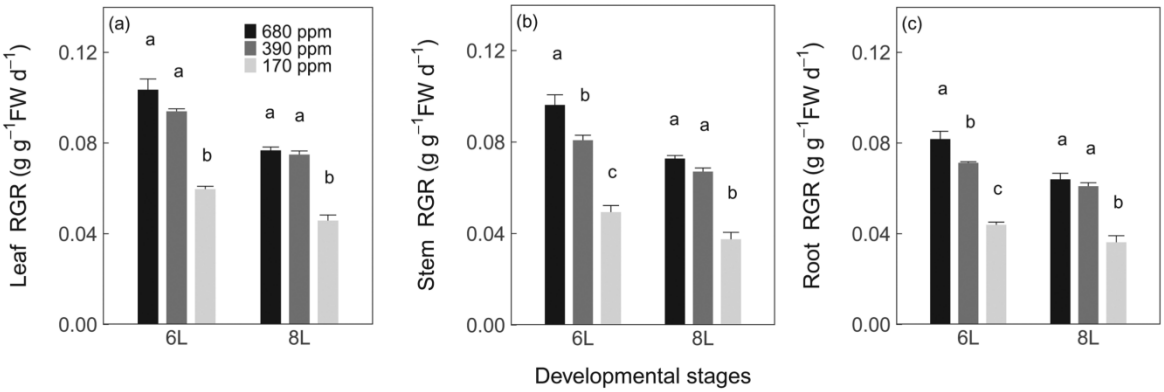

Fig. 2. Relative growth rate (RGR) of leaves (a), stems (b), and roots (c) of winter wheat (*Triticum aestivum*) for the three [CO_2] treatments. Values are the mean (g g^{-1} FW d^{-1}) ±SE of three individual chambers. Significant differences between [CO_2] treatments are indicated by different letters (P<0.05, Tukey's HSD). We harvested plants after emergence of three, six, and eight leaf sheaths, and RGR between three and six leaf sheaths and between six and eight leaf sheaths are denoted by 6L and 8L, respectively.

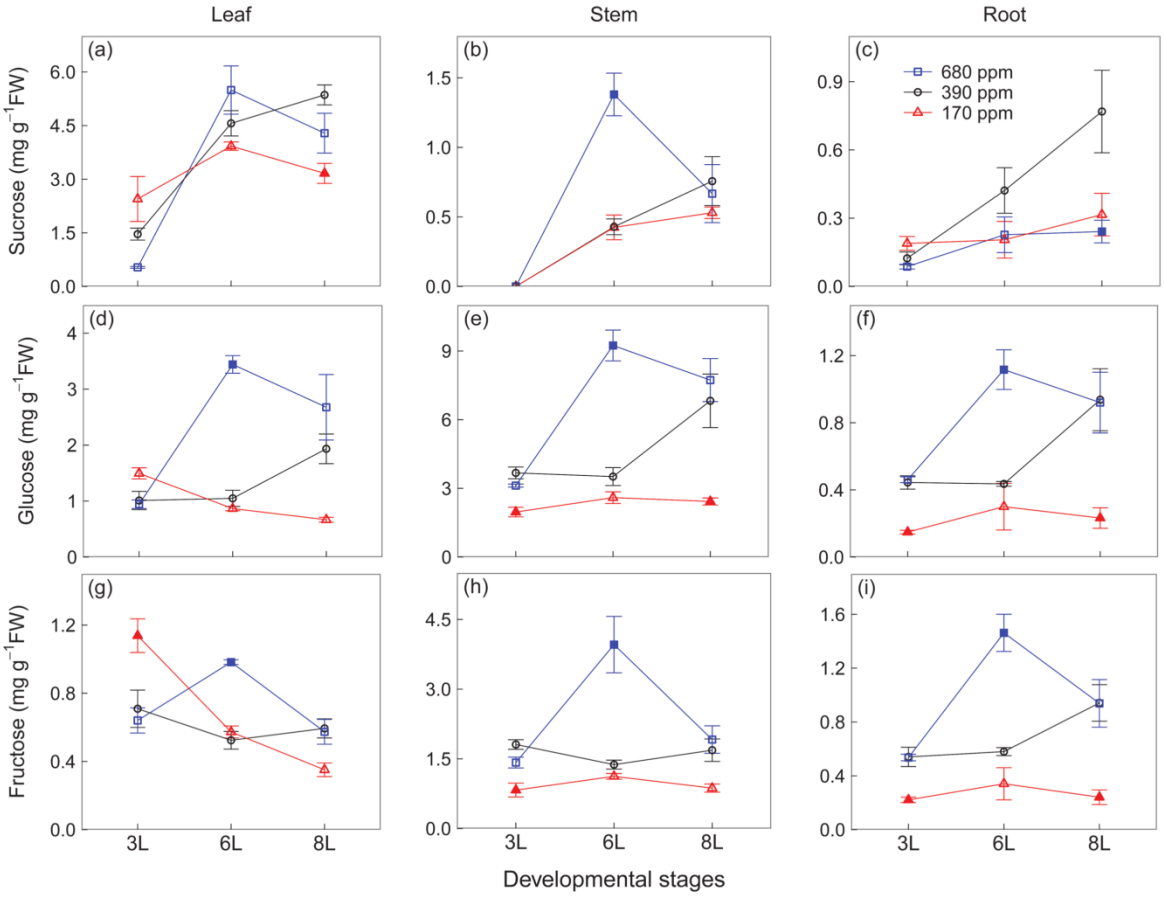

Fig. 3. Sucrose (a–c), glucose (d–f), and fructose (g–i) concentrations of winter wheat (*Triticum aestivum*) for the three [CO_2] treatments (squares, 680 ppm; circles, 390 ppm; triangles, 170 ppm). Values are the mean (mg g^{-1} FW) ±SE of three individual chambers. Filled symbols of 680 ppm and 170 ppm [CO_2] treatments indicate significant differences compared with 390 ppm [CO_2] treatment (P<0.05, Tukey's HSD). Note that the concentrations are expressed on a fresh weight basis and at different scales. We harvested plants after emergence of three, six, and eight leaf sheaths, denoted by 3L, 6L, and 8L, respectively. (This figure is available in colour at *JXB* online.)

much higher in leaves than in stems and roots, whereas glucose and fructose concentrations were generally higher in stems (Fig. 3a–i).

At 3L, plants grown at contrasting [CO_2] showed similar SM concentrations in leaves and roots. However, at 6L and 8L, leaf SM concentrations decreased with declining

[CO_2], but the decrease was greater at 170 ppm (compared with 390 ppm) than at 390 ppm (compared with 680 ppm). In contrast, at 6L and 8L, root SM concentrations remained unchanged between 390 ppm and 680 ppm [CO_2] treatments, but they were lower at 170 ppm than at 390 ppm and 680 ppm [CO_2], although not statistically significant at 8L (Table 1).

Hormonal profiling

At 6L and 8L, IAA concentrations decreased at 170 ppm [CO_2] in all tissues compared with 390 ppm and 680 ppm [CO_2], but the difference between the two higher [CO_2] treatments varied with developmental stages and tissues (Fig. 4a–c). IAA concentrations in stems were generally twice more than those in leaves and roots (Fig. 4a–c). In contrast to IAA, at 3L and 6L, ABA concentrations increased at 170 ppm [CO_2] in leaves but not in stems and roots, compared with 390 ppm and 680 ppm [CO_2] (Fig. 4d, e). From 3L to 8L, a consistent decrease in leaf ABA concentrations was observed at 170 ppm [CO_2], while the opposite was the case for 390 ppm and 680 ppm [CO_2] treatments (Fig. 4d). Note that ABA concentrations were much lower in roots than in leaves and stems (Fig. 4d, e).

Similar to IAA, at 6L and 8L, JA and JA-Ile concentrations were much lower in plants grown at 170 ppm than at 390 ppm and 680 ppm [CO_2], but at 6L there was no difference in leaves and stems between these two higher [CO_2] treatments (Fig. 5a–e). Plants grown at contrasting [CO_2] exhibited relatively similar 12-OH-JA concentrations in leaves and stems (Fig. 5g–i). Note that leaves and stems had lower concentrations of JA and JA-Ile but higher concentrations of 12-OH-JA compared with roots, in particular at 390 ppm and 680 ppm [CO_2] (Fig. 5a–i).

In contrast, plants grown at 170 ppm [CO_2] had higher leaf SA concentrations than at 390 ppm and 680 ppm [CO_2] (Fig. 6a). However, at 3L and 8L, there were no differences between the two higher [CO_2] treatments, and only at 6L were leaf SA concentrations lower at 390 ppm [CO_2] than at 680 ppm [CO_2] (Fig. 6a). SA concentrations remained relatively constant in stems and roots across [CO_2] treatments (Fig. 6b, c). Note that SA concentrations were relatively lower in stems and roots than in leaves (Fig. 6a–c).

Correlations of phytohormones to RGR, stomatal conductance, SMs, and soluble sugars

As expected, the decline in whole-plant RGR with decreasing [CO_2] was positively correlated with weighted IAA concentrations (R^2=0.84, P=0.01) (Fig. 7a). In contrast, RGR was negatively correlated with weighted ABA concentrations (R^2=0.15), but not statistically significantly (Fig. 7b). There was no correlation between stomatal conductance and leaf ABA concentrations (Fig. 7c). Weighted SM concentrations were also positively correlated with weighted JA concentrations (R^2=0.79, P=0.02) as well as concentrations of its bioactive derivative JA-Ile (R^2=0.51, P=0.11), but not with weighted SA concentrations (Fig. 7d, f). We also found a significant positive correlation between weighted soluble sugar concentrations and weighted IAA and JA concentrations, but not weighted ABA and SA concentrations (Fig. 8a–d).

Discussion

Manipulating whole-plant carbon availability along a gradient of [CO_2] combined with whole-plant hormonal analysis allowed unravelling of the mechanisms by which plants cope with abiotic stresses. As summarized in Fig. 9, our study revealed that low [CO_2] increased ABA and SA concentrations in leaves, probably in order to cope with potential oxidative stress from excess light excitation energy. With increasing C availability, wheat plants increased growth and

Table 1. *Secondary metabolite concentrations in leaves, stems, and roots of winter wheat (*Triticum aestivum*) for the three [CO_2] treatments: 680 ppm [CO_2], 390 ppm [CO_2], and 170 ppm [CO_2]*

Values are mean (μg g^{-1} FW) ±SD of three individual chambers. Note that the concentrations are expressed on a fresh weight basis.

Development	CO_2 ppm	Leaf					Stem	Root		
		Ferulic acid	Luteolin	Apigenin	Chrysoeriol	Tricin	Ferulic acid	Putrescine	DIMBOA-Glc	HDMBOA-Glc
3L	680	88.8 (6.1) a	59.8 (9.8) a	155.9 (15.5) a	43.5 (3.7) a	47.0 (3.9) a	55.9 (2.2) a	16.0 (4.3) a	46.3 (10.7) a	47.9 (6.5) a
	390	92.5 (10.2) a	51.3 (10.6)ab	163.1 (13.7) a	45.1 (4.5) a	48.3 (3.0) a	53.0 (4.7) a	20.3 (4.9) a	48.9 (6.2) a	44.5 (7.6) a
	170	87.9 (1.9) a	29.4 (5.5) b	134.2 (17.4) a	35.4 (4.8) a	43.3 (4.2) a	42.5 (3.7) b	18.2 (4.2) a	61.5 (24.4) a	58.0 (3.4) a
6L	680	57.9 (2.8) a	56.1 (4.7) a	193.8 (4.5) a	45.1 (2.5) a	70.7 (6.9) a	34.5 (0.5) a	32.1 (6.6) ab	59.4 (8.9) a	31.2 (2.4) a
	390	53.9 (6.3) ab	36.7 (3.2) b	164.4 (7.8) b	39.1 (3.0) b	50.2 (2.4) b	30.5 (2.5) b	45.6 (6.8) a	65.7 (13.4) a	27.8 (2.3) ab
	170	45.6 (2.6) b	11.8 (2.6) c	112.0 (11.3) c	25.4 (1.2) c	38.4 (4.0) b	29.0 (0.3) b	20.6 (4.3) b	44.0 (3.6) a	22.8 (2.3) b
8L	680	40.6 (3.4) a	39.8 (2.9) a	179.2 (8.8) a	39.5 (2.6) a	67.5 (7.4) a	29.2 (1.7) a	48.4 (5.6) a	56.1 (6.9) a	26.1 (4.3) a
	390	43.7 (1.5) a	26.9 (1.0) b	158.0 (10.7) a	33.4 (1.7) a	53.0 (7.4) b	31.4 (0.8) a	54.5 (12.9) a	57.4 (5.3) a	22.8 (1.3) a
	170	37.9 (4.7) a	6.1 (2.1) c	101.5 (10.7) b	17.7 (3.2) b	35.9 (2.5) c	23.6 (5.1) a	32.5 (10.9) a	44.8 (7.6) a	21.7 (7.4) a

Different letters indicate significant differences between [CO_2] treatments (P<0.05, Tukey's HSD).
We harvested plants after emergence of three, six, and eight leaf sheaths, denoted by 3L, 6L, and 8L, respectively.
DIMBOA-Glc, 2-(2,4-dihydroxy-7-methoxy-1,4-benzoxazin-3-one)-β-D-glucopyranose; HDMBOA-Glc, 2-(2-hydroxy-4,7-dimethoxy-1,4-benzoxazin-3-one)-β-D-glucopyranose. See also supporting information from Huang *et al*. (2016).

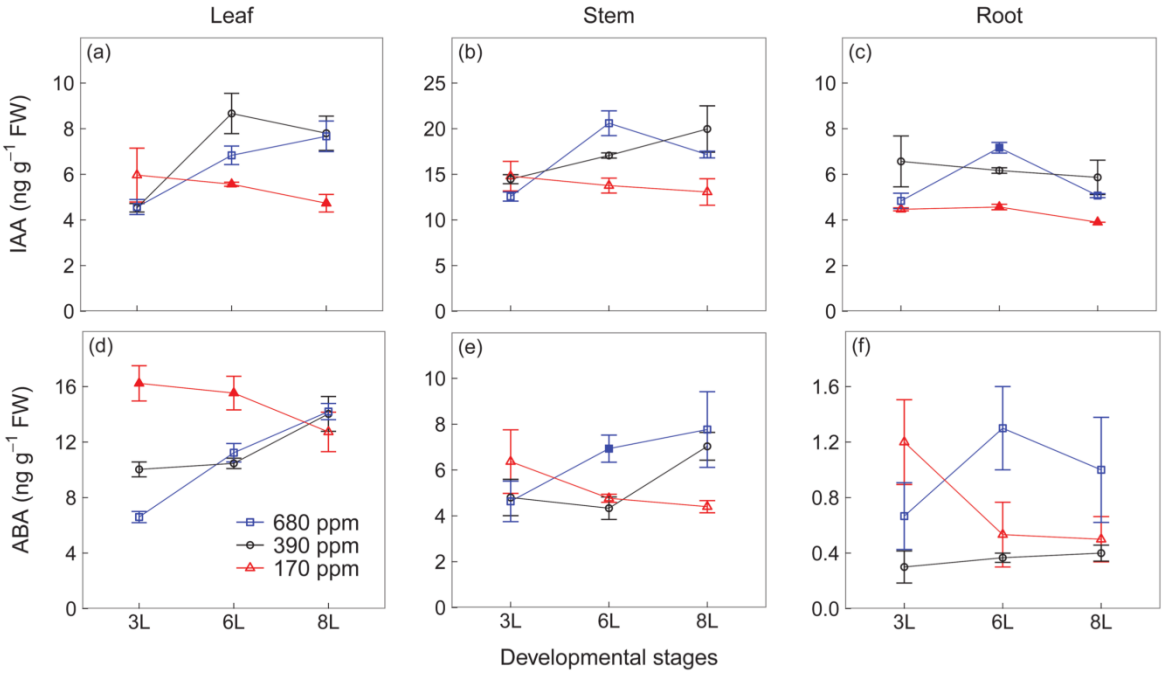

Fig. 4. Auxin (IAA) (a–c) and abscisic acid (ABA) concentrations of winter wheat (*Triticum aestivum*) for the three [CO_2] treatments (squares, 680 ppm; circles, 390 ppm; triangles, 170 ppm). Values are the mean (ng g^{-1} FW) ±SE of three individual chambers. Filled symbols of 680 ppm and 170 ppm [CO_2] treatments indicate significant differences compared with 390 ppm [CO_2] treatment (P<0.05, Tukey's HSD). Note that the concentrations are expressed on a fresh weight basis and at different scales. We harvested plants after emergence of three, six, and eight leaf sheaths, denoted by 3L, 6L, and 8L, respectively. (This figure is available in colour at *JXB* online.)

SM production via increases in IAA and JA (JA-Ile) levels and probably triggered by sugar signalling pathways.

Stomatal regulation

Transpiration rates and stomatal conductance were higher at low [CO_2] than at ambient and elevated [CO_2], and this difference increased over time. However, contrary to our expectation, stomatal conductance was not associated with leaf ABA concentrations under contrasting [CO_2]. Although it is well established that ABA can induce stomatal closure (Osakabe *et al.*, 2014), a lack of response to changes in bulk ABA cannot rule out ABA-dependent stomatal regulation, as mutants with only 10% of wild-type ABA concentrations showed stomatal closure under elevated [CO_2] (Merilo *et al.*, 2013). A recent study of ABA-deficient plants suggested that stomatal regulation under elevated [CO_2] requires increases in ABA in both stomatal precursor cells and guard cells, rather than in bulk ABA (Chater *et al.*, 2015). Furthermore, increasing leaf ABA concentration between 3L and 8L at elevated [CO_2] may be due to a down-regulation of stomatal density under elevated [CO_2] (Chater *et al.*, 2014).

Growth regulation

RGR increased in all tissues with increasing [CO_2] and were, at the whole-plant level, positively correlated with IAA but not with ABA, suggesting that IAA may be involved in growth regulation under low C availability. Growth modulation via IAA has also been observed under elevated [CO_2] in Arabidopsis (Hachiya *et al.*, 2014) and in tomato seedlings (Wang *et al.*, 2009), and during drought and low temperatures in rice (*Oryza sativa*) (Zhang *et al.*, 2009; Du *et al.*, 2013).

While leaves, stems, and roots showed similar RGR, IAA concentrations in stems were more than twice as high as in leaves and roots. IAA is synthesized mainly in the shoot apex and then transported to roots (Ljung *et al.*, 2001) so high IAA concentrations in stems may be an inactive transitory pool. Moreover, the basipetal transport of IAA from shoot to roots remained relatively constant even under low C availability, as the ratio of stem to root IAA concentrations remained relatively constant across [CO_2] treatments. In addition, at 8L, when RGR and soluble sugar concentrations at elevated [CO_2] declined in all tissues to ambient [CO_2] levels, we also observed a decrease in stem IAA concentrations. This decrease highlights the potential role of IAA in photosynthetic acclimation (Xu *et al.*, 2015), especially under elevated [CO_2].

We observed a weak relationship between RGR and ABA, and inconsistent temporal changes across tissues, suggesting that bulk ABA is not a main regulator for tissue growth. However, the ratio of leaf to stem ABA was, throughout the experiment, consistently higher at low than at ambient [CO_2], possibly because ABA is involved in photosynthetic acclimation to low [CO_2]. However, our data set cannot provide deeper insights into this mechanism, and assessments of other parameters, such as enhanced production of reactive oxygen species (ROS) from excess excitation energy at

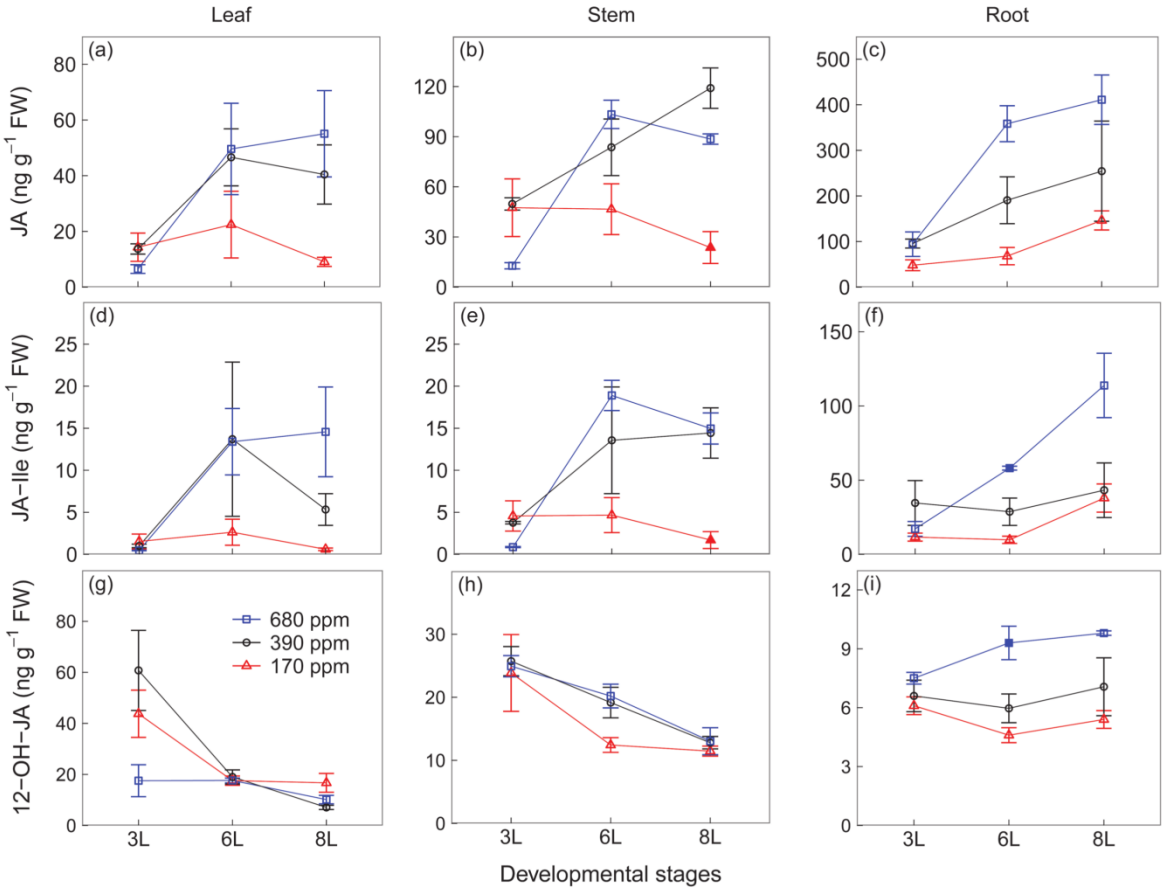

Fig. 5. Jasmonic acid (JA) (a–c), the isoleucine (Ile) conjugate of JA (JA-Ile) (d–f), and 12-hydroxy-JA (12-OH-JA) (g–i) concentrations of winter wheat (*Triticum aestivum*) for the three [CO_2] treatments (squares, 680 ppm; circles, 390 ppm; triangles, 170 ppm). Values are the mean (ng g^{-1} FW) ±SE of three individual chambers. Filled symbols of 680 ppm and 170 ppm [CO_2] treatments indicate significant differences compared with 390 ppm [CO_2] treatment (P<0.05, Tukey's HSD). Note that the concentrations are expressed on a fresh weight basis and at different scales. We harvested plants after emergence of three, six, and eight leaf sheaths, denoted by 3L, 6L, and 8L, respectively. (This figure is available in colour at *JXB* online.)

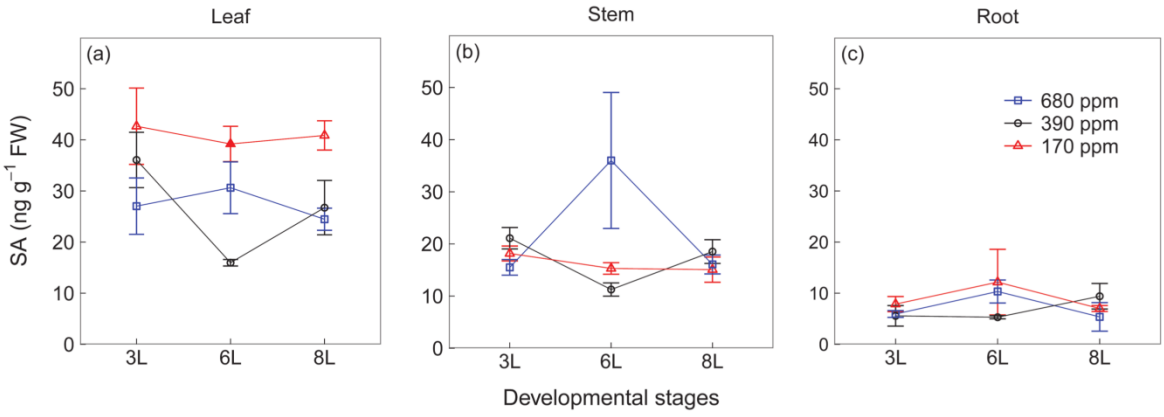

Fig. 6. Salicylic acid (SA) (a–c) concentrations of winter wheat (*Triticum aestivum*) for the three [CO_2] treatments (squares, 680 ppm; circles, 390 ppm; triangles, 170 ppm). Values are the mean (ng g^{-1} FW) ±SE of three individual chambers. Filled symbols of 680 ppm and 170 ppm [CO_2] treatments indicate significant differences compared with 390 ppm [CO_2] treatment (P<0.05, Tukey's HSD). Note that the concentrations are expressed on a fresh weight basis. We harvested plants after emergence of three, six, and eight leaf sheaths, denoted by 3L, 6L, and 8L, respectively. (This figure is available in colour at *JXB* online.)

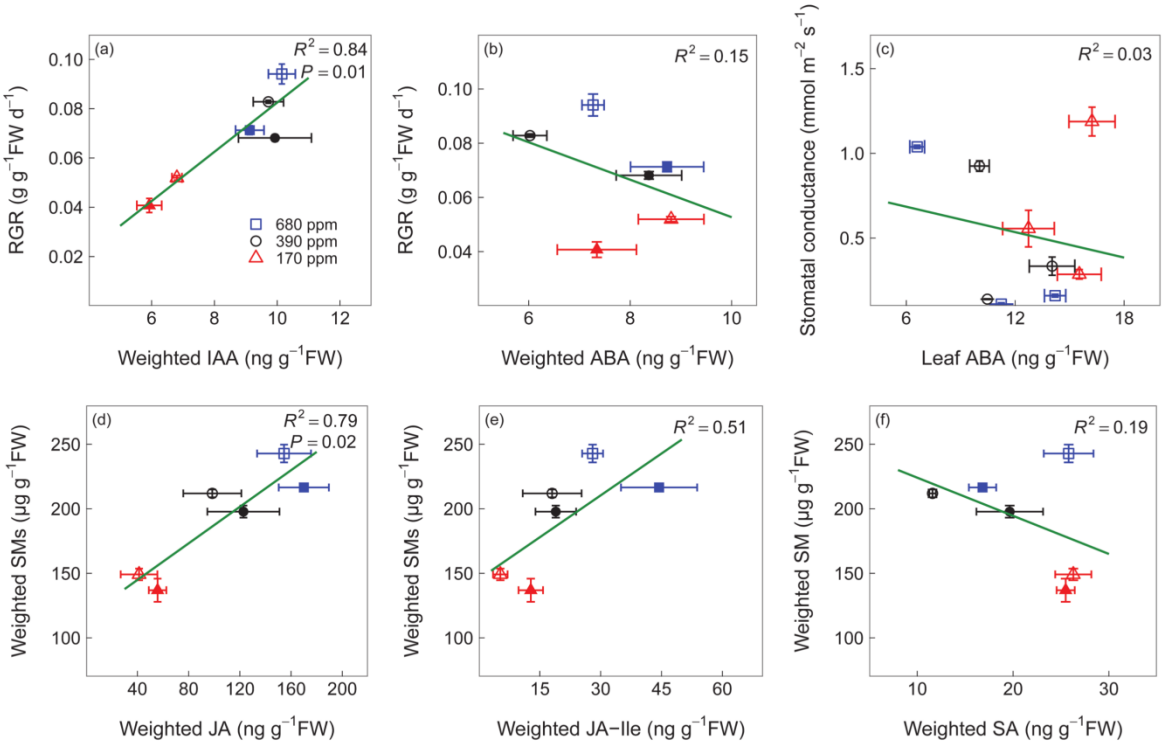

Fig. 7. Pearson's correlations of whole-plant relative growth rate (RGR) to weighted auxin (IAA) (a) and abscisic acid (ABA) (b) concentrations, between leaf area-based stomatal conductance and leaf ABA concentrations (c), and Pearson's correlations of weighted secondary metabolite (SM) concentration to jasmonic acid (JA) (d), isoleucine (Ile) conjugate of JA (e), and salicylic acid (SA) concentrations (f) in winter wheat (*Triticum aestivum*). The three [CO_2] treatments: squares, 680 ppm; circles, 390 ppm; triangles, 170 ppm. We harvested plants after emergence of three, six, and eight leaf sheaths, denoted by 3L, 6L, and 8L, respectively. However, before 3L, RGR and SM concentrations were also affected by seed storage, independent of [CO_2]; therefore, we only show RGR and SM concentrations of 6L and 8L, where open symbols represent 6L and filled symbols represent 8L. In contrast, we show stomatal conductance from 3L, 6L, and 8L, and all values are shown by open symbols. Values are the mean ±SE of three individual chambers. Note that the concentrations are expressed on a fresh weight basis and at different scales. (This figure is available in colour at *JXB* online.)

low [CO_2] (Galvez-Valdivieso *et al.*, 2009), are required to elucidate the role of ABA in stress mitigation (Mittler and Blumwald, 2015).

Regulation of secondary metabolite synthesis

Low [CO_2] reduced leaf flavonoids and root putrescine-based compounds as well as root benzoxazinoid derivatives, and this response was strongly associated with reduced JA and its bioactive derivative JA-Ile, but not with its inactive derivative 12-OH-JA. Jasmonates are involved in the biosynthesis of a wide range of SMs including flavonoids (Gundlach *et al.*, 1992), putrescine (Horbowicz *et al.*, 2011), and benzoxazinoid derivatives (Oikawa *et al.*, 2002). That low [CO_2] reduced SM synthesis via down-regulation of JA-dependent pathways is corroborated by evidence that deficiencies in potassium (Troufflard *et al.*, 2010) and phosphate (Khan *et al.*, 2016) can enhance SM production via up-regulation of JA and JA-Ile in Arabidopsis (Troufflard *et al.*, 2010; Khan *et al.*, 2016). In contrast, SA concentrations were higher in leaves at low than at ambient [CO_2], indicating that low C availability reduces leaf SM production independent of the SA signalling pathway. Given that SA and JA are antagonistic (Zavala *et al.*, 2013; Sun *et al.*, 2016), it is possible that the up-regulation of SA signalling is associated with the suppression of JA signalling at low C availability.

In contrast, under elevated [CO_2], leaf JA and SA levels changed independently from each other across developmental stages but both may nonetheless play a role in regulation of SMs. At 6L, leaf flavonoids and SA concentrations increased under elevated [CO_2] but that was not the case for JA and JA-Ile, indicating that elevated [CO_2] may stimulate short-term leaf flavonoid synthesis via SA (Zavala *et al.*, 2013; Sun *et al.*, 2016). At 8L, however, plants grown at elevated [CO_2] had higher leaf JA and JA-Ile concentrations than at ambient [CO_2] and probably induced flavonoid production. These dynamics mirror a potential long-term acclimation of photosynthesis at elevated CO_2, as indicated by declines in RGR and soluble sugars in all tissues at elevated [CO_2]. Deeper insights into such long-term leaf acclimation to elevated [CO_2] via hormonal regulation require assessments of hormones and SMs over the entire plant developmental gradient.

In roots, however, while SMs and SA remained relatively constant, JA and JA-Ile concentrations were higher at elevated [CO_2] than at ambient [CO_2]. We suggest here that JA-dependent signalling for SM production in roots was probably constrained by N availability, given that root SMs are N-rich compounds and that assimilation of nitrate into

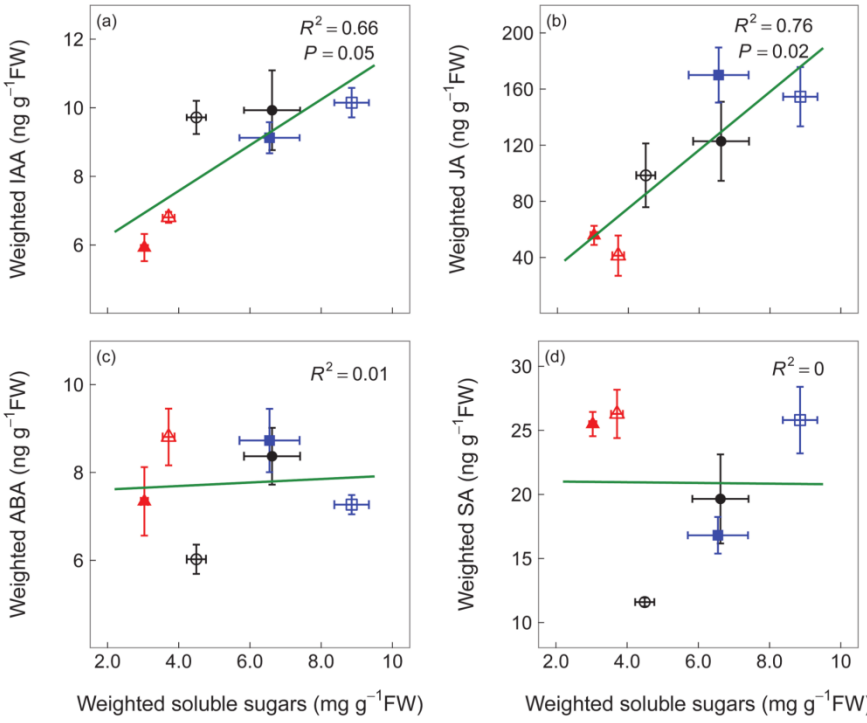

Fig. 8. Pearson's correlations of weighted soluble sugar concentration (mg g^{-1} FW) to weighted auxin (IAA) (a), jasmonic acid (JA) (b), abscisic acid (ABA) (c), and salicylic acid (SA) (d) concentrations (ng g^{-1} FW) in winter wheat (*Triticum aestivum*). The three [CO_2] treatments: squares, 680 ppm; circles, 390 ppm; triangles, 170 ppm. We harvested plants after emergence of three, six, and eight leaf sheaths, denoted by 3L, 6L, and 8L, respectively. However, before 3L, soluble sugar and SM concentrations were also affected by seed storage, independent of [CO_2]; therefore, we only show data of 6L and 8L, where open symbols represent 6L and filled symbols represent 8L. Values are the mean ±SE of three individual chambers. Note that the concentrations are expressed on a fresh weight basis and at different scales. (This figure is available in colour at *JXB* online.)

organic N compounds may be limited under elevated [CO_2] (Bloom *et al.*, 2010). Therefore, N availability, rather the JA- and JA-Ile-dependent signalling, determined the response of root SMs to elevated [CO_2].

Potential sugar signalling for IAA and JA synthesis

Soluble sugars are essential substrates for growth and metabolism (Hartmann and Trumbore, 2016), but also act as signalling molecules that interact with plant hormones to mediate plant stress responses (Rolland *et al.*, 2006; Lastdrager *et al.*, 2014). Our results revealed that accumulation of soluble sugars with increasing [CO_2] positively correlated with weighted IAA and JA concentrations, allowing our experiment to demonstrate nicely the interaction of soluble sugars and IAA and JA at the whole-plant level. It has been shown that glucose (Sairanen *et al.*, 2012) and sucrose (Lilley *et al.*, 2012) can both stimulate IAA biosynthesis and growth rates. In contrast, jasmonates reduced glucose and fructose concentrations in *Nicotiana attenuata* leaves (Machado *et al.*, 2015) and play a synergetic role with sucrose (Loreti *et al.*, 2008) and glucose (Guo *et al.*, 2013) in anthocyanin and glucosinolate biosynthesis. Hence, it is more likely that accumulation of soluble sugars at high [CO_2] stimulated whole-plant IAA and JA synthesis rather than vice versa. This sugar signalling pathway may also be a mechanism that triggers IAA and JA biosynthesis under cold, drought, and nutrient limitation, as these stresses decrease growth earlier than photosynthesis, thus allowing surplus carbon to be allocated to carbohydrates (Herms and Mattson, 1992; Palacio *et al.*, 2014). In contrast to IAA and JA, soluble sugars were not correlated with weighted ABA and SA concentrations, possibly because low [CO_2] may trigger leaf ABA and SA biosynthesis via signalling pathways independent of sugar availability, for example ROS accumulation from excess excitation energy and photorespiration (Galvez-Valdivieso *et al.*, 2009; Herrera-Vásquez *et al.*, 2015).

Light intensities (8 mol m^{-2} d^{-1}) were much lower in the greenhouse than usually occur in the field, and it might be that plants grown at ambient and elevated [CO_2] were light limited. However, the general agreement of plant responses in our study with results from field experiments downplays the importance of light limitation. Moreover, higher light intensities in the field are likely to amplify CO_2-induced responses, such as increases in assimilation, sugars, RGR, and secondary metabolites, as well as corresponding IAA and JA levels. Consequently, the suboptimal light conditions in the greenhouse underscore the robustness of our findings as the observed patterns are likely to be more pronounced in field-grown plants.

Outlook

Our study is an initial step towards unravelling whole-plant hormonal regulation of growth and defence in response to changing [CO_2] including low [CO_2]. We hypothesize that low

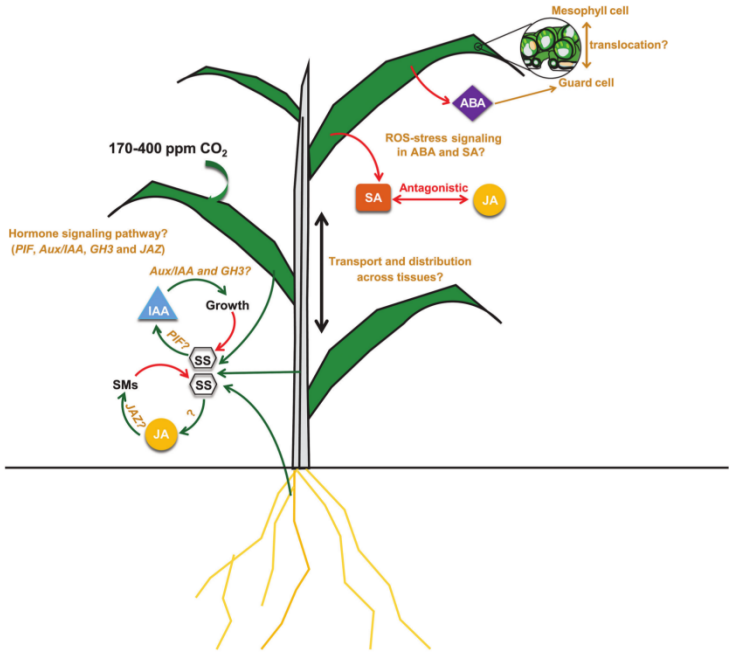

Fig. 9. Conceptual model and research needs of whole-plant hormonal regulation in response to changing [CO_2], derived from our experimental results and published literature. The leaf cross-section figure was modified from an original figure provided by Zephyris (Richard Wheeler) and Wikipedia. Increased [CO_2] stimulates photosynthesis and results in accumulation of soluble sugars at the whole-plant level which may elicit a cascade of downstream IAA and JA regulation of plant growth and defence, respectively. Increasing [CO_2] may dissipate the reducing power from the photosynthetic electron transfer chain and reduce photorespiration, which theoretically reduce ROS production (Galvez-Valdivieso *et al.*, 2009). Low [CO_2]-induced ROS accumulation may trigger ABA (Mittler and Blumwald, 2015) and SA biosynthesis (Herrera-Vásquez *et al.*, 2015), which in turn promote ROS accumulation or scavenging. Low [CO_2] could increase translocation of ABA from mesophyll chloroplast to guard cells and, as reported by Chater *et al.* (2015), the increase in guard cell ABA is sufficient to reduce stomatal conductance and density. Up-regulation of SA signalling may be associated with suppression of JA signalling (Zavala *et al.*, 2013; Sun *et al.*, 2016). Interactive signalling pathways via sugars for growth regulation and synthesis of secondary metabolites but also transport and distribution of phytohormones across tissues are still uncertain. Soluble sugars may stimulate IAA via the *PIF* family of transcription factors (Lilley *et al.*, 2012; Sairanen *et al.*, 2012). Furthermore, IAA may induce the *GH3* family which in turn catalyses the conjugation of IAA to amino acids (Sauer *et al.*, 2013). IAA and JA may stimulate growth and SM production via degradation of the repressor *Aux/IAA* (Enders and Strader, 2015) and *JAZ* (Riemann *et al.*, 2015), respectively. ABA, abscisic acid; IAA, auxin; JA, jasmonic acid; *JAZ*, jasmonate ZIM-domain protein; *PIF*, phytochrome-interacting factor; ROS, reactive oxygen species; SA, salicylic acid; SMs, secondary metabolites; SS, soluble sugars. Green arrows indicate positive, red negative, and brown uncertain.

[CO_2]-induced changes in ROS play important roles in leaf ABA and SA signalling, but this must be specifically addressed in future low [CO_2] studies. Hormones are highly interactive (Peleg and Blumwald, 2011), and therefore interactions between hormones, such as JA and SA, will help to establish a conceptual framework for the complex hormonal regulatory mechanisms of plant response to changing [CO_2] (Fig. 9).

Further progress in our understanding of hormonal whole-plant growth regulation can be achieved by combining measurements of bulk tissue hormone concentrations with investigations on hormone distribution and translocation across different tissues/organs. For example, root growth and development is regulated by auxin that has been synthesized in the shoot apex and transported to root tips to result in local auxin concentration peaks (Peer *et al.*, 2011). Similarly, ABA is stored mainly in the mesophyll cell, but a recent study shows that only ABA concentrations in guard cells control stomatal responses to elevated [CO_2] (Chater *et al.*, 2015). Experiments with mutants will provide more direct evidence for causality in hormonal regulation, and future studies at the transcriptional level should focus on biosynthetic and, in particular, responsive genes involved in hormonal signalling pathways. For example, soluble sugars may stimulate IAA via the phytochrome-interacting factor (PIF) family of transcription factors (Lilley *et al.*, 2012; Sairanen *et al.*, 2012). Auxin-responsive *GH3* (Du *et al.*, 2012, 2013) and *Aux/IAA* genes (Jung *et al.*, 2015), and the JA-responsive jasmonate ZIM-domain (JAZ) gene family (Du *et al.*, 2013; Riemann *et al.*, 2015) are signalling repressors and have been shown to be involved in drought and cold tolerance.

Acknowledgements

The authors thank Olaf Kolle, Waldemar Ziegler, and René Schwalbe for their assistance in [CO_2] manipulation, Savoyane Lambert and Iris Kuhlmann for their assistance in sample processing, and Jessica Heublein for the measurements of soluble sugars. We also thank Susan Trumbore and Jonathan Gershenzon for their support with the measurements of secondary metabolites and phytohormones. J.H. was funded by Chinese Scholarship Council and Max Planck Institute.

References

Achard P, Cheng H, De Grauwe L, Decat J, Schoutteten H, Moritz T, Van Der Straeten D, Peng J, Harberd NP. 2006. Integration of plant

responses to environmentally activated phytohormonal signals. Science **311,** 91–94.

Albacete A, Ghanem ME, Martínez-Andújar C, Acosta M, Sánchez-Bravo J, Martínez V, Lutts S, Dodd IC, Pérez-Alfocea F. 2008. Hormonal changes in relation to biomass partitioning and shoot growth impairment in salinized tomato (*Solanum lycopersicum* L.) plants. Journal of Experimental Botany **59,** 4119–4131.

Ballaré CL. 2014. Light regulation of plant defense. Annual Review of Plant Biology **65,** 335–363.

Bloom AJ, Burger M, Rubio Asensio JS, Cousins AB. 2010. Carbon dioxide enrichment inhibits nitrate assimilation in wheat and *Arabidopsis*. Science **328,** 899–903.

Casal JJ. 2013. Photoreceptor signaling networks in plant responses to shade. Annual Review of Plant Biology **64,** 403–427.

Chater C, Peng K, Movahedi M, *et al*. 2015. Elevated CO_2-induced responses in stomata require ABA and ABA signaling. Current Biology **25,** 2709–2716.

Chater CC, Oliver J, Casson S, Gray JE. 2014. Putting the brakes on: abscisic acid as a central environmental regulator of stomatal development. New Phytologist **202,** 376–391.

Cubasch U, Wuebbles D, Chen D, Facchini MC, Frame D, Mahowald N, Winther J-G. 2013. Introduction. In: Stocker TF, Qin D, Plattner G-K, Tignor M, Allen SK, Boschung J, Nauels A, Xia Y, Bex V, Midgley PM, eds. *Climate change 2013: the physical science basis. Contribution of Working Group I to the Fifth Assessment Report of the Intergovernmental Panel on Climate Change*. Cambridge: Cambridge University Press, 119–158.

Du H, Liu H, Xiong L. 2013. Endogenous auxin and jasmonic acid levels are differentially modulated by abiotic stresses in rice. Frontiers in Plant Science **4,** 397.

Du H, Wu N, Fu J, Wang S, Li X, Xiao J, Xiong L. 2012. A GH3 family member, OsGH3-2, modulates auxin and abscisic acid levels and differentially affects drought and cold tolerance in rice. Journal of Experimental Botany **63,** 6467–6480.

Enders TA, Strader LC. 2015. Auxin activity: past, present, and future. American Journal of Botany **102,** 180–196.

Erb M, Meldau S, Howe GA. 2012. Role of phytohormones in insect-specific plant reactions. Trends in Plant Science **17,** 250–259.

Franks PJ, Adams MA, Amthor JS, *et al*. 2013. Sensitivity of plants to changing atmospheric CO_2 concentration: from the geological past to the next century. New Phytologist **197,** 1077–1094.

Galvez-Valdivieso G, Fryer MJ, Lawson T, *et al*. 2009. The high light response in Arabidopsis involves ABA signaling between vascular and bundle sheath cells. The Plant Cell **21,** 2143–2162.

Gerhart LM, Ward JK. 2010. Plant responses to low [CO2] of the past. New Phytologist **188,** 674–695.

Gundlach H, Müller MJ, Kutchan TM, Zenk MH. 1992. Jasmonic acid is a signal transducer in elicitor-induced plant cell cultures. Proceedings of the National Academy of Sciences, USA **89,** 2389–2393.

Guo R, Shen W, Qian H, Zhang M, Liu L, Wang Q. 2013. Jasmonic acid and glucose synergistically modulate the accumulation of glucosinolates in *Arabidopsis thaliana*. Journal of Experimental Botany **64,** 5707–5719.

Hachiya T, Sugiura D, Kojima M, Sato S, Yanagisawa S, Sakakibara H, Terashima I, Noguchi K. 2014. High CO_2 triggers preferential root growth of *Arabidopsis thaliana* via two distinct systems under low pH and low N stresses. Plant and Cell Physiology **55,** 269–280.

Hartmann H, McDowell NG, Trumbore S. 2015. Allocation to carbon storage pools in Norway spruce saplings under drought and low CO_2. Tree Physiology **35,** 243–252.

Hartmann H, Trumbore S. 2016. Understanding the roles of nonstructural carbohydrates in forest trees—from what we can measure to what we want to know. New Phytologist **211,** 386–403.

Hartmann H, Ziegler W, Kolle O, Trumbore S. 2013. Thirst beats hunger—declining hydration during drought prevents carbon starvation in Norway spruce saplings. New Phytologist **200,** 340–349.

Herms DA, Mattson WJ. 1992. The dilemma of plants: to grow or defend. Quarterly Review of Biology **67,** 283–335.

Herrera-Vásquez A, Salinas P, Holuigue L. 2015. Salicylic acid and reactive oxygen species interplay in the transcriptional control of defense genes expression. Frontiers in Plant Science **6,** 171.

Hoagland DR, Arnon DI. 1950. The water culture method for growing plants without soil. California Agricultural Experiment Station Circular **347,** 1–32.

Horbowicz M, Kosson R, Wiczkowski W, Koczkodaj D, Mitrus J. 2011. The effect of methyl jasmonate on accumulation of 2-phenylethylamine and putrescine in seedlings of common buckwheat (*Fagopyrum esculentum*). Acta Physiologiae Plantarum **33,** 897–903.

Huang J, Hammerbacher A, Forkelová L, Hartmann H. 2016. Release of resource constraints allows greater carbon allocation to secondary metabolites and storage in winter wheat. Plant, Cell & Environment. doi:10.1111/pce.12885.

Jung H, Lee DK, Choi YD, Kim JK. 2015. OsIAA6, a member of the rice Aux/IAA gene family, is involved in drought tolerance and tiller outgrowth. Plant Science **236,** 304–312.

Kazan K. 2013. Auxin and the integration of environmental signals into plant root development. Annals of Botany **112,** 1655–1665.

Kelly G, Moshelion M, David-Schwartz R, Halperin O, Wallach R, Attia Z, Belausov E, Granot D. 2013. Hexokinase mediates stomatal closure. The Plant Journal **75,** 977–988.

Khan GA, Vogiatzaki E, Glauser G, Poirier Y. 2016. Phosphate deficiency induces the jasmonate pathway and enhances resistance to insect herbivory. Plant Physiology **171,** 632–644.

Khan MI, Fatma M, Per TS, Anjum NA, Khan NA. 2015. Salicylic acid-induced abiotic stress tolerance and underlying mechanisms in plants. Frontiers in Plant Science **6,** 462.

Koo AJ, Howe GA. 2012. Catabolism and deactivation of the lipid-derived hormone jasmonoyl-isoleucine. Frontiers in Plant Science **3,** 19.

Kramell R, Schmidt J, Schneider G, Sembdner G, Schreiber K. 1988. Synthesis of n-(jasmonoyl)amino acid conjugates. Tetrahedron **44,** 5791–5807.

Lake JA, Woodward FI. 2008. Response of stomatal numbers to CO_2 and humidity: control by transpiration rate and abscisic acid. New Phytologist **179,** 397–404.

Lastdrager J, Hanson J, Smeekens S. 2014. Sugar signals and the control of plant growth and development. Journal of Experimental Botany **65,** 799–807.

León P, Sheen J. 2003. Sugar and hormone connections. Trends in Plant Science **8,** 110–116.

Lilley JL, Gee CW, Sairanen I, Ljung K, Nemhauser JL. 2012. An endogenous carbon-sensing pathway triggers increased auxin flux and hypocotyl elongation. Plant Physiology **160,** 2261–2270.

Ljung K, Bhalerao RP, Sandberg G. 2001. Sites and homeostatic control of auxin biosynthesis in *Arabidopsis* during vegetative growth. The Plant Journal **28,** 465–474.

Loreti E, Povero G, Novi G, Solfanelli C, Alpi A, Perata P. 2008. Gibberellins, jasmonate and abscisic acid modulate the sucrose-induced expression of anthocyanin biosynthetic genes in *Arabidopsis*. New Phytologist **179,** 1004–1016.

Machado RA, Arce CC, Ferrieri AP, Baldwin IT, Erb M. 2015. Jasmonate-dependent depletion of soluble sugars compromises plant resistance to *Manduca sexta*. New Phytologist **207,** 91–105.

McDowell NG, White S, Pockman WT. 2008. Transpiration and stomatal conductance across a steep climate gradient in the southern Rocky Mountains. Ecohydrology **1,** 193–204.

Merilo E, Laanemets K, Hu H, *et al*. 2013. PYR/RCAR receptors contribute to ozone-, reduced air humidity-, darkness-, and CO2-induced stomatal regulation. Plant Physiology **162,** 1652–1668.

Miersch O, Neumerkel J, Dippe M, Stenzel I, Wasternack C. 2008. Hydroxylated jasmonates are commonly occurring metabolites of jasmonic acid and contribute to a partial switch-off in jasmonate signaling. New Phytologist **177,** 114–127.

Mittler R, Blumwald E. 2015. The roles of ROS and ABA in systemic acquired acclimation. The Plant Cell **27,** 64–70.

Moheb A, Ibrahim RK, Roy R, Sarhan F. 2011. Changes in wheat leaf phenolome in response to cold acclimation. Phytochemistry **72,** 2294–2307.

Nakamura Y, Mithöfer A, Kombrink E, Boland W, Hamamoto S, Uozumi N, Tohma K, Ueda M. 2011. 12-Hydroxyjasmonic acid

glucoside is a COI1-JAZ-independent activator of leaf-closing movement in *Samanea saman*. Plant Physiology **155,** 1226–1236.

Niu Y, Jin C, Jin G, Zhou Q, Lin X, Tang C, Zhang Y. 2011. Auxin modulates the enhanced development of root hairs in *Arabidopsis thaliana* (L.) Heynh. under elevated CO(2). Plant, Cell and Environment **34,** 1304–1317.

Oikawa A, Ishihara A, Iwamura H. 2002. Induction of HDMBOA-Glc accumulation and DIMBOA-Glc 4-O-methyltransferase by jasmonic acid in poaceous plants. Phytochemistry **61,** 331–337.

Osakabe Y, Yamaguchi-Shinozaki K, Shinozaki K, Tran LS. 2014. ABA control of plant macroelement membrane transport systems in response to water deficit and high salinity. New Phytologist **202,** 35–49.

Palacio S, Hoch G, Sala A, Körner C, Millard P. 2014. Does carbon storage limit tree growth? New Phytologist **201,** 1096–1100.

Peer WA, Blakeslee JJ, Yang H, Murphy AS. 2011. Seven things we think we know about auxin transport. Molecular Plant **4,** 487–504.

Peleg Z, Blumwald E. 2011. Hormone balance and abiotic stress tolerance in crop plants. Current Opinion in Plant Biology **14,** 290–295.

Piñero MC, Houdusse F, Garcia-Mina JM, Garnica M, Del Amor FM. 2014. Regulation of hormonal responses of sweet pepper as affected by salinity and elevated CO2 concentration. Physiologia Plantarum **151,** 375–389.

R Development Core Team. 2014. R: a language and environment for statistical computing. Vienna, Austria: R Foundation for Statistical Computing. http://www.r-project.org.

Raessler M, Wissuwa B, Breul A, Unger W, Grimm T. 2010. Chromatographic analysis of major non-structural carbohydrates in several wood species—an analytical approach for higher accuracy of data. Analytical Methods **2,** 532–538.

Riemann M, Dhakarey R, Hazman M, Miro B, Kohli A, Nick P. 2015. Exploring jasmonates in the hormonal network of drought and salinity responses. Frontiers in Plant Science **6,** 1077.

Rolland F, Baena-Gonzalez E, Sheen J. 2006. Sugar sensing and signaling in plants: conserved and novel mechanisms. Annual Review of Plant Biology **57,** 675–709.

Rowe JH, Topping JF, Liu J, Lindsey K. 2016. Abscisic acid regulates root growth under osmotic stress conditions via an interacting hormonal network with cytokinin, ethylene and auxin. New Phytologist **211,** 225–239.

Sairanen I, Novák O, Pěnčík A, Ikeda Y, Jones B, Sandberg G, Ljung K. 2012. Soluble carbohydrates regulate auxin biosynthesis via PIF proteins in *Arabidopsis*. The Plant Cell **24,** 4907–4916.

Sauer M, Robert S, Kleine-Vehn J. 2013. Auxin: simply complicated. Journal of Experimental Botany **64,** 2565–2577.

Schnyder H. 1992. Long-term steady-state labelling of wheat plants by use of natural (13)CO 2/(12)CO 2 mixtures in an open, rapidly turned-over system. Planta **187,** 128–135.

Sun YC, Guo HJ, Ge F. 2016. Plant–aphid interactions under elevated CO2: some cues from aphid feeding behavior. Frontiers in Plant Science **7,** 10.

Teng N, Wang J, Chen T, Wu X, Wang Y, Lin J. 2006. Elevated CO2 induces physiological, biochemical and structural changes in leaves of *Arabidopsis thaliana*. New Phytologist **172,** 92–103.

Thines B, Katsir L, Melotto M, *et al*. 2007. JAZ repressor proteins are targets of the SCF(COI1) complex during jasmonate signalling. Nature **448,** 661–665.

Troufflard S, Mullen W, Larson TR, Graham IA, Crozier A, Amtmann A, Armengaud P. 2010. Potassium deficiency induces the biosynthesis of oxylipins and glucosinolates in *Arabidopsis thaliana*. BMC Plant Biology **10,** 172.

Vadassery J, Reichelt M, Hause B, Gershenzon J, Boland W, Mithöfer A. 2012. CML42-mediated calcium signaling coordinates responses to Spodoptera herbivory and abiotic stresses in *Arabidopsis*. Plant Physiology **159,** 1159–1175.

Valluru R, Davies WJ, Reynolds MP, Dodd IC. 2016. Foliar abscisic acid-to-ethylene accumulation and response regulate shoot growth sensitivity to mild drought in wheat. Frontiers in Plant Science **7,** 461.

Wang Y, Du S-T, Li L-L, Huang L-D, Fang P, Lin X-Y, Zhang Y-S, Wang H-L. 2009. Effect of CO2 elevation on root growth and its relationship with indole acetic acid and ethylene in tomato seedlings. Pedosphere **19,** 570–576.

Wojakowska A, Perkowski J, Góral T, Stobiecki M. 2013. Structural characterization of flavonoid glycosides from leaves of wheat (*Triticum aestivum* L.) using LC/MS/MS profiling of the target compounds. Journal of Mass Spectrometry **48,** 329–339.

Wouters FC, Reichelt M, Glauser G, Bauer E, Erb M, Gershenzon J, Vassão DG. 2014. Reglucosylation of the benzoxazinoid DIMBOA with inversion of stereochemical configuration is a detoxification strategy in lepidopteran herbivores. Angewandte Chemie **126,** 11502–11506.

Xu Z, Jiang Y, Zhou G. 2015. Response and adaptation of photosynthesis, respiration, and antioxidant systems to elevated CO2 with environmental stress in plants. Frontiers in Plant Science **6,** 701.

Zavala JA, Nabity PD, DeLucia EH. 2013. An emerging understanding of mechanisms governing insect herbivory under elevated CO_2. Annual Review of Entomology **58,** 79–97.

Zhang SW, Li CH, Cao J, Zhang YC, Zhang SQ, Xia YF, Sun DY, Sun Y. 2009. Altered architecture and enhanced drought tolerance in rice via the down-regulation of indole-3-acetic acid by TLD1/OsGH3.13 activation. Plant Physiology **151,** 1889–1901.

CHAPTER 4

New Phytologist Research

Eyes on the future – evidence for trade-offs between growth, storage and defense in Norway spruce

Jianbei Huang[1], Almuth Hammerbacher[2,3], Alexander Weinhold[4], Michael Reichelt[2], Gerd Gleixner[1], Thomas Behrendt[1], Nicole M. van Dam[4,5], Anna Sala[6], Jonathan Gershenzon[2], Susan Trumbore[1] and Henrik Hartmann[1]

[1]Max Planck Institute for Biogeochemistry, Hans-Knöll-Str. 10, 07745 Jena, Germany; [2]Max Planck Institute for Chemical Ecology, Hans-Knöll-Str. 8, 07745 Jena, Germany; [3]Department of Zoology and Entomology, Forestry and Agricultural Biotechnology Institute, University of Pretoria, Private Bag X20, 0028 Pretoria, South Africa; [4]German Centre for Integrative Biodiversity Research, Deutscher Platz 5e, 04103 Leipzig, Germany; [5]Institute of Biodiversity, Friedrich Schiller University, Dornburger-Str. 159, 07743 Jena, Germany; [6]Division of Biological Sciences, The University of Montana, Missoula, MT 59812, USA

Author for correspondence:
Jianbei Huang
Tel: +49 3641 576150
Email: hjianbei@bgc-jena.mpg.de

Received: *26 July 2018*
Accepted: *28 September 2018*

New Phytologist (2018)
doi: 10.1111/nph.15522

Key words: biogenic volatile organic compounds (BVOCs), carbon allocation, carbon limitation, CO_2, growth–defense trade-offs, nonstructural carbohydrate (NSC) storage, Norway spruce (*Picea abies*), secondary metabolites (SM).

Summary

- Carbon (C) allocation plays a central role in tree responses to environmental changes. Yet, fundamental questions remain about how trees allocate C to different sinks, for example, growth vs storage and defense.
- In order to elucidate allocation priorities, we manipulated the whole-tree C balance by modifying atmospheric CO_2 concentrations [CO_2] to create two distinct gradients of declining C availability, and compared how C was allocated among fluxes (respiration and volatile monoterpenes) and biomass C pools (total biomass, nonstructural carbohydrates (NSC) and secondary metabolites (SM)) in well-watered Norway spruce (*Picea abies*) saplings. Continuous isotope labelling was used to trace the fate of newly-assimilated C.
- Reducing [CO_2] to 120 ppm caused an aboveground C compensation point (i.e. net C balance was zero) and resulted in decreases in growth and respiration. By contrast, soluble sugars and SM remained relatively constant in aboveground young organs and were partially maintained with a constant allocation of newly-assimilated C, even at expense of root death from C exhaustion.
- We conclude that spruce trees have a conservative allocation strategy under source limitation: growth and respiration can be downregulated to maintain 'operational' concentrations of NSC while investing newly-assimilated C into future survival by producing SM.

Introduction

Trees are long-lived sessile organisms that adjust their metabolic processes to survive under a rapidly changing climate (Trumbore *et al.*, 2015). Carbon (C) plays a fundamental role in plant metabolism due to its ability to bond with hydrogen and oxygen, as well as many other elements, to form primary and secondary metabolites (SM). Thus, studying 'the fate of C' in plant metabolism is crucial for understanding tree responses to environmental change (Atkin, 2015). C allocation is thought to be driven by the C balance between supply (source) and demand (sink). Changes in resource availability such as CO_2, light, temperature, nutrients and water (Fatichi *et al.*, 2014), may in turn influence source and sink activity and thus indirectly control plant C allocation. Of particular interest is the atmospheric CO_2 concentration [CO_2], which directly influences source activity but not sink activity. Manipulations of [CO_2] thus allow investigations on the roles of source activity in C allocation relative to other limiting factors. For example, at high [CO_2], when C is nonlimiting, growth may be limited by the availability of nutrients (Lewis *et al.*, 2010; Reich *et al.*, 2014) or water (Reich *et al.*, 2014; Faralli *et al.*, 2017). By contrast, at low [CO_2], photosynthesis and growth are strongly C-limited (Lewis *et al.*, 2010; Schmid *et al.*, 2017). The latter has been the case in trees under preindustrial concentrations of 280 ppm [CO_2] or glacial maximum concentrations of 170 ppm [CO_2] (Gerhart *et al.*, 2012), and the exposure and survival of trees during low CO_2 periods suggests strong ability to optimize C allocation strategies. However, it remains unclear how changing [CO_2] and resulting alteration of C availability may alter plant allocation strategies; for example, whether allocation to storage and defence that are essential for survival comes at the cost of other sinks like growth and its associated respiratory requirements. Such information will provide mechanistic insight into plant response to C availability under the influences of environmental constraints (e.g. long-term severe drought, cold and shading) as well as of biotic stress.

Nonstructural carbohydrates (NSC) are primary metabolites and serve multiple functions such as storage, transport of C (and

energy) and osmotic adjustment (Dietze *et al.*, 2014; Hartmann & Trumbore, 2016). Moderate C limitation induced by reducing [CO_2] to 280 ppm (Ayub *et al.*, 2011) or 170 ppm (Huang *et al.*, 2017a) decreased total NSC (in particular starch) whereas respiration rate remained constant, indicating that NSC are remobilized to meet respiratory demand. By contrast, under extremely limiting [CO_2] (40 ppm, Hartmann *et al.*, 2013) and under complete shading (Sevanto *et al.*, 2014; Fischer *et al.*, 2015), respiration decreased over time along with NSC reserves, suggesting that respiration may be downregulated to reduce the consumption of NSC storage and thereby prolong survival. Hence, respiration can be fuelled by NSC storage but only up to a threshold below which long-term survival is at risk. Likewise, there has been an active debate about whether growth can be limited by NSC storage in order to ensure future survival under drought and cold stress (Sala *et al.*, 2012; Wiley & Helliker, 2012; Palacio *et al.*, 2014). Drought and cold decrease growth (C demand) earlier and to a greater degree than photosynthesis (C supply). This leads plants to accumulate C which is stored as NSC pools through an 'overflow' mechanism – namely, when C is available in excess of sink demands (*sensu* accumulation; Chapin *et al.*, 1990). By contrast, recent studies have provided evidence that NSC may be prioritized over growth under defoliation (Wiley *et al.*, 2017a), drought (Galiano *et al.*, 2017) and low [CO_2] (Hartmann *et al.*, 2015), suggesting a trade-off between storage and growth (*sensu* reserve formation; Chapin *et al.*, 1990).

Secondary metabolites (SM) are compounds not directly involved in primary metabolic activities (e.g. growth and reproduction). Often SM fulfil important functions such as detoxification (Neilson *et al.*, 2013), anti-herbivore (Mithöfer & Boland, 2012) and anti-pathogen defense (Ullah *et al.*, 2017; Hammerbacher *et al.*, 2018). The biosynthesis of these compounds may be costly when resources are limited because they divert resources away from other sinks, such as growth. An assumption of the C–nutrient balance hypothesis (Bryant *et al.*, 1983) and the growth–differentiation balance hypothesis (Herms & Mattson, 1992) is that allocation to SM depends on the availability of NSC, which in turn depends on resource availability and the balance of C to nitrogen. They postulate that the process is driven by the balance between C supply via photosynthesis and C demand for growth. Such hypotheses are supported by the decrease in SM under shading (Roberts & Paul, 2006). However, shading results in negative C balance where growth is also strongly limited, making it difficult to determine the trade-offs between SM and growth. In addition, shading may also stimulate growth (i.e. allocation) via phytochromes (Casal, 2013) and thus suppress SM production, independent of C availability.

Unlike SM stored in tissues, responses of volatile SM (including isoprene and terpenoids) to changes in C availability have received less attention. This is despite the fact that they represent a considerable C investment to the plant and play important roles in protection against oxidants (Vickers *et al.*, 2009) and herbivory (Unsicker *et al.*, 2009). It is established that reducing atmospheric [CO_2] stimulates isoprene emissions (Way *et al.*, 2013). This is likely because ATP and NADPH may exceed the demands for Calvin cycle and thus reduce more carbohydrates to isoprene precursor, dimethylallyl diphosphate (Harrison *et al.*, 2013). However, it remains unclear how changes in C availability may influence emissions of monoterpenes. Given that the isoprene precursor also is used for monoterpene synthesis (Vickers *et al.*, 2009), we may expect similar effects on monoterpene emissions.

Our study aims to elucidate C allocation priorities in trees via reducing C availability. Reducing [CO_2] has been suggested to be a good approach for manipulating whole-plant C balance (Hartmann & Trumbore, 2016) without causing artificial effects on sink activities as compared to shading and defoliation. For example, severe defoliation may induce synthesis of defence compounds (Massad *et al.*, 2014), independent of C availability. We therefore exposed plants to a gradient of atmospheric [CO_2] (400, 280, 170, 120 and 50 ppm) in a step-wise fashion (Fig. 1a), and measured whole-plant C fluxes (assimilation, respiration and volatile monoterpenes) and biomass partitioning (structural biomass, NSC and SM). Continuous isotope labelling was applied to trace the allocation of the C assimilated during reduced [CO_2] into C sinks (i.e. growth, soluble sugars and phenolic compounds). We assume that pools with higher allocation priority will decline less than those with lower priority under C limitation. We also assume that any NSC and SM found in dead organs are inaccessible pools regardless of C availability.

The plant chosen for our experiments is Norway spruce (*Picea abies* L.), which survived ice age conditions in the refugia of Scandinavia (Parducci *et al.*, 2012). Given its potential longevity, we hypothesize that Norway spruce may have a conservative allocation strategy that prioritizes NSC and SM over other sinks (e.g. growth and respiration) to ensure survival during periodic stresses such as shading, defoliation and drought. Specifically, we hypothesize that (see Fig. 1b): (1) under 280 and 170 ppm [CO_2], spruce trees use accumulated NSC storage for growth and respiration whilst still having positive C balance; (2) as [CO_2] decreases and reaches a C compensation point, NSC and SM are reserved at the expense of growth and respiration, particularly in young developing leaves; (3) reducing [CO_2] to 50 ppm causes a negative C balance and thereby decreases all sink activities.

Materials and Methods

Plant material

Norway spruce clones (S21K04200232, Sweden) were initially grown in pots with soil and placed outdoors. In June 2015, one year before the experiment, *c.* 7-yr-old seedlings were pruned to fit in growth chambers and transplanted into pots filled with sand (i.e. carbon-free substrate not interfering with measurements of the C balance) and a slow-releasing inorganic fertilizer (Osmocote Start, Everris International BV, Geldermalsen, the Netherlands).

Growth chambers and [CO_2] manipulation

The study was carried out during summer 2016. Manipulation of atmospheric [CO_2] was achieved by twelve glass chambers

New Phytologist Research 3

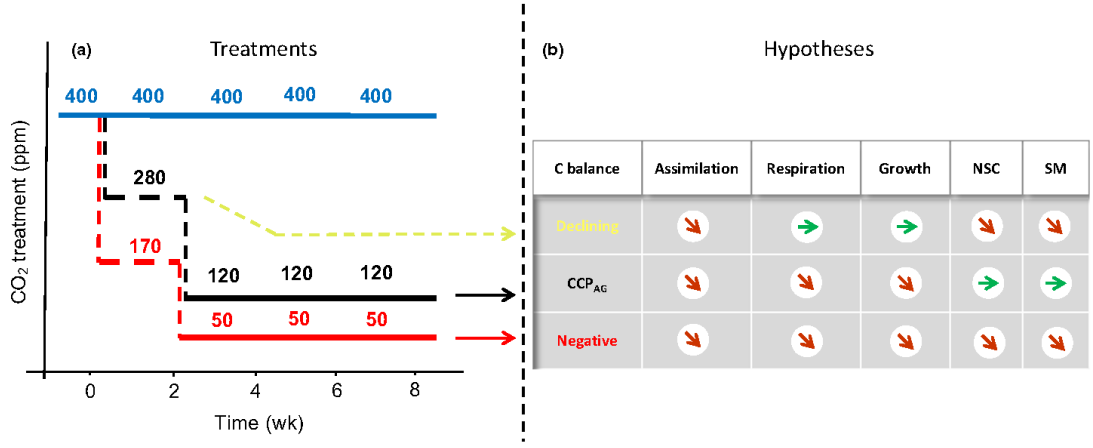

Fig. 1 (a) Atmospheric CO_2 concentration ($[CO_2]$, ppm) applied over time and (b) the predicted carbon (C) allocation trade-offs in *Picea abies* along a gradient of C availability. The treatments are shown in (a): blue line indicates 400 ppm $[CO_2]$, maintained throughout the experiment; black line indicates reducing $[CO_2]$ from 400 to 280 ppm, maintained for 2 wk (dashed line), then further to 120 ppm, maintained for 6 wk; red line indicates reducing $[CO_2]$ from 400 to 170 ppm, maintained for 2 wk (dashed line), and then further to 50 ppm, maintained for 6 wk. The predicted C balance and allocation are shown in (b): yellow dashed arrow indicates low CO_2 treatments that lead to declining C availability but C balance still maintains positive, whereas the black arrow and red arrow indicate treatments that result in aboveground C compensation point (CCP_{AG}) and negative C balance, respectively; at positive C balance but limited C supply, nonstructural carbohydrates (NSC) are used to fuel growth and respiration; at CCP_{AG}, allocation to NSC and secondary metabolites (SM) are maintained at the expense of growth and respiration in order to ensure future survival; under negative C balance, all sink activities decrease, but NSC cannot be completely depleted as they are required for osmoregulation, and SM remobilization is limited due to a lack of catabolic enzymes or limited enzymatic access. All hypothesized changes are relative to the control treatment, that is, 400 ppm $[CO_2]$.

coupled to a system allowing scrubbing ambient CO_2 from air and re-adding CO_2 from a gas tank. The facility had been built previously in the glasshouse of the Max Planck Institute for Biogeochemistry in Jena (see Hartmann *et al.*, 2013 for more details). Importantly, the CO_2 re-added to the CO_2-free air had a $\delta^{13}C$ of −38‰, whereas the outside air in which plants were grown before the experiment had $\delta^{13}C$ of *c.* −9‰. Thus, all C fixed by the plants under different $[CO_2]$ manipulations received a continuous label that could be traced through plant C metabolism. One spruce sapling was placed into every glass chamber, with roots grown in an airtight pot separated from the aboveground compartment. Supplemental glasshouse lamps were provided during the early morning and later afternoon, and purposefully adjusted to avoid high temperature stress during hot days and recovery period (2–3 d after root sampling). Light intensity was measured inside the glass chamber between 05:00 and 21:00 h, with overall means of 6.16 ± 0.72 mol m^{-2} d^{-1}, similar to previous experiments (Hartmann *et al.*, 2013; Huang *et al.*, 2017a). Twelve chambers were divided into three $[CO_2]$ treatments, thus yielding four replicates for each of the three treatments, as shown in Fig. 1(a).

Whole-plant gas exchange measurement

Aboveground and belowground CO_2 exchange were measured with Picarro® cavity ring-down spectrometers, 2131-i and 2101-i, respectively (see Hartmann *et al.*, 2013 for more details). C flux during hour *i* was assumed to be constant within the 2 h cycle and therefore calculated using the following equation:

$$\text{C flux}\ (\text{mg h}^{-1}) = ([CO_2]_{in} - [CO_2]_{out})(\mu\text{mol mol}^{-1}) \times \frac{\text{VFR}(\text{l min}^{-1}) \times 60(\text{min h}^{-1}) \times 12(\text{g mol}^{-1})}{22.4(\text{l mol}^{-1})} \times 10^{-3} \quad \text{Eqn 1}$$

($[CO_2]_{in}$ and $[CO_2]_{out}$, $[CO_2]$ of air entering and exiting the chambers, respectively; VFR, volumetric flow rate of air passing through the chamber (*c.* 22 l min^{-1} for aboveground glass chamber, and *c.* 3 l min^{-1} belowground pots); 22.4 l mol^{-1}, molar volume of gas under normal conditions). We then compute daytime assimilation, night-time respiration and belowground respiration according to the duration over which each occurred (16, 8 and 24 h, respectively).

Stem diameter and growth measurement

The basal stem diameter variation of each tree (precision 0.8 µm) was monitored continuously with a custom-made dendrometer, averaged every 10 min and recorded with a datalogger (CR23X; Campbell Scientific Inc., Logan, UT, USA). Each pot with the corresponding sapling was placed on a balance (PCB 10000-1; Kern & Sohn GmbH, Balingen, Germany) inside the growth chamber for continuously measuring the weight. To minimize noise during weighing from watering, a specific watering system was developed: the lower *c.* 2 cm of

sand were constantly immersed into water thereby wetting the upper layers of sand by capillary action. Water was constantly supplied from a separate reservoir of which the water level was kept constant using a sensor-activated valve.

Relative growth rate (RGR) of total tree fresh biomass at time i was calculated based on the initial fresh biomass at time 0 and the fresh biomass at each harvest using the following equation:

$$RGR_i = \frac{\log(M_i/M_0)}{t_i - t_0} \quad \text{Eqn 2}$$

(M_i, fresh biomass of the tree at time t_i (Hunt, 1982)).

Sampling and biomass processing

Sampling was carried out once every 2 wk between 14:00 and 21:00 h. Approximately 10–15 g of young and old aboveground organs (needles + branches) were sampled using a sharp branch cutter, immediately weighed and then frozen in liquid nitrogen. Fine roots were sampled using scissors, washed and dried before freezing in liquid nitrogen. All fresh tissues were transferred and stored in a freezer (−80°C) until further processing. Before metabolite analysis, fresh needles and branches were separated and homogenized in liquid nitrogen in a mortar. Part of the samples was weighed, freeze-dried and weighed again for determination of the relative water content. Freeze-dried tissues were then ground to fine powder using a ball mill (Retsch® MM400, Haan, Germany) and stored at −20°C until analysis of soluble sugars, starch and phenolic compounds. The other samples were ground with liquid nitrogen using a mortar and pestle, and stored at −80°C until analysis of monoterpenes. At the end of the experiment, all trees were destructively harvested for determination of dry biomass of each organ (leaves, branches and roots). From Week 8 onwards, we observed that all old needles and most young needles exposed to 50 ppm [CO_2] withered and began to fall, all fine roots had died and this resulted in *c.* 90% reduction in whole-plant aboveground transpiration compared to 400 and 120 ppm [CO_2].

Soluble sugars and starch analysis

Soluble sugars (glucose, sucrose and fructose) were extracted from freeze-dried samples with distilled water at 65°C and determined with High Performance Liquid Chromatography–Pulsed Amperometric Detection (HPLC-PAD), as described by Hartmann *et al.* (2013). For starch determination, the pellet from soluble sugar extraction was digested with a-amylase and amyloglucosidase (Sigma-Aldrich), followed by glucose determination with HPLC-PAD (S. Landhaeusser, unpublished).

Phenolic compounds analysis

Phenolic compounds were extracted from 30 mg freeze-dried samples in methanol containing 20 μg ml^{-1} of apigenin-7-glucoside (Carl Roth GmbH, Karlsruhe, Germany) as an internal standard (see Huang *et al.* (2017a) for extraction procedures), and then analysed with a HPLC coupled to a tandem mass spectrometer as described previously (Hammerbacher *et al.*, 2014). Catechin, gallocatechin, proanthocyanidin B1, astringin and isorhapontin were identified by comparison of retention time and mass spectra with standards, and then quantified using the experimentally determined response factors relative to an internal standard (Supporting Information Table S1). The sum of these compounds was reported as phenolic compounds. Note that quantification of phenolic compounds was restricted to the availability of standards (Hammerbacher *et al.*, 2014).

Monoterpene analysis

Approximately 100 mg of fresh samples was extracted with 1 ml tert-Butyl methyl ether (TBME) containing 30 μg ml^{-1} 1,9-decadiene (Sigma-Aldrich) as an internal standard. The extraction followed the same procedure used for phenolic compounds, but the supernatant was dehydrated by filtering through a Pasteur pipette filled with glass wool and anhydrous $MgSO_4$. Monoterpenes were identified by GC-MS and quantified with Gas chromatography-Flame Ionization Detector (GC-FID), as described previously by Martin *et al.* (2002) with slight modifications. α-pinene, camphene, β-pinene, myrcene, limonene, 1,8-cineole and bornyl acetate were identified by comparison of mass spectra with of the standards or reference spectra of data bases (Wiley 275, NIST 98, Adams 2205), and quantified with relative response factors (Table S1) estimated based on the effective C number concept (Scanlon & Willis, 1985). The sum of these compounds was reported as monoterpenes.

Volatiles collection, identification and quantification

Before tissue sampling (10:00 to 14:00 h), we collected biogenic volatile organic compounds (BVOC) of the air entering and exiting the chambers by using adsorbent tubes filled with 5 mm Quarz Wool, Tenax TA 35/60, Carbograph 5TD 40/60 (Markes Environmental, Sacramento, CA, USA). The collection was operated at a flow rate of 215 ml min^{-1} for 30 min achieved by using an air sampler (SG350ex; GSA GmbH & Co. KG, Germany). The BVOC were analysed by a thermal desorption-GC-MS consisting of a thermo desorption unit (Markes, Llantrisant, UK) equipped with an auto-sampler (Markes, Ultra 50/50). For details of conditions, please see Method S1. The major BVOC including α-pinene, β-pinene, 1,8-cineole and linalool were identified by comparison of retention time and mass spectra with standards (Sigma Aldrich), and then quantified using the external calibration curves. δ-3-carene was quantified using the calibration curve of β-pinene due to lack of standard.

$\delta^{13}C$ of biomass, water-soluble C and phenolic compounds

Approximately 0.1 mg of freeze-dried samples was weighed into tin cups and analysed with an isotope-ratio-MS (ThermoFinnigan GmbH, Bremen, Germany). For $\delta^{13}C$ of

New Phytologist Research 5

water soluble C, an aliquot of hot water extract was pipetted into a tin cup and dried at 40°C. The procedure was repeated successively to achieve 0.1 mg dry samples, which were analysed for $\delta^{13}C$ as before. Solid phase extraction (SPE) was used to separate phenolic compounds from other compounds (e.g. sugars, lipids, internal standard) in the methanol extacts. Briefly, 0.5 ml methanol extact was diluted with 4.5 ml distilled water. The 5 ml mixture was then loaded onto a column (Chromabond HR-X, 45 µm, 1 ml/30 mg; Macherey-Nagel Gmbh, Germany) that was pre-conditioned by 1 ml methanol followed by 1 ml water. The column was then eluted sequentially by a gradient of methanol/water solution (v/v) from 10% to 100%. Solutions were collected and analysed with a LC-MS (Esquire 6000 ESI; Bruker Daltronics, Bremen, Germany). All sugars were washed out by 1 ml 20% methanol/water solution, whereas phenolic compounds such as catechin and gallocatechin were mainly dissolved by 35% methanol/water solution. Hence, an aliquot of 35% methanol/water elution was pipetted into a tin cup, dried at 40°C and analysed for $\delta^{13}C$ as before. All $\delta^{13}C$ values were reported relative to the international Vienna Pee Dee Belemnite (VPDB), and calculated using Eqn 3:

$$\delta^{13}C(‰) = \left[\frac{\left[\frac{^{13}C}{^{12}C}\right]_{sample}}{\left[\frac{^{13}C}{^{12}C}\right]_{VPDB}} - 1\right] \times 1000 \qquad \text{Eqn 3}$$

The precision of the measurement was < 0.1‰ based on the laboratory standard (caffeic acid: −40.46‰). Although water-soluble C may contain C from soluble sugars, amino acids and organic acids, it has been demonstrated that water-soluble C is an reliable proxy for the $\delta^{13}C$ value of soluble sugars in needles of *Pinus sylvestris* (Brandes *et al.*, 2006).

Data analysis

Each growth chamber was treated as a biological replicate ($n = 4$). All data were checked for normality and homogeneity of variances with Shapiro–Wilk test and Levene tests, respectively, and were log-transformed to meet normality and homoscedasticity as needed. Tukey's HSD ($P < 0.05$) was used to test significant differences between treatments. When values are negative and cannot be log-transformed (e.g. assimilation, stem diameter variation at 50 ppm $[CO_2]$ and $\delta^{13}C$ values), we used Wilcoxon's rank-sum test to test significant differences between treatments. To assess the significant differences in temporal trends of NSC and SM concentrations and isotope data, we used repeated-measures ANOVA after checking normality and sphericity with Shapiro–Wilk and Mauchly's tests, respectively. A Friedman test was used when assumption of normality or sphercity was violated. For data expressed as the percentage of control (400 ppm $[CO_2]$), coefficient of variation (i.e. relative standard error) was calculated for control treatment, and standard errors of lower $[CO_2]$ treatments were propagated according to error propagation rules. All statistical analysis was conducted in R (v.3.3.2; R Development Core Team, 2016).

Results

Whole-plant gas exchange

Net assimilation declined rapidly right after reducing $[CO_2]$ from 400 ppm to 280 and 170 ppm, whereas both aboveground and belowground respiration were not significantly affected (Fig. 2a,b,d). From Week 2 onwards, net assimilation at 400 ppm decreased from *c.* 600 to 300 mg C d^{-1} possibly due to glasshouse light limitation. However, net assimilation declined to < 100 mg at 120 ppm and dropped to negative values at 50 ppm $[CO_2]$ (i.e. daytime respiration exceeded gross assimilation; Fig. 2a). Likewise, respiration was significantly lower at 120 ppm than at 400 ppm ($P < 0.05$), but the decrease was proportionally more belowground (*c.* 60%) than aboveground (*c.* 40%) relative to 400 ppm (Fig. 2b,d). At 120 ppm, respiration was roughly equal to assimilation aboveground, leading to zero C gain after Week 2, which we define as aboveground C compensation point (CCP_{AG}; Fig. 2c). A further $[CO_2]$ reduction from 120 to 50 ppm reduced aboveground respiration, but had less effect on belowground respiration (Fig. 2b,d) and let to overall C loss (Fig. 2c).

Growth

During the first 2 wk, stem diameter increased at 400 ppm but not at 280 and 170 ppm. From Week 2 onwards, stem diameter remained relatively constant at 400 ppm, but showed a significant decline at 120 ppm and decreased even further at 50 ppm (Fig. 3a). By contrast, fresh biomass increments showed little difference between 400, 280 and 170 ppm during the first 2 wk. After Week 2, although biomass increased over time at 400 ppm, it remained relatively constant at 120 and 50 ppm, which were similar to each other (Fig. 3b).

Soluble sugars and starch

After reducing $[CO_2]$ from 400 to 280 and 170 ppm for 2 wk, soluble sugars declined by *c.* 0–30% in aboveground organs, and by *c.* 40% in roots (Fig. 4a–c). A rather rapid decline was observed at Week 4 in aboveground organs after reducing $[CO_2]$ from 280 and 170 to 120 and 50 ppm, respectively; after which there were no further reductions in young needles and branches ($P > 0.05$, repeated measures ANOVA or Friedman test; Fig. 4a, b). Similar effects also were observed in old organs (Fig. S1). By contrast, reducing $[CO_2]$ to 50 ppm caused a significant decline in root soluble sugars towards the end of the experiment ($P < 0.05$, repeated-measures ANOVA; Fig. 4c). Note that at 50 ppm, concentrations of soluble sugars declined to between 10 and 20 mg g^{-1} in aboveground organs, but to almost zero in roots (Fig. S2).

Reducing $[CO_2]$ from 400 to 280 and 170 ppm caused a stronger decline in aboveground starch than in soluble sugars at

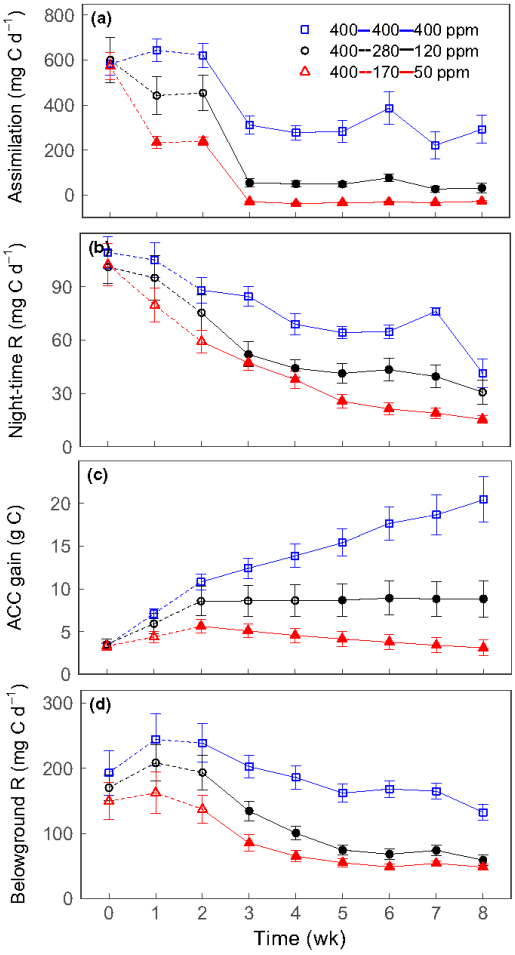

Fig. 2 Weekly aboveground (a) net carbon (C) assimilation (mg C d^{-1}), (b) night-time respiration (R; mg C d^{-1}), (c) aboveground accumulative C gain (ACC gain; g C); and (d) belowground respiration (mg C d^{-1}) in *Picea abies* for several different atmospheric CO_2 concentration ($[CO_2]$) treatments: 400 ppm $[CO_2]$ (squares, blue lines); 400–280–120 ppm $[CO_2]$ (circles, black line); 400–170–50 ppm $[CO_2]$ (triangles, red lines). The black and red dashed lines indicate reducing $[CO_2]$ from 400 to 280 ppm and from 400 to 170 ppm, respectively, maintained for 2 wk; the black and red solid lines indicate a further reduction from 280 to 120 ppm and from 170 to 50 ppm, respectively, maintained for 6 wk. Values are the means (mg C) of four individual chambers; error bars represent ± SE. Significant differences between the two lower $[CO_2]$ treatments and ambient $[CO_2]$ (400 ppm) are indicated by closed symbols ($P < 0.05$, Tukey's HSD or Wilcoxon's rank-sum test).

Week 2 (Fig. 4d,e). Starch concentrations continuously declined after a further reduction from 280 and 170 ppm to 120 and 50 ppm, respectively (Fig. 4d–f); at Week 8, starch concentrations in all organs declined to almost zero at 120 and 50 ppm (Fig. S2). Because concentrations of starch were much lower than of soluble

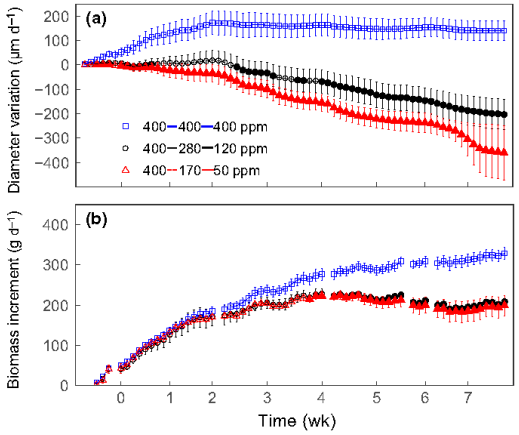

Fig. 3 Daily (a) stem diameter variation (μm d^{-1}) and (b) biomass increment (g d^{-1}) in *Picea abies* for the different atmospheric CO_2 concentration ($[CO_2]$) treatments: 400 ppm $[CO_2]$ (squares); 400–280–120 ppm $[CO_2]$ (circles); 400–170–50 ppm $[CO_2]$ (triangles). Values are the means of four individual chambers; error bars represent ± SE. Significant differences between the two lower $[CO_2]$ treatments and ambient $[CO_2]$ (400 ppm) are indicated by closed symbols ($P < 0.05$, Tukey's HSD or Wilcoxon's rank-sum test).

sugars across organs and treatments (Fig. S2), responses of total NSC (soluble sugars + starch; Fig. 4g–i) concentrations were similar to those of soluble sugars.

Phenolic compounds and monoterpenes

The response of phenolic compounds and monoterpenes to low $[CO_2]$ (expressed as a percentage of control, 400 ppm $[CO_2]$) differed among organs (Fig. 5). Reducing $[CO_2]$ from 400 to 280 and 170 ppm had no effects on phenolic compounds by Week 2 in all organs except in young branches, where there was a decline at 170 ppm (Fig. 5a–c). A further reduction to 120 ppm at Week 2 slightly decreased aboveground concentrations of phenolic compounds, but not significant relative to 400 ppm ($P > 0.05$; Fig. 5a,b). However, reducing $[CO_2]$ to 50 ppm eventually strongly decreased phenolic compounds by Week 8, by 85% and 50% in young needles and young branches, respectively, relative to 400 ppm; by contrast, there were no differences in old branches except a significant increase at Week 4 (Fig. S3). Under 50 ppm $[CO_2]$, root concentrations of phenolic compounds significantly decreased over time ($P < 0.05$; Friedman test). Note that concentrations of phenolic compounds in young needles declined to almost zero at 50 ppm $[CO_2]$ towards the end of the experiment (Fig. S4).

Aboveground concentrations of monoterpenes also were similar between 400 and 120 ppm and remained relatively constant over time ($P > 0.05$, repeated measures ANOVA or Friedman test; Fig. 5d,e). However, reducing $[CO_2]$ to 50 ppm resulted in *c.* 30–40% decrease in concentrations of monoterpenes relative to 400 ppm, although not statistically significant (Fig. 5d,e). By

New Phytologist Research 7

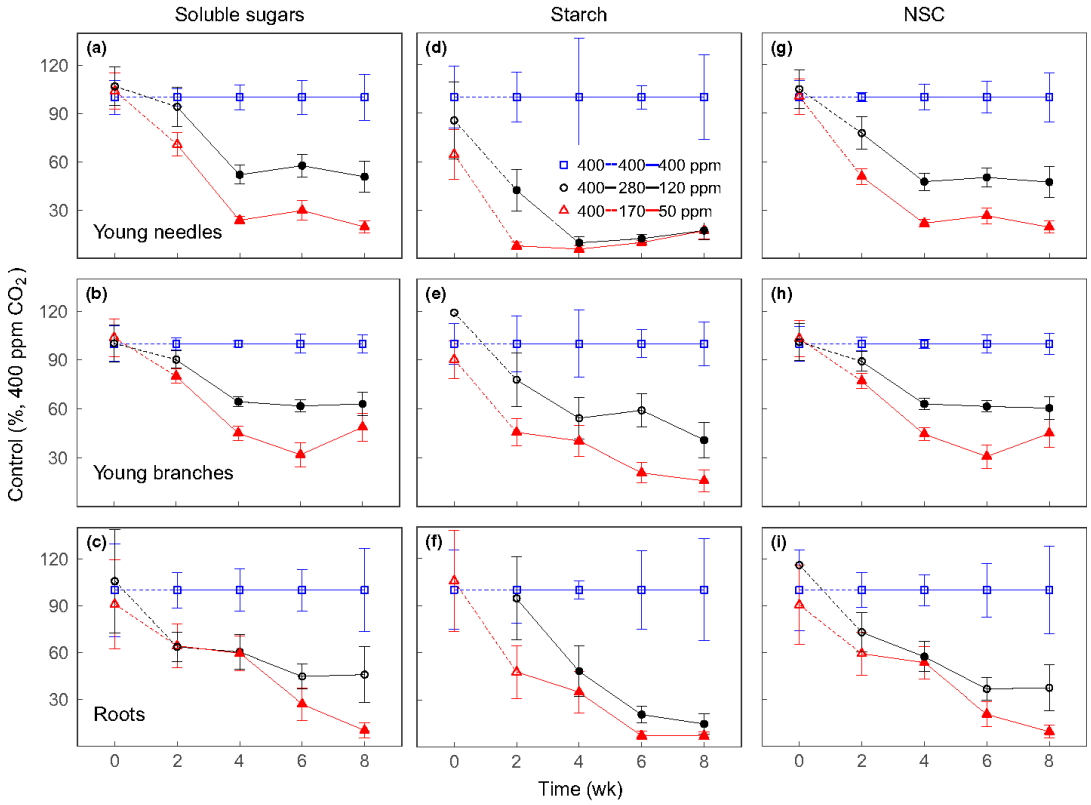

Fig. 4 Concentrations of (a–c) soluble sugars, (d–f) starch and (g–i) total nonstructural carbohydrates (NSC; soluble sugars + starch) of young needles, young branches and roots in *Picea abies* for the different atmospheric CO_2 concentration ($[CO_2]$) treatments: 400 ppm $[CO_2]$ (squares, blue line); 400–280–120 ppm $[CO_2]$ (circles, black line); 400–170–50 ppm $[CO_2]$ (triangles, red line), expressed as a percentage of control (400 ppm $[CO_2]$). The black and red dashed lines indicate reducing $[CO_2]$ from 400 to 280 ppm and from 400 to 170 ppm, respectively, maintained for 2 wk; the black and red solid lines indicate a further reduction from 280 to 120 ppm and from 170 to 50 ppm, respectively, maintained for 6 wk. Error bars at 400 ppm $[CO_2]$ represent coefficient of variation (i.e. relative SE). Error bars at 280, 170, 120 and 50 ppm $[CO_2]$ represent propagated SE. Significant differences between the two lower $[CO_2]$ treatments and ambient $[CO_2]$ (400 ppm) are calculated based on the raw concentrations, and indicated by closed symbols ($P < 0.05$, Tukey's HSD).

contrast, monoterpenes remained relatively constant in old needles and branches (Fig. S3). Root monoterpenes gradually decreased in both low $[CO_2]$ treatments which did not differ (Fig. 5f). Concentrations of phenolic compounds were generally higher than of monoterpenes across organs (Fig. S4), thereby total SM (phenolic compounds + monoterpenes; Fig. 5g–i) followed similar trends to phenolic compounds.

Unlike for monoterpenes stored in tissues, emissions of volatile monoterpenes exhibited large variations over time (Fig. 6). After Week 2, emissions of α- and β-pinene at 400 and 120 ppm $[CO_2]$ remained relatively constant and only slightly increased at Week 8, but there was a much stronger increase at 50 ppm $[CO_2]$ by Week 8, although not statistically significant compared to 400 ppm $[CO_2]$ (Fig. 6a,b). By contrast, linalool emissions declined to almost zero at 50 ppm $[CO_2]$, which were significantly < 400 ppm $[CO_2]$ at weeks 6 and 8 ($P < 0.05$; Fig. 6e). There were no clear differences in emissions of δ-3-carene, 1,8-cineole (Fig. 6c,d). The contrasting emissions of pinenes vs linalool to 50 ppm $[CO_2]$, resulted in no differences in total emissions of summed monoterpenes across $[CO_2]$ treatments (Fig. 6f).

Allocation of newly-assimilated C into biomass, water-soluble C and phenolic compounds

Before the treatments, the $\delta^{13}C$ of biomass and of water-soluble C were higher than those of phenolic compounds across organs (Fig. 7). Decreases in $\delta^{13}C$ indicate incorporation of newly-assimilated C. Reducing $[CO_2]$ from 400 to 280 and 170 ppm significantly decreased allocation of newly-assimilated C to

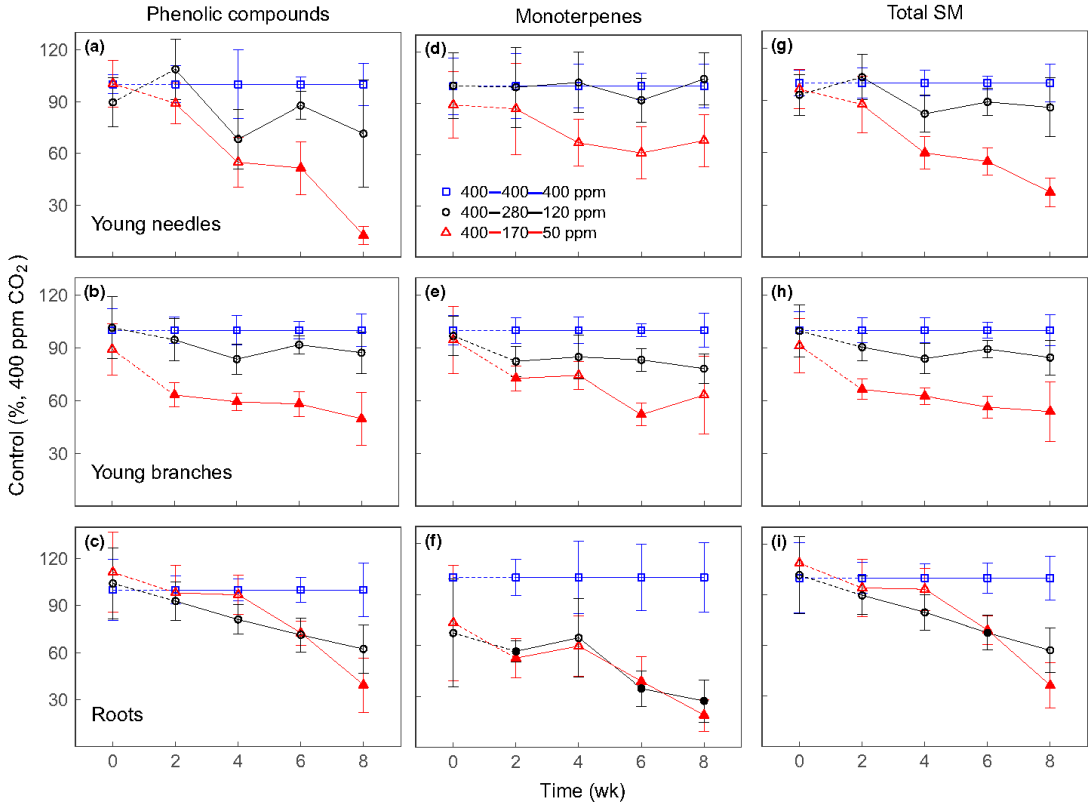

Fig. 5 Concentrations of (a–c) phenolic compounds, (d–f) monoterpenes and (g–i) total secondary metabolites (SM; phenolic compounds + monoterpenes) of young needles, young branches and roots in *Picea abies* for the different atmospheric CO_2 concentration ($[CO_2]$) treatments: 400 ppm $[CO_2]$ (squares, blue line); 400–280–120 ppm $[CO_2]$ (circles, black line); 400–170–50 ppm $[CO_2]$ (triangles, red line), expressed as a percentage of control (400 ppm $[CO_2]$). The black and red dashed lines indicate reducing $[CO_2]$ from 400 to 280 ppm and from 400 to 170 ppm, respectively, maintained for 2 wk; the black and red solid lines indicate a further reduction from 280 to 120 ppm and from 170 to 50 ppm, respectively, maintained for 6 wk. Error bars at 400 ppm $[CO_2]$ represent coefficient of variation (i.e. relative SE). Error bars at 280, 170, 120 and 50 ppm $[CO_2]$ represent propagated SE. Significant differences between the two lower $[CO_2]$ treatments and ambient $[CO_2]$ (400 ppm) are calculated based on the raw concentrations, and indicated by closed symbols ($P < 0.05$, Tukey's HSD).

biomass (bulk) and water-soluble C at Week 2 ($P < 0.05$; Fig. 7a–f). After reducing $[CO_2]$ to 120 ppm at Week 2, the $\delta^{13}C$ of biomass and water-soluble C significantly declined over time in aboveground organs ($P < 0.05$, repeated measures ANOVA or Friedman test) except for the $\delta^{13}C$ of biomass of young needles (Fig. 7a,b,d,e), indicating a continuous allocation of newly-assimilated C, but this apparently did not occur in roots (Fig. 7c,f). At 50 ppm $[CO_2]$, only minor allocation of newly-assimilated C was observed in young needles, and $\delta^{13}C$ of water-soluble C even showed an increase in young branches and roots (Fig. 7e,f).

For phenolic compounds, newly-assimilated C was observed at 280 and 170 ppm in young organs, although < 400 ppm (Fig. 7g,h); in old organs, however, there was little incorporation of newly-assimilated C (Fig. S5). After a reduction to 120 ppm at Week 2, $\delta^{13}C$ of phenolic compounds declined only slightly in young needles, but declined significantly over time in young branches ($P < 0.05$, repeated measures ANOVA; Fig. 7h), suggesting a continuous allocation of newly-assimilated C. After a reduction from 170 to 50 ppm $[CO_2]$, $\delta^{13}C$ of phenolic compounds slightly increased in young branches by Week 8 (Fig. 7h). By contrast, $\delta^{13}C$ of phenolic compounds remained relatively constant in old branches, irrespective of $[CO_2]$ treatments ($P > 0.05$, Friedman test; Fig. S5).

After reducing $[CO_2]$ from 400 to 280 and 170 ppm, assimilation strongly decreased but C balance still maintained positive; NSC decreased faster than respiration and RGR, but SM remained relatively constant (Fig. 8). A further reduction from 280 to 120 ppm $[CO_2]$ caused an aboveground C compensation

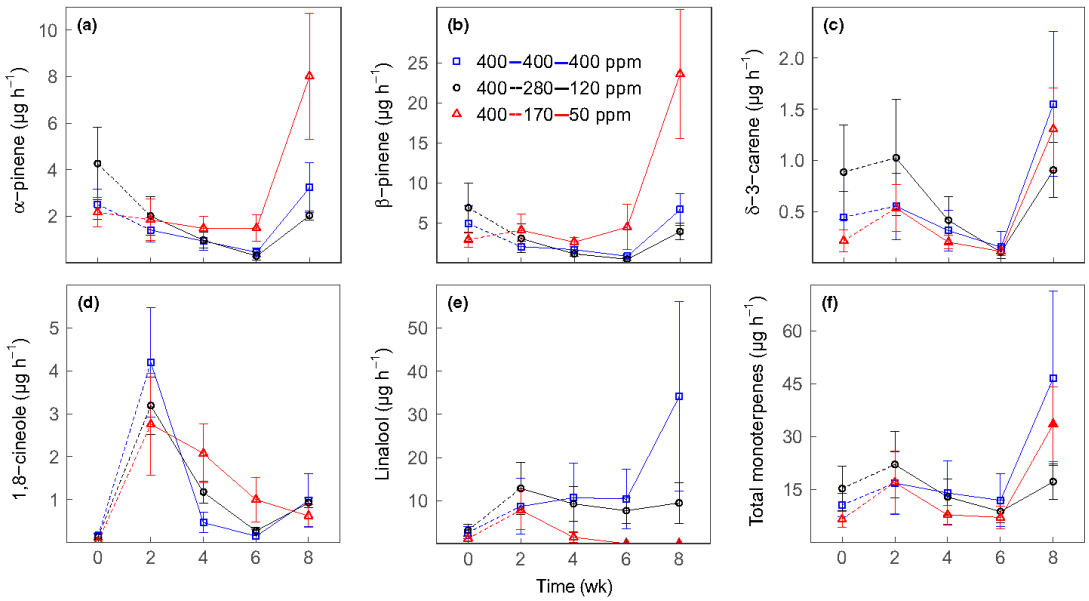

Fig. 6 Aboveground emissions (μg h^{-1}) of (a) α-pinene, (b) β-pinene, (c) δ-3-carene, (d) 1,8-cineole, (e) linalool and (f) total monoterpenes in *Picea abies* for the different atmospheric CO_2 concentration ($[CO_2]$) treatments: 400 ppm $[CO_2]$ (squares, blue lines); 400–280–120 ppm $[CO_2]$ (circles, black lines); 400–170–50 ppm $[CO_2]$ (triangles, red lines). The black and red dashed lines indicate reducing $[CO_2]$ from 400 to 280 ppm and from 400 to 170 ppm, respectively, maintained for 2 wk; the black and red solid lines indicate a further reduction from 280 to 120 ppm and from 170 to 50 ppm, respectively, maintained for 6 wk. Values are the means of four individual chambers; error bars represent ± SE. Significant differences between the two lower $[CO_2]$ treatments and ambient $[CO_2]$ (400 ppm) are indicated by close symbols ($P < 0.05$, Tukey's HSD).

point, and decreased growth more than NSC and SM. Reducing $[CO_2]$ to 50 ppm led to negative C balance, where activities of all sinks strongly declined apart from SM, which declined by only 20–30% relative to 400 ppm $[CO_2]$ (Fig. 8).

Discussion

Manipulation of the whole-tree carbon (C) balance via changing atmospheric CO_2 concentration ($[CO_2]$), coupled with application of isotopic labelling, allowed us to explore how trees allocate stored/newly-assimilated C for growth, storage and defence under different amounts of C supply. Our treatments were intended to create a situation of declining C availability to force trees into a severe resource trade-off, not necessarily to a new steady state. At aboveground C compensation point (CCP_{AG} (120 ppm), whole-plant growth decreased as root nonstructural carbohydrate (NSC) reserves declined continuously, whereas aboveground concentrations of soluble sugars initially declined but then remained constant due to a continuous allocation of newly-assimilated C. Soluble sugar concentrations further decreased under negative C balance (50 ppm), resulting in a complete depletion in roots, probably due to impeded transport of newly-assimilated C. By contrast, concentrations of secondary metabolites (SM) (phenolic compounds + monoterpenes) remained relatively constant in young organs until CCP_{AG}, which was also the case in old branches of dying trees below CCP_{AG} at Week 8. Above and at CCP_{AG}, newly-assimilated C was continuously allocated to phenolic compounds in young branches, but not in old organs. The emissions of aboveground volatile monoterpenes were unaffected by $[CO_2]$ treatments.

Downregulation of growth and respiration to maintain soluble sugars for survival

How trees build up NSC pools (i.e. accumulation vs reserve formation; Chapin *et al.*, 1990), has been hotly debated in recent years (Sala *et al.*, 2012; Wiley & Helliker, 2012; Dietze *et al.*, 2014; Palacio *et al.*, 2014). Our results showed that moderate C limitation (280 and 170 ppm $[CO_2]$) resulted in rapid declines in assimilation, leading trees to use NSC storage for maintaining growth and respiration (Fig. 8). This may indicate that NSC storage is at least partially driven by the balance between C supply and C demand – namely, accumulation (Chapin *et al.*, 1990; Hartmann & Trumbore, 2016). These responses at the whole-tree level are in agreement with results from studies on *Eucalypts* grown at 280 ppm $[CO_2]$, where leaf NSC concentrations decreased (Ayub *et al.*, 2011) yet leaf respiration (Ayub *et al.*, 2011, 2014) or growth did not (Ghannoum *et al.*, 2010).

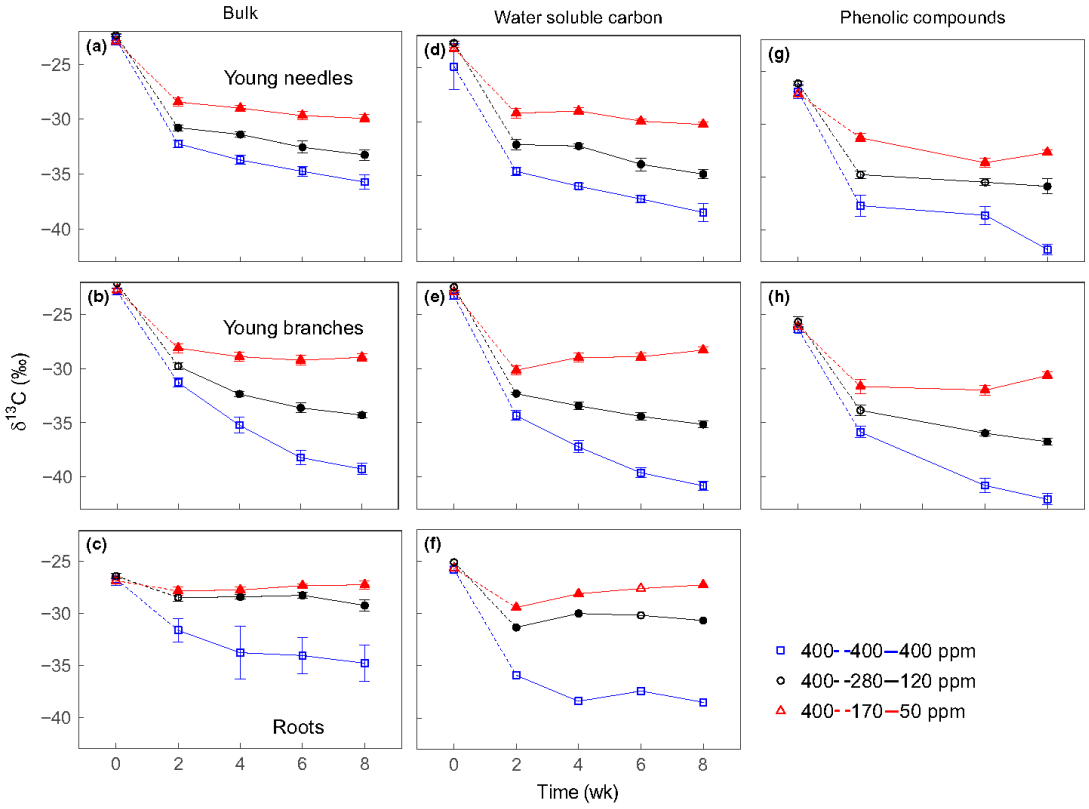

Fig. 7 $\delta^{13}C$ (‰) of (a–c) bulk tissue, (d–f) water soluble carbon and (g–i) phenolic compounds in *Picea abies* for the different atmospheric CO_2 concentration ($[CO_2]$) treatments: 400 ppm $[CO_2]$ (squares, blue lines); 400–280–120 ppm $[CO_2]$ (circles, black lines); 400–170–50 ppm $[CO_2]$ (triangles, red lines). The black and red dashed lines indicate reducing $[CO_2]$ from 400 to 280 ppm and from 400 to 170 ppm, respectively, maintained for 2 wk; the black and red solid lines indicate a further reduction from 280 to 120 ppm and from 170 to 50 ppm, respectively, maintained for 6 wk. Values are the means of four individual chambers; error bars represent ± SE. Significant differences between the two lower $[CO_2]$ treatments and ambient $[CO_2]$ (400 ppm) are indicated by closed symbols ($P < 0.05$, Tukey's HSD or Wilcoxon's rank-sum test).

A further reduction to 120 ppm (i.e. CCP_{AG}) decreased growth faster than NSC concentrations (Fig. 8), as aboveground concentrations of soluble sugars initially declined and then remained constant (Fig. 4). Soluble sugars were apparently available for metabolism because concentrations further declined when $[CO_2]$ was reduced to 50 ppm (i.e. negative C balance). This may indicate that under CCP_{AG}, soluble sugars are preferentially maintained in aboveground organs at the expense of growth. Isotope data further show continuous incorporation of newly-assimilated C into water-soluble C at CCP_{AG}, in particular in young organs (Fig. 7). This suggests that C fluxes in and out of soluble sugar pools were fine-tuned to achieve 'operational' levels. Such regulation of soluble sugar pools may represent a safety margin to avoid C exhaustion, and thus can be interpreted as reserve formation that occurred at the expense of growth (Chapin *et al.*, 1990; Hartmann & Trumbore, 2016; Martínez-Vilalta *et al.*, 2016). Similar patterns also were observed at the leaf level in Arabidopsis (Gibon *et al.*, 2009). By contrast, starch declined almost to zero at CCP_{AG}, suggesting that soluble sugars were prioritized over starch as long-term storage. Overall, total NSC responses generally support the theoretical model that NSC pools reflect two processes: accumulation that supports growth, and reserve formation that ensures future survival at the expense of immediate development.

Reducing C availability to the point where there is no net plant C gain (CCP_{AG}) may affect the sink strength of growth and respiration to different degrees in different organs. These are, in turn, reflected in the dynamics of their substrates, the soluble sugars. We found organ-specific response of growth sink strength by tracing the allocation of newly-assimilated C across organs. At CCP_{AG}, spruce invested more newly-assimilated C into growth of aboveground organs than of roots, consistent with the functional equilibrium hypothesis that resources are allocated to organs which are responsible for acquiring the most limiting

New Phytologist Research 11

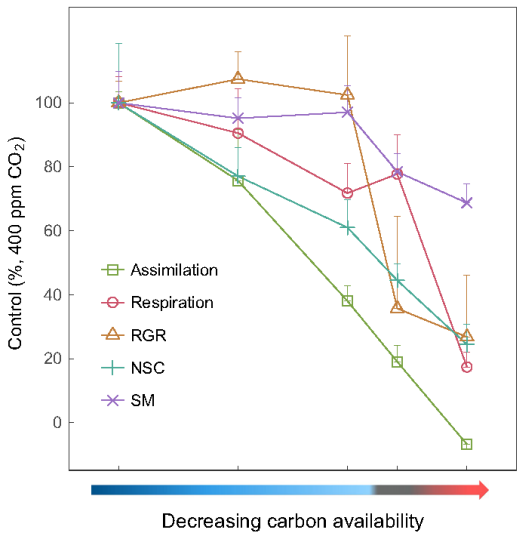

Fig. 8 Trade-offs between aboveground daytime net assimilation (squares, green line) and night-time respiration (circles, pink line), whole-tree relative growth rate (RGR, triangles, brown line), and weighted nonstructural carbohydrates (NSC; plus symbol, blue line) and secondary metabolites (SM; cross symbol, violet line) in *Picea abies* along a gradient of carbon (C) availability, expressed as a percentage of control (400 ppm atmospheric CO_2 concentration ($[CO_2]$)). The arrow below the x-axis indicates decreasing gradients of C availability, spanning from positive C balance (blue; 400, 280, 170 ppm $[CO_2]$) to the aboveground C compensation point (black; 120 ppm $[CO_2]$) and then to a negative C balance (red; 50 ppm $[CO_2]$). Whole-aboveground daytime assimilation and nighttime respiration were averaged over the last 2 d before organ sampling. Whole-tree RGR was calculated using intervals between Weeks 0 and 2, and between Weeks 2 and 6. NSC and SM concentrations were weighted by multiplying concentrations in needles, branches (averaged from young and old organs) and roots with the relative contribution of dry biomass of each organ (needles, branches and roots) that was assessed at the end of the experiment and accounting the biomass loss of organs from each sampling. The dry biomass ratio between needles, branches and roots was assumed to be constant after Week 2, as most growth occurred during the first 2 wk. Values are the means of three or four chambers; error bars at 400 ppm $[CO_2]$ represent coefficient of variation (i.e. relative SE, $n = 3$ or 4). Error bars at 280, 170, 120 and 50 ppm represent propagated SE.

resource – in this case, CO_2 (Poorter *et al.*, 2012). Those results contrast with the results from the study of Hartmann *et al.* (2015), which showed a continuous allocation of newly-assimilated C into roots at 40 ppm $[CO_2]$. The contrasting patterns were likely because allocation priorities vary with phenology. In our study, we exposed spruce trees to low CO_2 treatments between May and July when aboveground growth of aboveground tissues is a strong sink for C, whereas Hartmann *et al.* (2015) applied 40 ppm $[CO_2]$ treatment after growth and lignification of aboveground tissues were completed.

Reducing $[CO_2]$ to CCP_{AG} (120 ppm) constrained respiration more in belowground (*c.* 60% decline) than aboveground (*c.* 40% decline) organs compared to plants grown under ambient $[CO_2]$. This possibly reflects that respiratory demands of aboveground processes (e.g. sucrose synthesis, phloem loading and turnover of photosynthetic proteins) are prioritized over root processes (e.g. ion uptake). Unfortunately, our experimental setup did not allow differentiating root respiration from heterotrophic respiration (i.e. microorganisms decomposing root exudates and litter). Given that belowground respiration was similar between roots grown at CCP_{AG} (120 ppm) and roots dying from negative C balance (50 ppm) at Week 8, it is likely that belowground respiration in both low $[CO_2]$ treatments were mainly from microorganisms decomposing root litter. This would mean that C limitation on root respiration may have been underestimated in our experiment.

Preferential maintenance of NSC over respiration occurred at 50 ppm when NSC declined from *c.* 45% of controls at 120 ppm to *c.* 25% at 50 ppm, whereas respiration declined from *c.* 75% of controls at 120 ppm to *c.* 20% at 50 ppm (Fig. 8). This is consistent with the results of Martínez-Vilalta *et al.* (2016), which showed that average minimum NSC (mostly as soluble sugars) across diverse plant species are *c.* 36% of seasonal maximums. Such minimums may represent thresholds below which plants cannot survive and, therefore, are tightly regulated. Even when trees were dying under 50 ppm $[CO_2]$-induced C starvation, aboveground concentrations of soluble sugars maintained relatively constant over time (Fig. 4), in agreement with results from starvation treatments induced by shading (Sevanto *et al.*, 2014; Wiley *et al.*, 2017b; Weber *et al.*, 2018) and low $[CO_2]$ (Hartmann *et al.*, 2015). By contrast with aboveground organs, spruce roots completely depleted soluble sugars in the starvation treatment, which may have caused root death from C exhaustion. These results suggest that spruce saplings at CCP_{AG} (i.e. source limitation) prioritize investment of newly-assimilated C into aboveground processes, causing a depletion of locally stored carbohydrates in roots.

Downregulation of growth under C limitation to maintain defence

Similar to NSC storage, allocation to SM is often thought to be driven by the balance between C assimilated via photosynthesis (source process) and C demand for growth and respiration (sink processes). Our results show that spruce trees continuously invested C into SM (phenolic compounds + monoterpenes) in young organs until CCP_{AG} (120 ppm), resulting in no significant decline in SM relative to control (400 ppm). This occurred at the expense of other sinks (e.g. NSC storage, growth and respiration), suggesting that C was preferentially allocated to SM production. This is contrary to the theoretical predictions of the C–nutrient balance (Bryant *et al.*, 1983) and the growth–differentiation balance hypotheses (Herms & Mattson, 1992), and against empirical evidence from induced C starvation by shading (Roberts & Paul, 2006).

In Norway spruce, those phenolic (Hammerbacher *et al.*, 2014, 2018) and monoterpene compounds (Martin *et al.*, 2002) have been shown to play an important role in defence against

biotic attack. In addition, phenolic compounds (Neilson *et al.*, 2013) and volatile monoterpenes (Vickers *et al.*, 2009) are known to have antioxidant properties, therefore maybe required for reducing oxidative damage induced by excess electron transport under low [CO_2] (Galvez-Valdivieso *et al.*, 2009). Hence, prioritization of SM over growth and respiration may reflect increased demands for protecting aboveground young organs, which are of great value for assimilation especially under limited C supply, in agreement with the optimal defence hypothesis that organs that are of greater value should be better protected (Tomonori *et al.*, 2017). However, such allocation patterns were not seen in wheat plants, which produced significantly less concentrations of phenolic compounds in aboveground organs at 170 than at 400 ppm [CO_2] (Huang *et al.*, 2017a). The contrasting responses indicate that allocation to defence may follow a different strategy in long-lived organisms such as trees compared to annual herbaceous plants, as suggested by the resource availability hypothesis (Coley *et al.*, 1985). The long lifespan of trees increases the risk of encountering periods of abiotic (i.e. drought, heat waves and cold) or biotic stresses (i.e. insect attack and pathogen infestation) and a conservative allocation strategy that prioritizes SM over growth may therefore ensure long-term survival.

Terpene emissions serve a double role in plants: they scavenge reactive oxygen species (Vickers *et al.*, 2009), and defend against herbivores and pathogens (Holopainen & Gershenzon, 2010; Heil, 2014). We observed contrasting emissions of α- and β-pinene vs linalool as [CO_2] decreased. Both α- and β-pinene emissions increased under negative C balance which may be attributed to the physical release from the loss of old foliage, whereas linalool emissions are likely produced *de novo* and thus declined in trees dying under negative C balance at Week 8. Linalool has been shown to be the major terpenoid emitted from methyl jasmonate (MeJA)-treated Norway spruce (Martin *et al.*, 2003), herbivore-attacked mountain birch (*Betula pubescens*) and poplar trees (Eberl *et al.*, 2017). Hence, a decrease in linalool emissions under negative C balance may diminish the ability of Norway spruce to defend against herbivores such bark beetles. Such changes in blends of terpenoids provide new perspectives on how abiotic stress such as drought increases susceptibility of spruce trees to bark beetle attack (Ryan *et al.*, 2015).

By using a complete mass-balance approach, we found that decreasing [CO_2] treatments led to a net loss of NSC storage. By contrast, allocation to SM, calculated as changes in SM as a percentage of newly-assimilated C, remained relative constant (*c.* 3–5%) across [CO_2] treatments. This also suggests allocation to SM was preferentially maintained at the expense of NSC storage (Table S2). However, we underscore here that differences between measurement devices and techniques, as well as the incompleteness of the dataset (stems and tap roots were not assessed, also not root exudation or microbial decomposition of root litter), still prevent an accurate estimation of quantitative partitioning of available C into different sinks. For example, we did not measure the C allocation in root exudates, which may

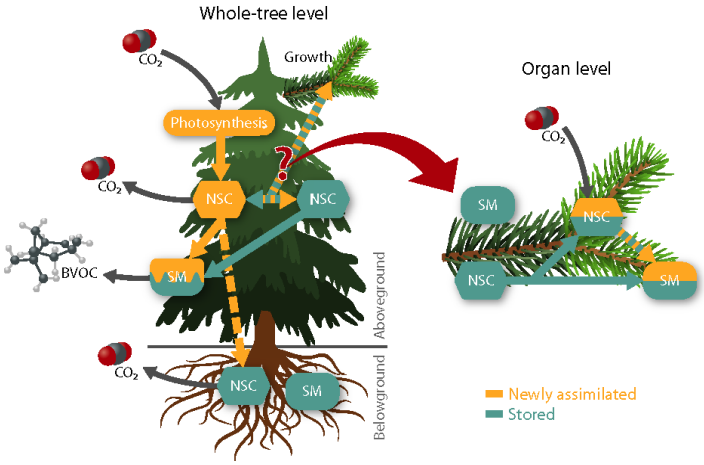

Fig. 9 A schematic summary of carbon (C) allocation patterns at the whole-tree and organ level in *Picea abies*. As C availability decreases, transport of newly-assimilated (yellow arrows and boxes) nonstructural carbohydrates (NSC) from aboveground to belowground decreases (dashed line). As a result, locally stored NSC (blue arrows and boxes) are depleted, causing reduced respiratory activity and constrained production of secondary metabolites (SM) in roots. Although newly-assimilated sugars are mixed into stored soluble sugar pools, aboveground respiration decreases as CO_2 supply and total NSC decrease, particularly when NSC reach the minimum operational concentrations (*c.* 25% of control) necessary for survival. Both newly-assimilated and stored NSC contribute to growth but only up to a threshold (*c.* 45% of control) below which operational NSC storage and survival may be compromised. The production of SM of aboveground (yellow-blue) is prioritized over NSC storage and growth, resulting in relatively constant emissions of biogenic volatile organic compounds (BVOCs). C pool dynamics at organ level revealed that little newly-assimilated C is allocated to SM in old organs, and stored SM cannot be mobilized or metabolized in old branches; however, NSC stored in old organs can be mobilized to young organs and provide, along with newly-assimilated NSC, substrates for growth and maintenance of NSC concentrations and the production of SM.

constitute ≤50% of the daily C assimilation (van Dam & Bouwmeester, 2016).

Our experiment was carried out in the glasshouse, and therefore the relative changes in NSC and SM as a percentage of control indicate treatment effects under the given conditions. Extrapolation of those results to field conditions where other environmental factors may come into play, should be carried out with caution. By contrast to the glasshouse, higher light intensities and lower air temperatures in the field along with an elevated risk of herbivory and pathogen attack may impact assimilation, RGR, NSC and SM more under ambient [CO_2] than under low [CO_2] conditions. Consequently, the effects of C limitation on NSC and SM in the glasshouse would likely be exacerbated under field conditions.

Conclusion and outlook

We provide mechanistic evidence for allocation strategies that appear to be consistent with coordination of supply and demand in the long run, and for trade-offs in the allocation of photosynthetic products to growth, storage and defence. We conclude that spruce trees have a conservative allocation strategy where growth and respiration can be downregulated to maintain 'operational' concentrations of NSC while investing in future survival by producing SM (Fig. 9). Moreover, by tracing fluxes of newly-assimilated C, we highlight an optimal allocation strategy: under source limitation, plants prioritize investment of newly-assimilated C to aboveground young tissues even at expense of root death from C exhaustion (Fig. 9). Such changes in C allocation strategies are important for us to understand and predict how trees respond to environmental changes such as drought (Anderegg *et al.*, 2015; Ryan *et al.*, 2015), shading (Roberts & Paul, 2006), defoliation (Anderegg & Callaway, 2012) and biotic interactions.

Future studies should integrate the allocation strategies uncovered in small trees in highly controlled growth chambers to large trees in field conditions known to have different light quantity and temperature, and thus different source–sink relationships (McDowell *et al.*, 2013; Poorter *et al.*, 2016). Moreover, active constraints on growth via phytohormonal regulation have been observed under a variety of stresses including drought (Skirycz *et al.*, 2010) and cold (Achard *et al.*, 2008) in Arabidopsis, and low [CO_2] in wheat (Huang *et al.*, 2017b). However, addressing the regulatory mechanisms in long-lived trees, where the genome is largely unknown, remains a major challenge that requires combining interdisciplinary approaches including ecological field manipulations, biochemical assays and molecular tools.

Acknowledgements

We thank Savoyane Lambert and Jessica Heublein for their help with sample collection and processing, Olaf Kolle and René Schwalbe for their help with [CO_2] manipulation. Agnes Fastnacht helped us in the glasshouse, Iris Kuhlmann and Anett Enke supported us in the laboratory. Heiko Moossen and Heike Geilmann carried out isotope measurements. JH was funded by the Chinese Scholarship Council and Max Planck Institute for Biogeochemistry, and acknowledges support from the International Max Planck Research School for Global Biogeochemical Cycles.

Author contribution

HH, JH, ST, AH, TB, JG, GG, NMvD and AS contributed to the plan and design of the work; JH performed experiments; MR and AH conducted analysis of secondary metabolites; AW conducted analysis of volatiles; JH analysed the data and wrote the manuscript with the assistance of HH All authors contributed to revisions.

ORCID

Nicole M. van Dam http://orcid.org/0000-0003-2622-5446
Jonathan Gershenzon http://orcid.org/0000-0002-1812-1551
Gerd Gleixner http://orcid.org/0000-0002-4616-0953
Almuth Hammerbacher http://orcid.org/0000-0002-0262-2634
Henrik Hartmann http://orcid.org/0000-0002-9926-5484
Jianbei Huang http://orcid.org/0000-0001-5286-5645
Susan Trumbore http://orcid.org/0000-0003-3885-6202
Alexander Weinhold http://orcid.org/0000-0003-1418-7788

References

Achard P, Gong F, Cheminant S, Alioua M, Hedden P, Genschik P. 2008. The cold-inducible CBF1 factor-dependent signaling pathway modulates the accumulation of the growth-repressing DELLA proteins via its effect on gibberellin metabolism. *Plant Cell* **20**: 2117–2129.

Anderegg WRL, Callaway ES. 2012. Infestation and hydraulic consequences of induced carbon starvation. *Plant Physiology* **159**: 1866–1874.

Anderegg WRL, Hicke JA, Fisher RA, Allen CD, Aukema J, Bentz B, Hood S, Lichstein JW, Macalady AK, McDowell N *et al.* 2015. Tree mortality from drought, insects, and their interactions in a changing climate. *New Phytologist* **208**: 674–683.

Atkin O. 2015. New Phytologist and the 'fate' of carbon in terrestrial ecosystems. *New Phytologist* **205**: 1–3.

Ayub G, Smith RA, Tissue DT, Atkin OK. 2011. Impacts of drought on leaf respiration in darkness and light in *Eucalyptus saligna* exposed to industrial-age atmospheric CO_2 and growth temperature. *New Phytologist* **190**: 1003–1018.

Ayub G, Zaragoza-Castells J, Griffin KL, Atkin OK. 2014. Leaf respiration in darkness and in the light under pre-industrial, current and elevated atmospheric CO_2 concentrations. *Plant Science* **226**: 120–130.

Brandes E, Kodama N, Whittaker K, Weston C, Rennenberg H, Keitel C, Adams MA, Gessler A. 2006. Short-term variation in the isotopic composition of organic matter allocated from the leaves to the stem of *Pinus sylvestris*: effects of photosynthetic and postphotosynthetic carbon isotope fractionation. *Global Change Biology* **12**: 1922–1939.

Bryant J, Chapin S, Klein D. 1983. Carbon/nutrient balance of boreal plants in relation to vertebrate herbivory. *Oikos* **40**: 357.

Casal JJ. 2013. Photoreceptor signaling networks in plant responses to shade. *Annual Review of Plant Biology* **64**: 403–427.

Chapin FS, Schulze E-D, Mooney HA. 1990. The ecology and economics of storage in plants. *Annual Review of Ecology and Systematics* **21**: 423–447.

Coley PD, Bryant JP, Chapin FS. 1985. Resource availability and plant antiherbivore defense. *Science* **230**: 895–899.

van Dam NM, Bouwmeester HJ. 2016. Metabolomics in the rhizosphere: tapping into belowground chemical communication. *Trends in Plant Science* **21**: 256–265.

Dietze MC, Sala A, Carbone MS, Czimczik CI, Mantooth JA, Richardson AD, Vargas R. 2014. Nonstructural carbon in woody plants. *Annual Review of Plant Biology* **65**: 667–687.

Eberl F, Hammerbacher A, Gershenzon J, Unsicker SB. 2017. Leaf rust infection reduces herbivore-induced volatile emission in black poplar and attracts a generalist herbivore. *New Phytologist* **220**: 760–772.

Faralli M, Grove IG, Hare MC, Kettlewell PS, Fiorani F. 2017. Rising CO_2 from historical concentrations enhances the physiological performance of *Brassica napus* seedlings under optimal water supply but not under reduced water availability. *Plant, Cell & Environment* **40**: 317–325.

Fatichi S, Leuzinger S, Korner C. 2014. Moving beyond photosynthesis: from carbon source to sink-driven vegetation modeling. *New Phytologist* **201**: 1086–1095.

Fischer S, Hanf S, Frosch T, Gleixner G, Popp J, Trumbore S, Hartmann H. 2015. *Pinus sylvestris* switches respiration substrates under shading but not during drought. *New Phytologist* **207**: 542–550.

Galiano L, Timofeeva G, Saurer M, Siegwolf R, Martínez-Vilalta J, Hommel R, Gessler A. 2017. The fate of recently fixed carbon after drought release: towards unravelling C storage regulation in *Tilia platyphyllos* and *Pinus sylvestris*. *Plant, Cell & Environment* **40**: 1711–1724.

Galvez-Valdivieso G, Fryer MJ, Lawson T, Slattery K, Truman W, Smirnoff N, Asami T, Davies WJ, Jones AM, Baker NR *et al.* 2009. The high light response in *Arabidopsis* involves ABA signaling between vascular and bundle sheath cells. *Plant Cell* **21**: 2143–2162.

Gerhart LM, Harris JM, Nippert JB, Sandquist DR, Ward JK. 2012. Glacial trees from the La Brea tar pits show physiological constraints of low CO_2. *New Phytologist* **194**: 63–69.

Ghannoum O, Phillips NG, Conroy JP, Smith RA, Attard RD, Woodfield R, Logan BA, Lewis JD, Tissue DT. 2010. Exposure to preindustrial, current and future atmospheric CO_2 and temperature differentially affects growth and photosynthesis in *Eucalyptus*. *Global Change Biology* **16**: 303–319.

Gibon Y, Pyl E-T, Sulpice R, Lunn JE, Höhne M, Günther M, Stitt M. 2009. Adjustment of growth, starch turnover, protein content and central metabolism to a decrease of the carbon supply when *Arabidopsis* is grown in very short photoperiods. *Plant, Cell & Environment* **32**: 859–874.

Hammerbacher A, Paetz C, Wright LP, Fischer TC, Bohlmann J, Davis AJ, Fenning TM, Gershenzon J, Schmidt A. 2014. Flavan-3-ols in Norway spruce: biosynthesis, accumulation, and function in response to attack by the bark beetle-associated fungus *Ceratocystis polonica*. *Plant Physiology* **164**: 2107–2122.

Hammerbacher A, Raguschke B, Wright LP, Gershenzon J. 2018. Gallocatechin biosynthesis via a flavonoid 3′,5′-hydroxylase is a defense response in Norway spruce against infection by the bark beetle-associated sap-staining fungus *Endoconidiophora polonica*. *Phytochemistry* **148**: 78–86.

Harrison SP, Morfopoulos C, Dani KGS, Prentice IC, Arneth A, Atwell BJ, Barkley MP, Leishman MR, Loreto F, Medlyn BE *et al.* 2013. Volatile isoprenoid emissions from plastid to planet. *New Phytologist* **197**: 49–57.

Hartmann H, McDowell NG, Trumbore S. 2015. Allocation to carbon storage pools in Norway spruce saplings under drought and low CO_2. *Tree Physiology* **35**: 243–252.

Hartmann H, Trumbore S. 2016. Understanding the roles of nonstructural carbohydrates in forest trees – from what we can measure to what we want to know. *New Phytologist* **211**: 386–403.

Hartmann H, Ziegler W, Kolle O, Trumbore S. 2013. Thirst beats hunger – declining hydration during drought prevents carbon starvation in Norway spruce saplings. *New Phytologist* **200**: 340–349.

Heil M. 2014. Herbivore-induced plant volatiles: targets, perception and unanswered questions. *New Phytologist* **204**: 297–306.

Herms DA, Mattson WJ. 1992. The dilemma of plants: to grow or defend. *Quarterly Review of Biology* **67**: 283–335.

Holopainen JK, Gershenzon J. 2010. Multiple stress factors and the emission of plant VOCs. *Trends in Plant Science* **15**: 176–184.

Huang J, Hammerbacher A, Forkelová L, Hartmann H. 2017a. Release of resource constraints allows greater carbon allocation to secondary metabolites and storage in winter wheat. *Plant, Cell & Environment* **40**: 672–685.

Huang J, Reichelt M, Chowdhury S, Hammerbacher A, Hartmann H. 2017b. Increasing carbon availability stimulates growth and secondary metabolites via modulation of phytohormones in winter wheat. *Journal of Experimental Botany* **68**: 1251–1263.

Hunt R. 1982. *Plant growth curves: a functional approach to plant growth analysis*. London, UK: Edward Arnold.

Lewis JD, Ward JK, Tissue DT. 2010. Phosphorus supply drives nonlinear responses of cottonwood (*Populus deltoides*) to increases in CO_2 concentration from glacial to future concentrations. *New Phytologist* **187**: 438–448.

Martin D, Tholl D, Gershenzon J, Bohlmann J. 2002. Methyl jasmonate induces traumatic resin ducts, terpenoid resin biosynthesis, and terpenoid accumulation in developing xylem of Norway spruce stems. *Plant Physiology* **129**: 1003–1018.

Martin DM, Gershenzon J, Bohlmann J. 2003. Induction of volatile terpene biosynthesis and diurnal emission by methyl jasmonate in foliage of Norway spruce. *Plant Physiology* **132**: 1586–1599.

Martínez-Vilalta J, Sala A, Asensio D, Galiano L, Hoch G, Palacio S, Piper FI, Lloret F. 2016. Dynamics of non-structural carbohydrates in terrestrial plants: a global synthesis. *Ecological Monographs* **86**: 495–516.

Massad TJ, Trumbore SE, Ganbat G, Reichelt M, Unsicker S, Boeckler A, Gleixner G, Gershenzon J, Ruehlow S. 2014. An optimal defense strategy for phenolic glycoside production in *Populus trichocarpa* – isotope labeling demonstrates secondary metabolite production in growing leaves. *New Phytologist* **203**: 607–619.

McDowell NG, Ryan MG, Zeppel MJB, Tissue DT. 2013. Improving our knowledge of drought-induced forest mortality through experiments, observations, and modeling. *New Phytologist* **200**: 289–293.

Mithöfer A, Boland W. 2012. Plant defense against herbivores: chemical aspects. *Annual Review of Plant Biology* **63**: 431–450.

Neilson EH, Goodger JQD, Woodrow IE, Møller BL. 2013. Plant chemical defense: at what cost? *Trends in Plant Science* **18**: 250–258.

Palacio S, Hoch G, Sala A, Körner C, Millard P. 2014. Does carbon storage limit tree growth? *New Phytologist* **201**: 1096–1100.

Parducci L, Jørgensen T, Tollefsrud MM, Elverland E, Alm T, Fontana SL, Bennett KD, Haile J, Matetovici I, Suyama Y *et al.* 2012. Glacial survival of boreal trees in northern Scandinavia. *Science* **335**: 1083–1086.

Poorter H, Fiorani F, Pieruschka R, Wojciechowski T, van der Putten WH, Kleyer M, Schurr U, Postma J. 2016. Pampered inside, pestered outside? Differences and similarities between plants growing in controlled conditions and in the field. *New Phytologist* **212**: 838–855.

Poorter H, Niklas KJ, Reich PB, Oleksyn J, Poot P, Mommer L. 2012. Biomass allocation to leaves, stems and roots: meta-analyses of interspecific variation and environmental control. *New Phytologist* **193**: 30–50.

R Development Core Team. 2016. *R: a language and environment for statistical computing, v.3.3.2*. Vienna, Austria: R foundation for Statistical Computing. URL http://www.r-project.org.

Reich PB, Hobbie SE, Lee TD. 2014. Plant growth enhancement by elevated CO_2 eliminated by joint water and nitrogen limitation. *Nature Geoscience* **7**: 920–924.

Roberts MR, Paul ND. 2006. Seduced by the dark side: integrating molecular and ecological perspectives on the inflence of light on plant defence against pests and pathogens. *New Phytologist* **170**: 677–699.

Ryan MG, Sapes G, Sala A, Hood SM. 2015. Tree physiology and bark beetles. *New Phytologist* **205**: 955–957.

Sala A, Woodruff DR, Meinzer FC. 2012. Carbon dynamics in trees: feast or famine? *Tree Physiology* **32**: 764–775.

Scanlon JT, Willis DE. 1985. Calculation of flame ionization detector relative response factors using the effective carbon number concept. *Journal of Chromatographic Science* **23**: 333–340.

Schmid S, Palacio S, Hoch G. 2017. Growth reduction after defoliation is independent of CO_2 supply in deciduous and evergreen young oaks. *New Phytologist* **214**: 1479–1490.

Sevanto S, McDowell NG, Dickman LT, Pangle R, Pockman WT. 2014. How do trees die? A test of the hydraulic failure and carbon starvation hypotheses. *Plant, Cell & Environment* **37**: 153–161.

Skirycz A, De Bodt S, Obata T, De Clercq I, Claeys H, De Rycke R, Andrianka ja M, Van Aken O, Van Breusegem F, Fernie AR *et al.* 2010. Developmental stage specificity and the role of mitochondrial metabolism in

the response of Arabidopsis leaves to prolonged mild osmotic stress. *Plant Physiology* **152**: 226–244.
Tomonori T, Sebastian K, van Dam NM. 2017. Root and shoot glucosinolate allocation patterns follow optimal defence allocation theory. *Journal of Ecology* **105**: 1256–1266.
Trumbore S, Brando P, Hartmann H. 2015. Forest health and global change. *Science* **349**: 814–818.
Ullah C, Unsicker SB, Fellenberg C, Constabel CP, Schmidt A, Gershenzon J, Hammerbacher A. 2017. Flavan-3-ols are an effective chemical defense against rust infection. *Plant Physiology* **175**: 1560–1578.
Unsicker SB, Kunert G, Gershenzon J. 2009. Protective perfumes: the role of vegetative volatiles in plant defense against herbivores. *Current Opinion in Plant Biology* **12**: 479–485.
Vickers CE, Gershenzon J, Lerdau MT, Loreto F. 2009. A unified mechanism of action for volatile isoprenoids in plant abiotic stress. *Nature Chemical Biology* **5**: 283–291.
Way DA, Ghirardo A, Kanawati B, Esperschütz J, Monson RK, Jackson RB, Schmitt-Kopplin P, Schnitzler J-P. 2013. Increasing atmospheric CO_2 reduces metabolic and physiological differences between isoprene- and non-isoprene-emitting poplars. *New Phytologist* **200**: 534–546.
Weber R, Schwendener A, Schmid S, Lambert S, Wiley E, Landhäusser SM, Hartmann H, Hoch G. 2018. Living on next to nothing: tree seedlings can survive weeks with very low carbohydrate concentrations. *New Phytologist* **218**: 107–118.
Wiley E, Casper BB, Helliker BR. 2017a. Recovery following defoliation involves shifts in allocation that favour storage and reproduction over radial growth in black oak. *Journal of Ecology* **105**: 412–424.
Wiley E, Helliker B. 2012. A re-evaluation of carbon storage in trees lends greater support for carbon limitation to growth. *New Phytologist* **195**: 285–289.
Wiley E, Hoch G, Landhäusser SM. 2017b. Dying piece by piece: carbohydrate dynamics in aspen (*Populus tremuloides*) seedlings under severe carbon stress. *Journal of Experimental Botany* **68**: 5221–5232.

Supporting Information

Additional Supporting Information may be found online in the Supporting Information section at the end of the article.

Fig. S1 Concentrations of soluble sugars, starch and NSC (soluble sugars + starch) expressed as percentage of control (400 ppm [CO_2]) at the whole-tree level.

Fig. S2 Concentrations of soluble sugars, starch and NSC (soluble sugars + starch) at the whole-tree level.

Fig. S3 Concentrations of phenolic compounds, monoterpenes and total secondary metabolites expressed as percentage of control (400 ppm [CO_2]) at the whole-tree level.

Fig. S4 Concentrations of phenolic compounds, monoterpenes and total secondary metabolites (phenolic compounds + monoterpenes) at the whole-tree level.

Fig. S5 $\delta^{13}C$ (‰) of bulk tissue, water soluble C and phenolic compounds at the whole-tree level.

Methods S1 TD-GC-MS conditions for BVOC analysis.

Table S1 Internal standards, weight-based response factors and methods used for the measurements of secondary metabolites.

Table S2 A rough estimation of allocation of newly-assimilated carbon.

Please note: Wiley Blackwell are not responsible for the content or functionality of any Supporting Information supplied by the authors. Any queries (other than missing material) should be directed to the *New Phytologist* Central Office.

CHAPTER 5

Environmental Science & Technology

Article

Cite This: Environ. Sci. Technol. XXXX, XXX, XXX−XXX

pubs.acs.org/est

New Perspectives on CO_2, Temperature, and Light Effects on BVOC Emissions Using Online Measurements by PTR-MS and Cavity Ring-Down Spectroscopy

Jianbei Huang,*[,†] Henrik Hartmann,[†] Heidi Hellén,[‡] Armin Wisthaler,[§] Erica Perreca,[∥] Alexander Weinhold,[⊥] Alexander Rücker,[†] Nicole M. van Dam,[⊥,#] Jonathan Gershenzon,[∥] Susan Trumbore,[†] and Thomas Behrendt*[,†]

[†]Max-Planck-Institute for Biogeochemistry, Jena, Germany
[‡]Finnish Meteorological Institute, Helsinki, Finland
[§]Department of Chemistry, University of Oslo, Oslo, Norway
[∥]Max Planck Institute for Chemical Ecology, Jena, Germany
[⊥]German Centre for Integrative Biodiversity Research, Leipzig, Germany
[#]Institute of Ecology, Friedrich Schiller University, Jena, Germany

Supporting Information

ABSTRACT: Volatile organic compounds (VOC) play important roles in atmospheric chemistry, plant ecology, and physiology, and biogenic VOC (BVOC) emitted by plants is the largest VOC source. Our knowledge about how environmental drivers (e.g., carbon, light, and temperature) may regulate BVOC emissions is limited because they are often not controlled. We combined a greenhouse facility to manipulate atmospheric CO_2 ($[CO_2]$) with proton-transfer-reaction mass spectrometry (PTR-MS) and cavity ring-down spectroscopy to investigate the regulation of BVOC in Norway spruce. Our results indicate a direct relationship between $[CO_2]$ and methanol and acetone emissions, and their temperature and light dependencies, possibly related to substrate availability. The composition of monoterpenes stored in needles remained constant, but emissions of mono-(linalool) and sesquiterpenes (β-farnesene) increased at lower $[CO_2]$, with the effects being most pronounced at the highest air temperature. Pulse-labeling suggested an immediate incorporation of recently assimilated carbon into acetone, mono- and sesquiterpene emissions even under 50 ppm $[CO_2]$. Our results provide new perspectives on CO_2, temperature and light effects on BVOC emissions, in particular how they depend on stored pools and recent photosynthetic products. Future studies using smaller but more seedlings may allow sufficient replication to examine the physiological mechanisms behind the BVOC responses.

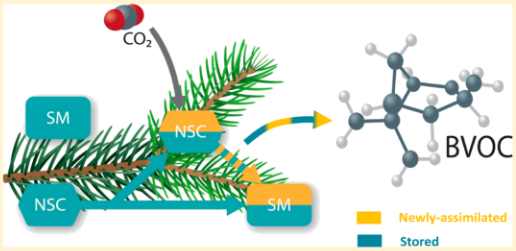

INTRODUCTION

Volatile organic compounds (VOC) play important roles in atmospheric chemistry and climate by altering the oxidative capacity of the atmosphere,[1−3] ozone production in the presence of NO_x ($NO+NO_2$),[4] and the formation of secondary organic aerosols.[5] Biogenic VOC (BVOC) is the largest VOC source, representing up to ∼90% of total emissions.[6] However, our limited understanding of the function and regulation of BVOC results in large uncertainties in estimating and predicting BVOC emissions.[7,8]

Temperature and light are commonly viewed as key environmental factors controlling BVOC emissions.[6] A rise in the mean global temperature of ∼2−3 °C is expected to increase total BVOC emissions by 30−45%.[9] In global vegetation models such as ORCHIDEE,[10] light intensity is the main driver of the emissions, accounting for 80% and 60% of methanol and monoterpenes, repectively. However, changing atmospheric $[CO_2]$ may also affect BVOC emissions, as increasing $[CO_2]$ from low (∼190 ppm) to high (∼600 ppm) has been shown to suppress isoprene emissions.[11,12] While such mechanisms that give rise to isoprene emissions have been implemented in models,[13,14] the information on the physiological regulation of other BVOC emissions, for example, mono- and sesquiterpenes as well as oxygenated BVOC, is still limited.

Mono- and sesquiterpenes serve important biological and ecological functions, such as repelling herbivores and attracting

Received: March 16, 2018
Revised: September 21, 2018
Accepted: October 18, 2018
Published: October 18, 2018

DOI: 10.1021/acs.est.8b01435
Environ. Sci. Technol. XXXX, XXX, XXX−XXX

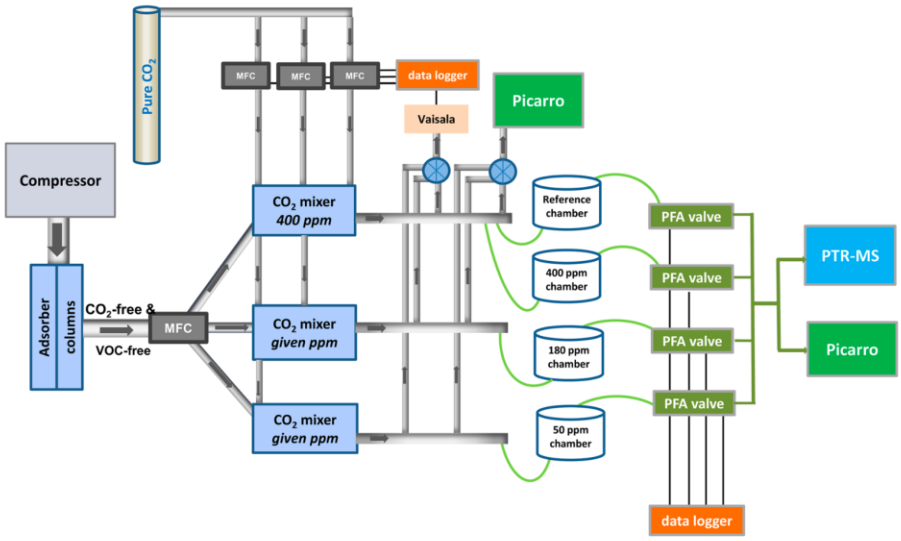

Figure 1. Schematic view of [CO_2] manipulation system in the greenhouse. MFC, mass flow controller; PTR-MS, proton-transfer-reaction mass spectrometry.

their predators,[15] or scavenging harmful reactive oxygen species (ROS) in plants.[16] Hence, their emissions are often induced by biotic and abiotic stresses such as herbivory, intense light and high temperature.[17,18] It remains unclear whether emitted monoterpenes are released from stored pools or synthesized de novo. Data on the third group of isoprenoids, sesquiterpenes, are still sparse because these compounds degrade rapidly due to their high chemical reactivity with radicals (e.g., hydroxyl radical, OH) and ozone (O_3).[19,20]

Plants also emit large quantities of oxygenated VOC (e.g., methanol and acetone) into the atmosphere.[10,21] Methanol is thought to be a byproduct of pectin demethylation during cell wall extension,[22,23] and is therefore often used as an indicator of growth.[24] Saccharides including glucose and sucrose are required for pectin synthesis,[25] which may play an important role in regulating methanol emissions.[26] The metabolic pathways involved in the synthesis of acetone are not yet fully understood, but it is likely that acetone is produced via pyruvate metabolism.[27] Field observations demonstrate that emissions of methanol and acetone are temperature- and light-dependent,[28−30] but their dependence on carbon has received less attention. In particular, quantification of interactions between temperature, light and [CO_2] on emissions and dynamics of these fluxes are still not well understood.

To fill this gap, we constructed a greenhouse facility specifically designed to induce contrasting carbon availability, spanning very low to ambient [CO_2] concentrations (400, 180, and 50 ppm). We combined proton transfer reaction mass spectrometry (PTR-MS) with gas chromatography−mass spectrometry (GC−MS) to investigate emissions of terpenoids and oxygenated BVOC from whole-canopies (including stem, branches and needles) of 8-year-old Norway spruce (*Picea abies*). We also monitored CO_2 and water vapor gas exchange, air temperature, and photosynthetically active radiation (PAR) to investigate their relationships to BVOC emissions. Concentrations of metabolites including soluble sugars and monoterpenes in tissues were measured to investigate the role of substrate availability in BVOC emissions. Isotope labeling allows partitioning the contribution of stored pools and recent photosynthetic products to BVOC emissions. Such an approach has been successfully applied for determining carbon source for isoprene emissions under different [CO_2],[31−33] and monoterpene emissions following herbivory.[34] Hence, we also employed $^{13}CO_2$ pulse-labeling and traced labeled C into emissions of acetone, mono-, and sesquiterpenes in all [CO_2] treatments.

MATERIALS AND METHODS

Plant Material. We conducted two experiments, one in 2016 (experiment I) one and 2017 (experiment II) using two genotypes of 8-year-old Norway Spruce saplings (S21K0420117 and S21K04200232 from Sweden). Prior to each experiment, trees were grown outdoors in pots filled with sand and a slow-releasing fertilizer (Osmocote Start, Everris International B.V., Netherlands). All saplings were pruned in July 2015 to make them fit into the growth chambers and were watered regularly before the start of the experiment.

Growth Chambers. Four cylindrical chambers (height = 70 cm, diameter = 70 cm, volume = 270 L) covered with fluorinated ethylene propylene (FEP) foil were built to enclose the whole aboveground portion of the spruce saplings (Supporting Information Figure S1). Previous studies found that FEP foil transmits about 95% of photosynthetically active radiation (PAR, 400−700 nm) and about 90% for wavelengths <400 nm.[35,36] Four FEP chambers were placed side-by-side on a greenhouse table and three of these were used to grow spruce clones. The fourth chamber served as a plant-free reference chamber to measure the VOC derived from the incoming air, chemical reactions in the gas phase, and adsorption/desorption to the walls of the chamber and tubing.[35] Previous work has shown that these spruce clones have little differences in concentrations of soluble sugars and monotperenes at the whole aboveground level (SI Figure S2). Except monoterpene emissions were induced by tissue damage during transferring trees and sampling, there were little differences in emissions of methanol, acetone, and sesquiterpenes (SI Figure S3). Each

DOI: 10.1021/acs.est.8b01435
Environ. Sci. Technol. XXXX, XXX, XXX−XXX

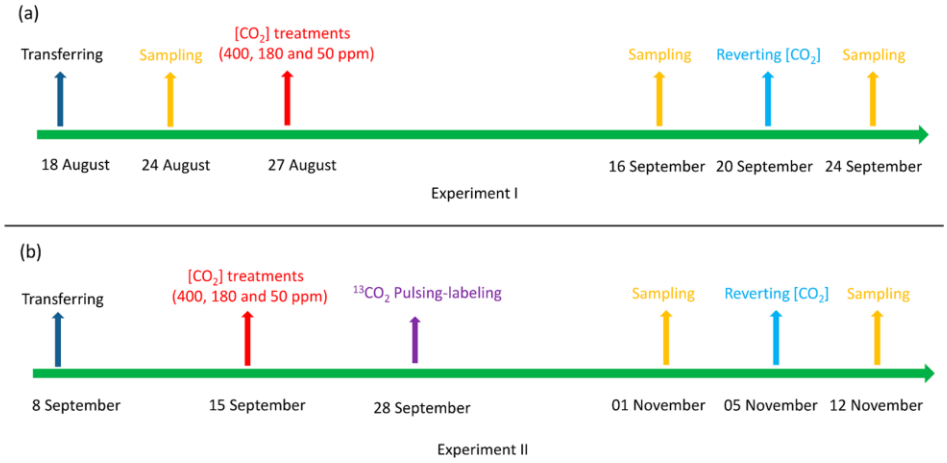

Figure 2. Treatment and sampling timeline.

chamber was flushed continuously through perforated Teflon tubing located at the bottom and an outlet at the top of the chamber. A light/dark regime of 16/8 h was maintained using supplemental greenhouse lamps (Son-T Agro 430W HPS bulbs, primary light range = 520−610 nm, Philips Lighting Co., Somerset, NJ) in 2016 and changed to LED lamps (ultraviolet, < 400 nm, 1%; blue, 400−500 nm, 20%; green, 500−600 nm, 39%; red, 600−700 nm, 35%; far-red, 700−800 nm, 5%; Valoya, Finland) in 2017. Ambient light was complemented with artificial lighting. Air temperature and PAR were monitored continuously using Type T Thermocouple and custom-made high-stability photovoltaic detectors (BPW21, OSRAM Opto Semiconductors GmbH, Regensburg, Germany), respectively. All PAR sensors have been calibrated vs a LI-COR quantum sensor (LI-COR, USA) with 604 Ohm millivolt adaptor. Temperature and light data were recorded every 30 min using a data logger (CR 23X, Campbell, U.K.) for each chamber.

[CO_2] Manipulation and Elimination of Ambient VOC. Ambient air from a compressor was passed through a molecular sieve to remove all CO_2 and most VOC (Figure 1). Pure CO_2 was then added to the CO_2-free air via mass flow controllers (Bronckhorst, Germany) to achieve target concentrations that were measured sequentially with a CO_2 sensor (*GMP 343,* Vaisala, Finland) (switching at 10 min intervals) and saved on a data-logger (CR1000, Campbell, U.K.). Concentrations were compared against target values (400, 180, and ∼50 ppm) and, if required, adjusted by the data-logger via the mass flow controllers. Air from each mixer was then delivered into each chamber through a custom-built manifold and controlled by a rotameter (MR3000, Key Instruments, Germany) (Figure 1).

Treatments, Sampling, and Biomass Processing. The treatment schedule and the sampling scheme are described in Figure 2. The entire aboveground portion of three 8 to 10-year-old spruce saplings was transferred into individual FEP film coated chambers, while the below-ground portions were kept in the original pot outside of the chamber. Aboveground, the headspace in each chamber was acclimated at 400 ppm [CO_2] for a week, then exposed to different [CO_2] (400, 180, and 50 ppm), followed by reverting the lower [CO_2] treatments to 400 ppm. The soil and roots (kept outside the atmospheric treatments) were watered to achieve field capacity every 2 days. Aboveground biomass samples (10−15 g each of needles and branches) were collected prior to [CO_2] reduction treatment (only in experiment I), at the end of treatment, and following reversion of [CO_2] to 400 ppm. In experiment I, we started [CO_2] reduction treatments 3 days after sampling, and waited 4 days after sampling at the end of [CO_2] reduction treatment in order to reduce artifacts on BVOC measurements (in particular terpenoids) caused by wounding during sampling; after which we reverted CO_2 back to 400 ppm. At the end of the experiment we destructively harvested all trees to determine total above-ground biomass. Needle samples collected for quantification of NSC (nonstructural carbohydrates) and monoterpenes were immediately frozen and homogenized in liquid nitrogen and then stored at −80 °C. Around half of the samples were freeze-dried and ground using a ball mill (Retsch MM400, Haan) and stored at −20 °C for analysis of soluble sugars. The other samples were ground in liquid nitrogen using a mortar and pestle for analysis of monoterpenes. Whole aboveground biomass was harvested and dried at 60 °C and weighed. The experiment carried out in 2016 was repeated in 2017 using the same procedure but with extended treatment duration, and different genotypes, radiation exposure, and temperatures.

Online Monitoring of Aboveground Gas Exchange. [CO_2] of air exiting each chamber was measured with a cavity ring-down spectrometer (2101-*i*, Picarro Inc. Santa Clara, CA, precision 200 ppbv at 10 Hz) once within a 2 h cycle from 6:00 to 20:00 (CET), using a custom-built magnetic valve unit (Sirai, Germany) controlled by a data-logger (CR1000, Campbell, UK) (Figure 1). [CO_2] of air exiting the chambers was measured with a second cavity ring-down spectrometer (2131-*i*, Picarro Inc. Santa Clara, CA) in 30 min intervals using four-coupled PFA valves (VWR International GmbH, Germany) also controlled by a data-logger (CR 23X, Campbell, U.K.). Reference gases were used to ensure comparability between the two Picarro devices. Transition periods after valve switching were excluded from the calculation of average [CO_2] and H_2O for each chamber. The instantaneous whole aboveground carbon assimilation (A_{net}) and transpiration rate (T_{net}) at hour j were defined as

DOI: 10.1021/acs.est.8b01435
Environ. Sci. Technol. XXXX, XXX, XXX−XXX

$$A_{net} \text{ or } T_{net} = \frac{[CO_2HH_2O]_{in} - [CO_2HH_2O]_{out}}{\text{molar volume}} \times \frac{\text{VFR}}{\text{biomass}} \quad (1)$$

where $[CO_2]_{in}$ is the $[CO_2]$ of air entering the chambers, and $[CO_2]_{out}$ is the $[CO_2]$ of air exiting the chambers. VFR is the volumetric flow rates of air passing through the chambers. The molar volume of gas (V_m) was calculated according to the air temperature using

$$V_m = \frac{RT}{P} \quad (2)$$

where R is the universal gas constant (8.31 J mol^{-1} K^{-1}), P is the atmospheric pressure (1 atm = 0.76 × 9.8 × 13.6 × 10^3 N/m^2), and T is the air temperature (K).

Online Monitoring of Whole Aboveground BVOC Emissions. VOC mixing ratios of air exiting Teflon chambers were measured by a proton-transfer-reaction mass spectrometer (PTR-QMS 500, Ionicon Analytik GmbH, Austria) operated in parallel with $[CO_2]$ measurements using the same four-coupled PFA valves switching unit (Figure 1). The inlet tubing was insulated and heated to 60 °C to avoid condensation. BVOC were detected by using proton transfer reactions with H_3O^+. The instrument was operated at 2.2 mbar drift pressure and 600 V drift voltage. The reduced electric field strength E/N (E being the electric field strength and N being the gas number density) was 145 Td (1 Td = 10^{-17} V cm^2). A gas calibration unit (Ionicon Analytik GmbH, Austria) was used for VOC calibration. In 2016, the instrumental response factors were 7.1 ncps ppb^{-1} for methanol (m/z 33), 16.7 ncps ppb^{-1} for acetone (m/z 59), 3.1 ncps ppb^{-1} for isoprene (m/z 69) and 10.8 ncps ppb^{-1} for monoterpenes (m/z 81 + 95 + 137). Both acetone and propanal can be detected as m/z 59. We consider m/z 59 as acetone because acetone has been reported to be one of the main BVOC emitted by *Picea abies*.[3,29,37,38] Previous work by Tani[39,40] and Brown[41] have shown that m/z 81 and m/z 137 are the two major ions produced from all monoterpenes including oxygenated species like linalool, even under high E/N of ca. 140. By considering only m/z's 81, 95, and 137 we collect ≥90% of the total monoterpene signal. We assume m/z 95 to be monoterpene fragment, because there was a strong relationship between m/z 137 and m/z 95 across treatments (R^2=0.84; SI Figure S4). Taking into account the different reaction rate coefficients for monoterpene isomers with H_3O^+ and the potential interferences from phenols, we estimated that the accumulative error of the reported total monoterpene emissions is within 15% of the true values. Hence, we believe that the sum of m/z 137 + 95 + 81 reflects a general trend of monoterpene emissions in plants and their responses to our treatment, as shown in many other studies.[3,29,30,42] In 2017, the instrumental response factors were 11.6 ncps ppb^{-1} for methanol (m/z 33), 19.1 ncps ppb^{-1} for acetone (m/z 59), 3.1 ncps ppb^{-1} for isoprene (m/z 69) and 10.1 ncps ppb^{-1} for monoterpenes (m/z 81 + 137). The instrumental response factor (0.5 ncps ppb^{-1}) for sesquiterpenes (m/z 205) was estimated so the reported concentrations are indicative only. The instantaneous specific whole aboveground BVOC emissions were defined as

$$\text{BVOC}(\text{nmol}\,\text{g}^{-1}\text{s}^{-1}) = \frac{\text{BVOC}_{\text{Tree}} - \text{VOC}_{\text{Ref}}(\text{nmol}\,\text{mol}^{-1})}{\text{molar volume}(\text{l}\,\text{mol}^{-1})} \times \frac{\text{VFR}(\text{l}\,\text{s}^{-1})}{\text{biomass}(\text{g})} \quad (3)$$

where $\text{BVOC}_{\text{tree}}$ represents the mixing ratio of specific BVOC (methanol, acetone, mono- or sesquiterpenes) of air exiting the chambers with tree, and VOC_{ref} is the mixing ratio of specific VOC of air exiting the reference chamber. VFR and the molar volume of gas were the same as used in eq 1. Biomass is calculated as the sum of dry weight of samples collected for substrate analysis and of whole aboveground (including stem, branches, and needles) harvested at the end of the experiment. $[CO_2]$ and BVOC of air exiting each chamber were measured every 2 h from 6:00 to 20:00 (CET). Emissions of BVOC during nighttime were shown to be much lower than during daytime, and thus excluded from our study.

$^{13}CO_2$ Pulse-Labeling. On 28 September 2017 in experiment II, the air supply system was disconnected and replaced for 1 h, between 13:00 and 14:00, by inlets from aluminum gas tanks of synthetic air premixed with 99 atom % $^{13}CO_2$ (Sigma-Aldrich) at 400, 180, and 50 ppm at the same flow rate. Afterward, the original air supply system reconnected and treatments continued. We traced the ^{13}C into acetone, mono-, and sesquiterpenes by measuring isotopologue emissions: Acetone, m/z 59 and 60; monoterpenes, m/z 137−142; sesquiterpenes, m/z 205−210.

Identification of Emitted Monoterpenes and Sesquiterpenes. At the end of $[CO_2]$ reverting treatment, air exiting each chamber was drawn through adsorbent tubes filled with 5 mm Quarz Wool, Tenax TA 35/60 and Carbograph 5TD 40/60 (Markes Environmental, Sacramento, CA) in parallel to the PTR-MS measurements. Each sample was collected at a flow rate of 215 mL min^{-1} for 30 min using a flow-controlled hand-held pump (SG350ex, GSA GmbH & CO KG Germany). Samples collected from experiment I were identified and quantified by a thermal desorption−gas chromatograph−mass spectrometer (TD−GC−MS) system described in detail elsewhere.[43] Samples collected from experiment II were also analyzed by TD−GC−MS but with slight modifications. Tubes were desorbed using the following conditions: dry purge 5 min at 20 mL/min, pre purge 2 min at 20 mL/min, desorption 8 min at 280 °C with 20 mL/min, pre trap fire purge 1 min at 30 mL/min, trap heated to 300 °C and hold for 4 min. The BVOCs were separated on a gas chromatograph (Bruker, GC-456, Bremen, Germany) connected to a triple-quad mass spectrometer (Bruker, SCION). Separation took place on a DB-5MS column (30 m × 0.25 mm × 0.25 μm. Restek, Germany). The conditions of the GC were as follows: 40 °C for 6 min, 20 °C/min to 120 °C, 5 °C/min to 200 °C, 30 °C/min to 260 °C and hold for 6 min. The mass spectrometer was operated in full scan mode with the following parameters: transfer line temperature 260 °C, ion source temperature 240 C, scan time 250 ms, scan range 40 to 550 m/z, ionization 70 eV.

Analysis of Soluble Sugars and Stored Monoterpenes. Soluble sugars were extracted with distilled water at 65 °C and determined with high-performance liquid chromatography−pulsed amperometric detection (HPLC−PAD), as previously described in Hartmann et al.[44] Stored monoterpenes were extracted with *tert*-butylmethyl ether using 30 μg/mL 1,9-decadiene as internal standard. Stored monoterpenes were qualitatively and quantitatively analyzed with an Agilent 6890 series gas chromatograph (Santa Clara, CA) (injection: 1 μL splitless, 220 °C, flow: 2 mL min^{-1} constant, temperature: 70 °C for 3 min, 70−240 °C gradient with 6 °C min^{-1} and 240 °C for 3 min) coupled to either a flame

DOI: 10.1021/acs.est.8b01435
Environ. Sci. Technol. XXXX, XXX, XXX−XXX

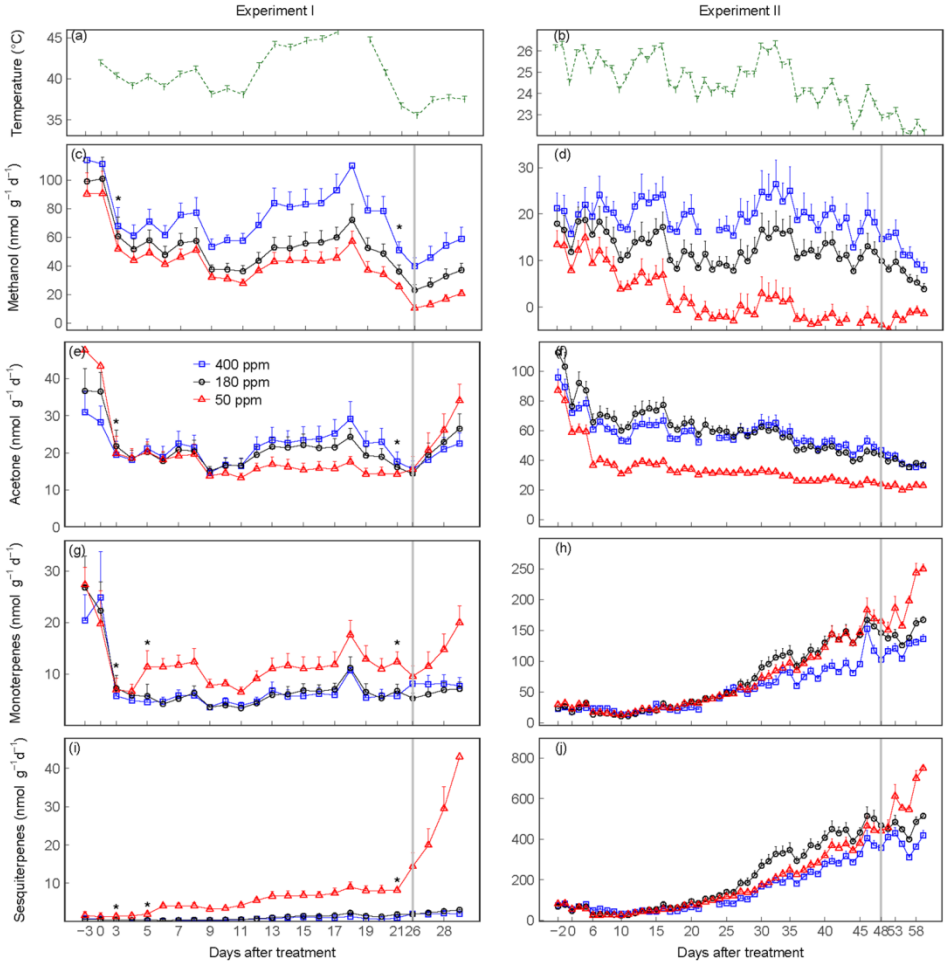

Figure 3. Daytime temperature (a, b), whole aboveground methanol (c, d), acetone (e, f), mono- (g, h), and sesquiterpenes (i, j) emissions. Values (nmol g^{-1} day^{-1}) are from individual FEP chamber; error bars represent daytime variations of BVOC emissions measured every 2 h from 6:00 to 20:00 (CET) within each chamber (n = 7). [CO_2] were reduced from 400 to 180 and 50 ppm from day 1, followed by reverting [CO_2] from 180 and 50 back to 400 ppm as indicated by the gray line. Emissions for days −3, −2, −1, and 0 were measured prior to the [CO_2] treatments. The tentative quantification of sesquiterpenes was based on estimated instrumental mass discrimination and fragmentation of protonated sesquiterpenes. Asterisks indicate data were averaged from less than five data points due to disturbance, for example, PTR-MS malfunction and sampling. Note the different scales on y-axes.

ionization detector (FID; operated at 300 °C) or an Agilent 5973 series mass spectrometer (MS; transferline temperature: 270 °C, quadrupole temperature: 150 °C, source temperature: 230 °C, electron energy: 70 eV, 4.49 scans s^{-1}, 33−350 amu), respectively. The volatile blend was separated on a DB-5MS column (30 m × 0.25 mm × 0.25 μm; Agilent) with H_2 (FID) or He (MS) as carrier gas. Peak integration was done with Agilent ChemStation Software. In order to identify the compounds, their mass spectra were matched with reference spectra from databases (Wiley 275, NIST 98, Adams 2205), or compared to those of authentic standards. The amount of each compound was determined from GC−FID data based on the peak area in relation to the internal standard peak area. The relative response factor was estimated with the effective carbon number concept, and normalized to fresh weight and duration of collection.[45]

Data Analysis. The correlations of methanol, acetone, mono-, and sesquiterpene emissions to variations in temperature, light and net carbon assimilation along the CO_2 gradient, all averaged half-hourly, were assessed by Pearson's correlation. The effects of temperature, light and [CO_2] and their interactions on BVOC, all averaged half-hourly, were assessed by three-way ANOVA, with temperature, light and A_{net} as independent variables and BVOC emissions as dependent variable. All statistical analysis was conducted in R version 3.23,[46]

RESULTS

In both experiments, whole aboveground daytime A_{net} rapidly declined after reducing [CO_2] from 400 to 180 or 50 ppm, but rapidly recovered after reverting [CO_2] back to 400 ppm [CO_2] (SI Figure S5a, b).

To investigate the carbon dependence of BVOC emissions, we measured methanol, acetone, mono-, and sesquiterpenes emissions from entire aboveground portion of Norway spruce

DOI: 10.1021/acs.est.8b01435
Environ. Sci. Technol. XXXX, XXX, XXX−XXX

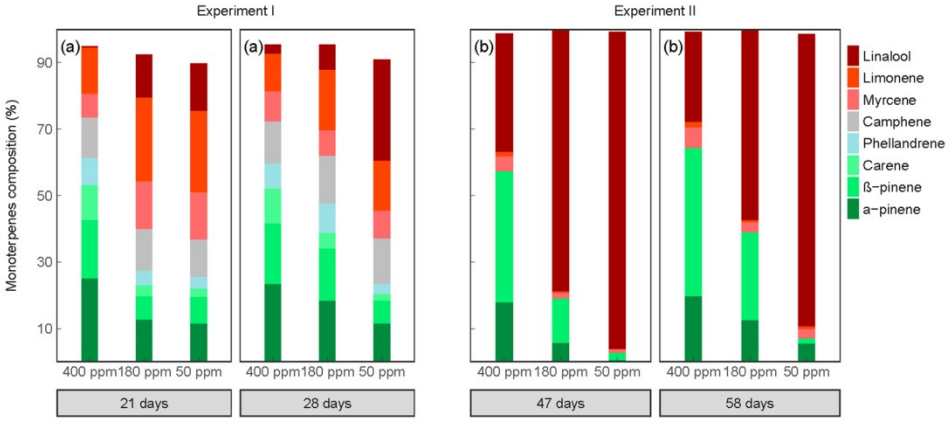

Figure 4. Changes in relative proportions of monoterpene emissions. In experiment I, air samples were collected 21 days after reducing [CO_2] from 400 ppm to 180 and 50 ppm (shown as day 21) and 4 days after reverting the two lower [CO_2] treatments back to 400 ppm (shown as day 28). In experiment II, air samples were collected 48 days after reducing [CO_2] from 400 ppm to 180 and 50 ppm (shown as day 48) and 7 days after reverting the two lower [CO_2] treatments back to 400 ppm (shown as day 59).

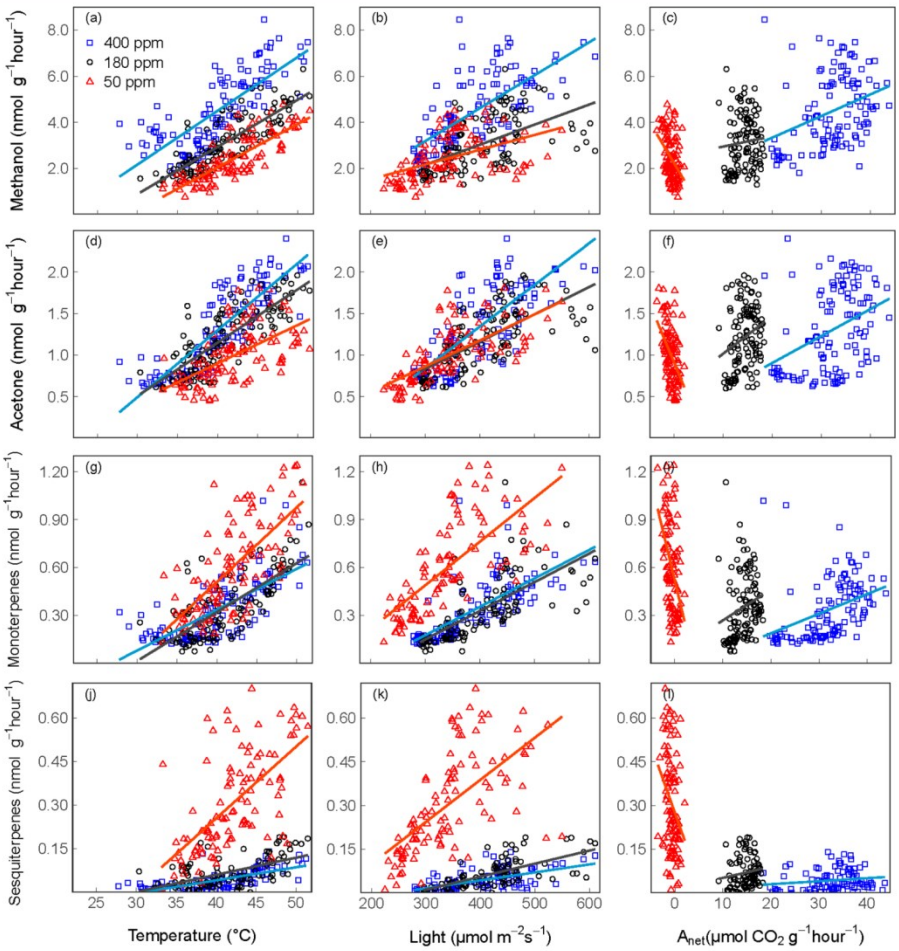

Figure 5. Relationships of experiment I between methanol (a–c), acetone (d–f), mono- (g–i), and sesquiterpenes (j–l) and temperature, light, and net carbon assimilation (A_{net}). A linear regression fit was used for each [CO_2] treatment. The tentative quantification of sesquiterpenes was based on estimated instrumental mass discrimination and fragmentation of protonated sesquiterpenes.

DOI: 10.1021/acs.est.8b01435
Environ. Sci. Technol. XXXX, XXX, XXX−XXX

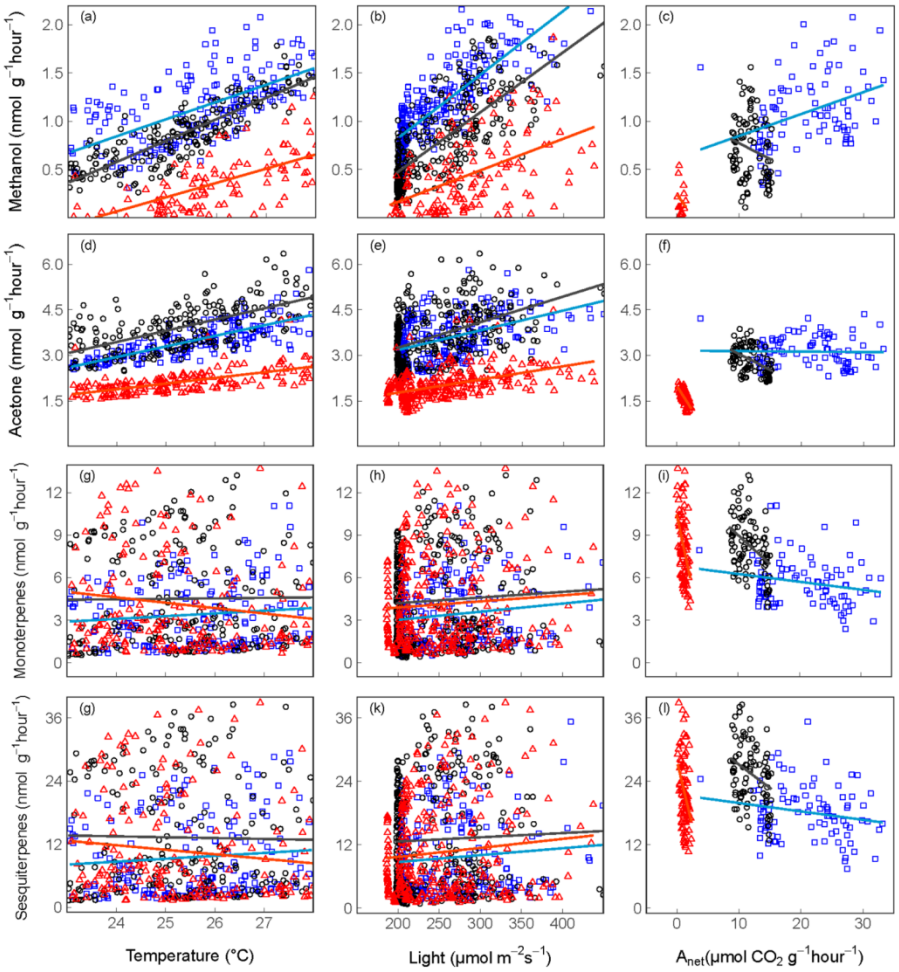

Figure 6. Relationships of experiment II between methanol (a–c), acetone (d–f), mono- (g–i), and sesquiterpenes (j–l) and temperature, light and net carbon assimilation (A_{net}). A linear regression fit was used for A_{net} for each [CO_2] treatment. The tentative quantification of sesquiterpenes was based on estimated instrumental mass discrimination and fragmentation of protonated sesquiterpenes.

trees exposed to 400, 180, and 50 ppm [CO_2] (Figure 3). Methanol and acetone were the most abundant oxygenated BVOC in both experiments (10–100 nmol g^{-1} day^{-1}). In experiment I, methanol emissions showed little difference initially at 400 ppm [CO_2], but decreased by more than 30 nmol g^{-1} day^{-1} from 400 to 180 ppm [CO_2] and decreased by 15 nmol g^{-1} day^{-1} from 180 to 50 ppm [CO_2] at day 18 (Figure 3c). In experiment II, methanol emission rates declined to zero over time at 50 ppm [CO_2] (Figure 3d). Similarly, acetone emissions were lower at 50 ppm [CO_2] than at 180 and 400 ppm [CO_2] which did not differ, in both experiments (Figure 3e, f). ANOVA results showed there was a significant CO_2 effects on methanol and acetone emissions (SI Table S1, S2). After reverting [CO_2] from 50 and 180 ppm back to 400 ppm, difference in methanol emissions between treatments persisted within the 4/7 days of observations (Figure 3c, d), while difference in acetone emission rates recovered to rates observed prior to CO_2 reduction treatments in experiment I, but tended to decrease in experiment II (Figure 3e, f).

Emissions of mono- and sesquiterpenes showed little difference initially at 400 ppm [CO_2], in both experiments. In experiment I, emissions of mono- and sesquiterpenes at 400 and 180 ppm [CO_2] were similar but much lower than at 50 ppm [CO_2] (Figure 3g, (i). In experiment II, emissions were low initially and increased by orders of magnitude over time in all [CO_2] treatments, and the increase was stronger at 180 and 50 ppm than at 400 ppm [CO_2] (Figure 3h, j). In both experiments, there was a significant CO_2 effect on emissions of mono- and sesquiterpenes (SI Table S1, S2). Strikingly, in both experiments, the difference in emission rates of mono- and sesquiterpenes further increased after reverting [CO_2] from 50 back to 400 ppm [CO_2] (Figure 3g–j). Note that in experiment I, emissions of methanol, acetone, and monoterpenes strongly declined from days −3 and 0 (prior to sampling and treatments, respectively) to day 3, likely reflecting aboveground acclimation to the dry air and high temperatures in the chamber.

To investigate how changing [CO_2] alters the composition of monoterpenes, we analyzed the air samples by using GC–MS. (Figure 4). In both experiments, reducing [CO_2] from

DOI: 10.1021/acs.est.8b01435
Environ. Sci. Technol. XXXX, XXX, XXX−XXX

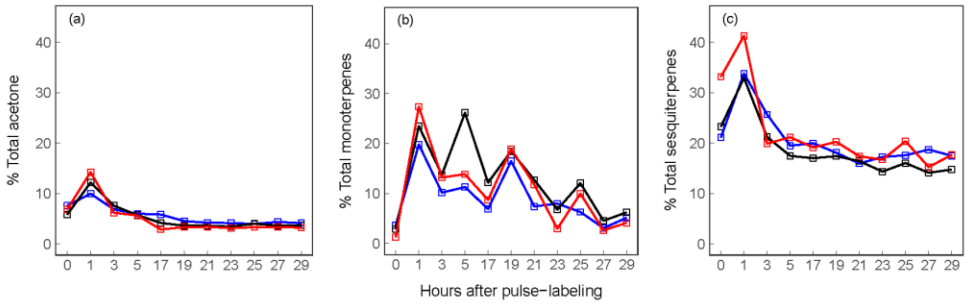

Figure 7. ^{13}C Labeled BVOC emissions as a percentage of total BVOC emissions during and during and after 1 h pulse-labeling: (a) [$^{13}C_1$]acetone; (b) [$^{13}C_{1-3}$]monoterpenes; (c) [$^{13}C_{1-3}$]sesquiterpenes.

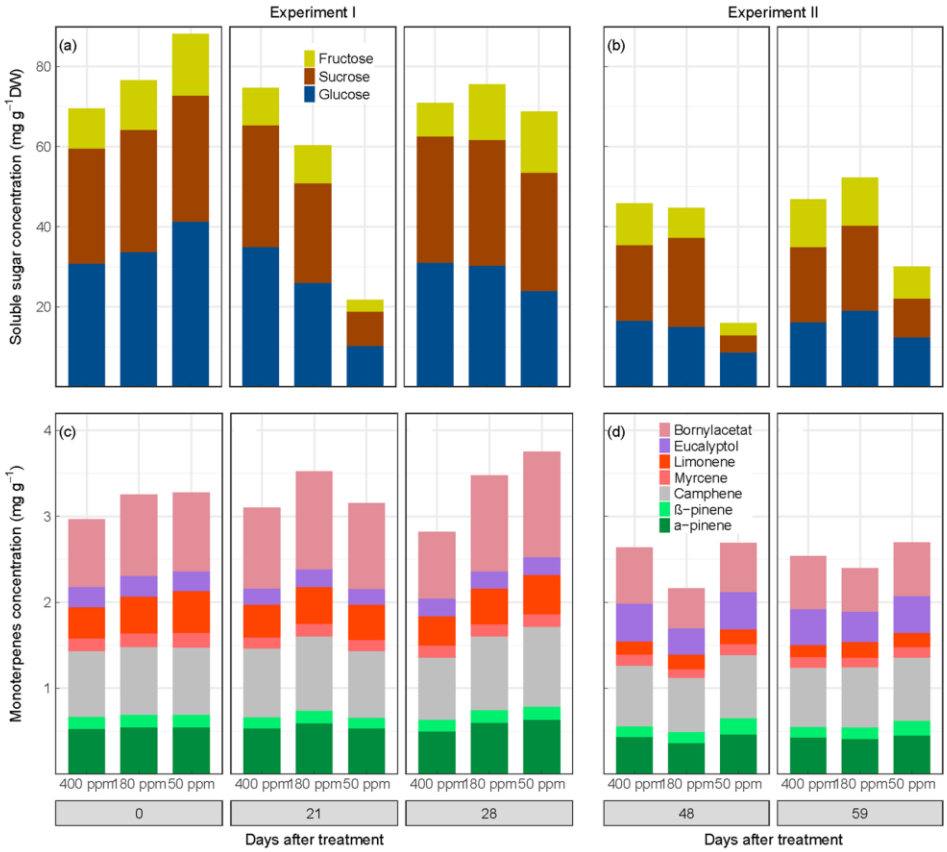

Figure 8. Concentrations of soluble sugars (mg g^{-1} dry weight, a, b) and monoterpenes (mg g^{-1} fresh weight, c, d) in current-year needles of in *Picea abies*.

400 to 50 ppm decreased the proportion of α-pinene and β-pinene, but increased linalool. Although similar changes in the composition of monoterpenes were found in the two experiments, the lack of replication within each experiment increases uncertainty. These patterns remained consistent after reverting [CO_2] from 50 and 180 ppm to 400 pm (Figure 4a, b). The spruce genotype used in experiment I emitted α−farnesene, β−farnesene and α−bisabolene (SI Figure S6). By contrast, the spruce genotype used in experiment II emitted (*E*)-β-farnesene only.

To investigate the interactions of temperature, light, and carbon assimilation in controlling BOVC emissions, we plotted half-hourly measurements of BVOC emissions against temperature, light and A_{net} within each [CO_2] treatment. In both experiments, methanol and acetone emissions strongly increased with air temperature and PAR (Figure 5 and Figure 6a, b, d, e). Methanol emissions exhibited a greater dependence on air temperature (mean R^2 = 0.68) than on light (mean R^2 = 0.42) (SI Tables S3, S4). The temperature sensitivity of methanol and acetone emissions varied significantly across [CO_2] treatment (temperature × [CO_2]

DOI: 10.1021/acs.est.8b01435
Environ. Sci. Technol. XXXX, XXX, XXX−XXX

interaction, $P < 0.01$; SI Tables S1, S2). Relationships were not as evident with respect to net carbon assimilation at 400 and 180 ppm [CO_2] (A_{net}) ($R^2 < 0.3$), but methanol emissions were more dependent on A_{net} across [CO_2] treatments (R^2 is 0.33 and 0.65 in experiment I and II, respectively) than within each [CO_2] treatment (SI Tables S3, S4).

In experiment I, emissions of mono- and sesquiterpenes also increased strongly with air temperature and PAR but not with A_{net} (Figure 5g–l). Sesquiterpene emissions were more dependent on A_{net} ($R^2 = 0.40$) across [CO_2] treatments than within each [CO_2] treatment (SI Table S3). Temperature and light response curves were also influenced by [CO_2], as emissions increased more at 50 ppm [CO_2] than at 400 ppm [CO_2] with air temperature and PAR (Figure 5g, h, j, k). In experiment II, however, emissions of mono- and sesquiterpenes were not correlated with air temperature or light (Figure 6g, h, j, k). From the ANOVA, interactions between [CO_2] and air temperature on emissions of mono- and sesquiterpenes were stronger in experiment I ($P < 0.01$, SI Table S1) than in experiment II ($P = 0.05$, SI Table S2).

To determine the relative contribution of newly assimilated vs old carbon to BVOC emissions, we applied $^{13}CO_2$ pulse-labeling and traced ^{13}C labeled BVOC emissions with PTR-MS. Newly assimilated carbon was incorporated into acetone and sesquiterpene emissions directly after pulsing-labeling (shown at hour 0, Figure 7). Labeled BVOC peaked 1 h after labeling, with higher incorporation of labeled C in mono- and sesquiterpenes emissions than in acetone emissions. By using $^{13}CO_2$ labeling, we estimated that ca. 15% of total sesquiterpene emissions were [$^{13}C_{1-3}$]sesquiterpenes emissions. Interestingly, reducing [CO_2] from 400 to 50 ppm increased the proportion of labeled C in all three BVOC emissions (Figure 7).

To link changes in BVOC emissions to changes in substrate availability, we measured concentrations of soluble sugars and monoterpenes in needles (Figure 8). In experiment I, trees showed little differences in concentrations and composition of soluble sugars and monoterpenes (Figure 8a, c). However, reducing [CO_2] to 50 ppm strongly decreased soluble sugar concentrations in both experiments (Figure 8a, b). Soluble sugar concentrations at 50 ppm [CO_2] rapidly recovered 4 days after reverting [CO_2] to 400 ppm in experiment I (Figure 8a), whereas the recovery was much slower in experiment II (Figure 8b). By contrast, in both experiments, reducing [CO_2] had no effect on monoterpene concentrations or on the composition of individual compounds in current-year needles. Similarly, monoterpenes remained relatively constant after reverting [CO_2] treatments, and only slightly increased after reverting [CO_2] from 50 to 400 ppm [CO_2] in experiment I (Figure 8c).

DISCUSSION

Coupling PTR-MS and cavity ring-down spectroscopy to [CO_2] manipulation allowed highly time-resolved (half-hourly) measurements of BVOC emissions and [CO_2], as well as environmental factors (temperature and light) along a gradient of [CO_2]. TD–GC–MS analysis further showed compound-specific response of terpenoid emissions. In addition, the pulse-labeling approach clearly revealed the incorporation of newly assimilated carbon versus old stored carbon to BVOC emissions, even under 50 ppm [CO_2]. Combining all these techniques no doubt contributes to the understanding of the complexity of BVOC regulation but also requires careful experimental design, significant investment, and collaboration across disciplines. The financial and technical expense of facilities including large FEP chambers and PFA valves switching unit, along with the fact that only one PTR-QMS was available, necessarily limited the number of biological replicates. We note that this is an apparent weakness in our approach, and one reason repeated the same experiment in different years. While not without weaknesses, our study provides new perspectives on CO_2, temperature and light effects on BVOC emissions, in particular how they depend on stored pools and recent photosynthetic products.

Interactions between [CO_2], Temperature and Light in Controlling Methanol and Acetone Emissions. Previous work has shown that Norway spruce-dominated forests emit large amounts of methanol.[29] We found that the percentage of net carbon assimilation (ca. 500 and 300 μmol g^{-1} day^{-1} for experiment I and II, respectively) emitted as methanol (ca. 50–100 and 15–30 nmol g^{-1} day^{-1} for experiment I and II, respectively) ranged from 0.005% to 0.02%, similar to previous enclosure measurements.[47] Reduced [CO_2] progressively decreased the absolute magnitude of daily methanol emissions (Figure 3), possibly due to declining growth activity.[24] Also, half-hourly variations in emissions of these compounds were mainly driven by temperature and light, rather than instantaneous A_{net} under low CO_2 treatments (Figure 4, 5), indicating that low [CO_2] may influence BVOC emissions not via immediate effects on photosynthesis.

While A_{net} rapidly declined after reducing [CO_2] to 180 and 50 ppm and immediately recovered after reverting back to 400 ppm [CO_2], methanol emissions showed little change relative to 400 ppm [CO_2], within the 4/7 days of observations (Figure 3). This may indicate, on the one hand, that reserves may have provided substrate for maintaining methanol pathway activity, but, on the other hand, that reactivating this pathway is a slow process, which did not occur 1 week after return to 400 ppm conditions. Substrate limitations of pectin methylesterase (PME) may play an important role in regulating methanol emissions.[26] We did not assess PME substrate availability in our study. However, it may be expected that pectins, that is, galacturonic acid-rich polysaccharides,[25] have been reduced at low [CO_2] because the levels of saccharides including glucose and sucrose that are required for pectins synthesis have been strongly decreased here (Figure 8) and in previous low [CO_2] studies.[44,48] In addition, the fact that methanol emissions at low [CO_2] varied with air temperature and light, and they did not recover though soluble sugars increased upon reverting [CO_2], suggesting substrate limitation alone cannot explain the reduction in methanol emissions. Studies have shown that auxin initiates PME activity,[49] which catalyzes demethylation of pectin and thereby causes methanol emissions. Low [CO_2] has been found to decrease auxin levels[50] and this may also explain reduced methanol emissions.

Acetone emissions were not dependent on instantaneous A_{net} at 400 ppm [CO_2], but progressively declined under reduced [CO_2], again indicating that reserves may be important for maintaining acetone emissions (Figure 3). By using pulse-labeling, our results suggest that less than 15% of acetone was produced from newly assimilate carbon (Figure 7). Acetone is likely derived from metabolism of pyruvic acid,[27] which is produced from glucose during glycolysis. Hence, decreasing glucose availability at low [CO_2] may become a limiting factor for glycolysis reactions that provide

DOI: 10.1021/acs.est.8b01435
Environ. Sci. Technol. XXXX, XXX, XXX–XXX

pyruvic acid as precursor for acetone emissions. In contrast to methanol reactivation, acetone emissions recovered quickly from reverting [CO_2] in experiment I (Figure 3), indicating the pyruvate pool can be rapidly fuelled by recently assimilated carbon.

Interestingly, low [CO_2] also decreased the responses of methanol and acetone emissions to air temperature and PAR conditions (Figures 5 and 6), suggesting substrate limitation at low [CO_2] may not allow emissions to increase as would be expected from higher enzymatic activities at elevated air temperature and light. The mechanisms underlying these interactions between [CO_2], temperature and light are currently unknown but important for understanding and predicting methanol and acetone emissions.

Monoterpene (e.g., linalool) and Sesquiterpene (e.g., farnesene) Emission Rates Increased at Low Carbon Availability. Our observations that monoterpenes had higher emission rates than isoprene (SI Figure S7) agree with previous results on Norway spruce using in situ gas chromatography.[51] Mono- and sesquiterpene emission rates remained constant or increased at low [CO_2], possibly to protect plants against oxidative stress via scavenging ROS.[16] It is known that reducing [CO_2] may exacerbate ROS production from excess light excitation energy,[52] and reduce the ability of plants to scavenge ROS via reducing sugar.[53] In addition, terpenoid emissions are also known to protect plants against herbivory,[15,54] and this is corroborated by the burst following sampling and ensuing tissue damage (SI Figure S8). Hence, enhanced terpenoid emissions may also reflect increased defense demand at low [CO_2] where tissues become relatively more valuable for carbon assimilation and more costly to repair following attack. A defense-related response is also supported by strong increases in linalool and farnesene emissions at low [CO_2], as they are also the major terpenoids emitted from Norway spruce after methyl jasmonate (MeJA) treatment[55] and from mountain birch (*Betula pubescens*) after herbivory.[56]

Interestingly, our results showed interactions between [CO_2] and air temperature, and [CO_2] and light, in controlling mono- and sesquiterpene emissions but only in experiment I (Figure 5), possibly because sodium lamps were used in experiment I to provide supplemental light, but also created much higher air temperatures than did LED lamps used in experiment II. Nevertheless, in experiment I increased temperature dependence at low [CO_2] may result from increased stomatal conductance, as emission responses to variations in transpiration rates also increased at low [CO_2] (Figure S9). Interactions between intercellular CO_2 and temperature,[57] between growth [CO_2] and light[58] have also been reported on isoprene emissions.

Half-hourly emissions of mono- and sesquiterpenes were not correlated with A_{net} ($R^2 < 0.3$), suggesting that total terpenoid emissions are not mainly driven by variations in recently assimilated carbon (Figures 5 and 6). By using $^{13}CO_2$ labeling, our results also indicate that less than 30% of terpenoid emissions were produced from recently assimilated carbon after 1 h pulse-labeling (Figure 7). This is in agreement with a previous study showing that ca. 30% of monoterpene emissions under ambient [CO_2] are produced de novo in Norway spruce.[59] Interestingly, we found that more newly assimilated carbon was allocated to terpenoid emissions at low [CO_2] than at ambient [CO_2], suggesting low [CO_2]-induced increases in terpenoid emissions might be synthesized de novo, rather than stored terpenoid pools. This is corroborated by the contrasting profiles in monoterpene emissions versus monoterpenes stored in needles, as low [CO_2] reduced the proportion of α- and β-pinene emissions and increased the proportion of linalool emissions, whereas in needles the composition and concentrations of monoterpenes remained unaffected and no linalool was detected in both experiments (Figure 8).

Reverting [CO_2] from 50 to 400 ppm strongly increased mono- in particular sesquiterpene emissions (Figure 3), suggesting that the de novo production is limited by newly assimilated carbon at low CO_2. In our study, linalool, α- and β-farnesene were the major terpenoid compounds produced upon reverting [CO_2] (Figure 4), a result that is corroborated by previous studies showing that linalool and β-farnesene are synthesized de novo after methyl jasmonate treatment in Norway spruce.[55] Further advances of our understanding of the roles of terpenoid emissions can be achieved by starving transgenic plants that differ in production of terpenoids, for example, linalool and farnesene, similar to what has been done on isoprene emissions.[11,24]

In summary, we provide new evidence for the dependency of plant methanol and acetone emissions on carbon availability, temperature and light. Our work demonstrates reducing carbon availability has similar impacts on methanol and acetone emissions to those of temperature and light. Based on our findings one would expect that methanol and acetone may have strongly increased from the past (glacial [CO_2], ~170 ppm) to current climatic scenarios (ambient [CO_2], ~400 ppm), and may continue to increase as [CO_2] rises in the future. Moreover, by tracing the fate of newly assimilated C into emissions of BVOC, we provide new perspectives on the physiological regulation of BVOC emissions. Under conditions of low carbon supply (e.g., from drought, nutrient deficiency and defoliation), stored compounds (e.g., NSC and monoterpenes) along with newly assimilated carbon can provide substrates for BVOC production that may play an important role in plant protection and defense.

Investigations of physiological mechanisms behind the observed BVOC responses can be carried out on small seedling clones, as they allow less costly constructions and manipulations,[60] for example, FEP chambers constructed at a smaller size. Moreover, PTR-QMS uses a quadrupole mass analyzer that measures only one VOC at a time and may not capture all fragments of BVOCs, and thus preventing an accurate quantification. Instead, PTR-TOF-MS uses a time-of-flight mass spectrometer that gives an entire mass range therefore may significantly reduce the measurement time for each chamber. Such approaches may allow sufficient replication to examine the physiological mechanisms, that is, the carbon and temperature dependencies of enzyme−substrate interactions involved in methanol and acetone emissions, and the role of terpenoid emissions in stress responses.

■ ASSOCIATED CONTENT

Supporting Information

The Supporting Information is available free of charge on the ACS Publications website at DOI: 10.1021/acs.est.8b01435.

Table S1 and S2: Three-way ANOVA testing in experiment I and II, respectively. Tables S3 and S4: Coefficient of determination and probability for the correlations between BVOC emissions and air temperature, light and assimilation in experiment I and II,

DOI: 10.1021/acs.est.8b01435
Environ. Sci. Technol. XXXX, XXX, XXX−XXX

respectively. Table S5 Coefficient of determination and probability for the correlations between terpenoid emissions and transpiration rate in experiment I(PDF) Figure S1 Photograph of the four Teflon chambers in the greenhouse. Figure S2 Additional data sets on concentrations of soluble sugars and monoterpenes of aboveground organs. Figure S3 Additional data set on BVOC emissions from trees grown under 400 ppm [CO_2]. Figure S4 The correlation between m/z 95 and m/z 137. Figure S5 CO_2 and water vapor gas exchange. Figure S6 Changes in relative proportions of sesquiterpene emissions in experiment I. Figure S7 A comparison between monoterpenes and isoprenes emissions in experiment I and II. Figure S8 Screenshot of PTR-MS monitor after sampling damage. Figure S9 Relationships between terpenoid emissions and transpiration rate in experiment I (PDF)

AUTHOR INFORMATION

Corresponding Authors

*(J.H) E-mail: hjianbei@bgc-jena.mpg.de.

*(T.B.) E-mail: tbehr@bgc-jena.mpg.de.

ORCID

Jianbei Huang: 0000-0001-5286-5645

Armin Wisthaler: 0000-0001-5050-3018

Notes

The authors declare no competing financial interest.

ACKNOWLEDGMENTS

We thank Waldemar Ziegler, Frank Voigt, Karl Kübler, Olaf Kolle, Savoyane Lambert, and René Schwalbe for their help with chamber and light construction and [CO_2] manipulation. We thank Louwrance Wright for his assistance in setting up the PTR-MS measurement. We also thank Agnes Fastnacht and Somak Chowdhury for support in the greenhouse, Iris Kuhlmann and Anett Enke for assistance in the laboratory. We thank Michael Reichelt for GC−MS and GC−FID analysis. The work has been funded by the Deutsche Forschungsgemeinschaft (DFG) CRC 1076 "AquaDiva". We thank the Hainich CZE site manager Robert Lehmann, Christine Hess for scientific coordination and the Hainich National Park. J.H. was funded by Chinese Scholarship Council and Max Planck Institute for Biogeochemistry, and acknowledges support from the International Max Planck Research School for Global Biogeochemical Cycles.

REFERENCES

(1) Lelieveld, J.; Butler, T. M.; Crowley, J. N.; Dillon, T. J.; Fischer, H.; Ganzeveld, L.; Harder, H.; Lawrence, M. G.; Martinez, M.; Taraborrelli, D.; Williams, J. Atmospheric oxidation capacity sustained by a tropical forest. *Nature* **2008**, *452* (7188), 737−740.

(2) Di Carlo, P.; Brune, W. H.; Martinez, M.; Harder, H.; Lesher, R.; Ren, X.; Thornberry, T.; Carroll, M. A.; Young, V.; Shepson, P. B.; Riemer, D.; Apel, E.; Campbell, C. Missing OH reactivity in a forest: evidence for unknown reactive biogenic VOCs. *Science* **2004**, *304* (5671), 722−725.

(3) Nölscher, A. C.; Bourtsoukidis, E.; Bonn, B.; Kesselmeier, J.; Lelieveld, J.; Williams, J. Seasonal measurements of total OH reactivity emission rates from Norway spruce in 2011. *Biogeosciences* **2013**, *10* (6), 4241−4257.

(4) Monks, P. S.; Archibald, A. T.; Colette, A.; Cooper, O.; Coyle, M.; Derwent, R.; Fowler, D.; Granier, C.; Law, K. S.; Mills, G. E.; Stevenson, D. S.; Tarasova, O.; Thouret, V.; von Schneidemesser, E.; Sommariva, R.; Wild, O.; Williams, M. L. Tropospheric ozone and its precursors from the urban to the global scale from air quality to short-lived climate forcer. *Atmos. Chem. Phys.* **2015**, *15* (15), 8889−8973.

(5) Hallquist, M.; Wenger, J. C.; Baltensperger, U.; Rudich, Y.; Simpson, D.; Claeys, M.; Dommen, J.; Donahue, N. M.; George, C.; Goldstein, A. H.; Hamilton, J. F.; Herrmann, H.; Hoffmann, T.; Iinuma, Y.; Jang, M.; Jenkin, M. E.; Jimenez, J. L.; Kiendler-Scharr, A.; Maenhaut, W.; McFiggans, G.; Mentel, T. F.; Monod, A.; Prévôt, A. S. H.; Seinfeld, J. H.; Surratt, J. D.; Szmigielski, R.; Wildt, J. The formation, properties and impact of secondary organic aerosol: current and emerging issues. *Atmos. Chem. Phys.* **2009**, *9* (14), 5155−5236.

(6) Guenther, A.; Hewitt, C. N.; Erickson, D.; Fall, R.; Geron, C.; Graedel, T.; Harley, P.; Klinger, L.; Lerdau, M.; McKay, W. A.; Pierce, T.; Scholes, B.; Steinbrecher, R.; Tallamraju, R.; Taylor, J.; Zimmerman, P. A global model of natural volatile organic compound emissions. *J. Geophys. Res.* **1995**, *100* (D5), 8873−8892.

(7) Kessler, A. Introduction to a Virtual Special Issue on plant volatiles. *New Phytol.* **2016**, *209* (4), 1333−1337.

(8) Loreto, F.; Dicke, M.; Schnitzler, J.-P.; Turlings, T. C. J. Plant volatiles and the environment. *Plant, Cell Environ.* **2014**, *37* (8), 1905−1908.

(9) Peñuelas, J.; Llusià, J. BVOCs: plant defense against climate warming? *Trends Plant Sci.* **2003**, *8* (3), 105−109.

(10) Messina, P.; Lathière, J.; Sindelarova, K.; Vuichard, N.; Granier, C.; Ghattas, J.; Cozic, A.; Hauglustaine, D. A. Global biogenic volatile organic compound emissions in the ORCHIDEE and MEGAN models and sensitivity to key parameters. *Atmos. Chem. Phys.* **2016**, *16* (22), 14169−14202.

(11) Way, D. A.; Ghirardo, A.; Kanawati, B.; Esperschütz, J.; Monson, R. K.; Jackson, R. B.; Schmitt-Kopplin, P.; Schnitzler, J.-P. Increasing atmospheric CO_2 reduces metabolic and physiological differences between isoprene- and non-isoprene-emitting poplars. *New Phytol.* **2013**, *200* (2), 534−546.

(12) Possell, M.; Hewitt, C. N. Isoprene emissions from plants are mediated by atmospheric CO_2 concentrations. *Global Change Biology* **2011**, *17* (4), 1595−1610.

(13) Sharkey, T. D.; Monson, R. K. The future of isoprene emission from leaves, canopies and landscapes. *Plant, Cell Environ.* **2014**, *37* (8), 1727−1740.

(14) Harrison, S. P.; Morfopoulos, C.; Dani, K. G. S.; Prentice, I. C.; Arneth, A.; Atwell, B. J.; Barkley, M. P.; Leishman, M. R.; Loreto, F.; Medlyn, B. E.; Niinemets, Ü.; Possell, M.; Peñuelas, J.; Wright, I. J. Volatile isoprenoid emissions from plastid to planet. *New Phytol.* **2013**, *197* (1), 49−57.

(15) Holopainen, J. K.; Gershenzon, J. Multiple stress factors and the emission of plant VOCs. *Trends Plant Sci.* **2010**, *15* (3), 176−184.

(16) Vickers, C. E.; Gershenzon, J.; Lerdau, M. T.; Loreto, F. A unified mechanism of action for volatile isoprenoids in plant abiotic stress. *Nat. Chem. Biol.* **2009**, *5* (5), 283−291.

(17) Penuelas, J.; Staudt, M. BVOCs and global change. *Trends Plant Sci.* **2010**, *15* (3), 133−144.

(18) Loreto, F.; Schnitzler, J.-P. Abiotic stresses and induced BVOCs. *Trends Plant Sci.* **2010**, *15* (3), 154−166.

(19) Atkinson, R.; Arey, J. Gas-phase tropospheric chemistry of biogenic volatile organic compounds: a review. *Atmos. Environ.* **2003**, *37* (Supplement 2), 197−219.

(20) Jardine, K.; Yañez Serrano, A.; Arneth, A.; Abrell, L.; Jardine, A.; van Haren, J.; Artaxo, P.; Rizzo, L. V.; Ishida, F. Y.; Karl, T.; Kesselmeier, J.; Saleska, S.; Huxman, T. Within-canopy sesquiterpene ozonolysis in Amazonia. *J. Geophys. Res.* **2011**, *116* (D19), D19301.

(21) Sindelarova, K.; Granier, C.; Bouarar, I.; Guenther, A.; Tilmes, S.; Stavrakou, T.; Müller, J. F.; Kuhn, U.; Stefani, P.; Knorr, W. Global data set of biogenic VOC emissions calculated by the MEGAN model over the last 30 years. *Atmos. Chem. Phys.* **2014**, *14* (17), 9317−9341.

(22) Pelloux, J.; Rustérucci, C.; Mellerowicz, E. J. New insights into pectin methylesterase structure and function. *Trends Plant Sci.* **2007**, *12* (6), 267−277.

DOI: 10.1021/acs.est.8b01435
Environ. Sci. Technol. XXXX, XXX, XXX−XXX

(23) Fall, R. Abundant oxygenates in the atmosphere: a biochemical perspective. *Chem. Rev.* **2003**, *103* (12), 4941−4952.
(24) Vanzo, E.; Jud, W.; Li, Z. R.; Albert, A.; Domagalska, M. A.; Ghirardo, A.; Niederbacher, B.; Frenzel, J.; Beemster, G. T. S.; Asard, H.; Rennenberg, H.; Sharkey, T. D.; Hansel, A.; Schnitzler, J. P. Facing the future: effects of short-term climate extremes on isoprene-emitting and nonemitting poplar. *Plant Physiol.* **2015**, *169* (1), 560−575.
(25) Mohnen, D. Pectin structure and biosynthesis. *Curr. Opin. Plant Biol.* **2008**, *11* (3), 266−277.
(26) Oikawa, P. Y.; Giebel, B. M.; da Silveira Lobo O'Reilly Sternberg, L.; Li, L.; Timko, M. P.; Swart, P. K.; Riemer, D. D.; Mak, J. E.; Lerdau, M. T. Leaf and root pectin methylesterase activity and $^{13}C/^{12}C$ stable isotopic ratio measurements of methanol emissions give insight into methanol production in *Lycopersicon esculentum*. *New Phytol.* **2011**, *191* (4), 1031−1040.
(27) Jardine, K. J.; Sommer, E. D.; Saleska, S. R.; Huxman, T. E.; Harley, P. C.; Abrell, L. Gas phase measurements of pyruvic acid and its volatile metabolites. *Environ. Sci. Technol.* **2010**, *44* (7), 2454−60.
(28) Brilli, F.; Gioli, B.; Fares, S.; Terenzio, Z.; Zona, D.; Gielen, B.; Loreto, F.; Janssens, I. A.; Ceulemans, R. Rapid leaf development drives the seasonal pattern of volatile organic compound (VOC) fluxes in a 'coppiced' bioenergy poplar plantation. *Plant, Cell Environ.* **2016**, *39* (3), 539−555.
(29) Bourtsoukidis, E.; Williams, J.; Kesselmeier, J.; Jacobi, S.; Bonn, B. From emissions to ambient mixing ratios: online seasonal field measurements of volatile organic compounds over a Norway spruce-dominated forest in central Germany. *Atmos. Chem. Phys.* **2014**, *14* (13), 6495−6510.
(30) Yanez-Serrano, A. M.; Nolscher, A. C.; Williams, J.; Wolff, S.; Alves, E.; Martins, G. A.; Bourtsoukidis, E.; Brito, J.; Jardine, K.; Artaxo, P.; Kesselmeier, J. Diel and seasonal changes of biogenic volatile organic compounds within and above an Amazonian rainforest. *Atmos. Chem. Phys.* **2015**, *15* (6), 3359−3378.
(31) Jardine, K.; Chambers, J.; Alves, E. G.; Teixeira, A.; Garcia, S.; Holm, J.; Higuchi, N.; Manzi, A.; Abrell, L.; Fuentes, J. D.; Nielsen, L. K.; Torn, M. S.; Vickers, C. E. Dynamic balancing of isoprene carbon sources reflects photosynthetic and photorespiratory responses to temperature stress. *Plant Physiol.* **2014**, *166* (4), 2051−U1293.
(32) Trowbridge, A. M.; Asensio, D.; Eller, A. S. D.; Way, D. A.; Wilkinson, M. J.; Schnitzler, J.-P.; Jackson, R. B.; Monson, R. K. Contribution of various varbon sources toward isoprene biosynthesis in poplar leaves mediated by altered atmospheric CO_2 concentrations. *PLoS One* **2012**, *7* (2), e32387.
(33) Schnitzler, J. P.; Graus, M.; Kreuzwieser, J.; Heizmann, U.; Rennenberg, H.; Wisthaler, A.; Hansel, A. Contribution of different carbon sources to isoprene biosynthesis in poplar leaves. *Plant Physiol.* **2004**, *135* (1), 152−60.
(34) Brilli, F.; Ciccioli, P.; Frattoni, M.; Prestininzi, M.; Spanedda, A. F.; Loreto, F. Constitutive and herbivore-induced monoterpenes emitted by *Populus x euroamericana* leaves are key volatiles that orient *Chrysomela populi* beetles. *Plant, Cell Environ.* **2009**, *32* (5), 542−52.
(35) Breuninger, C.; Oswald, R.; Kesselmeier, J.; Meixner, F. X. The dynamic chamber method: trace gas exchange fluxes (NO, NO_2, O_3) between plants and the atmosphere in the laboratory and in the field. *Atmos. Meas. Tech.* **2012**, *5* (5), 955−989.
(36) Pape, L.; Ammann, C.; Nyfeler-Brunner, A.; Spirig, C.; Hens, K.; Meixner, F. X. An automated dynamic chamber system for surface exchange measurement of non-reactive and reactive trace gases of grassland ecosystems. *Biogeosciences* **2009**, *6* (3), 405−429.
(37) Filella, I.; Wilkinson, M. J.; Llusià, J.; Hewitt, C. N.; Peñuelas, J. Volatile organic compounds emissions in Norway spruce (*Picea abies*) in response to temperature changes. *Physiol. Plant.* **2007**, *130* (1), 58−66.
(38) Cojocariu, C.; Kreuzwieser, J.; Rennenberg, H. Correlation of short-chained carbonyls emitted from *Picea abies* with physiological and environmental parameters. *New Phytol.* **2004**, *162* (3), 717−727.
(39) Tani, A. Fragmentation and Reaction Rate Constants of Terpenoids Determined by Proton Transfer Reaction-mass Spectrometry. *Environ. Control Biol.* **2013**, *51* (1), 23−29.
(40) Tani, A.; Hayward, S.; Hewitt, C. N. Measurement of monoterpenes and related compounds by proton transfer reaction-mass spectrometry (PTR-MS). *Int. J. Mass Spectrom.* **2003**, *223*−*224*, 561−578.
(41) Brown, P. A. *Investigations of proton transfer reaction mass spectrometry for applications in organophosphate detection and breath analysis*. The University of Birmingham, 2012.
(42) Bracho-Nunez, A.; Knothe, N. M.; Welter, S.; Staudt, M.; Costa, W. R.; Liberato, M. A. R.; Piedade, M. T. F.; Kesselmeier, J. Leaf level emissions of volatile organic compounds (VOC) from some Amazonian and Mediterranean plants. *Biogeosciences* **2013**, *10* (9), 5855−5873.
(43) Mäki, M.; Heinonsalo, J.; Hellén, H.; Bäck, J. Contribution of understorey vegetation and soil processes to boreal forest isoprenoid exchange. *Biogeosciences* **2017**, *14* (5), 1055−1073.
(44) Hartmann, H.; Ziegler, W.; Kolle, O.; Trumbore, S. Thirst beats hunger − declining hydration during drought prevents carbon starvation in Norway spruce saplings. *New Phytol.* **2013**, *200* (2), 340−349.
(45) Scanlon, J. T.; Willis, D. E. Calculation of Flame Ionization Detector relative response factors using the effective carbon number concept. *J. Chromatogr. Sci.* **1985**, *23* (8), 333−340.
(46) R Development Core Team R: *A Language and Environment for Statistical Computing*; R foundation for Statistical computing: Vienna, Austria, 2014, http://www.r-project.org.
(47) Harley, P.; Greenberg, J.; Niinemets, Ü.; Guenther, A. Environmental controls over methanol emission from leaves. *Biogeosciences* **2007**, *4* (6), 1083−1099.
(48) Huang, J.; Hammerbacher, A.; Forkelová, L.; Hartmann, H. Release of resource constraints allows greater carbon allocation to secondary metabolites and storage in winter wheat. *Plant, Cell Environ.* **2017**, *40* (5), 672−685.
(49) Micheli, F. Pectin methylesterases: cell wall enzymes with important roles in plant physiology. *Trends Plant Sci.* **2001**, *6* (9), 414−419.
(50) Huang, J.; Reichelt, M.; Chowdhury, S.; Hammerbacher, A.; Hartmann, H. Increasing carbon availability stimulates growth and secondary metabolites via modulation of phytohormones in winter wheat. *J. Exp. Bot.* **2017**, *68* (5), 1251−1263.
(51) Hakola, H.; Tarvainen, V.; Praplan, A. P.; Jaars, K.; Hemmilä, M.; Kulmala, M.; Bäck, J.; Hellén, H. Terpenoid and carbonyl emissions from Norway spruce in Finland during the growing season. *Atmos. Chem. Phys.* **2017**, *17* (5), 3357−3370.
(52) Das, K.; Roychoudhury, A. Reactive oxygen species (ROS) and response of antioxidants as ROS-scavengers during environmental stress in plants. *Front. Environ. Sci.* **2014**, *2* (53), 1−13.
(53) Keunen, E. L. S.; Peshev, D.; Vangronsveld, J.; Van Den Ende, W. I. M.; Cuypers, A. N. N. Plant sugars are crucial players in the oxidative challenge during abiotic stress: extending the traditional concept. *Plant, Cell Environ.* **2013**, *36* (7), 1242−1255.
(54) Ghimire, R. P.; Markkanen, J. M.; Kivimäenpää, M.; Lyytikäinen-Saarenmaa, P.; Holopainen, J. K. Needle removal by pine sawfly larvae increases branch-level VOC emissions and reduces below-ground emissions of Scots pine. *Environ. Sci. Technol.* **2013**, *47* (9), 4325−4332.
(55) Martin, D. M.; Gershenzon, J.; Bohlmann, J. Induction of volatile terpene biosynthesis and diurnal emission by methyl jasmonate in foliage of Norway spruce. *Plant Physiol.* **2003**, *132* (3), 1586−99.
(56) Yli-Pirilä, P.; Copolovici, L.; Kannaste, A.; Noe, S.; Blande, J.; Mikkonen, S.; Klemola, T.; Pulkkinen, J.; Virtanen, A.; Laaksonen, A.; Joutsensaari, J.; Niinemets, Ü.; Holopainen, J. Herbivory by an outbreaking moth increases emissions of biogenic volatiles and leads to enhanced secondary organic aerosol formation capacity. *Environ. Sci. Technol.* **2016**, *50*, 11501−11510.

DOI: 10.1021/acs.est.8b01435
Environ. Sci. Technol. XXXX, XXX, XXX−XXX

(57) Monson, R. K.; Neice, A. A.; Trahan, N. A.; Shiach, I.; McCorkel, J. T.; Moore, D. J. P. Interactions between temperature and intercellular CO_2 concentration in controlling leaf isoprene emission rates. *Plant, Cell Environ.* **2016**, *39* (11), 2404−2413.
(58) Sun, Z.; Niinemets, Ü.; Hüve, K.; Noe, S. M.; Rasulov, B.; Copolovici, L.; Vislap, V. Enhanced isoprene emission capacity and altered light responsiveness in aspen grown under elevated atmospheric CO_2 concentration. *Global Change Biology* **2012**, *18* (11), 3423−3440.
(59) Ghirardo, A.; Koch, K.; Taipale, R.; Zimmer, I.; Schnitzler, J. P.; Rinne, J. Determination of *de novo* and pool emissions of terpenes from four common boreal/alpine trees by $^{13}CO_2$ labelling and PTR-MS analysis. *Plant, Cell Environ.* **2010**, *33* (5), 781−92.
(60) McDowell, N. G.; Ryan, M. G.; Zeppel, M. J. B.; Tissue, D. T. Improving our knowledge of drought-induced forest mortality through experiments, observations, and modeling. *New Phytol.* **2013**, *200* (2), 289−293.

DOI: 10.1021/acs.est.8b01435
Environ. Sci. Technol. XXXX, XXX, XXX−XXX

CHAPTER 6 General discussion and outlook

Whether and to what extent the build-up of non-structural carbohydrate (NSC) storage pools and secondary metabolites (SM) occur at the expense of growth is poorly understood but of critical importance for understanding and predicting how plants respond to changing environmental conditions. The carbon-nutrient balance hypothesis (CNBH, Bryant *et al.*, 1983) and growth-differentiation balance hypothesis (GDBH, Herms & Mattson, 1992) both suggest that any moderate stress that limits growth more than photosynthesis may result in accumulation of NSC and SM, assuming that growth receives carbon allocation priority over growth and SM. Empirical evidence supporting this view has until now been very limited. By changing carbon availability and then assessing carbon allocation into functional fluxes (respiration and volatile monoterpenes) and biomass partitioning (total biomass, NSC and SM as well as phytohormonal changes, my thesis provides new insights into allocation trade-offs and their underlying mechanisms.

6.1 General discussion

6.1.1 Dynamics of nonstructural carbohydrates

Despite a general recognition of the important roles of NSC in plant resilience to biotic and abiotic stresses (Hartmann & Trumbore, 2016), mechanisms of carbon storage in plants are still debated. Chapin *et al.* (1990) suggested almost 30 years ago that storage in plant results from both resource accumulation (carbon supply via photosynthesis (source) exceeds carbon demand for growth (sink)) and reserve formation (upregulation of storage at the expense of growth), but so far research has not provided empirical evidence for the regulation of these processes (Dietze *et al.*, 2014). The fact that abiotic stresses such as drought and cold decrease growth (C demand) earlier and to a greater degree than photosynthesis (C supply), has led to the view that NSC pools passively accumulate when C supply is in excess of sink demands (Palacio *et al.*, 2014). Recent attempts in manipulating carbon availability via defoliation (Wiley

et al., 2013; Wiley *et al.*, 2017a) and shading (Bahn *et al.*, 2013) have also provided empirical evidence in support of reserve formation. However, defoliation may artificially decrease nitrogen storage thereby limiting growth independent of carbon availability, especially in evergreen species where nitrogen is stored mainly in foliage (Millard & Grelet, 2010; Piper & Fajardo, 2014), and shading may trigger phytochrome-induced growth stimulation (Casal, 2013). To address these shortcomings, I manipulated carbon availability via reducing [CO_2] to varying degrees, which imposes direct limit on the factor of interest, carbon availability, thereby allowing new insights into this ongoing debate.

In both wheat plants and spruce saplings, carbon limitation induced by low [CO_2] (170 ppm) decreased NSC storage more than it decreased growth and respiration, indicating that NSC storage was at least partially used as a carbon source to satisfy growth and respiration under carbon limitation (chapter 2 and 4). However, wheat growth was apparently limited by carbon supply even while substantial NSC were still present in leaves and stems. Thus, NSC may be preserved to enhance future survival at the expense of growth like during reserve formation, or they may be required to serve non-metabolic roles, such as maintaining osmoregulation. However, in the spruce study (chapter 4), further reducing carbon availability down to the aboveground carbon compensation point (CCP_{AG}, net assimilation – respiration = 0, at ~120 ppm [CO_2]) decreased growth and respiration more than NSC storage. That was likely the result of continuous incorporation of newly-assimilated carbon in the NSC pool, suggesting that allocation to growth and respiration may be constrained by NSC storage as is expected during reserve formation. We also demonstrated that reserves were at least partly available for metabolism when the carbon balance was negative (50 ppm [CO_2]). However, NSC pools at death were not completely depleted in aboveground organs, in agreement with recent results observed under drought or shading (Sevanto *et al.*, 2014; Hartmann *et al.*, 2015; Piper & Fajardo, 2016; Wiley *et al.*, 2017b), again likely due to the non-metabolic functions of NSC (Dietze *et al.*, 2014).

Phloem transport may be involved in shifting carbon allocation in response to environmental changes (Savage *et al.*, 2016). I tested this hypothesis by assessing NSC dynamics

in different organs and along a gradient of carbon availability. In both wheat and spruce, regulation of NSC storage appears to be organ-specific in response to low carbon availability: wheat plants grown at 170 ppm [CO_2] prioritized allocation of NSC to leaves over stems and roots (chapter 2) while spruce NSC storage at CCP_{AG} remained constant in aboveground organs, but continuously declined in roots due to impeded transport of newly-assimilated sugars (chapter 4). This suggests that phloem transport may play a central role in regulating carbon allocation in an attempt to achieve a functional equilibrium under changing resource availability. In my experiment, where carbon was limiting, leaves were of greater importance to the plants and thus had a higher allocation priority than stems or roots.

Taken together, my thesis provides evidence that plants regulate NSC pools at the organ level to adjust the balance of source and sink activities under different carbon availability. NSC pools can be used to support respiration and growth when carbon is limited, but may also compete with growth and respiration at CCP_{AG} in order to ensure future survival. Remaining minimum pools probably serve non-metabolic functions and are therefore not accessible for mobilization at death.

My thesis on NSC dynamics under changing carbon availability provides new insights into understanding and predicting plant response to abiotic and biotic stresses. For example, changes in NSC have long been thought as an indicator of carbon balance. However, I argue that this may only be the case for plants subjected to moderate stress where carbon supply exceeds carbon demand. Under zero and negative carbon balance that may result from harsh abiotic (e.g. extremes of drought (Adams *et al.*, 2017), cold (Susiluoto *et al.*, 2010)) and biotic stresses (e.g. defoliation, Wiley *et al.* (2017a)), accumulation ceases over time and thereafter reserve formation may come into play in order to enhance future survival, i.e. growth and respiration may be constrained to maintain NSC storage. Furthermore, the fact that not all sugars were depleted at tree death raises the problematic issue of using bulk NSC concentrations as an indicator of carbon starvation under stresses like drought and shading, instead we should identify the minimum NSC threshold below which a tree can die of carbon starvation. The non-linear responses of NSC and SM along a gradient of carbon availability also

highlight the need to manipulate the whole-plant carbon balance to varying degrees and for NSC dynamics to be assessed for each organ.

6.1.2 Dynamics of secondary metabolites

While CNBH and GDBH have provided a conceptual framework which suggests that allocation to SM is driven by the balance between carbon supply via photosynthesis and carbon demand for growth, empirical evidence does not always support these hypotheses (Niinemets, 2016). In particular, the effects of drought on SM appear to be compound-specific (McKiernan *et al.*, 2016), raising the possibility of active regulation of SM production in order to cope with environmental stresses, independent of carbon availability. Lowering carbon availability via reducing CO_2 may impose allocation trade-offs between SM and growth thereby allowing a quantitative understanding of whether and to what extent allocation to SM occur at the expense of growth.

My results showed contrasting SM dynamics in winter wheat and spruce trees exposed to a gradient of CO_2 availability. A reduction of [CO_2] caused both NSC and SM in wheat plants to decline, suggesting that SM production strongly depended on NSC availability (chapter 2). By contrast, in spruce growing at the carbon compensation point growth and NSC storage decreased but had little effects on SM, suggesting an up-regulation of SM production even at the expense of growth and NSC storage (chapter 4). Thus, different SM dynamics may result from contrasting life-history strategies. Annual herbaceous wheat plants die at the end of their fruiting season and allocation to SM, in the absence of herbivory, reduces both growth and final reproductive success. By contrast, long-lived tree species like spruce have a greater risk of encountering periods of abiotic (i.e. drought, heat waves and cold) or biotic stresses (i.e. insect attack and pathogen infestation) and preferential allocation to SM over growth may enhance long-term survival and overall fitness (Sala *et al.*, 2012; Becklin *et al.*, 2014).

Dynamics of SM were more complex than predicted by CNBH and GDBH when accessibility of SM is taken into consideration. For example, CNBH and GDBH suggest that constitutive SM are accumulated in tissues at high to moderate levels of stress but reduced at moderate to low levels of stress. However, during the progression of stress severity, SM that are initially

produced and accumulated may be inaccessible, leading to stationary bulk concentrations of SM even when stress becomes severe over time and results in negative carbon balance. As a result, changes in total SM concentrations may not reflect actual dynamics of allocation to SM in response to changing carbon availability. By contrast, there is also evidence that SM (e.g. glucosides) can be recycled and reallocated to metabolism (Neilson *et al.*, 2013). My results show that, while growth-defense tradeoffs may mainly occur in young organs, recycling may explain SM responses in old organs, with an amplitude that is organ-specific. Previously stored phenolic compounds were at least partly recycled prior to death in old needles but not in branches, whereas monoterpenes that were previously stored in needles and branches remained constant throughout the experiment (chapter 4 and 5). This evidence raises the question of whether and to what extent highly variable SM responses that have been observed under drought (Niinemets, 2016) can be explained by a trade-off between growth and defense. Interpretation of SM responses must therefore consider effects of primary source activity (carbon assimilation) from recycling of constitutive resources and how this may change with developmental stages and across organ types.

Plants not only store SM in tissues but also emit them into the atmosphere for communication and protection (Loreto & Schnitzler, 2010). For example, emissions of isoprenoids can help plants to scavenge harmful reactive oxygen species (ROS) during stress like heat and drought (Vickers *et al.*, 2009). I thus also investigated how spruce trees regulate biogenic volatile organic compounds (BVOC) under different carbon availability. Carbon limitation at 50 ppm CO_2 decreased emissions of methanol and acetone, possibly due to reduced substrate availability. By contrast, emissions of mono- (i.e. limonene and linalool) and sesquiterpenes (i.e. α- and β-farnesene) increased under carbon limitation, in particular after releasing carbon limitation, possibly as a means of stress mitigation (chapter 5). While these fluxes may not represent a large carbon cost compared to what has been stored in organs (chapter 2 and 4), their changes provide new insights into plant functioning under carbon limitation. For example, as tree mortality during drought often occurs due to insects, the changes in BVOC may play a role in hastening or delaying death.

Resource allocation in response to changing resource availability requires regulation at the molecular level. Phytohormones have been shown to regulate plant growth (Albacete *et al.*, 2008; Rowe *et al.*, 2016) and defense (Riemann *et al.*, 2015) under drought or salinity stress, but a whole-plant perspective on phytohormonal regulation of allocation in response to changing carbon availability is still limited. My thesis investigates whether phytohormones, such as auxin, abscisic acid and jasmonic acid (JA) are involved in orchestrating carbon allocation patterns under changing carbon availability. My results show that in wheat plants, increasing carbon availability stimulates growth and production of SM via upregulation of auxin and JA, respectively (chapter 3). However, this potential mechanism was not seen in spruce trees as reducing CO_2 to 50 ppm resulted in negative carbon balance, where auxin, abscisic acid and JA levels dramatically increased (data not shown). Hence, while phytohormones may be involved in controlling allocation to growth and SM in plants experiencing positive carbon balance, they may also function as signalling compounds that possibly trigger apoptosis under negative carbon balance. Our understanding of the role of hormones in response to carbon availability is still limited, and requires biochemistry experiments using mutants to provide direct evidence for causality in hormonal regulation.

Taken together, my thesis on SM dynamics under changing carbon availability suggests allocation to SM can be explained by changes in carbon supply via photosynthesis and carbon demand for growth in annual plants, but not in spruce trees where SM production may be prioritized over NSC storage and growth (Fig 6.1). While keeping in mind that SM accessibility should be taken into consideration when interpreting dynamics of SM during the progression of stress severity (Fig 6.1). Furthermore, SM emitted into atmosphere can be good indicators of plant functioning under carbon limitation.

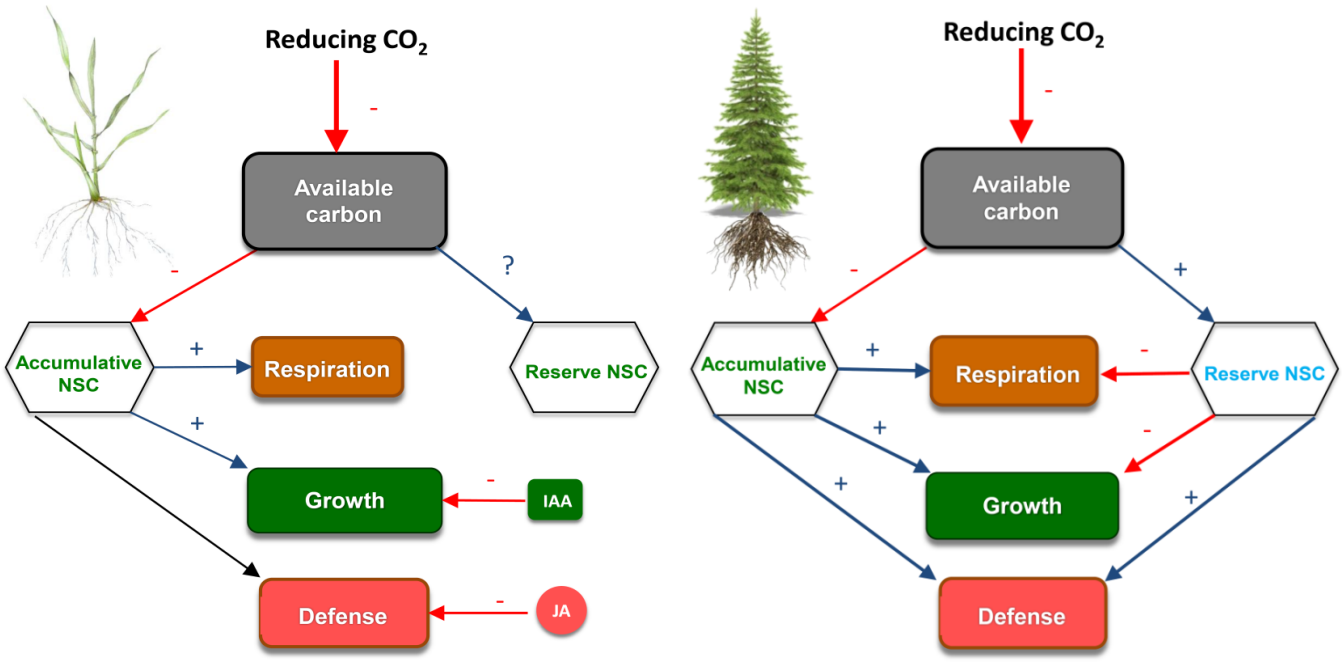

Figure 6.1 A schematic model showing the trade-offs between storage, defense and growth under low carbon availability in winter wheat (*Triticum aestivum*) and Norway spruce (*Picea abies*), derived from the results of this thesis. Arrows indicates carbon flow between pools, blue arrows indicate positive, red negative, and black constant. IAA, auxin; JA, jasmonic acid.

6.2 General outlook

My thesis provides new evidence for trade-offs between growth, storage and defense in winter wheat and Norway spruce. However, carbon allocation strategies most likely vary among species with contrasting life histories, e.g., between fast- vs slow-growing species. Fast-growing species are generally adapted to resource-rich environments and characterized by a 'fast return' economic strategy. These species prioritize growth in order to rapidly exploit more resources (e.g. nutrients, water and light) to outcompete neighbours. In this strategy investment into survival (e.g. storage and defense) has a high opportunity cost which does not outweigh the benefits achieved from allocation to growth. By contrast, slow-growing species are often adapted to resource-poor environments, and their 'slow return' economic strategy that prioritizes allocation to storage (Atkinson *et al.*, 2012) and defense (Endara & Coley, 2011) is advantageous to promote survival (Rose *et al.*, 2009). In addition, allocation strategies may also differ in plant species with different leaf habits, e.g. between deciduous vs evergreen species.

Leaves of evergreen species have a longer lifespan than of deciduous species and this poses a greater risk of encountering abiotic (i.e. drought, heat waves and cold) or biotic (i.e. insect attack and pathogen infestation) stresses. To ensure leaf survival over several growing seasons evergreen species thus adapt a conservative allocation strategy that prioritize storage (Sala *et al.*, 2012) and defense (Endara & Coley, 2011) at the expense of growth. By contrast, deciduous leaves with shorter lifetime may invest proportionally more carbon into growth than storage or defense (Piper & Fajardo, 2014). These different strategies may have been shaped by a different evolutionary trajectory and result in contrasting allocation patterns under resource limitation. Fast-growing and deciduous species may respond to resource limitation by investing storage to growth, whereas slow-growing and evergreen species may instead invest more limited resources to storage and defense to ensure their survival.

Prioritization of storage and defense over growth is achieved by either up-regulation of genes involved in biosynthesis of NSC and SM or down-regulation of genes involved in growth or both. For example, in *Arabidopsis*, up-regulation of genes involved in starch synthesis has been found to avoid low light-induced C starvation (Smith & Stitt, 2007; Gibon *et al.*, 2009); drought and salinity stress may stimulate SM production via down-regulation of the repressor jasmonate ZIM-domain (JAZ) gene family (Riemann *et al.*, 2015). Moreover, down-regulation of growth via gibberellin-mediated accumulation of repressing proteins has been shown to enhance survival under salt (Achard *et al.*, 2006), cold (Achard *et al.*, 2008) and osmotic stress (Skirycz *et al.*, 2010). However, these are generally short-term (hours to days) response mechanisms found in model organism *Arabidopsis*, where many genes and their functions have been identified. Addressing regulatory mechanisms that act over diurnal and seasonal dynamics in long-lived trees where the genome is largely unknown, remains a major challenge that requires combining interdisciplinary approaches including ecological field manipulations, biochemical assays and molecular tools (Dietze *et al.*, 2014).

Summary

Plants are sessile organisms that have to adjust metabolic processes to face challenges under rapidly changing climate. Because carbon (C) is a fundamental element in plant metabolism allocation of carbon plays a central role in plant responses to environmental changes. Yet, fundamental questions remain about how plants partition C resources among competing sinks (e.g. growth versus storage and defense) and across organs (e.g. above- versus belowground). Resolving these questions is challenging and of critical importance for understanding and predicting plant functioning and, in particular, climate-induced vegetation mortality that has been increasingly observed (Allen *et al.*, 2015) and predicted to increase in the future (Anderegg *et al.*, 2015a).

To address these questions, I increased the level of competition between sinks by manipulating C availability via changing atmospheric CO_2 concentration ($[CO_2]$). Under reduced C availability, plant allocation patterns can reveal allocation priorties and thus plant functional strategies. During my PhD I assessed functional C fluxes (e.g. respiration (R) and biogenic volatile organic compounds (BVOC)), biomass partitioning (e.g.structural growth (SG), non-structural carbohydrates (NSC) and secondary metabolites (SM)) and investigated phytohormonal changes (signalling mechanisms) during organ ontogeny (e.g. young vs old) and across organ types (e.g. leaf vs stem vs root) in different plant species types (e.g. herbaceous vs. woody plants).

In chapter 2, I quantified the percentage of daytime whole-plant net assimilation (A) allocated to night-time R, SG, NSC and SM during 8 weeks of vegetative growth in winter wheat growing at low, ambient, and elevated $[CO_2]$ (170, 390 and 680 ppm). R/A remained relatively constant over a large gradient of $[CO_2]$. However, with decreasing C availability, the fraction of assimilation allocated to biomass (SG + NSC + SM), in particular NSC and SM decreased. Assuming these pools are accurately assessed, a mass balance approach would suggest

allocation to C export (e.g. root exudates and BVOCs) increases with decreasing C availability. In addition, at low [CO_2] biomass and NSC increased in leaves but decreased in stems and roots, which may help plants achieve a functional equilibrium, i.e. overcome the most severe resource limitation. These results reveal that carbon limitation from low [CO_2] forces plants to reduce investment into long-term survival while optimizing allocation of scarce resources to biomass and NSC in tissues responsible for assimilation.

In chapter 3, I then quantified the phytohormones including abscisic acid (ABA), auxin (IAA), jasmonic acid (JA) and salicylic acid (SA) at the whole-plant level in winter wheat. My results show that RGR positively correlated with IAA but not ABA, and SM positively correlated with JA and JA-Ile but not SA. Moreover, soluble sugars positively correlated with IAA and JA but not ABA and SA. I conclude that increasing carbon availability stimulates growth and production of SM via upregulation of IAA and JA, respectively, likely in response to sugar-mediated signalling.

Chapters 4 and 5 focus on carbon allocation trade-offs in trees. In chapter 4, I manipulated the whole-tree carbon balance by modifying [CO_2] along a gradient (400, 280, 170, 120, and 50 ppm) and then assessed carbon allocation into competing fluxes and biomass sinks. Continuous isotope labelling was applied to trace the fate of newly-assimilated C in small Norway spruce trees. I found that carbon limitation from lowering [CO_2] from 400 to 280 to 170 ppm forced spruce trees to invest NSC storage (starch + soluble sugars) into growth and respiration. A further reduction to 120 ppm resulted in the aboveground C compensation point (CCP, daily assimilation flux = daily respiration flux), and caused decreases in growth and respiration while partially maintaining soluble sugars and keeping SM constant (phenolic compounds + monoterpenes). Allocation to NSC and SM was fuelled by a low but constant allocation of newly assimilated C, with the rate being dependent on C availability. Trees died of C starvation at 50 ppm [CO_2] although aboveground soluble sugar concentrations never reached zero and SM stored in old branches were not remobilized or recycled. Emission rates of volatile monoterpenes remained relatively constant across [CO_2]. I conclude that spruce trees have an evolutionarily conservative allocation strategy where growth and respiration can be down-regulated to maintain ‘operational’ levels of NSC while investing into future survival by

producing SM. While keep in mind that NSC and SM may also serve non-metabolic functions thus not accessible for mobilization at death.

In chapter 5, I continuously monitored BVOC emissions from whole-aboveground of Norway spruce exposed to a gradient of [CO_2] (400, 180, and 50 ppm) over three weeks and followed by reverting the lower [CO_2] treatments to 400 ppm. Soluble sugar and monoterpene concentrations in needles were measured to further investigate the mechanisms by which changing [CO_2] may regulate BVOC emissions. My results show that reducing [CO_2] decreased emissions of methanol and acetone as well as their temperature and light dependencies, likely related to reduced substrate availability. By contrast, emissions of mono- (i.e. limonene and linalool) and sesquiterpenes (i.e. α- and β-farnesene) and their temperature and light dependencies increased at low [CO_2], maybe as a means of stress mitigation.

Overall, my results show contrasting allocation strategies in winter wheat and Norway spruce that may have been shaped by a different evolutionary trajectory. Winter wheat, an annual herbaceous plant species that completes its life cycle within one year, prioritizes growth over storage and defense in order to rapidly acquire resources thereby enhancing final reproduction. By contrast, Norway spruce is a long-lived species with a high likelihood of encountering abiotic stresses (i.e. drought, heat waves and cold) and biotic stresses (i.e. insect attack and pathogen infestation) during its lifetime. This, apparently, leads to a conservative strategy where NSC storage is partially maintained (future resource buffer) and C preferentially invested into SM even at the expense of growth to enhance future survival. Furthermore, under C limitation, both species strive to achieve a functional equilibrium, that is, grow more leaves to alleviate resource constraints. Leaves thus have a higher allocation priority than roots. Future studies should investigate whether allocation strategies change in species with different life-histories (fast- vs slow-growing) and leaf habits (evergreen vs deciduous). Investigations of the underlying molecular mechanisms would provide information on active regulation of genes involved in jasmonates and gibberellin signalling networks controlling the allocation trade-off between defense and growth.

Zusammenfassung

Pflanzen sind sessile Organismen und können schwierigen Umweltbedingungen nicht entfliehen: um sich den Herausforderungen des sich rasch ändernden Klimas zu stellen, müssen sie daher ihre Stoffwechselprozesse anpassen. Kohlenstoff (C) ist ein grundlegendes Element des Pflanzenstoffwechsels und Allokation von Kohlenstoff spielt eine zentrale Rolle bei der Reaktion der Pflanzen auf Umweltveränderungen. Grundsätzlich stellt sich die Frage, wie Pflanzen die C-Ressourcen zwischen konkurrierenden Senken (z.B. Wachstum versus Speicherung und Verteidigung) und Organen (z.B. ober- versus unterirdisch) verteilen. Die Klärung dieser Fragen ist sowohl für das Verständnis von Pflanzenfunktion als auch für die Vorhersage der Zusammensetzung von Pflanzengemeinschaften von entscheidender Bedeutung. Dies gilt insbesondere in Anbetracht der klimabedingten Vegetationsmortalität, die zunehmend beobachtet wurde (Allen et al., 2015) und weiter zunehmen wird (Anderegg et al., 2015a).

Um diese Fragen zu beantworten, soll der Wettbewerb zwischen verschiedenen Senken durch eine Verringerung der C-Verfügbarkeit mittels Veränderung der atmosphärischen CO2-Konzentration ([CO2]) verstärkt werden. Bei verminderter C-Verfügbarkeit zeigen Zuordnungsmuster gleichzeitig Prioritäten und Strategien der pflanzlichen Allokations auf. Im Rahmen meiner Doktorarbeit habe ich C-Flüsse (z.B. Atmung (R) und biogene flüchtige organische Verbindungen (BVOC)), Biomassenaufteilung (z.B. Wachstum struktureller Biomasse (SG), nicht-strukturelle Kohlenhydrate (NSC) und Sekundärmetaboliten (SM)) und Signalmechanismen (phytohormonelle Veränderungen) im Verlauf der Ontogenese (z.B. jung vs. alt) und über Organtypen hinweg (z.B. Blatt vs. Stamm vs. Wurzel) bei verschiedenen Pflanzenarten (z.B. krautige vs. holzige Pflanzen) untersucht.

In Kapitel 2 quantifizierte ich den Prozentsatz der pflanzlichen Nettoassimilation (A) bei Winterweizen. Dieser wurde im Verlauf von 8 Wochen vegetativen Wachstums unter niedrigem, bestehendem und erhöhtem [CO2] (170, 390 und 680 ppm) an R, SG, NSC und SM ermittelt. Ich

konnte zeigen, dass das Verhältnis von R/A über diesen recht großen [CO2] Gradienten relativ konstant blieb. Mit abnehmender C-Verfügbarkeit sank jedoch der Anteil der Assimilation, der der Biomasse (SG + NSC + NSC + SM) zugewiesen wurde, insbesondere NSC und SM. Unter der Annahme der Massenbilanz konnte ich ermitteln, dass der Export von C (z.B. Wurzelexsudate und BVOCs) mit abnehmender C-Verfügbarkeit zunimmt. Darüber hinaus nahmen Biomasse und NSC bei niedrigem CO2-Gehalt in den Blättern zu, in Stämmen und Wurzeln jedoch ab. Dies könnte den Pflanzen helfen, ein funktionelles Gleichgewicht zu erreichen, d.h. starke Ressourcenlimitierung zu überwinden. Diese Ergebnisse zeigen, dass Einschränkungen des C-Haushaltes die Pflanzen dazu zwingt, Investitionen in langfristiges Überleben zu reduzieren. Gleichzeitig sollte die Einteilung knapper Ressourcen so optimiert werden, dass Gewebe, welche kurzfristige Assimilation steigern, begünstigt werden.

In Kapitel 3 erfolgte die Quantifizierung mehrerer Phytohormone, wie z.B. wachstumsregulierende Abscisinsäure (ABA) und Auxin (IAA) oder für die Abwehr wichtige Jasmonsäure (JA) und Salicylsäure (SA), in allen Organen des Winterweizens. Meine Ergebnisse zeigen, dass Wachstum positiv mit IAA korreliert, aber nicht mit ABA, und Konzentrationen von SM positiv mit JA und JA-Ile korrelieren, aber nicht mit SA. Außerdem korrelieren lösliche Zucker positiv mit IAA und JA, aber nicht mit ABA und SA. Ich schließe daraus, dass die Erhöhung der Kohlenstoffverfügbarkeit das Wachstum und die Produktion von SM durch die Hochregulierung von IAA bzw. JA stimuliert, wahrscheinlich aufgrund zuckervermittelter Signalgebung.

Die Kapitel 4 und 5 konzentrieren sich auf Kompromisssituationen in der Kohlenstoffallokation bei Bäumen. In Kapitel 4 habe ich die Kohlenstoffbilanz der untersuchten Bäume entlang eines [CO_2] Gradienten (400, 280, 170, 120 und 50 ppm) verändert und kontinuierliche Isotopenmarkierung angewandt, um den Verbleib von frisch-assimiliertem C in kleinen Fichten zu verfolgen. Ich fand heraus, dass die Begrenzung von [CO_2] von 400 auf 280 und weiter auf 170 ppm die Fichten dazu zwang, die NSC-Speicherung (Stärke + lösliche Zucker) aufzugeben und verfügbaren C in Wachstum und Atmung zu investieren. Eine weitere

Reduktion auf 120 ppm und der damit einhergehenden C-Kompensationspunkt (CCP, Daily Assimilation Flux = Daily Respiration Flux) führte zu einer Abnahme von Wachstum und Atmung bei gleichbleibenden Konzentrationen von löslichen Zucker und SM (Phenolverbindungen + Monoterpene). NSC und SM wurden durch eine niedrige aber konstante Zuteilung von neu assimiliertem C genährt, wobei die Flussrate von der C-Verfügbarkeit bestimmt wurde. Bäume starben bei 50 ppm[CO_2] an C-Auszehrung, obwohl lösliche Zuckerkonzentrationen in oberirdischen Organen nie Null erreichten. SM, die in älteren Zweigen gelagert waren, konnten nicht mobilisiert oder recycelt werden. Emissionsraten von flüchtigen Monoterpenen blieben über den [CO_2] Gradienten relativ konstant. Ich schließe daraus, dass Fichten eine evolutionär konservative Allokationsstrategie besitzen - Wachstum und Atmung können dabei herunterreguliert werden, um ein lebenswichtiges Niveau an NSC für Pflanzen aufrechtzuerhalten. Gleichzeitig werden SM als Vorsichtsmaßnahme produziert, um somit ebenfalls langfristiges Überleben zu sichern. Allokation zu NSC und SM ist daher zum Teil eine nicht recycelbare C-Investition, und unabhängig von C-Flüssen.

In Kapitel 5 beobachtete ich BVOC-Emissionen von Fichten die entlang eines [CO_2] Gradienten (400, 180 und 50 ppm, anschließend erneut 400 ppm) über einen Zeitraum von drei Wochen kontinuierlich untersucht wurden. Konzentrationen von löslichem Zuckern und Monoterpenen in Nadeln wurden gemessen, um bessere Einblicke in grundlegende Mechanismen zu gewähren. Meine Ergebnisse zeigen, dass die Temperatur- und Lichtabhängigkeit der Emissionen von Methanol und Aceton durch die Reduzierung von [CO2] verringert wurde. Dies hängt wahrscheinlich mit einer reduzierten Substratverfügbarkeit zusammen. Die Emissionen von Mono- (d.h. Limonen und Linalool) und Sesquiterpenen (d.h. α- und β-Farnesene) und deren Temperatur- und Lichtabhängigkeiten stiegen hingegen bei niedrigem CO_2-Gehalt, offenbar zur Linderung von Oxidationsstress.

Insgesamt zeigen meine Ergebnisse kontrastierende Allokationsstrategien für Winterweizen und Fichte, die möglicherweise durch unterschiedliche evolutionäre Entwicklungen geprägt sind. Winterweizen ist eine einjährige krautige Pflanzenart und vollendet ihren Lebenszyklus

innerhalb eines Jahres; sie muss daher Ressourcen so investieren, dass die einmalige Reproduktion erreicht und optimiert wird. Im Gegensatz dazu ist die Fichte eine langlebige Art mit einem hohen Risiko abiotischen (z.B. Trockenheit, Hitzewellen und Kälte) und biotischen Belastungen (z.B. Insektenbefall und Krankheiten) ausgesetzt zu sein. Dies führt offenbar zu einer konservativen Strategie, bei der NSC-Speicher teilweise beibehalten werden (zukünftiger Ressourcenpuffer) und C bevorzugt in Abwehr investiert wird. Dies geschieht auch auf Kosten des Wachstums, um Überlebenschancen langfristig zu erhöhen. Beide Arten streben jedoch unter C-Limitierung ein funktionelles Gleichgewicht an, d.h. sie produzieren mehr Blätter, um Resourcen-Knappheit, hier niedrige [CO_2], auszugleichen. Blätter erhalten somit eine höhere Allokationspriorität als Wurzeln.

Zukünftige Studien sollten untersuchen, ob und wie sich Allokationsstrategien bei Arten mit unterschiedlichen biologisch-ökologischen Merkmalen (immergrün vs. sommergrün, schnell- vs. langsam-wüchsig) unterscheiden. Untersuchungen der zugrundeliegenden molekularen Mechanismen könnten dabei Aufschluss über die genetische Regulierung geben, die den Jasmonat- und Gibberellin-Signalnetzwerken zugrunde liegen und den Allokationskompromiss zwischen Abwehr und Wachstum mechanistisch modulieren.

Bibliography

Achard P, Cheng H, De Grauwe L, Decat J, Schoutteten H, Moritz T, Van Der Straeten D, Peng J, Harberd NP. 2006. Integration of plant responses to environmentally activated phytohormonal signals. *Science* **311**: 91-94.

Achard P, Gong F, Cheminant S, Alioua M, Hedden P, Genschik P. 2008. The cold-inducible CBF1 factor-dependent signaling pathway modulates the accumulation of the growth-repressing DELLA proteins via its effect on gibberellin metabolism. *The Plant Cell* **20**: 2117-2129.

Adams HD, Zeppel MJB, Anderegg WRL, Hartmann H, Landhäusser SM, Tissue DT, Huxman TE, Hudson PJ, Franz TE, Allen CD, et al. 2017. A multi-species synthesis of physiological mechanisms in drought-induced tree mortality. *Nature Ecology & Evolution*.

Albacete A, Ghanem ME, Martínez-Andújar C, Acosta M, Sánchez-Bravo J, Martínez V, Lutts S, Dodd IC, Pérez-Alfocea F. 2008. Hormonal changes in relation to biomass partitioning and shoot growth impairment in salinized tomato (*Solanum lycopersicum* L.) plants. *Journal of Experimental Botany* **59**: 4119-4131.

Allen CD, Breshears DD, McDowell NG. 2015. On underestimation of global vulnerability to tree mortality and forest die-off from hotter drought in the Anthropocene. *Ecosphere* **6**: 1-55.

Allen CD, Macalady AK, Chenchouni H, Bachelet D, McDowell N, Vennetier M, Kitzberger T, Rigling A, Breshears DD, Hogg EH, et al. 2010. A global overview of drought and heat-induced tree mortality reveals emerging climate change risks for forests. *Forest Ecology and Management* **259**: 660-684.

Anderegg WRL, Flint A, Huang C-y, Flint L, Berry JA, Davis Frank W, Sperry JS, Field CB. 2015a. Tree mortality predicted from drought-induced vascular damage. *Nature Geoscience* **8**: 367.

Anderegg WRL, Hicke JA, Fisher RA, Allen CD, Aukema J, Bentz B, Hood S, Lichstein JW, Macalady AK, McDowell N, et al. 2015b. Tree mortality from drought, insects, and their interactions in a changing climate. *New Phytologist* **208**: 674-683.

Armstrong AF, Logan DC, Atkin OK. 2006. On the developmental dependence of leaf respiration: responses to short- and long-term changes in growth temperature. *American Journal of Botany* **93**: 1633-1639.

Atkin O. 2015. New Phytologist and the 'fate' of carbon in terrestrial ecosystems. *New Phytologist* **205**: 1-3.

Atkin OK, Scheurwater I, Pons TL. 2007. Respiration as a percentage of daily photosynthesis in whole plants is homeostatic at moderate, but not high, growth temperatures. *New Phytologist* **174**: 367-380.

Atkinson RRL, Burrell MM, Osborne CP, Rose KE, Rees M. 2012. A non-targeted metabolomics approach to quantifying differences in root storage between fast- and slow-growing plants. *New Phytologist* **196**: 200-211.

Bahn M, Lattanzi FA, Hasibeder R, Wild B, Koranda M, Danese V, Bruggemann N, Schmitt M, Siegwolf R, Richter A. 2013. Responses of belowground carbon allocation dynamics to extended shading in mountain grassland. *New Phytologist* **198**: 116-126.

Barton KE, Koricheva J. 2010. The ontogeny of plant defense and herbivory: characterizing general patterns using meta‐analysis. *The American Naturalist* **175**: 481-493.

Becklin KM, Medeiros JS, Sale KR, Ward JK. 2014. Evolutionary history underlies plant physiological responses to global change since the last glacial maximum. *Ecology Letters* **17**: 691-699.

Becklin KM, Walker SM, Way DA, Ward JK. 2017. CO_2 studies remain key to understanding a future world. *New Phytologist* **214**: 34-40.

Boeckler GA, Gershenzon J, Unsicker S. 2013. Gypsy moth caterpillar feeding has only a marginal impact on phenolic compounds in old-growth black poplar. *Journal of Chemical Ecology* **39**: 1301-1312.

Bryant J, Chapin S, Klein D. 1983. Carbon/nutrient balance of boreal plants in relation to vertebrate herbivory. *Oikos* **40**: 357.

Casal JJ. 2013. Photoreceptor signaling networks in plant responses to shade. *Annual Review of Plant Biology* **64**: 403-427.

Chapin FS, Schulze E-D, Mooney HA. 1990. The ecology and economics of storage in plants. *Annual Review of Ecology and Systematics* **21**: 423-447.

Cubasch U, Wuebbles D, Chen D, Facchini MC, Frame D, Mahowald N, Winther J-G 2013. Introduction. In: Stocker TF, Qin D, Plattner G-K, Tignor M, Allen SK, Boschung J, Nauels A, Xia Y, Bex V, Midgley PM eds. *Climate Change 2013: The Physical Science Basis. Contribution of Working Group I to the Fifth Assessment Report of the Intergovernmental Panel on Climate Change*. Cambridge, United Kingdom and New York, NY, USA: Cambridge University Press, 119–158.

Di Carlo P, Brune WH, Martinez M, Harder H, Lesher R, Ren X, Thornberry T, Carroll MA, Young V, Shepson PB, et al. 2004. Missing OH reactivity in a forest: evidence for unknown reactive biogenic VOCs. *Science* **304**: 722-725.

Dietze MC, Sala A, Carbone MS, Czimczik CI, Mantooth JA, Richardson AD, Vargas R. 2014. Nonstructural carbon in woody plants. *Annual Review of Plant Biology* **65**: 667-687.

Donaldson JR, Kruger EL, Lindroth RL. 2006. Competition- and resource-mediated tradeoffs between growth and defensive chemistry in trembling aspen (Populus tremuloides). *New Phytologist* **169**: 561-570.

Donaldson JR, Lindroth RL. 2007. Genetics, environment, and their interaction determine efficacy of chemical defense in trembling aspen. *Ecology* **88**: 729-739.

Endara MJ, Coley PD. 2011. The resource availability hypothesis revisited: a meta-analysis. *Functional Ecology* **25**: 389-398.

Enders TA, Strader LC. 2015. AUXIN ACTIVITY: PAST, PRESENT, AND FUTURE. *American Journal of Botany* **102**: 180-196.

Faralli M, Grove IG, Hare MC, Kettlewell PS, Fiorani F. 2017. Rising CO_2 from historical concentrations enhances the physiological performance of *Brassica napus* seedlings under optimal water supply but not under reduced water availability. *Plant, Cell & Environment* **40**: 317-325.

Farrar J, Hawes M, Jones D, Lindow S. 2003. HOW ROOTS CONTROL THE FLUX OF CARBON TO THE RHIZOSPHERE. *Ecology* **84**: 827-837.

Fatichi S, Leuzinger S, Korner C. 2014. Moving beyond photosynthesis: from carbon source to sink-driven vegetation modeling. *New Phytologist* **201**: 1086-1095.

Fischer S, Hanf S, Frosch T, Gleixner G, Popp J, Trumbore S, Hartmann H. 2015. *Pinus sylvestris* switches respiration substrates under shading but not during drought. *New Phytologist* **207**: 542-550.

Galiano Pérez L, Timofeeva G, Saurer M, Siegwolf R, Martínez-Vilalta J, Hommel R, Gessler A. 2017. The fate of recently fixed carbon after drought release: towards unravelling C storage regulation in *Tilia platyphyllos* and *Pinus sylvestris*. *Plant, Cell & Environment*: n/a-n/a.

Gerhart LM, Harris JM, Nippert JB, Sandquist DR, Ward JK. 2012. Glacial trees from the La Brea tar pits show physiological constraints of low CO_2. *New Phytologist* **194**: 63-69.

Gibon Y, Pyl E-T, Sulpice R, Lunn JE, Höhne M, Günther M, Stitt M. 2009. Adjustment of growth, starch turnover, protein content and central metabolism to a decrease of the carbon supply when *Arabidopsis* is grown in very short photoperiods. *Plant, Cell & Environment* **32**: 859-874.

Gifford RM. 1995. Whole plant respiration and photosynthesis of wheat under increased CO_2 concentration and temperature: long-term vs. short-term distinctions for modelling. *Global Change Biology* **1**: 385-396.

Godoy-Hernández G, Loyola-Vargas VM. 1997. Effect of acetylsalicylic acid on secondary metabolism of Catharanthus roseus tumor suspension cultures. *Plant Cell Reports* **16**: 287-290.

Grimoldi AA, Kavanova M, Lattanzi FA, Schaufele R, Schnyder H. 2006. Arbuscular mycorrhizal colonization on carbon economy in perennial ryegrass: quantification by $^{13}CO_2/^{12}CO_2$ steady-state labelling and gas exchange. *New Phytol* **172**: 544-553.

Guenther A, Hewitt CN, Erickson D, Fall R, Geron C, Graedel T, Harley P, Klinger L, Lerdau M, McKay WA, et al. 1995. A global model of natural volatile organic compound emissions. *Journal of Geophysical Research: Atmospheres* **100**: 8873-8892.

Gundlach H, Müller MJ, Kutchan TM, Zenk MH. 1992. Jasmonic acid is a signal transducer in elicitor-induced plant cell cultures. *Proceedings of the National Academy of Sciences of the United States of America* **89**: 2389-2393.

Hachiya T, Sugiura D, Kojima M, Sato S, Yanagisawa S, Sakakibara H, Terashima I, Noguchi K. 2014. High CO_2 triggers preferential root growth of *Arabidopsis thaliana* via two distinct systems under low pH and low N stresses. *Plant and Cell Physiology* **55**: 269-280.

Hallquist M, Wenger JC, Baltensperger U, Rudich Y, Simpson D, Claeys M, Dommen J, Donahue NM, George C, Goldstein AH, et al. 2009. The formation, properties and impact of secondary organic aerosol: current and emerging issues. *Atmos. Chem. Phys.* **9**: 5155-5236.

Harding SA, Jarvie MM, Lindroth RL, Tsai CJ. 2009. A comparative analysis of phenylpropanoid metabolism, N utilization, and carbon partitioning in fast- and slow-growing Populus hybrid clones. *Journal of Experimental Botany* **60**: 3443-3452.

Hartmann H, McDowell NG, Trumbore S. 2015. Allocation to carbon storage pools in Norway spruce saplings under drought and low CO_2. *Tree Physiology* **35**: 243-252.

Hartmann H, Trumbore S. 2016. Understanding the roles of nonstructural carbohydrates in forest trees – from what we can measure to what we want to know. *New Phytologist* **211**: 386-403.

Hartmann H, Ziegler W, Kolle O, Trumbore S. 2013a. Thirst beats hunger – declining hydration during drought prevents carbon starvation in Norway spruce saplings. *New Phytologist* **200**: 340-349.

Hartmann H, Ziegler W, Trumbore S. 2013b. Lethal drought leads to reduction in nonstructural carbohydrates in Norway spruce tree roots but not in the canopy. *Functional Ecology* **27**: 413-427.

Herms DA, Mattson WJ. 1992. The dilemma of plants: to grow or defend. *The Quarterly Review of Biology* **67**: 283-335.

Herrera-Vásquez A, Salinas P, Holuigue L. 2015. Salicylic acid and reactive oxygen species interplay in the transcriptional control of defense genes expression. *Frontiers in Plant Science* **6**: 171.

Hoch G, Richter A, Korner C. 2003. Non-structural carbon compounds in temperate forest trees. *Plant, Cell & Environment* **26**: 1067-1081.

Holeski LM, Zinkgraf MS, Couture JJ, Whitham TG, Lindroth RL. 2013. Transgenerational effects of herbivory in a group of long-lived tree species: maternal damage reduces offspring allocation to resistance traits, but not growth. *Journal of Ecology* **101**: 1062-1073.

Horbowicz M, Kosson R, Wiczkowski W, Koczkodaj D, Mitrus J. 2011. The effect of methyl jasmonate on accumulation of 2-phenylethylamine and putrescine in seedlings of common buckwheat (*Fagopyrum esculentum*). *Acta Physiologiae Plantarum* **33**: 897-903.

Johansson EM, Fransson PMA, Finlay RD, van Hees PAW. 2009. Quantitative analysis of soluble exudates produced by ectomycorrhizal roots as a response to ambient and elevated CO_2. *Soil Biology and Biochemistry* **41**: 1111-1116.

Johnson D, Leake JR, Ostle N, Ineson P, Read DJ. 2002. *In situ* (CO_2) C^{13} pulse-labelling of upland grassland demonstrates a rapid pathway of carbon flux from arbuscular mycorrhizal mycelia to the soil. *New Phytologist* **153**: 327-334.

Kannenberg SA, Novick KA, Phillips RP. 2017. Coarse roots prevent declines in whole-tree non-structural carbohydrate pools during drought in an isohydric and an anisohydric species. *Tree Physiology*: 1-9.

Kazan K. 2013. Auxin and the integration of environmental signals into plant root development. *Annals of Botany*.

Khan MIR, Fatma M, Per TS, Anjum NA, Khan NA. 2015. Salicylic acid-induced abiotic stress tolerance and underlying mechanisms in plants. *Frontiers in Plant Science* **6**: 17.

Kiddle GA, Doughty KJ, Wallsgrove RM. 1994. Salicylic acid-induced accumulation of glucosinolates in oilseed rape (*Brassica napus* L.) leaves. *Journal of Experimental Botany* **45**: 1343-1346.

Kim HJ, Fonseca JM, Choi JH, Kubota C. 2007. Effect of methyl jasmonate on phenolic compounds and carotenoids of romaine lettuce (*Lactuca sativa* L.). *Journal of Agricultural and Food Chemistry* **55**: 10366-10372.

Körner C. 2006. Plant CO2 responses: an issue of definition, time and resource supply. *New Phytologist* **172**: 393-411.

Kreuzwieser J, Cojocariu C, Jüssen V, Rennenberg H. 2002. Elevated atmospheric CO_2 causes seasonal changes in carbonyl emissions from *Quercus ilex*. *New Phytologist* **154**: 327-333.

Lacointe A. 2000. Carbon allocation among tree organs: A review of basic processes and representation in functional-structural tree models. *Ann. For. Sci.* **57**: 521-533.

Lelieveld J, Butler TM, Crowley JN, Dillon TJ, Fischer H, Ganzeveld L, Harder H, Lawrence MG, Martinez M, Taraborrelli D, et al. 2008. Atmospheric oxidation capacity sustained by a tropical forest. *Nature* **452**: 737-740.

Lewis JD, Ward JK, Tissue DT. 2010. Phosphorus supply drives nonlinear responses of cottonwood (*Populus deltoides*) to increases in CO_2 concentration from glacial to future concentrations. *New Phytologist* **187**: 438-448.

Loreto F, Schnitzler J-P. 2010. Abiotic stresses and induced BVOCs. *Trends in Plant Science* **15**: 154-166.

Martin D, Tholl D, Gershenzon J, Bohlmann J. 2002. Methyl jasmonate induces traumatic resin ducts, terpenoid resin biosynthesis, and terpenoid accumulation in developing xylem of Norway spruce stems. *Plant Physiology* **129**: 1003-1018.

McKiernan AB, Potts BM, Brodribb TJ, Hovenden MJ, Davies NW, McAdam SA, Ross JJ, Rodemann T, O'Reilly-Wapstra JM. 2016. Responses to mild water deficit and rewatering differ among secondary metabolites but are similar among provenances within *Eucalyptus* species. *Tree Physiology* **36**: 133-147.

Messina P, Lathière J, Sindelarova K, Vuichard N, Granier C, Ghattas J, Cozic A, Hauglustaine DA. 2016. Global biogenic volatile organic compound emissions in the ORCHIDEE and MEGAN models and sensitivity to key parameters. *Atmos. Chem. Phys.* **16**: 14169-14202.

Millard P, Grelet G-a. 2010. Nitrogen storage and remobilization by trees: ecophysiological relevance in a changing world. *Tree Physiology* **30**: 1083-1095.

Mitchell PJ, O'Grady AP, Tissue DT, White DA, Ottenschlaeger ML, Pinkard EA. 2013. Drought response strategies define the relative contributions of hydraulic dysfunction and carbohydrate depletion during tree mortality. *New Phytologist* **197**: 862-872.

Miyazawa SI, Terashima I. 2001. Slow development of leaf photosynthesis in an evergreen broad-leaved tree, *Castanopsis sieboldii*: relationships between leaf anatomical characteristics and photosynthetic rate. *Plant, Cell & Environment* **24**: 279-291.

Monks PS, Archibald AT, Colette A, Cooper O, Coyle M, Derwent R, Fowler D, Granier C, Law KS, Mills GE, et al. 2015. Tropospheric ozone and its precursors from the urban to the global scale from air quality to short-lived climate forcer. *Atmos. Chem. Phys.* **15**: 8889-8973.

Mooney HA. 1972. The carbon balance of plants. *Annual Review of Ecology and Systematics* **3**: 315-346.

Neilson EH, Goodger JQD, Woodrow IE, Møller BL. 2013. Plant chemical defense: at what cost? *Trends in Plant Science* **18**: 250-258.

Niinemets U. 2016. Uncovering the hidden facets of drought stress: secondary metabolites make the difference. *Tree Physiology* **36**: 129-132.

Niu Y, Jin C, Jin G, Zhou Q, Lin X, Tang C, Zhang Y. 2011. Auxin modulates the enhanced development of root hairs in *Arabidopsis thaliana* (L.) Heynh. under elevated CO_2. *Plant Cell and Environment* **34**: 1304-1317.

Nölscher AC, Bourtsoukidis E, Bonn B, Kesselmeier J, Lelieveld J, Williams J. 2013. Seasonal measurements of total OH reactivity emission rates from Norway spruce in 2011. *Biogeosciences* **10**: 4241-4257.

Oikawa A, Ishihara A, Iwamura H. 2002. Induction of HDMBOA-Glc accumulation and DIMBOA-Glc 4-O-methyltransferase by jasmonic acid in poaceous plants. *Phytochemistry* **61**: 331-337.

Osier TL, Lindroth RL. 2006. Genotype and environment determine allocation to and costs of resistance in quaking aspen. *Oecologia* **148**: 293-303.

Paajanen R, Julkunen-Tiitto R, Nybakken L, Petrelius M, Tegelberg R, Pusenius J, Rousi M, Kellomaki S. 2011. Dark-leaved willow (Salix myrsinifolia) is resistant to three-factor (elevated CO2, temperature and UV-B-radiation) climate change. *New Phytologist* **190**: 161-168.

Palacio S, Hoch G, Sala A, Körner C, Millard P. 2014. Does carbon storage limit tree growth? *New Phytologist* **201**: 1096-1100.

Pantin F, Simonneau T, Muller B. 2012. Coming of leaf age: control of growth by hydraulics and metabolics during leaf ontogeny. *New Phytologist* **196**: 349-366.

Paul-Victor C, Zust T, Rees M, Kliebenstein DJ, Turnbull LA. 2010. A new method for measuring relative growth rate can uncover the costs of defensive compounds in Arabidopsis thaliana. *New Phytologist* **187**: 1102-1111.

Penuelas J, Staudt M. 2010. BVOCs and global change. *Trends in Plant Science* **15**: 133-144.

Phillips RP, Bernhardt ES, Schlesinger WH. 2009. Elevated CO_2 increases root exudation from loblolly pine (*Pinus taeda*) seedlings as an N-mediated response. *Tree Physiology* **29**: 1513-1523.

Piper FI, Fajardo A. 2014. Foliar habit, tolerance to defoliation and their link to carbon and nitrogen storage. *Journal of Ecology* **102**: 1101-1111.

Piper FI, Fajardo A. 2016. Carbon dynamics of *Acer pseudoplatanus* seedlings under drought and complete darkness. *Tree Physiology* **36**: 1400-1408.

Pons TL, Poorter H. 2014. The effect of irradiance on the carbon balance and tissue characteristics of five herbaceous species differing in shade-tolerance. *Frontiers in Plant Science* **5**: 14.

Poorter H, Niklas KJ, Reich PB, Oleksyn J, Poot P, Mommer L. 2012. Biomass allocation to leaves, stems and roots: meta-analyses of interspecific variation and environmental control. *New Phytologist* **193**: 30-50.

Reich PB, Hobbie SE, Lee TD. 2014. Plant growth enhancement by elevated CO_2 eliminated by joint water and nitrogen limitation. *Nature Geoscience* **7**: 920-924.

Riemann M, Dhakarey R, Hazman M, Miro B, Kohli A, Nick P. 2015. Exploring jasmonates in the hormonal network of drought and salinity responses. *Frontiers in Plant Science* **6**: 1077.

Roberts MR, Paul ND. 2006. Seduced by the dark side: integrating molecular and ecological perspectives on the inflence of light on plant defence against pests and pathogens. *New Phytologist* **170**: 677-699.

Robinson EA, Ryan GD, Newman JA. 2012. A meta-analytical review of the effects of elevated CO_2 on plant-arthropod interactions highlights the importance of interacting environmental and biological variables. *New Phytologist* **194**: 321-336.

Rose KE, Atkinson RL, Turnbull LA, Rees M. 2009. The costs and benefits of fast living. *Ecology Letters* **12**: 1379-1384.

Rowe JH, Topping JF, Liu J, Lindsey K. 2016. Abscisic acid regulates root growth under osmotic stress conditions via an interacting hormonal network with cytokinin, ethylene and auxin. *New Phytologist* **211**: 225-239.

Sala A, Woodruff DR, Meinzer FC. 2012. Carbon dynamics in trees: feast or famine? *Tree Physiology* **32**: 764-775.

Savage JA, Clearwater MJ, Haines DF, Klein T, Mencuccini M, Sevanto S, Turgeon R, Zhang C. 2016. Allocation, stress tolerance and carbon transport in plants: how does phloem physiology affect plant ecology? *Plant, Cell & Environment* **39**: 709-725.

Schmid S, Palacio S, Hoch G. 2017. Growth reduction after defoliation is independent of CO_2 supply in deciduous and evergreen young oaks. *New Phytologist* **214**: 1479-1490.

Sevanto S, McDowell NG, Dickman LT, Pangle R, Pockman WT. 2014. How do trees die? A test of the hydraulic failure and carbon starvation hypotheses. *Plant, Cell & Environment* **37**: 153-161.

Sharkey TD, Monson RK. 2014. The future of isoprene emission from leaves, canopies and landscapes. *Plant, Cell & Environment* **37**: 1727-1740.

Sindelarova K, Granier C, Bouarar I, Guenther A, Tilmes S, Stavrakou T, Müller JF, Kuhn U, Stefani P, Knorr W. 2014. Global data set of biogenic VOC emissions calculated by the MEGAN model over the last 30 years. *Atmos. Chem. Phys.* **14**: 9317-9341.

Skirycz A, De Bodt S, Obata T, De Clercq I, Claeys H, De Rycke R, Andriankaja M, Van Aken O, Van Breusegem F, Fernie AR, et al. 2010. Developmental Stage Specificity and the Role of Mitochondrial Metabolism in the Response of Arabidopsis Leaves to Prolonged Mild Osmotic Stress. *Plant Physiology* **152**: 226-244.

Smith AM, Stitt M. 2007. Coordination of carbon supply and plant growth. *Plant, Cell & Environment* **30**: 1126-1149.

Sun YC, Guo HJ, Ge F. 2016. Plant-aphid interactions under elevated CO_2: some cues from aphid feeding behavior. *Frontiers in Plant Science* **7**: 10.

Susiluoto S, Hilasvuori E, Berninger F. 2010. Testing the growth limitation hypothesis for subarctic Scots pine. *Journal of Ecology* **98**: 1186-1195.

Teng N, Wang J, Chen T, Wu X, Wang Y, Lin J. 2006. Elevated CO_2 induces physiological, biochemical and structural changes in leaves of *Arabidopsis thaliana*. *New Phytologist* **172**: 92-103.

Velikova V, Tsonev T, Barta C, Centritto M, Koleva D, Stefanova M, Busheva M, Loreto F. 2009. BVOC emissions, photosynthetic characteristics and changes in chloroplast ultrastructure of *Platanus orientalis* L. exposed to elevated CO_2 and high temperature. *Environmental Pollution* **157**: 2629-2637.

Vickers CE, Gershenzon J, Lerdau MT, Loreto F. 2009. A unified mechanism of action for volatile isoprenoids in plant abiotic stress. *Nature Chemical Biology* **5**: 283-291.

Virjamo V, Julkunen-Tiitto R, Henttonen H, Hiltunen E, Karjalainen R, Korhonen J, Huitu O. 2013. Differences in Vole Preference, Secondary Chemistry and Nutrient Levels Between Naturally Regenerated and Planted Norway Spruce Seedlings. *Journal of Chemical Ecology* **39**: 1322-1334.

Virjamo V, Sutinen S, Julkunen-Tiitto R. 2014. Combined effect of elevated UVB, elevated temperature and fertilization on growth, needle structure and phytochemistry of young Norway spruce (Picea abies) seedlings. *Global Change Biology* **20**: 2252-2260.

Wang Y, Du S-T, Li L-L, Huang L-D, Fang P, Lin X-Y, Zhang Y-S, Wang H-L. 2009. Effect of CO_2 elevation on root growth and its relationship with indole acetic acid and ethylene in tomato seedlings. *Pedosphere* **19**: 570-576.

Way DA, Oren R. 2010. Differential responses to changes in growth temperature between trees from different functional groups and biomes: a review and synthesis of data. *Tree Physiology* **30**: 669-688.

Wiley E, Casper BB, Helliker BR. 2017a. Recovery following defoliation involves shifts in allocation that favour storage and reproduction over radial growth in black oak. *Journal of Ecology* **105**: 412-424.

Wiley E, Helliker B. 2012. A re-evaluation of carbon storage in trees lends greater support for carbon limitation to growth. *New Phytologist* **195**: 285-289.

Wiley E, Hoch G, Landhäusser SM. 2017b. Dying piece by piece: carbohydrate dynamics in aspen (Populus tremuloides) seedlings under severe carbon stress. *Journal of Experimental Botany* **68**: 5221-5232.

Wiley E, Huepenbecker S, Casper BB, Helliker BR. 2013. The effects of defoliation on carbon allocation: can carbon limitation reduce growth in favour of storage? *Tree Physiology* **33**: 1216-1228.

Zavala JA, Nabity PD, DeLucia EH. 2013. An emerging understanding of mechanisms governing insect herbivory under elevated CO_2. *Annual Review of Entomology* **58**: 79-97.

Zhang SW, Li CH, Cao J, Zhang YC, Zhang SQ, Xia YF, Sun DY, Sun Y. 2009. Altered architecture and enhanced drought tolerance in rice via the down-regulation of indole-3-acetic acid by TLD1/OsGH3.13 activation. *Plant Physiology* **151**: 1889-1901.

Curriculum Vitae

Name: Jianbei Huang

Date of birth: 01.04.1989

Place of birth: Shandong, China

EDUCATION

Since 05.2014: Ph.D student, department of Biogeochemical processes, Max Planck Institute for Biogeochemistry

09.2011-09.2013: College of Forestry, Sichuan Agricultural University, Sichuan, China
Master of Ecology
Thesis: Effects of Decomposing Leaf Litter of *Juglans Regia* L. on Growth of *Triticum Aestivum* L.

09.2007-09.2011: College of Geography & Planning, Lu Dong University, Shandong
Bachelor of Resources Environment and the Management of Urban and Rural Planning

PUBLICATIONS:

Huang J, Hu TX, Wu ZL, Hu HL, Chen H, Wang Q, Wei Z. 2014. Effects of decomposing leaf litter of *Juglans regia* on growth and physiological characteristics of *Triticum aestivum*. *Acta Ecologica Sinica* **40**(23): 6855-6863.

Huang J, Hammerbacher A, Forkelová L, Hartmann H. 2017. Release of resource constraints allows greater carbon allocation to secondary metabolites and storage in winter wheat. *Plant, Cell & Environment* **40**(5): 672-685.

Huang J, Reichelt M, Chowdhury S, Hammerbacher A, Hartmann H. 2017. Increasing carbon availability stimulates growth and secondary metabolites via modulation of phytohormones in winter wheat. *Journal of Experimental Botany* **68**(5): 1251-1263.

Huang J, Hammerbacher A, Weinhold A, Reichelt M, Gleixner G, Behrendt T, van Dam NM, Sala A, Gershenzon J, Trumbore S & Hartmann H. 2017. Eyes on the future – evidence for trade-offs between growth, respiration, storage and defense in Norway spruce. New phytologist. Doi: 10.1111/nph.15522.

Huang J, Hartmann H, Hellén H, Wisthaler A, Perreca E, Weinhold A, Rücker A, van Dam NM, Gershenzon J, Trumbore S, and Behrendt T. 2017. New perspectives on CO_2, temperature and light effects on BVOC emissions using online measurements by PTR-MS and cavity ring-down spectroscopy. Environmental Science &Technology. Doi: 10.1021/acs.est.8b01435.

Appendix

Supporting information for each chapter can be found in the published article at the publisher's web-site.

Author Contributions

Publication 1: Huang J, Hammerbacher A, Forkelová L, Hartmann H. 2017a. Release of resource constraints allows greater carbon allocation to secondary metabolites and storage in winter wheat. *Plant, Cell & Environment* 40(5): 672-685.

Jianbei Huang and Henrik Hartmann planned and designed the research. Jianbei Huang performed experiments. Almuth Hammerbacher conducted secondary metabolites analysis. Jianbei Huang and Lenka Forkelová analysed the data. Jianbei Huang wrote the manuscript with significant contributions by all co-authors.

Publication 2: Huang J, Reichelt M, Chowdhury S, Hammerbacher A, Hartmann H. 2017b. Increasing carbon availability stimulates growth and secondary metabolites via modulation of phytohormones in winter wheat. *Journal of Experimental Botany* 68(5): 1251-1263.

Jianbei Huang and Henrik Hartmann planned and designed the research. Jianbei Huang performed experiments. Michael Reichelt conducted phytohormones analysis. Jianbei Huang and Almuth Hammerbacher conducted secondary metabolites analysis. Jianbei Huang and Somak Chowdhury analysed the data. Jianbei Huang wrote the manuscript with significant contributions by all co-authors.

Publication 3: Huang J, Hammerbacher A, Weinhold A, Reichelt M, Gleixner G, Behrendt T, van Dam NM, Sala A, Gershenzon J, Trumbore S & Hartmann H. (2017) Eyes on the future – evidence for trade-offs between growth, respiration, storage and defense in Norway spruce. New phytologist. Doi: 10.1111/nph.15522.

All authors contributed to the design of the work. Jianbei Huang performed experiments, collected samples and extracted metabolites. Michael Reichelt and Almuth Hammerbacher conducted analysis of secondary metabolites. Alexander Weinhold conducted analysis of volatiles. Jianbei Huang analysed the data. Jianbei Huang wrote the manuscript with significant contributions by all co-authors.

Publication 4: Huang J, Hartmann H, Hellén H, Wisthaler A, Perreca E, Weinhold A, Rücker A, van Dam NM, Gershenzon J, Trumbore S, and Behrendt T. Contrasting emissions of methanol and acetone versus mono- and sesquiterpenes from Norway spruce under carbon limitation. Environmental Science &Technology. Doi: 10.1021/acs.est.8b01435.

Jianbei Huang, Henrik Hartmann, Susan Trumbore and Thomas Behrendt planned and designed the research. Jianbei Huang performed experiments, collected samples and extracted metabolites. Heidi Hellén and Alexander Weinhold conducted GC-MS analysis for volatiles. Armin Wisthaler and Thomas Behrendt performed PTR-MS calibration. Jianbei Huang analysed the data. The manuscript was written by Jianbei Huang with significant contributions by all co-authors.

Selbständigkeitserklärung

Ich erkläre, dass ich die vorliegende Arbeit selbständig und unter Verwendung der angegebenen Hilfsmittel, persönlichen Mitteilungen und Quellen angefertigt habe.

Jena